Unwinding or cutting ties for good: helicases and nucleases at stalled replication forks

Inauguraldissertation

zur

Erlangung der Würde eines Doktors der Philosophie

vorgelegt der

Philosophisch-Naturwissenschaftlichen Fakultät

der Universität Basel

von

Benoît Evan Falquet

Von Collonge-Bellerive, Genf

2020

Genehmigt von der Philosophisch-Naturwissenschaftlichen Fakultät
auf Antrag von

Prof. Dr. Susan M. Gasser
Prof. Dr. Ulrich Rass
Prof. Dr. Petr Cejka

Basel, den 15. Oktober 2019

Prof. Dr. Martin Spiess
Dekan

To Franz,

great friend and brilliant scientist.

Acknowledgments

I would like to express my gratitude to Pr. Ulrich Rass for his supervision, enthusiasm and extensive knowledge of the scientific literature. He was always open to discussions and to critically examine new data and ideas.

I would like to thank Susan Gasser for her mentoring and support especially during the second half of my doctorate and Petr Cejka for his constructive comments on my work.

This project would not have been possible without Gizem Ölmezer, who pioneered this work and supported me during my entire stay at FMI. She made me a better person and a better scientist.

Many of my results were obtained thanks to the dexterity, the intellectual agility and the generosity of several Rass and Gasser lab members. I am especially grateful to Dominique Klein, Kenji Shimada, Kiran Challa, Anais Cheblal , Verena Hurst and Franz Enkner. My thanks extend to all the Rass and Gasser lab members for their warm welcome and the friendly atmosphere they create. They never hesitated to spare some of their time to help me.

During this PhD, I had the chance to benefit from the technical assistance of several facilities of the FMI. I am especially grateful to Hubertus Kohler (FACS), Laurent Gelman (FAIM) and Steven Bourke (FAIM) and the team of the media kitchen for their diligence.

Finally, I would like to thank my family and friends, for their unconditional support outside of the lab. Türkiyeli aileme bana verdikleri karşılıksız destek ve sevgi için çok teşekkür ederim.

Unwinding or cutting ties for good: helicases and nucleases at stalled replication forks

Benoit Evan Falquet

Abstract

DNA replication is one of the most central processes of life. This task is performed by replicative machineries, which have to travel the entire length of each chromosome to ensure genome duplication. However, replication might stall due to natural impediments or external stress factors. The cells, then, rely on multiple accessory helicases and nucleases to unwind or cut the DNA in order to resume DNA synthesis and allow chromosome segregation at mitosis. Despite the importance of these factors, our understanding of their exact role remains incomplete.

In this work, we used budding yeast as a model organism to understand the role of the conserved nuclease-helicase Dna2 in replication. Taking advantage of its genetic interaction with Yen1, we first uncovered the role of the Dna2 helicase activity in the replication stress response and uncovered a non-canonical role of Yen1 in resolving DNA replication intermediates. We, then, extended our understanding and found that both the helicase and nuclease activities of Dna2 ensure an essential function in attending stalled replication forks to promote full genome duplication. These results offer new insights in the replication stress response and provide a new framework to understand the human pathologies associated with DNA2.

List of abbreviations

9-1-1	Ddc1-Rad17-Mec3 complex (human Rad9-Hus1-Rad1)
BIR	Break-induced replication
CDK	Cyclin-dependent kinase
CPT	Camptothecin
CFS	Common fragile site
D-loop	Displacement loop
DDK	Dbf4-dependent kinase
DSB	DNA double-strand break
dsDNA	Double-stranded DNA
HJ	Holliday junction
HR	Homologous recombination
HU	Hydroxyurea
MCM	Minichromosome maintenance
MMS	Methyl methanesulfonate
NHEJ	Non-homologous end joining
OFP	Okazaki fragment processing
ORC	Origin recognition complex
PCNA	Proliferating cell nuclear antigen
PIP	PCNA interacting peptide
Pol	Polymerase
pre-RC	Pre-replicative complex
rDNA	Ribosomal DNA
RDR	Recombination-dependent replication
RF	Replication fork
RFB	Replication fork barrier
RS	Replication stress
ssDNA	Single-stranded DNA
UFB	Ultrafine DNA bridges
UV	Ultraviolet

Overview

This thesis consists of eight chapters.

Chapter 1 gives an overview of the eukaryotic DNA replication system and examines the causes and the consequences of replication stress.

Chapter 2 consists of a published review examining the mechanisms that have evolved to prevent and mitigate the consequences of DNA underreplication, focusing on budding yeast and human.

Chapter 3 reviews the published roles of the conserved nuclease-helicase Dna2 focusing on the data obtained in budding yeast and human.

Chapter 4 examines the published roles of the helicase Pif1 with a particular emphasis on the budding yeast and the human proteins.

Chapter 5 consists of a published study and an opinion paper examining a role of the Dna2 helicase activity in the replication stress response and unraveling a novel function of Yen1 in the resolution of replication intermediates.

Chapter 6 consists of experimental data in the form of a manuscript in preparation showing that Dna2 and Yen1 fulfil together an essential function in the replication stress response.

Chapter 7 presents additional data obtained during my PhD studies.

Chapter 8 summarizes the main conclusions of this work and proposes directions for future research.

Table of content

Chapter 1: An introduction to eukaryotic DNA replication

A one light-year travel

20'000'000'000'000 km, twenty trillion kilometers, more than a light-year, is the unimaginable total length of DNA a human body produces in 70 years of life[1]. Yet, there we all are, originating from one microscopic cell encapsulating only a few meters of DNA in its nucleus. It is fascinating to consider that for each of our 10 trillion cells, the 3 billions of base pairs encoding our genome were accurately copied multiple times. The task is so immense that it seems beyond the capacities of a simple human being. However, replicating genetic information is an ancient problem and arguably one of the most fundamental properties of a living organism.

During the 3.5 billion years that has passed since the emergence of life on Earth, extremely robust mechanisms have evolved to safeguard the faithful transmission of genetic information from cell to cell. In eukaryotes, this relies on the tight organization both at the cellular level and the molecular level. While cellular surveillance mechanisms allow DNA replication only when favorable conditions are met, the molecular level of control monitors each and every DNA replication machinery constantly. As importantly, both mechanisms ensure that the full genome is duplicated once and only once per cell cycle (reviewed in[2])

Perturbation of DNA replication can be an existential threat to an organism's survival, regardless of whether they are unicellular or multicellular. Disruption of essential portions of the genome is lethal for unicellular life forms and can hamper the growth of multicellular organisms. Furthermore, mutation or amplification of genes implicated in cell proliferation can lead to the uncontrolled proliferation of a cell, which is characteristic of cancer. Understanding replication, therefore, does not only provide a glimpse at the most fundamental process of life, but also has important biomedical implications. With this in mind, I have used the budding yeast, *Saccharomyces cerevisiae*, as a model organism to investigate the role of the disease-associated Dna2 nuclease-helicase and its interplay with the Holliday junction resolvase Yen1 and the conserved helicase Pif1 helicase in DNA replication.

The eukaryotic cell cycle

DNA replication, the underlying mechanism of genetic inheritance, gives rise to two copies from one initial DNA molecule before transmission to the daughter cells. To prevent incomplete or excessive replication, this complex process operates through multiple steps that must occur

sequentially and in a strict order. Certain events are restricted to a particular window of the cell cycle. This ensure that every stage has been completed before progressing irreversibly to the next stage. For example, the cell first finishes bulk DNA replication and only then enters the phase of cell division.

The eukaryotic cell cycle is the series of events leading to the duplication of the genome and the generation of two daughter cells with identical genomes[3]. The cell cycle is divided into temporally distinct phases, and the transition from one to another is governed by the activity of cyclin-dependent kinases (CDKs)[4]. In G1 (gap 1) phase, cells grow in size and volume, producing proteins that set up replication origins and mark sites where DNA synthesis will later be initiated at[5].

Upon reaching a sufficient size, and if no DNA damage is detected, cells transit irreversibly to the next phase of the cell cycle, namely, S (synthesis) phase. During S phase, bulk DNA synthesis is completed. Subsequently, the cell, which has now doubled its DNA content, reaches the G2 (gap 2) phase where growth resumes and proteins are produced in preparation of the upcoming cell division. This is when damaged DNA is repaired in order to avoid deleterious consequences[6] in mitosis, which entails the separation of replicated sister chromatids into daughter cells.

M phase consists of four main stages: prophase, metaphase, anaphase and telophase. In metazoans, the nuclear envelope breaks down during prophase, while it remains intact in single celled species such as yeast, which perform a so-called "closed" mitosis. At this stage, each chromosome, containing two sister chromatids, undergo condensation. This compaction of the genetic material facilitates the separation of the genetic material between the daughter cells. Then, in metaphase, the chromosomes are aligned to form the metaphase plate and connect through their centromeres to the centrosomes by filaments of microtubules. Anaphase then sees the sister chromatids separate and being pulled to opposite poles by microtubules. Once the chromosomes are segregated equally, they begin to decondense. In telophase, the nuclear envelope reforms and the microtubule filaments disassemble. Finally, during cytokinesis, abscission of the plasma membrane (and of the nuclear membrane in case of a closed mitosis) gives rise to two separate daughter cells with identical genomes[7].

The initiation of DNA replication

The nucleus of each human cell contains ~2 meters of DNA comprising over 3 billion base-pairs[8]. In order to generate genetically identical offspring, cells have to accurately copy their entire genome before dividing. However, even with a DNA replication machinery synthetizing an astonishing 1000 base-pairs per second, full replication of the human genome would take more than a month if it were to be started from a single point.

To accelerate the process, cells initiate DNA replication from multiple locations simultaneously along each chromosome. In G1 phase of the cell cycle, eukaryotic cells establish multiple pre-replication complexes along the DNA at sites termed "origins of replication", by a process called "origin licensing". How the origins of replication are determined in metazoan species remains unclear since no consensus DNA sequences have been identified so far; yet, epigenetic marks, active transcription, secondary structures or the physical properties of DNA sequences have been proposed to play a role[9]. In yeast, the origins of replication are programmed by a consensus DNA sequence. Origin licensing starts with the recognition of initiation sites by the multi-components origin recognition complex (ORC), Cdc6 and Cdt1. These factors then promote the loading of two hexamers of the core replicative helicases, constituted by the minichromosome maintenance proteins 2 to 7 (MCM2-7). This leads to formation of the pre-replicative complex (pre-RC). At this stage, the chromosomes are prepared for replication, but the lack of Dbf4-dependent kinase activity (DDK) prevents the initiation of replication and the pre-RC remains stably bound to origins (reviewed in [10]).

Once cells reach S phase, rising CDK activity allows for pre-RC activation and "origin firing" while origin licensing shuts down. DDK releases pre-RC inhibition by phosphorylating the N-terminal tails of MCM2-7. This promotes the recruitment of the firing factors Sld3/7 and Cdc45. Subsequent phosphorylation, catalyzed by CDKs, allows the binding of Dpb11, Sld2 and the GINS complex. Several DNA polymerases and elongation factors are then recruited to perform DNA synthesis, forming a supramolecular complex called the "replisome" (reviewed in [10]).

On both DNA strands, the polymerase (Pol) α/primase initiates replication with the synthesis of a short RNA primer, leaving a free reactive -OH group at the 3-end of the molecule, as substrate for the replicative polymerases. It has been proposed that Polδ starts DNA synthesis

on both strands before Polε takes over this role on the leading strand, while Pol δ synthesizes the discontinuous lagging strand[11]. At each activated origin, this tightly regulated process gives rise to two replication forks (RFs) travelling on DNA in opposite directions. If RFs do not run in insurmountable road-blocks, the RFs travel until they meet another oncoming fork from a proximal origin or reach the end of the chromosome.

Road-blocks challenge DNA replication and generate replication stress

During replication, many obstacles may impede the progression of the RFs, hamper DNA synthesis or both. This phenomenon is referred to as "replication stress" (RS) and can compromise the completion of genome duplication. The sources of RS are diverse and ubiquitous and may stem from endogenous and exogenous factors (reviewed in [12]).

First of all, RS may be caused by a DNA template that differs from the canonical B-form DNA and adopts a conformation that renders its unwinding problematic. For instance, Hoogsteen pairing in Guanidine-rich regions can form a G-quadruplex structures, while repetitive sequences are prone to fold into a DNA "hairpin". Such structures require specialized helicases to be unfolded and timely replicated. The build-up of torsional stress by the replication machinery itself is another constant source of replication perturbation, such that topoisomerases are required to constantly release superhelical tension from the DNA template and allow smooth progression of the replisomes (reviewed in [13]).

DNA damage, stemming from internal and external factors, may affect the chemistry of the DNA, leading to RS. For example, it has been estimated that ultraviolet (UV) exposure following a day under the sun can induce the formation of up to 100'000 pyrimidine dimers in skin cells. Moreover, metabolic, environmental or artificial agents, such as methyl methanesulfonate (MMS) or the crosslinking agent cisplatin, may induce a wide variety of oxidative DNA damages and covalent DNA adducts, blocking the replication machinery, necessitating specialized pathways to overcome such lesions[12].

Certain factors, such as histones, are mainly produced during S-phase[14,15]. Ongoing transcription may become a cause for RS when the replisome collides head-on with the transcription machinery, transcription factors or RNA molecules that form stable complexes with DNA, called R-loops. In fact, recent research suggest that R-loops are one of the major causes of RF stalling[16].

The transcription machinery is, however, not the only protein prone susceptible to cause RF stalling. The budding yeast genome presents several sites where bound proteins obstruct RF progression. In the rDNA, Fob1 creates a replication fork barrier (RFB), a natural replication pausing site, which prevents the collision of the replication and transcription machineries[17]. Telomeric proteins including Rap1 causes replication fork pausing[18]. Moreover, the replisome slows down at centromeres due to the presence of the many factors that make up kinetochores[19]. Similar roadblocks are also present in the human genome (reviewed in [20]). While all these blocks are naturally present on the DNA and play a role in genome stability, they necessitate accessory factors such as specialized helicases to be overcome.

Yet another source of RS is the depletion of replication factors, such as dNTPs. When the ratio between the pool of available dNTPs and the number of ongoing forks is unfavorable, the DNA polymerases can no longer elongate the nascent DNA strands, while the replicative helicases still unwind the parental DNA duplex. This leads to the accumulation of long stretches of single-stranded DNA (ssDNA) at the fork resulting in RS[21]. This effect can be recapitulated artificially by using hydroxyurea (HU), an inhibitor of the ribonucleotide reductase or aphidicolin, a DNA polymerases poison[22]. ssDNA is more fragile than double-stranded DNA (dsDNA) and prolonged treatment with HU leads to chromosomal breaks, indicating that forks stalled by HU are susceptible to nucleolytic degradation and breakage[23].

Origin regulation limits replication stress

Since RS is a constant threat to proper genome duplication, the intrinsic regulation of DNA replication has evolved to minimize its deleterious consequences. The regulation of origin firing is a central pillar of the cellular RS response. On the one hand, origin firing is tightly controlled to prevent an exhaustion of replication factors; on the other hand, local activation of origins can mitigate the deleterious consequences of RF arrest.

The genome is divided in spatially clustered sites called replication domains, each of which comprises a set of origins of replication that are activated simultaneously[24]. While the origins are fired synchronously within a given replication domain, different replication domains are activated sequentially throughout the genome, which limits the levels of active RFs at any one time. Secondly, within each replication domain, only a fraction of the origins fire during each cell cycle. For instance, in fission yeast, only one fifth of the available origins at the rDNA locus are fired in

each S-phase[25] and this number is probably as low as one tenth in mammalian cells genome-wide[24]. The remaining origins are "dormant" but can be activated under stress conditions. Together, temporal separation of the replication clusters and control of origin firing limit the number of RFs that are concurrently present, avoiding the exhaustion of replication factors and dNTPs and preventing the accumulation of DNA damage[26-28].

Except telomeres, the chromosomes are replicated in segments by pairs of converging RFs. Therefore, the stalling of one RF can be compensated by the oncoming neighboring fork. However, unreplicated regions can still persist if two converging RFs stall. Double-stall events are unavoidable, especially under RS conditions. Local underreplication can be avoided by dormant origin firing in the vicinity. Since new origins cannot be licensed during replication, the cell relies on an overabundance of pre-assembled replication complexes to compensate for double RF stalling. An excess of loaded replicative complexes is, hence, critical to resist hinderance of RF progression and prevent underreplication[29,30]. It has been shown that the experimental reduction of origin licensing renders cells hypersensitive to RS[31-34] and results in genomic instability[35,36].

Theoretical calculations suggest that the partitioning of origins along the yeast chromosomes in yeast has evolved as a response to RF stalling. Thus, origins are dispersed in a more regular fashion than would be expected from random distribution. This is explained by the fact that the probability of two converging forks stalling is proportional to the square of the inter-origin distance, which makes big inter-origin segments quadratically more susceptible to under-replication. With a limited number of origins distributed over the length of the genome, the distribution that minimizes the probability of unreplicated DNA is a uniform partitioning of origins[37]. A solution that has been evolutionarily selected.

Despite intrinsic failsafe mechanisms that promote full genome duplication, local under-replication can occur. This is particularly the case in regions deprived of dormant origins, which is characteristic for common fragile sites (CFSs) in mammalian cells[22]. Mathematical modelling of underreplication shows that the principal factor influencing the probability of a double-stalling of converging RFs is the size of the genome. In human cells and other organisms with large genomes, some degree of underreplication is almost unavoidable in each cell cycle, with an estimated 80% of human cells experiencing at least one RF double-stall event per cell cycle[38]. Transition to mitosis with underreplicated chromosomes can have devastating consequences. Mitigating this danger, cells have evolved molecular circuits (checkpoints) that sense replication perturbations, trigger

mechanisms of RF recovery and delay cell-cycle progression. A robust replication checkpoint is essential for cell viability[39,40] and even partial disruption of the checkpoint is linked to severe pathologies in human[41].

The checkpoint response to replication stress

The checkpoint activation

DNA replication perturbations are sensed by the intra-S phase checkpoint and signaled throughout the cell through a phosphorylation cascade. A common outcome of RF stalling is an accumulation of ssDNA[21], which gets rapidly coated by the replication protein A (RPA)[42]. The accumulation of RPA molecules promotes the recruitment of the central signalling kinase of the intra-S phase checkpoint, namely, Mec1-Ddc2 (human ATR-ATRIP)[43,44]; yet is not sufficient to activate it.

The Rad24-RFC (human RAD17-RFC) complex recognizes the site where a ssDNA-dsDNA junction display a free 5'-end and directs the loading of the 9-1-1 clamp at the junction (yeast Rad17-Mec3-Ddc1, human Rad9-Hus1-Rad1)[45]. While it is the ssDNA-dsDNA junction end that is required to trigger the intra-S phase checkpoint, the length of the ssDNA stretch determines the intensity of the checkpoint response[46]. The close contact of Ddc1 with Mec1-Ddc2 kinase triggers the first wave of Mec1 activation and starts a positive feedback loop, in which Mec1 phosphorylates Ddc1 and promotes the recruitment of Dpb11 (human TopBP1), a factor that further promotes Mec1 kinase activity[47,48]. While Mec1 is primarily recruited to ssDNA, DNA double-strand breaks (DSBs) activate the Tel1 kinase (human ATM), which also contributes to the initiation of the checkpoint response[49].

Once Mec1 is activated, it can induce the phosphorylation hundreds of target proteins[50], including a critical component in the response of RS, the effector kinase Rad53 (functionally related to human CHK1). The mode of activation of Rad53 differs depending on the cell cycle phase it is targeted. In S phase, Mrc1 (human Claspin), a component of the replisome, promotes the recruitment of Rad53 onto Mec1 [51]. In G1 and G2, Rad9 (the homologue of human 53BP1 or BRCA1) is first recruited to stalled RFs by histone modifications and is in turn phosphorylated by Mec1 [52]. Rad9 is then able to recruit multiple Rad53 molecules, which are phosphorylation by Mec1, setting in motion its autophosphorylation activity[53]. Subsequently, phosphorylated Rad53 diffuses throughout the nucleus to translate the local sensing of RF problems into a global cellular response with consequences on several cellular functions.

The cellular response to replication stress

At the cellular level, the activation of the checkpoint following RS has several consequences. First, the progression towards M phase is slowed or blocked. In human, G2/M arrest is mediated by the inhibition of the cyclin-dependent kinases CDK1-CyclinA/E and CDK1-CyclineB, while in yeast, checkpoint mediated stabilization of Pds1, a mitotic inhibitor, halts the cell cycle in metaphase[54]. This prevents a premature entry into mitosis with underreplicated or damaged chromosomes.

In addition to its effect on cell cycle progression, the intra-S phase checkpoint regulates the dNTP level upon RS, and this regulation of dNTPs is critical for yeast cell viability[55]. One of the downstream targets of Mec1 is the ribonucleotide reductase complex (RNR). Upon activation, the checkpoint induces the degradation of Sml1, an RNR inhibitor, increasing the pool of dNTPs upon RS and allowing the restart of starved DNA polymerases. When Mec1 is deleted, Sml1 activity reduces dNTP production to an inviable level. Hence deletion of *SML1* gene rescues the lethality associated with the loss of Mec1[56].

The checkpoint plays a critical role also in the control of origin firing: while inhibiting the activation of origins in non-replicating clusters, it allows origin firing in the replicating domain [57,58]. As discussed earlier, this differential regulation promotes the completion of DNA synthesis while preventing replication factor exhaustion. In yeast, Cdc45 recruits Rad53 on the pre-RC complex[59] to promote the phosphorylation of Dbf4 and Sld3 , which prevents origin firing[60,61]. In metazoans, on the other hand, the mechanisms that inhibit origin firing upon checkpoint activation are not as clear, although Treslin (yeast Sld3[62]) and DDK are shown to be inhibited[63], indicating that the fundamental principles are conserved. How the cells identify origins located in a replicating cluster is yet unclear.

Interestingly, neither the inhibition of origin firing[61] nor the blocking of mitotic entry[64,65] determine for the cell survival following RS. Studies show that in checkpoint mutants RFs are prone to breakage[66], and cells are unable to reactivate stalled RFs[55,67,68], suggesting a yet another critical role for checkpoints in protecting stalled RFs from accumulating aberrant DNA structures.

A crucial factor that contributes to the stability of stalled RFs is the inhibition of unscheduled nucleolytic degradation of the forks. This can be achieved by downregulating the activity of the nucleases. For instance; in human, the exonuclease EXO1 is degraded in an ATR-dependent manner[69], while, in budding yeast, Exo1 is phosphorylated and deactivated by the

checkpoint machinery following DNA damage. The deletion of *EXO1* prevents the accumulation of ssDNA at replication forks in *rad53* mutant cells[70] and improves the resistance to DNA damaging agents[65], suggesting that the checkpoint protects the RFs from deleterious resection.

In addition to inhibiting RF degradation, the checkpoint machinery prevents the formation of aberrant DNA intermediates, either by coordinating RF progression or by controlling RF remodeling. In *rad53* mutants, the unwinding of the parental duplex is uncoupled from the synthesis activity of Polε[71], explaining the formation of long ssDNA stretches at the fork as observed in yeast and human cells exposed to RS[72,73]. The accumulation of ssDNA is deleterious because ssDNA structures are intrinsically more fragile than dsDNA and are dependent on RPA protein for their stability. When ssDNA accumulates to an extent that exhausts the pool of RPA, stalled RFs are left unprotected, leading to the breakage of chromosomes[27].

In addition to ssDNA, RS promotes the formation of reversed forks, an unusual DNA intermediate that arises from the remodeling of a canonical RF (three-way DNA junction) into a four-way junction. This structure, also referred to as a "regressed fork" or "chicken foot", is formed when the two nascent strands are extruded from the parental DNA and anneal with one another, while the parental strands re-anneal. It is still unclear which enzymes catalyzes RF reversal *in vivo* but numerous factors including RAD54, HTFL, FBH1, FANCM, SMARCAL1, ZRANB3, RecQ5, BLM and WRN in human and Sgs1, Rad5, Rrm3 and Pif1 in budding yeast have been suggested to play a role (reviewed by [74,75]). It is however still unclear how most of these enzyme are regulated and whether they are required for different DNA transactions or are cooperating with each other.

In budding yeast, the accumulation of regressed forks is considered pathological as it is observed mostly in checkpoint deficient yeast cell[66,70,72], or in yeast cells treated with CPT, an inhibitor of the topoisomerase I, creating lesions undetectable by the checkpoint[76]. The checkpoint is, therefore, proposed to be actively preventing RF regression or to promote the further processing of these intermediates.

The situation, however, appears different in metazoans where a wide variety of stresses induce RF reversal, even in checkpoint proficient cells[76,77]. In contrast to yeast, fork regression inhibition induces DNA breaks[76,78,79], suggesting that it constitutes an important mechanism to resist RS. Interestingly, fork reversal is not limited to the RFs affected by the replication block. In

a recent report, ATR was shown to induce a global RF slow-down and reversal in response to a local inter-strand DNA crosslink[80]. This mechanisms hints at a model where checkpoint-mediated RF reversal allows the stabilization of RF until the stress conditions are overcome.

Consequences of RS

The principal consequence of RS is the increased frequency of RF stalling events with higher probability of double stalling of converging forks. This raises the probability of underreplicated DNA regions, leading to incomplete chromosomal duplication and the persistence of unresolved DNA intermediates that are difficult to disentangle. While the checkpoint monitors stalled and ongoing forks[81], underreplication itself can go undetected and does not prevent entry to mitosis[82,83].

Due to the semi-conservative nature of canonical DNA replication, underreplicated sister chromatids remain intertwined during mitosis, hampering chromosome segregation. A common manifestation of underreplication is the formation of fine DNA links connecting the segregating sister chromatids[84-86]. These ultra-fine bridges (UFBs) are frequently observed at sites, such as the rDNA[87,88], telomeres [89,90], common fragile sites[86] and other difficult-to-replicate loci[22]. Contrary to the bulky anaphase bridges that can arise from chromosome fusion, UFBs are devoid of histones and are not stained by DAPI, which suggests that their structure differs from the classical B-form of DNA. A fraction of these bridges is bound by RPA, indicative of the presence of ssDNA, while the rest is either denatured or too stretched to bind intercalating agents[91].

Persistence of DNA bridges has several consequences. If the connection between sister chromatids is severed, fragmented chromosomes are transmitted to the daughter cells. In humans, these lesions are marked by 53BP1 bodies, shielding them from aberrant repair processes during the next G1 phase following the faulty mitosis[92]. On the other hand, non-disjunction subjects the sister chromatids to mechanical tension during anaphase, and may cause uncontrolled breakage and uneven segregation of the broken chromosome, leading to aneuploidy, micronuclei formation and other mitotic aberrations. It was also reported that UFBs can compromise cytokinesis, generating binucleated cells[87]. All of these defects are a source of genomic instability, a driving force of tumorigenesis. RS, therefore, represents a critical factor in cancer development[93].

Given the danger and the frequency of underreplication, several mechanisms have evolved to counteract terminal RF stalling. In the following chapter, we review the current knowledge on

how the cells use structure specific endonucleases to promote full genome duplication and safeguard chromosome segregation.

Chapter 2: The resolution of DNA underreplication

This chapter is based on:

Benoit Falquet and Ulrich Rass.

Structure-Specific Endonucleases and the Resolution of Chromosome Underreplication.

Genes, 2019 vol. 10 (3) p. 232.

Author Contributions:
Both authors contributed to defining the form and content of this review article and wrote the manuscript.

genes

MDPI

Review

Structure-Specific Endonucleases and the Resolution of Chromosome Underreplication

Benoît Falquet [1,2] and Ulrich Rass [3,*]

1 Friedrich Miescher Institute for Biomedical Research, Maulbeerstrasse 66, CH-4058 Basel, Switzerland; benoit.falquet@fmi.ch
2 Faculty of Natural Sciences, University of Basel, Petersplatz 10, CH-4003 Basel, Switzerland
3 Genome Damage and Stability Centre, School of Life Sciences, University of Sussex, Falmer, Brighton BN1 9RQ, UK
* Correspondence: u.w.rass@sussex.ac.uk

Received: 22 February 2019; Accepted: 13 March 2019; Published: 19 March 2019

Abstract: Complete genome duplication in every cell cycle is fundamental for genome stability and cell survival. However, chromosome replication is frequently challenged by obstacles that impede DNA replication fork (RF) progression, which subsequently causes replication stress (RS). Cells have evolved pathways of RF protection and restart that mitigate the consequences of RS and promote the completion of DNA synthesis prior to mitotic chromosome segregation. If there is entry into mitosis with underreplicated chromosomes, this results in sister-chromatid entanglements, chromosome breakage and rearrangements and aneuploidy in daughter cells. Here, we focus on the resolution of persistent replication intermediates by the structure-specific endonucleases (SSEs) MUS81, SLX1-SLX4 and GEN1. Their actions and a recently discovered pathway of mitotic DNA repair synthesis have emerged as important facilitators of replication completion and sister chromatid detachment in mitosis. As RS is induced by oncogene activation and is a common feature of cancer cells, any advances in our understanding of the molecular mechanisms related to chromosome underreplication have important biomedical implications.

Keywords: DNA replication; chromosome stability; replication stress; Holliday junction resolvase; structure-specific nuclease; ultrafine anaphase bridge; chromosome segregation; mitotic DNA synthesis; genome stability

1. Introduction

DNA replication requires the unwinding of the parental DNA duplex by the replicative helicase, which leads to the formation of branched DNA structures that are known as replication forks (RFs). Each parental DNA single-strand then acts as a template for DNA synthesis by DNA polymerases, which associate at RFs with large protein assemblies that are known as replisomes. During a human cell cycle, replisomes routinely synthesize DNA with a combined length of approximately two meters, consisting of billions of base pairs. Along the way, the replisomes have to negotiate numerous obstacles, including DNA damage, DNA secondary structures, proteins bound to the DNA template or sites of active transcription. Such obstacles can impede RF progression, causing replication stress (RS). This is mitigated by the replication checkpoint, which activates the pathways for RF recovery and promotes the resumption of DNA synthesis. RF recovery is critically dependent on homologous recombination (HR) and frequently entails the formation of branched DNA intermediates, notably Holliday junctions (HJs) [1,2], which physically link sister chromatids. These HR intermediates are removed by HJ dissolution along a decatenation pathway that is dependent on a complex of Bloom's syndrome helicase (BLM) and TopoIIIα-RMI1-RMI2 (Sgs1 helicase and Top3-Rmi1 in yeast) [3]. Alternatively,

replication-associated HR intermediates can be nucleolytically resolved by a class of structure-specific endonucleases (SSEs) that are known as HJ resolvases [4]. In addition, the cells rely on these same SSEs to cleave chromosomes at sites of potential sister chromatid non-disjunction arising from persistent replication intermediates [5]. This nucleolytic intervention, which leads to chromosome breakage, may appear to be drastic but helps to reinitiate DNA synthesis along HR-dependent repair pathways and serves as a failsafe mechanism for mitotic chromosome segregation. In this review, we provide an overview of the actions of the SSEs Mus81-Mms4/MUS81-EME1 or MUS81-EME2 (budding yeast/human), Slx1-Slx4/SLX1-SLX4 and Yen1/GEN1, highlighting their roles in mitigating genome instability and cell death that results from RS and unfinished DNA replication.

2. Intrinsic Safeguards Against Chromosomal Underreplication

Genome replication is a robust process. Eukaryotes have evolved a number of features that help to drive chromosomal replication to completion and minimize the need for SSE interventions [6–8]. Chromosomes are subdivided into replication units—or replicons—each initiated at an origin of replication that gives rise to bidirectional RFs. With the exception of the very tips of chromosomes, each inter-origin space is thus replicated by two converging RFs that have adjacent origins. This set-up compensates for local replication shortfalls caused by RF arrest through the actions of oncoming, neighboring RFs. A non-random origin distribution in yeast suggests that the inter-origin distances have been evolutionarily minimized, which reduces the risk of RF double-stalling events (inactivating a pair of converging forks) that may jeopardize replication completion [9]. Secondly, only a fraction of available replication-competent (licensed) origins are normally activated during the S phase of the cell cycle. This overabundance of licensed origins provides cells with a large pool of dormant origins that serve as failsafe replication initiation sites within the areas of insufficient RF progression. The contribution of dormant origins to bulk DNA synthesis is exemplified by the persistence of replication intermediates into the M phase, genome instability and tumor formation in mice upon the experimental depletion of dormant origins and in models with ineffective origin firing [10,11]. Consistently, excess origins have been shown to activate under replication stress conditions, protecting cells from underreplication and DNA damage [12–15]. Thirdly, the genome of higher eukaryotes is partitioned into multi-replicon replication domains [16]. Origins within a domain activate as a group but with distinct timing from those in other replication domains. This limits the number of active RFs at any one time during S phase, preventing RF destabilization and DNA damage caused by the exhaustion of replication factors or deoxyribonucleoside triphosphate pools (dNTPs) [17,18].

Other safety mechanisms couple DNA replication to cell-cycle progression and ensure that enough time has passed to synthesize a copy of the genome before the cells undergo mitosis. From yeast to humans, mitotic kinase activity is attenuated while DNA replication is ongoing and cells that are unable to initiate DNA replication due to experimental intervention subsequently enter mitosis prematurely [19–23]. This has been linked to a basal activity of the apical checkpoint kinase ATR (Mec1 and Rad3 in *Saccharomyces cerevisiae* and *Schizosaccharomyces pombe*, respectively) in response to single-stranded DNA exposed at active RFs. As a consequence, the expression of the mitotic gene network is suppressed and this avoids premature mitotic entry and carryover of underreplicated DNA into mitosis [24–26].

3. Preventing Underreplication in the Face of Replication Stress

Replication stress sets off additional cellular pathways that promote full genome replication. While unperturbed replication mildly activates ATR, RS provokes a full-blown ATR response and replication/S-phase checkpoint activation through the exposure of long stretches of RPA-coated single-stranded DNA and single-stranded/double-stranded DNA junctions at stalled RFs. After this, ATR and its orthologues in yeast act with their effector kinases CHK1 and Rad53 in budding yeast and Cds1 in fission yeast to stabilize RFs, upregulate dNTP supplies, modify the DNA replication program and control cell-cycle progression [27,28]. Across organisms, the inhibition of ATR makes

cells extremely sensitive to RS and unable to avoid frequent chromosome breakage at intrinsically difficult-to-replicate sites [29–33]. In budding yeast, Mec1-Rad53 signaling prevents RF collapse and promotes stable replication across damaged DNA templates [34,35] while checkpoint disruption results in chromosomal underreplication and accumulation of pathological DNA replication intermediates in the presence of RS [36,37]. Similar observations of RF inactivation and underreplication have been made in vertebrate cells that are acutely deprived of ATR activity [25,26]. RF collapse in yeast and human cells mediated by nucleases and helicases, including Mus81/MUS81, Exo1/EXO1 and SMARCAL1, in the absence of a functional replication checkpoint indicates that the regulation of DNA metabolic enzymes—including SSEs—is one way in which the checkpoint contributes to replication completion under RS conditions [38–43]. In addition, origin firing is restrained along the ATR-CHK1 axis across organisms [16,17,44–46]. Interestingly, the activation of the replication checkpoint attenuates origin firing globally but the origins at sites of ongoing replication maintain their ability to fire [12,45–47]. This limits the number RFs globally when cells experience RS, reducing the risk of excessive RF stalling and DNA-damage formation. At the same time, local origin activation within replicons or replication domains that are already affected by RF blockage promotes replication completion, which further benefits from critical resources (dNTPs, limiting replication factors) not being diverted to sites of newly initiated DNA synthesis in other parts of the genome [48]. Finally, replication checkpoint signaling antagonizes cell-cycle progression by dampening cyclin-dependent kinase (CDK) activity, preventing mitotic entry as long as the unresolved replication problems persist [27,28,49–54].

4. Structure-Specific Endonucleases and Their Roles in Protecting Cells from Chromosomal Underreplication

Despite the safeguards described above, accidental RF inactivation and collapse are unavoidable and routinely give rise to branched DNA intermediates that require the attention of SSEs. Cells enter the S phase with a large yet finite number of usable replication origins. It follows that double fork-failures affecting pairs of converging RFs without the possibility of compensatory origin firing in the intervening segments of DNA cannot be fully excluded. HR-dependent RF recovery (explained in more detail below) offers possibilities for re-initiating DNA synthesis and SSEs are involved in the timely removal of recombination intermediates that link sister chromatids [5]. On the other hand, theoretical considerations and experimental evidence indicate that the incidence of double-fork failure increases with genome size such that at least one unreplicated genomic site routinely persists until after bulk DNA synthesis in human cells [55,56]. While ongoing replication activity delays mitosis [24–26], replication completion appears not to be under stringent checkpoint control and segments of unreplicated DNA can thus be carried forth into mitosis [57]. After this, SSEs can intervene by processing persistent replication intermediates. Their actions resolve DNA entanglements at underreplicated chromosomal segments, which otherwise manifest as ultrafine anaphase bridges (UFBs) between segregating sister chromatids [58–61]. UFBs are strongly induced by RS and often localize to chromosomal fragile sites (CFSs), which are characterized by a number of features that make them difficult to replicate, such as being transcriptionally active, poor in usable origins and containing repetitive DNA sequences prone to DNA secondary-structure formation [32,33,62]. Fragile site expression—the appearance of metaphase chromosome gaps and breaks—is thought to be the cytogenetic manifestation of extremely late replication and perturbed chromosome condensation at intrinsically difficult-to-replicate, underreplicated chromosomal sites [62–66]. Importantly, fragile sites demarcate the breakpoints of recurrent chromosome rearrangements seen in cancer cells and give rise to deletions and duplications [31,67,68]. Therefore, SSEs play multiple roles in facilitating the completion of genome replication and suppressing genome instability associated with RF failure, incomplete replication and improper chromosome segregation.

5. Structure-Specific Endonucleases: Substrate Spectrum and Cell-Cycle Regulation

Mus81-Mms4/MUS81-EME1 or MUS81-EME2, Slx1-Slx4/SLX1-SLX4 and Yen1/GEN1 are three SSEs implicated in removing branched DNA intermediates that arise from stalled and broken RFs in eukaryotes [5] (Figure 1). Their shared ability to cleave DNA four-way junctions places them in the operationally-defined class of HJ resolvases [4]. The resolvases recognize the structure of HJs and catalyze the unique reaction that introduces symmetrically-related incisions across the junction branch point. This reaction completes HR processes by separating the recombining DNA duplexes into nicked duplex products, which can be repaired by simple nick ligation [4]. In contrast to the classic resolvase RuvC from bacteria [69], the eukaryotic HJ resolvases exhibit additional DNA debranching activities on DNA flap structures and DNA three-way junctions that are similar to RFs. Moreover, their actions are tightly regulated by post-translational modifications, protein–protein interactions and nucleocytoplasmic shuttling [70].

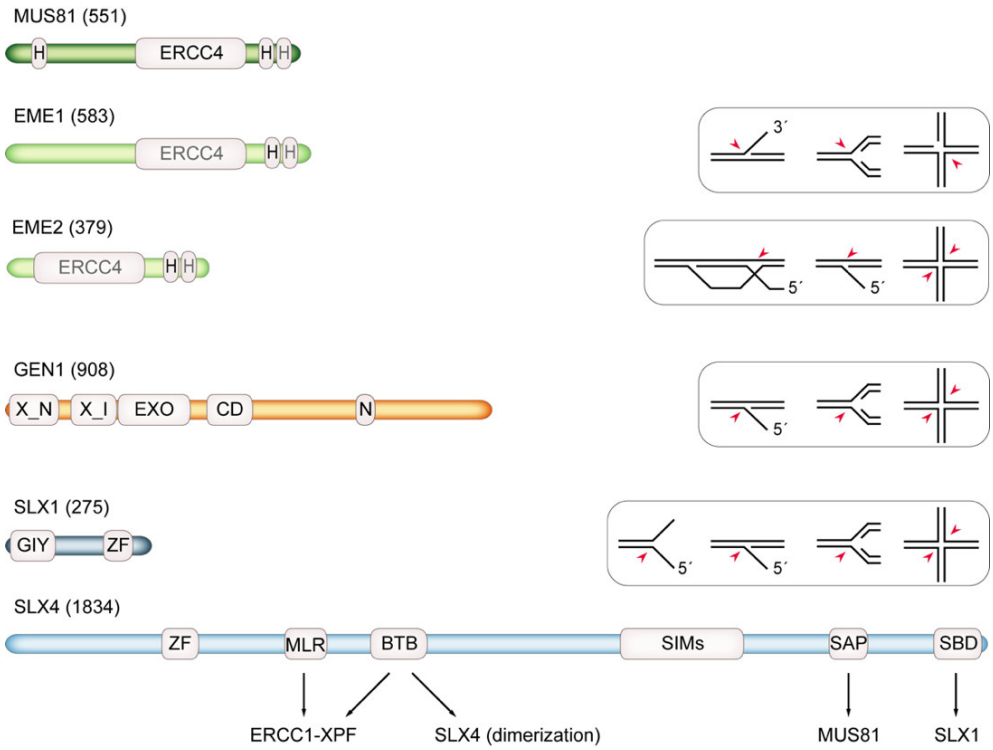

Figure 1. Human structure-specific endonuclease (SSE) domain structures and DNA substrate specificities. MUS81 and its alternative binding partners EME1 and EME2 (length in amino acids is indicated) contain ERCC4 endonuclease domain and helix-hairpin-helix (H) motifs (gray font denotes degenerate motifs). While MUS81-EME1 exhibits activity on 3′-flaps, replication forks (RFs) and nicked Holliday junctions (HJs) (red arrows), MUS81-EME2 additionally cleaves D-loop strand-invasion structures and 5′-flaps as well as being more active on intact HJs. As part of a SLX-MUS complex (see text), MUS81-EME1 effectively resolves HJs by symmetric cleavage after pre-nicking mediated by the SLX1-SLX4 nuclease. GEN1 contains N-terminal and internal XPG nuclease motifs (X_N and X_I), followed by a 5′-3′ exonuclease domain (EXO) and a chromodomain (CD) that promotes substrate recognition [71]; N denotes a nuclear export signal. GEN1 cuts 5′-flaps, RFs and HJs. SLX1 is a GIY-YIG nuclease with a zinc-finger (ZF) at the C-terminus. Associated with SLX4 via a C-terminal SLX1-binding domain (SBD), SLX1 cleaves splayed arm, 5′-flap, RF and HJ substrates. SLX4 contains a ZF domain (two copies of ubiquitin-binding UBZ4), multiple SUMO-interacting motifs (SIMs) [72] and scaffolds a tri-nuclease complex that is known as SMX containing SLX1, MUS81-EME1 (bound at its SAP domain) and ERCC1-XPF (bound via MLR, BTB). Figure is modified from [5].

5.1. MUS81

MUS81 was identified in a screen for genes that are essential in the absence of *BLM* homologue *SGS1* in budding yeast [73]. The lethality of *sgs1 mus81* double mutant cells was suppressed by inactivating HR [74], which indicates that an accumulation of recombination intermediates arising in the absence of Sgs1-mediated HJ dissolution imposes an essential requirement for Mus81 [73]. Mus81 is a member of the XPF structure-specific endonuclease family and possesses the typical ERCC4 nuclease domain and a pair of terminal helix–hairpin–helix motifs that mediate heterodimer formation with constitutive, non-catalytic subunits [75,76]. These are Mms4 in budding yeast, Eme1 in fission yeast and EME1 or EME2 in vertebrates [77–82]. Mus81 complexes from yeast and human were shown to cleave multiple branched DNA substrates, such as DNA 3′-flaps, RFs and HJs. Curiously, recombinant Mus81 consistently showed a clear preference for nicked HJ substrates while cleaving canonical, intact HJs inefficiently [77,83,84]. This is different for MUS81 in complex with EME2, an alternative heterodimeric partner found in vertebrates. The human MUS81-EME2 complex is catalytically more effective than MUS81-EME1 in biochemical assays and can, as a stand-alone nuclease, cleave a wider variety of substrates, including intact HJs and displacements loops (D-loops) generated by HR-mediated strand invasion [85,86] (Figure 1). MUS81-EME2 appears to play a particularly prominent role in the cleavage of RFs [87], which is discussed in more detail below.

Across organisms, Mus81/MUS81 activity is tightly regulated in a cell cycle-dependent manner. In yeast, the catalytic activity of Mus81 is boosted by CDK-dependent hyperphosphorylation of Mms4 (or Eme1 in fission yeast) when the cells approach the G2/M phase of the cell cycle [88,89]. Consistently, 3′-flaps, RFs and nicked HJs were efficiently cleaved by the purified Mus81-Mms4 complex from G2/M cells but not from G1 or S phase-arrested cells [90]. Mms4 hyper-phosphorylation is a multi-step process. First, Cdc5 and Dbf4-dependent kinase (DDK) associate with the scaffold protein Rtt107, which mediates the initial Mms4 phosphorylation together with CDK (Cdc28). This favors the association of Rtt107 and its binding partners with Mms4, providing a positive feedback loop that leads to the hyperphosphorylation of Mms4 when Cdc5 expression peaks towards the end of genome replication [90–92]. The cooperation of three kinases acts like a molecular switch, preventing Mus81 activity early in the cell cycle [93] but ensuring robust activation in G2/M. Following mitosis, Mms4 phosphorylation is no longer observed [90] but it is currently unclear whether this is achieved through protein turnover and/or active dephosphorylation. HJ cleavage by Mus81-Mms4 is further modulated by the sumo-like domain protein Esc2 [94] and the proliferating cell nuclear antigen (PCNA) sliding clamp and the clamp loader replication factor C (RFC), which might play a role in recruiting Mus81 to perturbed replication intermediates [95]. Similarly to yeast, the ability of human MUS81 to cleave HJ substrates correlates with the PLK1 and CDK1-dependent phosphorylation of EME1 [88,96]. However, human MUS81 effectively cleaves RF-type substrates at all stages of the cell cycle, indicating that it is not the nuclease activity per se that is cell-cycle regulated [97]. Instead, MUS81-EME1 associates with SLX1-SLX4 and XPF-ERCC1 to form a cell cycle-dependent tri-nuclease complex with HJ resolution activity [96,98–101] (see Section 5.3 below). The interaction with SLX1-SLX4 seems critical for the recruitment of MUS81 to chromatin during mitosis [97,102].

5.2. Slx1-Slx4/SLX1-SLX4

Slx1/SLX1 belongs to the UvrC family of endonucleases with an N-terminal GIY-YIG nuclease domain and a C-terminal zinc-finger domain. Associated with the much larger, multi-domain Slx4/SLX4 protein, Slx1/Slx1 cleaves a variety of DNA substrates, including 5′ flaps, RF analogs and HJs [98–100,103,104] (Figure 1). *SLX1* and *SLX4* were uncovered by the same screen for synthetic lethality with *sgs1* that identified *MUS81-MMS4* in budding yeast [73]. In contrast to *mus81 sgs1* cells, the lethality of *slx1 sgs1* or *slx4 sgs1* cells was not suppressed in the absence of HR. It has been proposed that Sgs1 and Slx1-Slx4 cooperate in maintaining the rDNA array in yeast, which might potentially happen by processing stalled RFs to initiate recombinational repair [103,105,106].

In human, SLX1-SLX4 interacts with MUS81-EME1 and XPF-ERCC1 to form the abovementioned tri-nuclease complex that is known as SMX, which functions as a highly effective HJ resolvase [96,98–101]. Consistently, epistasis analyses place *SLX1*, *SLX4* and *MUS81* in the same pathway of HJ resolution, suppressing sister-chromatid entanglements and mitotic chromosome non-disjunction [107]. However, the expression of SLX4 mutants that are unable to bind MUS81 or SLX1 partially rescues mitotic defects in SLX4-deficient cells [108], pointing to potential additional SLX1 and MUS81-independent roles of SLX4 in the processing of branched DNA intermediates [109]. In human, *SLX4* is one of the genes mutated in Fanconi anemia (and is therefore also known as *FANCP*), a rare genetic disorder characterized by defective repair of replication-blocking inter-strand DNA crosslinks, genome instability, bone marrow failure and a high susceptibility to cancer [110,111].

The crystal structure analyses of *Candida glabrata* Slx1 and the C-terminal region of Slx4 suggest that the formation of inactive Slx1 homodimers provides a means of regulating Slx1-Slx4 complex formation and activity [112]. However, as alluded to above, the control over MUS81 and SLX1-SLX4-dependent HJ resolution has to be considered in the context of cell cycle-dependent SMX complex formation.

5.3. The SMX Tri-Nuclease Complex

At its core, the SMX complex has the composite SLX-MUS resolvase that mediates HJ resolution by a SLX1-nick/MUS81-EME1-counternick mechanism [96,100,113]. Co-crystal structures of MUS81-EME1 with DNA have revealed a binding pocket for the 5′-end present at a nick that appears to provide substrate selectivity and enzyme positioning for HJ incision at a point precisely opposite a pre-existing nick [114]. Thus, HJ nicking by SLX1 creates a reference point for HJ resolution by MUS81-EME1, while SLX4 ensures coordinated cleavage by tethering MUS81 and SLX1. These observations provide an explanation for the increased efficiency of four-way DNA junction cleavage upon the association of MUS81-EME1 with SLX1-SLX4 [96,97]. The remaining subunit of SMX, the XPF-ERCC1 heterodimer, stimulates the HJ resolvase activity of SLX-MUS in a manner that is independent of its own nuclease activity [101].

SMX complex formation is governed by the activity of cell-cycle kinases. MUS81 exhibits the highest level of HJ resolution activity when purified from cells arrested in prometaphase by nocodazole at the time when MUS81-EME1 is found to be physically associated with SLX1-SLX4 [88,96]. This protein–protein interaction is dependent on CDK1 and, to a lesser extent, PLK1 activity, and is thus restricted to late cell-cycle phases [96]. CK2-dependent phosphorylation of MUS81 and CDK1-dependent phosphorylation of the SLX4 C-terminal SAP domain have been shown to promote MUS81-SLX4 interactions [72,97,115]. SLX1-SLX4 depletion or ablation of the MUS81 binding domain of SLX4 results in diminished HJ resolution activity of affinity-purified MUS81 or SLX1-SLX4, respectively [96,100]. These findings provide strong evidence that DNA four-way junction cleavage occurs in the context of the SLX-MUS complex in vivo.

In budding yeast, Mus81-Mms4, Slx1-Slx4 and Rad1-Rad10 (the homologue of XPF-ERCC1) have been shown to localize to the same sub-nuclear foci in response to RS and DNA damage [116]. Their localization was not interdependent and did not require the scaffolding function of Slx4, which is consistent with earlier experiments that failed to detect assemblies of a MUS-SLX resolvase in yeast after DNA damage treatment [117]. SSE colocalization occurred in the G1 and S phases and proteins became dispersed upon Mus81-Mms4 activation by hyperphosphorylation in G2/M [116]. These findings suggest that yeast SSEs may be recruited by a common stress-induced signal rather than physical interactions within an SMX complex. However, in a striking parallel to the human system, Mus81-Mms4 has been shown to join the abovementioned complex containing Slx4-Rtt107-Dpb11 as cells enter mitosis [118,119]. Rather than direct binding of Slx4, Mus81-Mms4 recruitment is dependent on a physical interaction between Mms4 and Dpb11, which is mediated by Cdc5 [119]. In contrast to the human system, the Slx4-Dpb11-Mus81-Mms4 complex facilitated the timely resolution of

branched DNA intermediates in a Slx1-independent manner and it remains to be determined whether a SLX-MUS-type resolvase is formed in yeast [119,120].

5.4. Yen1/GEN1

Yen1 and GEN1 were identified by a two-pronged approach that involved screening the affinity-purified protein complexes from yeast for HJ resolution activity and analyzing HeLa protein fractions with high specific HJ resolution activity by mass spectrometry [121,122]. Yen1/GEN1 are members of the Rad2/XPG nuclease family and possess a bi-partite N-terminal/internal XPG nuclease domain and helix-hairpin-helix domain [123]. While the enzyme is conserved from yeast to humans, it is conspicuously absent in fission yeast, where the heterologous expression of GEN1 can partially substitute for Mus81-Eme1 [71,124–129]. Like all other members of the XPG family, Yen1/GEN1 cuts 5′-flap structures but is the only family member that can cleave fully double-stranded three and four-way DNA junctions [121,130] (Figure 1). GEN1 is monomeric in solution and dimerizes on HJs, after which it triggers resolution by dual incision [71,129,131–134].

In contrast to Mus81-Mms4, Yen1 is inhibited by CDK. Phosphorylated Yen1 resides in the cytoplasm and accumulates in the nucleus after anaphase entry triggers its dephosphorylation by Cdc14. This activates a nuclear import signal and increases the DNA-binding activity of Yen1 [88,135–137]. In addition to the regulation by cell cycle-dependent phosphorylation, Yen1 is sumoylated in response to DNA damage. Yen1 sumoylation leads to Slx5-Slx8-dependent ubiquitination and release from DNA. It has been proposed that increased Yen1 turnover mediated by sumoylation limits the mutagenic effects of Yen1 actions on DNA [138].

Nuclear envelope breakdown during mitosis in mammalian cells necessitates a different form of regulation of GEN1 compared to Yen1 in yeast. Strikingly, GEN1 regulation also follows a strategy of cytoplasmic sequestration. A nuclear export signal within GEN1 mediates cytosolic localization throughout interphase (Figure 1), while GEN1 automatically gains access to mitotic chromosomes in prometaphase [139]. GEN1 is phosphorylated in M phase in a similar way to Yen1 although this does not appear to modulate its HJ resolvase activity and the functional consequences of this post-translational modification remain to be determined [139].

6. Holliday Junction Resolution by Structure-Specific Endonucleases Facilitates Chromosome Segregation

The canonical function of HJ resolvases is the removal of late HR intermediates. As mentioned above, RF recovery and post-replicative DNA repair pathways rely on HR [140,141] (Figure 2). After this, HJ processing severs any remaining DNA links that may compromise chromosome segregation. The loss of MUS-SLX and Yen1/Gen1-dependent branched-DNA processing sensitizes cells to a variety of agents that impair replication progression by inducing DNA damage and RS. Mus81-defective yeast cells exhibit RS sensitivity, spontaneous chromosome loss, persistence of anaphase-bridge structures and segregation failure and these phenotypes are exacerbated in the absence of Yen1 [119,142–147]. Many of the defects can be ameliorated by eliminating HR, which indicates an involvement of unresolved recombination intermediates [136,143,144]. In human cells, the perturbation of the MUS-SLX and GEN1 pathways leads to elevated levels of mitotic chromosome bridges and UFBs, chromosome segregation defects, micronuclei and transmission of DNA damage to daughter cells [96,107,108,148,149]. A recently described UFB sub-type, formed in a manner dependent on HR proteins RAD51 and BRCA2 (termed HR-UFBs), is strongly elevated upon the disruption of MUS81 and GEN1 under RS conditions. This provides evidence that SSE-dependent processing of HR intermediates arising at perturbed RFs is required to ensure that chromosomes are disentangled in time for segregation [150].

Being governed by the regulatory mechanisms described above, which direct the actions of Yen1/GEN1 and Mus81/MUS-SLX towards mitotic chromosomes, HJ resolution occurs late in the cell cycle. Disrupting cell-cycle control over HJ resolution leads to increased crossover formation

and loss of heterozygosity from yeast to humans [93,135,139,151]. This can be explained by the fact that HJ cleavage by SSEs produces crossover and non-crossover HR outcomes in equal measure. In contrast, HJ dissolution along the Sgs1/BLM-dependent decatenation pathways always leads to non-crossovers [152]. Thus, delaying the action of SSEs until after bulk DNA synthesis is completed provides a window of opportunity to dissolve—rather than resolve—HR intermediates, preventing sister chromatid exchange, chromosomal translocations (in case of non-allelic recombination) and loss of heterozygosity.

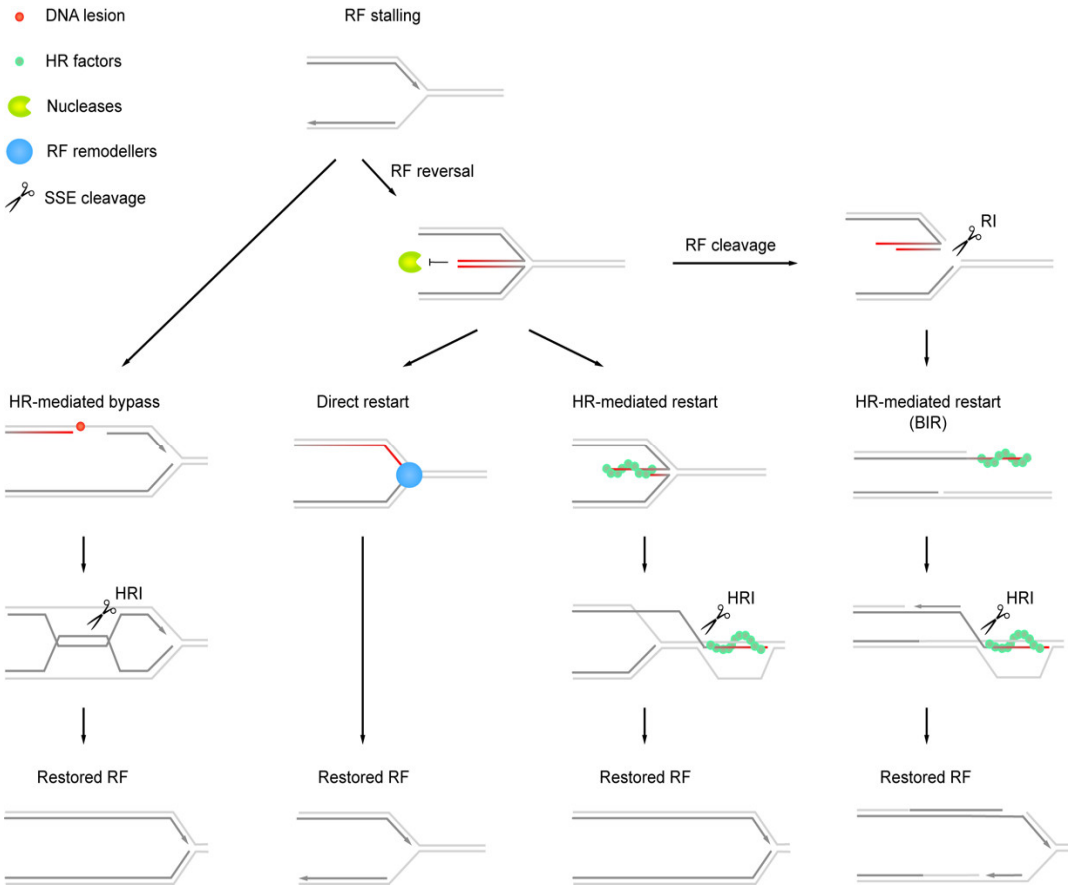

Figure 2. Multiple roles of SSEs in RF recovery. SSEs target replication (RI) and HR (HRI) intermediates to facilitate replication restart and completion. At DNA lesions, RF arrest may be overcome by HR-mediated bypass. Re-initiation of DNA synthesis downstream of lesions leaves daughter-strand gaps that are subsequently filled in by template switching. The ensuing HRIs may be removed by Sgs1/BLM-dependent dissolution (not depicted on figure) or cleavage by SSEs. RF reversal by disengagement of the leading and lagging strands at stalled forks followed by nascent-strand annealing generates HJ-like DNA four-way RIs. These intermediates are shielded from degradation, which facilitates passive rescue by converging RFs. If reversed RFs are not permanently inactivated, such as by replisome loss, remodeling for direct restart that is mediated by DNA helicases/translocases may be possible. Alternatively, functional RFs are restored by HR-mediated restart through invasion of the upstream template and associated HRIs are removed by SSEs. Persistent RIs have emerged as important non-HRI targets of SSEs. The cleavage of RF structures produces single-ended DNA double-strand breaks, triggering break-induced replication (BIR). Invasion of the unbroken sister chromatid generates a D-loop and subsequently a new processive RF. HRIs formed along the BIR pathway are once again resolved by SSEs.

Unscheduled nuclear entry of Yen1 during S phase has been shown to result in replication stress sensitivity [135,151]. Thus, the haphazard processing of DNA replication and repair intermediates is

another risk that is associated with SSE activity during S phase. Perhaps the most striking examples of chromosome breakage and genome instability upon SSE dysregulation are observed when CDK1 is prematurely activated by the inhibition of either the G2 checkpoint kinase WEE1 or checkpoint protein CHK1 [153–158]. Under these conditions, aberrant SLX-MUS complexes formed in the S phase can trigger a massive cleavage of replicating DNA, which results in a chromosome pulverization phenotype [97]. Restricting HJ resolution to mitosis thus serves a dual purpose of protecting ongoing replication, while ensuring that chromosomal DNA links can be fully removed when segregation is imminent.

7. Structure-Specific Endonucleases Cleave DNA Replication Intermediates to Promote Cell Viability

Despite the dangers associated with access of SSEs to replicating chromosomes, evidence has been solidifying in recent years that SSEs target persistent replication intermediates to promote the completion of genome replication. In mouse cells, protracted treatment with DNA replication inhibitors was shown to provoke MUS81-dependent chromosomal breaks that were correlated with replication restart [159,160]. These observations are compatible with the conversion of arrested RFs into transient DNA double-strand breaks, which subsequently serve as substrates for HR-dependent replication restart along the break-induced replication (BIR) pathway [161] (Figure 2). BIR can overcome replication breakdown by rebuilding RFs without the need for fresh origin firing, thus providing an opportunity to complete genome replication at difficult-to-replicate and damaged chromosomal sites. Consistently, MUS81 can promote chromosome breakage, replication restart and viability in human cells suffering various types of endogenous and exogenous replication stress [40,148,149,162–168]. MUS81-dependent DNA breaks result from alternative complexes containing MUS81-EME1 or MUS81-EME2, with the latter being particularly relevant to RF processing in S-phase cells [87,169]. Interestingly, in contrast to MUS81-EME1, MUS81-EME2 has the ability to process D-loop structures, such as those generated by strand invasion during BIR [86]. This raises the possibility that the actions of MUS81-EME2 may be involved in initiating replication restart by BIR and subsequently in limiting the extent of BIR-associated DNA synthesis. BIR-associated replication is error-prone and at least in yeast, Mus81-Mms4 has been shown to limit the mutagenic effects of BIR [170].

Replication stress is a hallmark of cancer, driving genome instability during tumorigenesis [171]. The involvement of MUS81-EME1 and MUS81-EME2 in RF processing and restart highlights the potential of these and other enzymes involved in RF recovery as possible anti-cancer targets.

8. Structure-Specific Endonuclease-Mediated Cleavage of DNA Replication Intermediates Initiates DNA Repair Synthesis in Mitosis

As mentioned above, underreplication gives rise to UFBs and chromosome segregation defects (Figure 3). UFBs, which remain undetected by conventional DNA dyes, are identified by their association with a characteristic set of proteins, including Polo-like kinase 1-interacting checkpoint helicase (PICH; also known as ERCC6-like protein) and BLM [58,59]. In contrast to HR-UFBs [172,173], UFBs believed to result from unreplicated segments of DNA, which are often found associated with CFSs, are flanked by foci of Fanconi anemia protein FANCD2 [60,174]. In early mitosis, a PLK1-dependent SMX complex containing the MUS81-EME1 and XPF-ERCC1 nucleases localizes with FANCD2 on chromosomes, suppresses UFBs and promotes fragile-site expression that is associated with new DNA synthesis [148,149,175]. Based on these observations, a pathway of mitotic DNA synthesis (MiDAS) has been proposed, which resolves persistent replication intermediates in an SSE-dependent manner and initiates repair DNA synthesis when the chromosomes condense in preparation for segregation [175]. MiDAS may be viewed as a last-ditch attempt to complete chromosome replication and a catchall for unreplicated DNA that may escape checkpoint surveillance and pose a serious threat to sister chromatid disjunction and chromosome integrity. In light of this, CFS-associated gaps on mitotic chromosomes are a manifestation of ongoing MiDAS, which

locally precludes chromosomal condensation, rather than unrepaired DNA damage [148,149,175] (Figure 3). MiDAS requires HR mediator RAD52 but is inhibited by the strand-exchange recombinase RAD51 [176,177]. RAD52 can catalyze strand annealing and supports BIR at regions bearing small homologies [178–180], which suggests that MiDAS represents microhomology-mediated BIR initiated at SSE-generated DNA breaks at arrested RFs [181]. Consistently, MiDAS requires the non-catalytic POLD3 subunit of polymerase δ and involves a conservative mode of DNA replication in a similar way to BIR [175,177]. However, a feature that clearly distinguishes MiDAS from other instances of RF collapse and BIR-dependent replication restart is its apparent dependence on chromosome compaction, making MiDAS a truly mitotic phenomenon. The inhibition of chromosome condensation or stabilization of cohesion on sister-chromatid arms prevented the recruitment of MUS81 and precluded MiDAS [175]. It has been suggested that DNA compaction may expose underreplicated segments of DNA, conceivably facilitating their processing by SSEs [175]. MiDAS is strongly elevated under RS conditions and particularly prevalent in aneuploid cell lines, which makes the pathway an attractive potential target for cancer therapy [175,182].

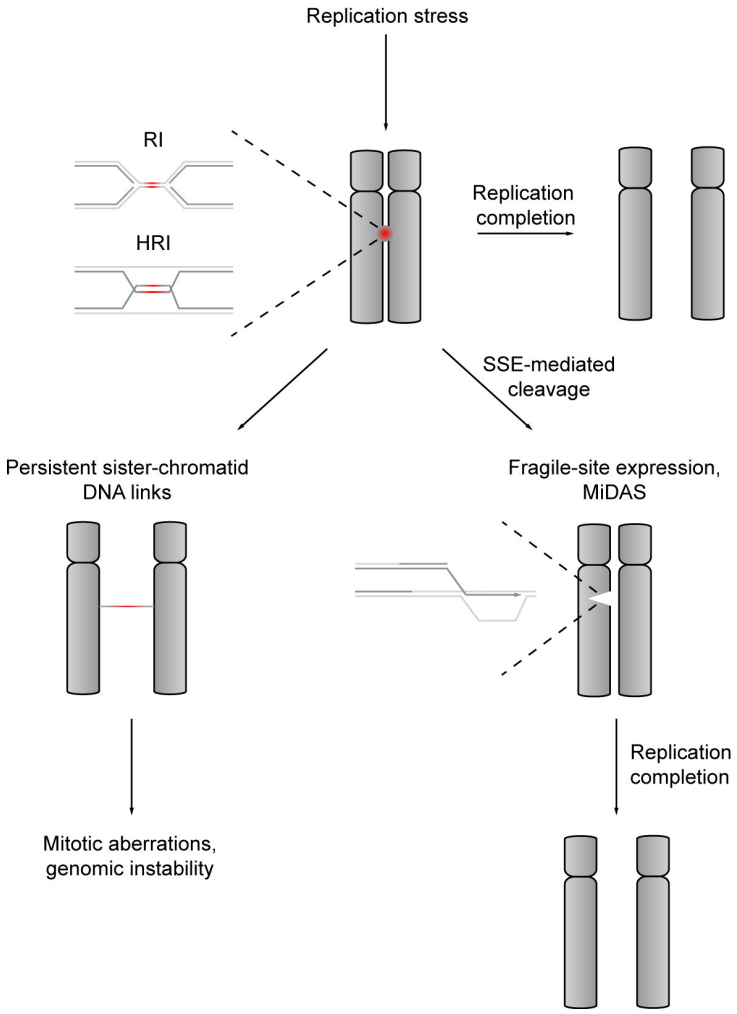

Figure 3. SSEs promote sister chromatid disjunction and replication completion. RS leads to an accumulation of unresolved replication (RI) and HR (HRI) intermediates linking nascent sister chromatids. If replication is not completed in S phase and not all RIs and HRIs are removed, SSEs resolve persistent intermediates in mitosis. RI cleavage initiates late DNA repair synthesis along the mitotic DNA synthesis (MiDAS) pathways, which promotes replication completion in mitotic cells and safeguards sister chromatid disjunction. Failure to resolve RI and HRI sister chromatid DNA links leads to BLM and PICH-bound UFBs, mitotic DNA damage and segregation failure.

In yeast, Yen1 has been implicated in the mitotic resolution of underreplicated DNA. Yen1-mutant cells exhibit hypersensitivity to RS upon inactivation of the helicase domain within the Dna2 nuclease-helicase [183–185]. This synthetic-sick relationship persisted in the absence of Rad52, indicating that Yen1 targets in Dna2-mutant cells arise independently of HR [185]. In human cells, DNA2 has been shown to promote DNA replication and facilitate the restart of stalled RFs [186–189]. Consistently, replication intermediates accumulate in Dna2 helicase-defective yeast cells and preclude chromosome segregation unless they are resolved by Yen1 [185]. Due to the fact that Yen1 activity is restricted to mitosis, Dna2-mutant cells are prone to terminal G2/M DNA damage checkpoint arrest when exposed to RS [185]. Conversely, Yen1^{ON}, which is a constitutively nuclear and active Yen1 mutant [135], supports the growth of otherwise inviable *dna2*Δ cells [190]. It remains to be determined whether Yen1 cleavage of persistent replication structures results in mitotic DNA synthesis or transmission of DNA breaks to daughter cells. Either way, DNA cleavage of replication intermediates that have escaped Dna2 activity prevents mitotic catastrophe and restores near wild-type levels of viability to Dna2 helicase-mutant cells [185]. In human, the mutations in *DNA2* are associated with Seckel syndrome, one of the microcephalic primordial dwarfism disorders that have been linked to defective RF recovery [191,192]. In cancer, on the other hand, *DNA2* is frequently overexpressed, potentially reflecting an adaptation to endogenous RS and elevated levels of RF stalling [193,194]. If a two-tiered DNA2-GEN1 mechanism for the processing of persistent replication intermediates is conserved in humans, inhibiting these enzymes may provide a means to kill cancer cells by stress overload.

9. Structure-Specific Endonuclease Targets Arising at Stalled Replication Forks

The versatile DNA debranching activities of Mus81-Mms4/MUS81-EME1, MUS81-EME2, Slx1-Slx4/SLX1-SLX4 and Yen1/GEN1 at three-way and four-way DNA junctions suggest that these SSEs may be capable of cleaving a wide variety of failing replication intermediates in vivo. Direct observations of DNA topology by electron microscopy have revealed reversed RF intermediates that are structurally equivalent to HJs [195] (Figure 2). These intermediates are ubiquitous in human cells but accumulate under RS conditions when MUS81 is absent, indicating that SSEs target the remodeled four-way replication structures or arrested RFs that give rise to them [40,196,197].

RF remodeling involving DNA strand separation and strand annealing can be catalyzed by a number of factors, including the DNA helicases and translocases RAD54, HTFL, FBH1, FANCM, SMARCAL1, ZRANB3, BLM and WRN [198]. RF reversal appears to protect from breakage, suggesting that changes in the architecture of forks that were originally perceived as pathologic and detrimental constitute a controlled response to RF stalling [40,165,195,199–201]. The regressed arm at reversed RFs has an exposed DNA end and is susceptible to degradation. In human cells, the tumor suppressor BRCA2 promotes the formation of protective RAD51 filaments on reversed RFs, acting in an HR-independent role to block MRE11-mediated nucleolytic degradation and RF demise [196,202–207]. Preserving reversed RFs may facilitate passive rescue by fork convergence upon the arrival of a neighboring RF. Alternatively, reversed RFs are converted back to three-way processive forks by the controlled resection of the regressed arm and/or branch migration [43,188,208] (see "direct restart" in Figure 2). Active three-way/four-way structure interconversions mediated by bacterial and viral DNA repair helicases in reconstituted in vitro systems suggest that RF recovery by fork remodeling is a ubiquitous mechanism [209,210]. If direct restart fails, RFs can be restored by cleavage-free HR-dependent mechanisms, involving the invasion of the upstream parental duplex by the regressed arm (see "HR-mediated restart" in Figure 2). However, persistent replication intermediates will eventually become susceptible to SSE cleavage late in the cell cycle, when the HJ resolvases are activated and targeted to chromatin as described above (see "RF cleavage" in Figure 2). This ensures sister chromatid disjunction when chromosome segregation approaches although MiDAS and/or DNA damage repair in daughter cells may subsequently be required for replication completion (Figure 3). It is tempting to speculate that reversed fork structures that are distinct from conventional three-way

RFs may attract SSEs in vivo but it is currently unclear whether proper nucleolytic processing is dependent upon prior RF remodeling. It will also be interesting to learn how MUS81-EME2 can be targeted to inactivated RFs in S phase while sparing similar structures that are actively engaged in DNA synthesis. The association of the replisome and other replication/repair factors crowding RFs certainly plays a role in the structural conformation and accessibility of RFs for SSEs.

10. Conclusions

In the last few years, there has been considerable progress in our understanding of the function and regulation of SSEs in the resolution of underreplication and sister chromatid non-disjunction. The general picture that has emerged is that SSEs are subject to multiple layers of regulation that largely restrict their activities to mitosis. This serves to protect ongoing replication in S phase and ensures that the persistent chromosomal DNA links are removed in time for chromosome segregation. Incomplete replication may escape checkpoint surveillance but SSEs are mobilized at every mitosis and are ready to avert anaphase-bridge formation and mitotic catastrophe. Perhaps one of the most striking discoveries is the SSE-mediated initiation of DNA synthesis along the MiDAS pathway, identifying a surprisingly late-acting mechanism of replication completion in mitosis. MiDAS provides an appealing solution for maintaining genome stability despite the inevitability of local underreplication during genome replication. The advances that are being made in our detailed understanding of the mechanisms related to RS and chromosomal underreplication will no doubt feed into strategies exploiting cancer-associated RS for new anti-cancer therapeutic approaches.

Author Contributions: Both authors contributed to defining the form and content of this review article and wrote the manuscript.

Funding: This research received no external funding.

Acknowledgments: Our work on SSEs and replication stress was supported by the Friedrich Miescher Institute for Biomedical Research in Basel and the Novartis Research Foundation. We thank Kok-Lung Chan for helpful discussions.

Conflicts of Interest: The authors declare no conflict of interest.

References

1. Holliday, R. A mechanism for gene conversion in fungi. *Genet. Res.* **1964**, *5*, 282–304. [CrossRef]
2. Liu, Y.; West, S.C. Happy Hollidays: 40th anniversary of the Holliday junction. *Nat. Rev. Mol. Cell Biol.* **2004**, *5*, 937–944. [CrossRef]
3. Wu, L.; Hickson, I.D. The Bloom's syndrome helicase suppresses crossing over during homologous recombination. *Nature* **2003**, *426*, 870–874. [CrossRef] [PubMed]
4. Wyatt, H.D.M.; West, S.C. Holliday junction resolvases. *Cold Spring Harb. Perspect. Biol.* **2014**, *6*, a023192. [CrossRef] [PubMed]
5. Rass, U. Resolving branched DNA intermediates with structure-specific nucleases during replication in eukaryotes. *Chromosoma* **2013**, *122*, 499–515. [CrossRef]
6. Rivera-Mulia, J.C.; Gilbert, D.M. Replicating large genomes: Divide and conquer. *Mol. Cell* **2016**, *62*, 756–765. [CrossRef]
7. Blow, J.J.; Ge, X.Q.; Jackson, D.A. How dormant origins promote complete genome replication. *Trends Biochem. Sci.* **2011**, *36*, 405–414. [CrossRef] [PubMed]
8. Fragkos, M.; Ganier, O.; Coulombe, P.; Méchali, M. DNA replication origin activation in space and time. *Nat. Rev. Mol. Cell Biol.* **2015**, *16*, 360–374. [CrossRef]
9. Newman, T.J.; Mamun, M.A.; Nieduszynski, C.A.; Blow, J.J. Replisome stall events have shaped the distribution of replication origins in the genomes of yeasts. *Nucleic Acids Res.* **2013**, *41*, 9705–9718. [CrossRef]
10. Kawabata, T.; Luebben, S.W.; Yamaguchi, S.; Ilves, I.; Matise, I.; Buske, T.; Botchan, M.R.; Shima, N. Stalled fork rescue via dormant replication origins in unchallenged S phase promotes proper chromosome segregation and tumor suppression. *Mol. Cell* **2011**, *41*, 543–553. [CrossRef]

11. Bellelli, R.; Borel, V.; Logan, C.; Svendsen, J.; Cox, D.E.; Nye, E.; Metcalfe, K.; O'Connell, S.M.; Stamp, G.; Flynn, H.R.; et al. Polε instability drives replication stress, abnormal development, and tumorigenesis. *Mol. Cell* **2018**, *70*, 707–721. [CrossRef] [PubMed]
12. Ge, X.Q.; Jackson, D.A.; Blow, J.J. Dormant origins licensed by excess Mcm2-7 are required for human cells to survive replicative stress. *Genes Dev.* **2007**, *21*, 3331–3341. [CrossRef]
13. Woodward, A.M.; Göhler, T.; Luciani, M.G.; Oehlmann, M.; Ge, X.; Gartner, A.; Jackson, D.A.; Blow, J.J. Excess Mcm2-7 license dormant origins of replication that can be used under conditions of replicative stress. *J. Cell Biol.* **2006**, *173*, 673–683. [CrossRef] [PubMed]
14. Ibarra, A.; Schwob, E.; Mendez, J. Excess MCM proteins protect human cells from replicative stress by licensing backup origins of replication. *Proc. Natl. Acad. Sci. USA* **2008**, *105*, 8956–8961. [CrossRef] [PubMed]
15. Kunnev, D.; Rusiniak, M.E.; Kudla, A.; Freeland, A.; Cady, G.K.; Pruitt, S.C. DNA damage response and tumorigenesis in Mcm2-deficient mice. *Oncogene* **2010**, *29*, 3630–3638. [CrossRef] [PubMed]
16. Maya-Mendoza, A.; Petermann, E.; Gillespie, D.A.F.; Caldecott, K.W.; Jackson, D.A. Chk1 regulates the density of active replication origins during the vertebrate S phase. *EMBO J.* **2007**, *26*, 2719–2731. [CrossRef]
17. Syljuåsen, R.G.; Sørensen, C.S.; Hansen, L.T.; Fugger, K.; Lundin, C.; Johansson, F.; Helleday, T.; Sehested, M.; Lukas, J.; Bartek, J. Inhibition of human Chk1 causes increased initiation of DNA replication, phosphorylation of ATR targets, and DNA breakage. *Mol. Cell. Biol.* **2005**, *25*, 3553–3562. [CrossRef]
18. Toledo, L.I.; Altmeyer, M.; Rask, M.-B.; Lukas, C.; Larsen, D.H.; Povlsen, L.K.; Bekker-Jensen, S.; Mailand, N.; Bartek, J.; Lukas, J. ATR prohibits replication catastrophe by preventing global exhaustion of RPA. *Cell* **2013**, *155*, 1088–1103. [CrossRef]
19. Christensen, P.U.; Bentley, N.J.; Martinho, R.G.; Nielsen, O.; Carr, A.M. Mik1 levels accumulate in S phase and may mediate an intrinsic link between S phase and mitosis. *Proc. Natl. Acad. Sci. USA* **2000**, *97*, 2579–2584. [CrossRef] [PubMed]
20. Lemmens, B.; Hegarat, N.; Akopyan, K.; Sala-Gaston, J.; Bartek, J.; Hochegger, H.; Lindqvist, A. DNA replication determines timing of mitosis by restricting CDK1 and PLK1 activation. *Mol. Cell* **2018**, *71*, 117–128. [CrossRef]
21. Sugimoto, K.; Shimomura, T.; Hashimoto, K.; Araki, H.; Sugino, A.; Matsumoto, K. Rfc5, a small subunit of replication factor C complex, couples DNA replication and mitosis in budding yeast. *Proc. Natl. Acad. Sci. USA* **1996**, *93*, 7048–7052. [CrossRef]
22. Hofmann, J.F.; Beach, D. Cdt1 is an essential target of the Cdc10/Sct1 transcription factor: Requirement for DNA replication and inhibition of mitosis. *EMBO J.* **1994**, *13*, 425–434. [CrossRef] [PubMed]
23. Piatti, S.; Lengauer, C.; Nasmyth, K. Cdc6 is an unstable protein whose de novo synthesis in G1 is important for the onset of S phase and for preventing a "reductional" anaphase in the budding yeast *Saccharomyces cerevisiae*. *EMBO J.* **1995**, *14*, 3788–3799. [CrossRef]
24. Bastos de Oliveira, F.M.; Kim, D.; Cussiol, J.R.; Das, J.; Jeong, M.C.; Doerfler, L.; Schmidt, K.H.; Yu, H.; Smolka, M.B. Phosphoproteomics reveals distinct modes of Mec1/ATR signaling during DNA replication. *Mol. Cell* **2015**, *57*, 1124–1132. [CrossRef]
25. Eykelenboom, J.K.; Harte, E.C.; Canavan, L.; Pastor-Peidro, A.; Calvo-Asensio, I.; Llorens-Agost, M.; Lowndes, N.F. ATR activates the S-M checkpoint during unperturbed growth to ensure sufficient replication prior to mitotic onset. *Cell Rep.* **2013**, *5*, 1095–1107. [CrossRef]
26. Saldivar, J.C.; Hamperl, S.; Bocek, M.J.; Chung, M.; Bass, T.E.; Cisneros-Soberanis, F.; Samejima, K.; Xie, L.; Paulson, J.R.; Earnshaw, W.C.; et al. An intrinsic S/G2 checkpoint enforced by ATR. *Science* **2018**, *361*, 806–810. [CrossRef]
27. Iyer, D.R.; Rhind, N. The intra-S checkpoint responses to DNA damage. *Genes* **2017**, *8*, 74. [CrossRef] [PubMed]
28. Saldivar, J.C.; Cortez, D.; Cimprich, K.A. The essential kinase ATR: Ensuring faithful duplication of a challenging genome. *Nat. Rev. Mol. Cell Biol.* **2017**, *18*, 622–636. [CrossRef]
29. Cha, R.S.; Kleckner, N. ATR homolog Mec1 promotes fork progression, thus averting breaks in replication slow zones. *Science* **2002**, *297*, 602–606. [CrossRef]
30. Casper, A.M.; Nghiem, P.; Arlt, M.F.; Glover, T.W. ATR regulates fragile site stability. *Cell* **2002**, *111*, 779–789. [CrossRef]

31. Barlow, J.H.; Faryabi, R.B.; Callén, E.; Wong, N.; Malhowski, A.; Chen, H.T.; Gutierrez-Cruz, G.; Sun, H.-W.; McKinnon, P.; Wright, G.; et al. Identification of early replicating fragile sites that contribute to genome instability. *Cell* **2013**, *152*, 620–632. [CrossRef]
32. Shastri, N.; Tsai, Y.-C.; Hile, S.; Jordan, D.; Powell, B.; Chen, J.; Maloney, D.; Dose, M.; Lo, Y.; Anastassiadis, T.; et al. Genome-wide identification of structure-forming repeats as principal sites of fork collapse upon ATR inhibition. *Mol. Cell* **2018**, *72*, 222–238. [CrossRef] [PubMed]
33. Tubbs, A.; Sridharan, S.; van Wietmarschen, N.; Maman, Y.; Callén, E.; Stanlie, A.; Wu, W.; Wu, X.; Day, A.; Wong, N.; et al. Dual roles of poly(dA:dT) tracts in replication initiation and fork collapse. *Cell* **2018**, *174*, 1127–1142. [CrossRef]
34. Tercero, J.A.; Longhese, M.P.; Diffley, J.F.X. A central role for DNA replication forks in checkpoint activation and response. *Mol. Cell* **2003**, *11*, 1323–1336. [CrossRef]
35. Tercero, J.A.; Diffley, J.F. Regulation of DNA replication fork progression through damaged DNA by the Mec1/Rad53 checkpoint. *Nature* **2001**, *412*, 553–557. [CrossRef] [PubMed]
36. Lopes, M.; Cotta-Ramusino, C.; Pellicioli, A.; Liberi, G.; Plevani, P.; Muzi-Falconi, M.; Newlon, C.S.; Foiani, M. The DNA replication checkpoint response stabilizes stalled replication forks. *Nature* **2001**, *412*, 557–561. [CrossRef]
37. Sogo, J.M.; Lopes, M.; Foiani, M. Fork reversal and ssDNA accumulation at stalled replication forks owing to checkpoint defects. *Science* **2002**, *297*, 599–602. [CrossRef]
38. Froget, B.; Blaisonneau, J.; Lambert, S.; Baldacci, G. Cleavage of stalled forks by fission yeast Mus81/Eme1 in absence of DNA replication checkpoint. *Mol. Biol. Cell* **2008**, *19*, 445–456. [CrossRef]
39. El-Shemerly, M.; Hess, D.; Pyakurel, A.K.; Moselhy, S.; Ferrari, S. ATR-dependent pathways control hEXO1 stability in response to stalled forks. *Nucleic Acids Res.* **2008**, *36*, 511–519. [CrossRef]
40. Neelsen, K.J.; Zanini, I.M.Y.; Herrador, R.; Lopes, M. Oncogenes induce genotoxic stress by mitotic processing of unusual replication intermediates. *J. Cell Biol.* **2013**, *200*, 699–708. [CrossRef] [PubMed]
41. Cotta-Ramusino, C.; Fachinetti, D.; Lucca, C.; Doksani, Y.; Lopes, M.; Sogo, J.; Foiani, M. Exo1 processes stalled replication forks and counteracts fork reversal in checkpoint-defective cells. *Mol. Cell* **2005**, *17*, 153–159. [CrossRef]
42. Segurado, M.; Diffley, J.F.X. Separate roles for the DNA damage checkpoint protein kinases in stabilizing DNA replication forks. *Genes Dev.* **2008**, *22*, 1816–1827. [CrossRef] [PubMed]
43. Couch, F.B.; Bansbach, C.E.; Driscoll, R.; Luzwick, J.W.; Glick, G.G.; Bétous, R.; Carroll, C.M.; Jung, S.Y.; Qin, J.; Cimprich, K.A.; et al. ATR phosphorylates SMARCAL1 to prevent replication fork collapse. *Genes Dev.* **2013**, *27*, 1610–1623. [CrossRef] [PubMed]
44. Seiler, J.A.; Conti, C.; Syed, A.; Aladjem, M.I.; Pommier, Y. The intra-S-phase checkpoint affects both DNA replication initiation and elongation: Single-cell and -DNA fiber analyses. *Mol. Cell. Biol.* **2007**, *27*, 5806–5818. [CrossRef]
45. Santocanale, C.; Diffley, J.F. A Mec1- and Rad53-dependent checkpoint controls late-firing origins of DNA replication. *Nature* **1998**, *395*, 615–618. [CrossRef] [PubMed]
46. Shirahige, K.; Hori, Y.; Shiraishi, K.; Yamashita, M.; Takahashi, K.; Obuse, C.; Tsurimoto, T.; Yoshikawa, H. Regulation of DNA-replication origins during cell-cycle progression. *Nature* **1998**, *395*, 618–621. [CrossRef]
47. Dimitrova, D.S.; Gilbert, D.M. Temporally coordinated assembly and disassembly of replication factories in the absence of DNA synthesis. *Nat. Cell Biol.* **2000**, *2*, 686–694. [CrossRef] [PubMed]
48. Yekezare, M.; Gómez-González, B.; Diffley, J.F.X. Controlling DNA replication origins in response to DNA damage—inhibit globally, activate locally. *J. Cell. Sci.* **2013**, *126*, 1297–1306. [CrossRef] [PubMed]
49. Lundgren, K.; Walworth, N.; Booher, R.; Dembski, M.; Kirschner, M.; Beach, D. mik1 and wee1 cooperate in the inhibitory tyrosine phosphorylation of cdc2. *Cell* **1991**, *64*, 1111–1122. [CrossRef]
50. Boddy, M.N.; Furnari, B.; Mondesert, O.; Russell, P. Replication checkpoint enforced by kinases Cds1 and Chk1. *Science* **1998**, *280*, 909–912. [CrossRef]
51. Zeng, Y.; Forbes, K.C.; Wu, Z.; Moreno, S.; Piwnica-Worms, H.; Enoch, T. Replication checkpoint requires phosphorylation of the phosphatase Cdc25 by Cds1 or Chk1. *Nature* **1998**, *395*, 507–510. [CrossRef] [PubMed]
52. Furnari, B.; Rhind, N.; Russell, P. Cdc25 mitotic inducer targeted by chk1 DNA damage checkpoint kinase. *Science* **1997**, *277*, 1495–1497. [CrossRef]

53. Sanchez, Y.; Wong, C.; Thoma, R.S.; Richman, R.; Wu, Z.; Piwnica-Worms, H.; Elledge, S.J. Conservation of the Chk1 checkpoint pathway in mammals: linkage of DNA damage to Cdk regulation through Cdc25. *Science* **1997**, *277*, 1497–1501. [CrossRef]
54. Palou, G.; Palou, R.; Zeng, F.; Vashisht, A.A.; Wohlschlegel, J.A.; Quintana, D.G. Three different pathways prevent chromosome segregation in the presence of DNA damage or replication stress in budding yeast. *PLoS Genet.* **2015**, *11*, e1005468. [CrossRef] [PubMed]
55. Al Mamun, M.; Albergante, L.; Moreno, A.; Carrington, J.T.; Blow, J.J.; Newman, T.J. Inevitability and containment of replication errors for eukaryotic genome lengths spanning megabase to gigabase. *Proc. Natl. Acad. Sci. USA* **2016**, *113*, E5765–E5774. [CrossRef]
56. Moreno, A.; Carrington, J.T.; Albergante, L.; Al Mamun, M.; Haagensen, E.J.; Komseli, E.-S.; Gorgoulis, V.G.; Newman, T.J.; Blow, J.J. Unreplicated DNA remaining from unperturbed S phases passes through mitosis for resolution in daughter cells. *Proc. Natl. Acad. Sci. USA* **2016**, *113*, E5757–E5764. [CrossRef] [PubMed]
57. Torres-Rosell, J.; De Piccoli, G.; Cordón-Preciado, V.; Farmer, S.; Jarmuz, A.; Machín, F.; Pasero, P.; Lisby, M.; Haber, J.E.; Aragón, L. Anaphase onset before complete DNA replication with intact checkpoint responses. *Science* **2007**, *315*, 1411–1415. [CrossRef] [PubMed]
58. Baumann, C.; Körner, R.; Hofmann, K.; Nigg, E.A. PICH, a centromere-associated SNF2 family ATPase, is regulated by Plk1 and required for the spindle checkpoint. *Cell* **2007**, *128*, 101–114. [CrossRef] [PubMed]
59. Chan, K.-L.; North, P.S.; Hickson, I.D. BLM is required for faithful chromosome segregation and its localization defines a class of ultrafine anaphase bridges. *EMBO J.* **2007**, *26*, 3397–3409. [CrossRef] [PubMed]
60. Naim, V.; Rosselli, F. The FANC pathway and BLM collaborate during mitosis to prevent micro-nucleation and chromosome abnormalities. *Nat. Cell Biol.* **2009**, *11*, 761–768. [CrossRef]
61. Fernández-Casañas, M.; Chan, K.-L. The Unresolved Problem of DNA Bridging. *Genes* **2018**, *9*, 623. [CrossRef]
62. Glover, T.W.; Wilson, T.E.; Arlt, M.F. Fragile sites in cancer: more than meets the eye. *Nat. Rev. Cancer* **2017**, *17*, 489–501. [CrossRef] [PubMed]
63. Glover, T.W.; Berger, C.; Coyle, J.; Echo, B. DNA polymerase α inhibition by aphidicolin induces gaps and breaks at common fragile sites in human chromosomes. *Hum. Genet.* **1984**, *67*, 136–142. [CrossRef]
64. Durkin, S.G.; Ragland, R.L.; Arlt, M.F.; Mulle, J.G.; Warren, S.T.; Glover, T.W. Replication stress induces tumor-like microdeletions in FHIT/FRA3B. *Proc. Natl. Acad. Sci. USA* **2008**, *105*, 246–251. [CrossRef] [PubMed]
65. Arlt, M.F.; Mulle, J.G.; Schaibley, V.M.; Ragland, R.L.; Durkin, S.G.; Warren, S.T.; Glover, T.W. Replication stress induces genome-wide copy number changes in human cells that resemble polymorphic and pathogenic variants. *Am. J. Hum. Genet.* **2009**, *84*, 339–350. [CrossRef] [PubMed]
66. Le Beau, M.M.; Rassool, F.V.; Neilly, M.E.; Espinosa, R.; Glover, T.W.; Smith, D.I.; McKeithan, T.W. Replication of a common fragile site, FRA3B, occurs late in S phase and is delayed further upon induction: implications for the mechanism of fragile site induction. *Hum. Mol. Genet.* **1998**, *7*, 755–761. [CrossRef] [PubMed]
67. Wilson, T.E.; Arlt, M.F.; Park, S.H.; Rajendran, S.; Paulsen, M.; Ljungman, M.; Glover, T.W. Large transcription units unify copy number variants and common fragile sites arising under replication stress. *Genome Res.* **2015**, *25*, 189–200. [CrossRef]
68. Le Tallec, B.; Millot, G.A.; Blin, M.E.; Brison, O.; Dutrillaux, B.; Debatisse, M. Common fragile site profiling in epithelial and erythroid cells reveals that most recurrent cancer deletions lie in fragile sites hosting large genes. *Cell Rep.* **2013**, *4*, 420–428. [CrossRef]
69. West, S.C. Processing of recombination intermediates by the RuvABC proteins. *Annu. Rev. Genet.* **1997**, *31*, 213–244. [CrossRef]
70. Kim, S.M.; Forsburg, S.L. Regulation of structure-specific endonucleases in replication stress. *Genes* **2018**, *9*, 634. [CrossRef]
71. Lee, S.-H.; Princz, L.N.; Klügel, M.F.; Habermann, B.; Pfander, B.; Biertümpfel, C. Human Holliday junction resolvase GEN1 uses a chromodomain for efficient DNA recognition and cleavage. *eLife* **2015**, *4*, 213. [CrossRef] [PubMed]
72. Guervilly, J.-H.; Takedachi, A.; Naim, V.; Scaglione, S.; Chawhan, C.; Lovera, Y.; Despras, E.; Kuraoka, I.; Kannouche, P.; Rosselli, F.; et al. The SLX4 complex is a SUMO E3 ligase that impacts on replication stress outcome and genome stability. *Mol. Cell* **2015**, *57*, 123–137. [CrossRef]

73. Mullen, J.R.; Kaliraman, V.; Ibrahim, S.S.; Brill, S.J. Requirement for three novel protein complexes in the absence of the Sgs1 DNA helicase in *Saccharomyces cerevisiae*. *Genetics* **2001**, *157*, 103–118. [PubMed]
74. Fabre, F.; Chan, A.; Heyer, W.-D.; Gangloff, S. Alternate pathways involving Sgs1/Top3, Mus81/ Mms4, and Srs2 prevent formation of toxic recombination intermediates from single-stranded gaps created by DNA replication. *Proc. Natl. Acad. Sci. USA* **2002**, *99*, 16887–16892. [CrossRef] [PubMed]
75. Newman, M.; Murray-Rust, J.; Lally, J.; Rudolf, J.; Fadden, A.; Knowles, P.P.; White, M.F.; McDonald, N.Q. Structure of an XPF endonuclease with and without DNA suggests a model for substrate recognition. *EMBO J.* **2005**, *24*, 895–905. [CrossRef]
76. Nishino, T.; Komori, K.; Ishino, Y.; Morikawa, K. Structural and functional analyses of an archaeal XPF/Rad1/Mus81 nuclease: asymmetric DNA binding and cleavage mechanisms. *Structure* **2005**, *13*, 1183–1192. [CrossRef] [PubMed]
77. Ciccia, A.; Constantinou, A.; West, S.C. Identification and characterization of the human mus81-eme1 endonuclease. *J. Biol. Chem.* **2003**, *278*, 25172–25178. [CrossRef] [PubMed]
78. Ciccia, A.; Ling, C.; Coulthard, R.; Yan, Z.; Xue, Y.; Meetei, A.R.; Laghmani, E.H.; Joenje, H.; McDonald, N.; de Winter, J.P.; et al. Identification of FAAP24, a Fanconi anemia core complex protein that interacts with FANCM. *Mol. Cell* **2007**, *25*, 331–343. [CrossRef] [PubMed]
79. Boddy, M.N.; Gaillard, P.H.; McDonald, W.H.; Shanahan, P.; Yates, J.R.; Russell, P. Mus81-Eme1 are essential components of a Holliday junction resolvase. *Cell* **2001**, *107*, 537–548. [CrossRef]
80. Kaliraman, V.; Mullen, J.R.; Fricke, W.M.; Bastin-Shanower, S.A.; Brill, S.J. Functional overlap between Sgs1-Top3 and the Mms4-Mus81 endonuclease. *Genes Dev.* **2001**, *15*, 2730–2740. [CrossRef]
81. Chen, X.B.; Melchionna, R.; Denis, C.M.; Gaillard, P.H.; Blasina, A.; Van de Weyer, I.; Boddy, M.N.; Russell, P.; Vialard, J.; McGowan, C.H. Human Mus81-associated endonuclease cleaves Holliday junctions in vitro. *Mol. Cell* **2001**, *8*, 1117–1127. [CrossRef]
82. Oğrünç, M.; Sancar, A. Identification and characterization of human MUS81-MMS4 structure-specific endonuclease. *J. Biol. Chem.* **2003**, *278*, 21715–21720. [CrossRef] [PubMed]
83. Fricke, W.M.; Bastin-Shanower, S.A.; Brill, S.J. Substrate specificity of the *Saccharomyces cerevisiae* Mus81-Mms4 endonuclease. *DNA Repair* **2005**, *4*, 243–251. [CrossRef] [PubMed]
84. Ehmsen, K.T.; Heyer, W.-D. A junction branch point adjacent to a DNA backbone nick directs substrate cleavage by *Saccharomyces cerevisiae* Mus81-Mms4. *Nucleic Acids Res.* **2009**, *37*, 2026–2036. [CrossRef] [PubMed]
85. Amangyeld, T.; Shin, Y.-K.; Lee, M.; Kwon, B.; Seo, Y.-S. Human MUS81-EME2 can cleave a variety of DNA structures including intact Holliday junction and nicked duplex. *Nucleic Acids Res.* **2014**, *42*, 5846–5862. [CrossRef]
86. Pepe, A.; West, S.C. Substrate specificity of the MUS81-EME2 structure selective endonuclease. *Nucleic Acids Res.* **2014**, *42*, 3833–3845. [CrossRef]
87. Pepe, A.; West, S.C. MUS81-EME2 promotes replication fork restart. *Cell Rep.* **2014**, *7*, 1048–1055. [CrossRef] [PubMed]
88. Matos, J.; Blanco, M.G.; Maslen, S.; Skehel, J.M.; West, S.C. Regulatory control of the resolution of DNA recombination intermediates during meiosis and mitosis. *Cell* **2011**, *147*, 158–172. [CrossRef] [PubMed]
89. Dehé, P.-M.; Coulon, S.; Scaglione, S.; Shanahan, P.; Takedachi, A.; Wohlschlegel, J.A.; Yates, J.R.; Llorente, B.; Russell, P.; Gaillard, P.-H.L. Regulation of Mus81-Eme1 Holliday junction resolvase in response to DNA damage. *Nat. Struct. Mol. Biol.* **2013**, *20*, 598–603. [CrossRef]
90. Gallo-Fernández, M.; Saugar, I.; Ortiz-Bazán, M.Á.; Vázquez, M.V.; Tercero, J.A. Cell cycle-dependent regulation of the nuclease activity of Mus81–Eme1/Mms4. *Nucleic Acids Res.* **2012**, *40*, 8325–8335. [CrossRef] [PubMed]
91. Princz, L.N.; Wild, P.; Bittmann, J.; Aguado, F.J.; Blanco, M.G.; Matos, J.; Pfander, B. Dbf4-dependent kinase and the Rtt107 scaffold promote Mus81-Mms4 resolvase activation during mitosis. *EMBO J.* **2017**, *36*, 664–678. [CrossRef] [PubMed]
92. Matos, J.; Blanco, M.G.; West, S.C. Cell-cycle kinases coordinate the resolution of recombination intermediates with chromosome segregation. *Cell Rep.* **2013**, *4*, 76–86. [CrossRef] [PubMed]
93. Szakal, B.; Branzei, D. Premature Cdk1/Cdc5/Mus81 pathway activation induces aberrant replication and deleterious crossover. *EMBO J.* **2013**, *32*, 1155–1167. [CrossRef] [PubMed]

94. Sebesta, M.; Urulangodi, M.; Stefanovie, B.; Szakal, B.; Pacesa, M.; Lisby, M.; Branzei, D.; Krejci, L. Esc2 promotes Mus81 complex-activity via its SUMO-like and DNA binding domains. *Nucleic Acids Res.* **2017**, *45*, 215–230. [CrossRef] [PubMed]
95. Sisakova, A.; Altmannova, V.; Sebesta, M.; Krejci, L. Role of PCNA and RFC in promoting Mus81-complex activity. *BMC Biol.* **2017**, *15*, 90. [CrossRef] [PubMed]
96. Wyatt, H.D.M.; Sarbajna, S.; Matos, J.; West, S.C. Coordinated actions of SLX1-SLX4 and MUS81-EME1 for Holliday Junction resolution in human Cells. *Mol. Cell* **2013**, *52*, 234–247. [CrossRef]
97. Duda, H.; Arter, M.; Gloggnitzer, J.; Teloni, F.; Wild, P.; Blanco, M.G.; Altmeyer, M.; Matos, J. A Mechanism for controlled breakage of under-replicated chromosomes during mitosis. *Dev. Cell* **2016**, *39*, 740–755. [CrossRef]
98. Fekairi, S.; Scaglione, S.; Chahwan, C.; Taylor, E.R.; Tissier, A.; Coulon, S.; Dong, M.-Q.; Ruse, C.; Yates, J.R.; Russell, P.; et al. Human SLX4 is a Holliday junction resolvase subunit that binds multiple DNA repair/recombination endonucleases. *Cell* **2009**, *138*, 78–89. [CrossRef] [PubMed]
99. Muñoz, I.M.; Hain, K.; Déclais, A.-C.; Gardiner, M.; Toh, G.W.; Sanchez-Pulido, L.; Heuckmann, J.M.; Toth, R.; Macartney, T.; Eppink, B.; et al. Coordination of structure-specific nucleases by human SLX4/BTBD12 is required for DNA repair. *Mol. Cell* **2009**, *35*, 116–127. [CrossRef]
100. Svendsen, J.M.; Smogorzewska, A.; Sowa, M.E.; O'Connell, B.C.; Gygi, S.P.; Elledge, S.J.; Harper, J.W. Mammalian BTBD12/SLX4 assembles a Holliday junction resolvase and is required for DNA repair. *Cell* **2009**, *138*, 63–77. [CrossRef]
101. Wyatt, H.D.M.; Laister, R.C.; Martin, S.R.; Arrowsmith, C.H.; West, S.C. The SMX DNA repair Tri-nuclease. *Mol. Cell* **2017**, *65*, 848–860. [CrossRef] [PubMed]
102. Yin, J.; Wan, B.; Sarkar, J.; Horvath, K.; Wu, J.; Chen, Y.; Cheng, G.; Wan, K.; Chin, P.; Lei, M.; et al. Dimerization of SLX4 contributes to functioning of the SLX4-nuclease complex. *Nucleic Acids Res.* **2016**, *44*, 4871–4880. [CrossRef]
103. Coulon, S.; Gaillard, P.-H.L.; Chahwan, C.; McDonald, W.H.; Yates, J.R.; Russell, P. Slx1-Slx4 are subunits of a structure-specific endonuclease that maintains ribosomal DNA in fission yeast. *Mol. Biol. Cell* **2004**, *15*, 71–80. [CrossRef]
104. Fricke, W.M.; Brill, S.J. Slx1-Slx4 is a second structure-specific endonuclease functionally redundant with Sgs1-Top3. *Genes Dev.* **2003**, *17*, 1768–1778. [CrossRef]
105. Kaliraman, V.; Brill, S.J. Role of SGS1 and SLX4 in maintaining rDNA structure in *Saccharomyces cerevisiae*. *Curr. Genet.* **2002**, *41*, 389–400. [CrossRef]
106. Coulon, S.; Noguchi, E.; Noguchi, C.; Du, L.-L.; Nakamura, T.M.; Russell, P. Rad22Rad52-dependent repair of ribosomal DNA repeats cleaved by Slx1-Slx4 endonuclease. *Mol. Biol. Cell* **2006**, *17*, 2081–2090. [CrossRef] [PubMed]
107. Sarbajna, S.; Davies, D.; West, S.C. Roles of SLX1-SLX4, MUS81-EME1, and GEN1 in avoiding genome instability and mitotic catastrophe. *Genes Dev.* **2014**, *28*, 1124–1136. [CrossRef]
108. Garner, E.; Kim, Y.; Lach, F.P.; Kottemann, M.C.; Smogorzewska, A. Human GEN1 and the SLX4-associated nucleases MUS81 and SLX1 are essential for the resolution of replication-induced Holliday junctions. *Cell Rep.* **2013**, *5*, 207–215. [CrossRef]
109. Guervilly, J.-H.; Gaillard, P.H. SLX4: Multitasking to maintain genome stability. *Crit. Rev. Biochem. Mol. Biol.* **2018**, *53*, 475–514. [CrossRef] [PubMed]
110. Kim, Y.; Lach, F.P.; Desetty, R.; Hanenberg, H.; Auerbach, A.D.; Smogorzewska, A. Mutations of the SLX4 gene in Fanconi anemia. *Nat. Genet.* **2011**, *43*, 142–146. [CrossRef]
111. Stoepker, C.; Hain, K.; Schuster, B.; Hilhorst-Hofstee, Y.; Rooimans, M.A.; Steltenpool, J.; Oostra, A.B.; Eirich, K.; Korthof, E.T.; Nieuwint, A.W.M.; et al. SLX4, a coordinator of structure-specific endonucleases, is mutated in a new Fanconi anemia subtype. *Nat. Genet.* **2011**, *43*, 138–141. [CrossRef] [PubMed]
112. Gaur, V.; Wyatt, H.D.M.; Komorowska, W.; Szczepanowski, R.H.; de Sanctis, D.; Gorecka, K.M.; West, S.C.; Nowotny, M. Structural and mechanistic analysis of the Slx1-Slx4 endonuclease. *Cell Rep.* **2015**, *10*, 1467–1476. [CrossRef]
113. Castor, D.; Nair, N.; Déclais, A.-C.; Lachaud, C.; Toth, R.; Macartney, T.J.; Lilley, D.M.J.; Arthur, J.S.C.; Rouse, J. Cooperative control of holliday junction resolution and DNA repair by the SLX1 and MUS81-EME1 nucleases. *Mol. Cell* **2013**, *52*, 221–233. [CrossRef] [PubMed]

114. Gwon, G.H.; Jo, A.; Baek, K.; Jin, K.S.; Fu, Y.; Lee, J.-B.; Kim, Y.; Cho, Y. Crystal structures of the structure-selective nuclease Mus81-Eme1 bound to flap DNA substrates. *EMBO J.* **2014**, *33*, 1061–1072. [CrossRef] [PubMed]
115. Palma, A.; Pugliese, G.M.; Murfuni, I.; Marabitti, V.; Malacaria, E.; Rinalducci, S.; Minoprio, A.; Sanchez, M.; Mazzei, F.; Zolla, L.; et al. Phosphorylation by CK2 regulates MUS81/EME1 in mitosis and after replication stress. *Nucleic Acids Res.* **2018**, *46*, 5109–5124. [CrossRef]
116. Saugar, I.; Jiménez-Martín, A.; Tercero, J.A. Subnuclear relocalization of structure-specific endonucleases in response to DNA damage. *Cell Rep.* **2017**, *20*, 1553–1562. [CrossRef]
117. Schwartz, E.K.; Wright, W.D.; Ehmsen, K.T.; Evans, J.E.; Stahlberg, H.; Heyer, W.-D. Mus81-Mms4 functions as a single heterodimer to cleave nicked intermediates in recombinational DNA repair. *Mol. Cell. Biol.* **2012**, *32*, 3065–3080. [CrossRef] [PubMed]
118. Ohouo, P.Y.; Bastos de Oliveira, F.M.; Almeida, B.S.; Smolka, M.B. DNA damage signaling recruits the Rtt107-Slx4 scaffolds via Dpb11 to mediate replication stress response. *Mol. Cell* **2010**, *39*, 300–306. [CrossRef]
119. Gritenaite, D.; Princz, L.N.; Szakal, B.; Bantele, S.C.S.; Wendeler, L.; Schilbach, S.; Habermann, B.H.; Matos, J.; Lisby, M.; Branzei, D.; et al. A cell cycle-regulated Slx4-Dpb11 complex promotes the resolution of DNA repair intermediates linked to stalled replication. *Genes Dev.* **2014**, *28*, 1604–1619. [CrossRef] [PubMed]
120. Princz, L.N.; Gritenaite, D.; Pfander, B. The Slx4-Dpb11 scaffold complex: coordinating the response to replication fork stalling in S-phase and the subsequent mitosis. *Cell Cycle* **2014**, *14*, 488–494. [CrossRef]
121. Ip, S.C.Y.; Rass, U.; Blanco, M.G.; Flynn, H.R.; Skehel, J.M.; West, S.C. Identification of Holliday junction resolvases from humans and yeast. *Nature* **2008**, *456*, 357–361. [CrossRef]
122. West, S.C. The search for a human Holliday junction resolvase. *Biochem. Soc. Trans.* **2009**, *37*, 519–526. [CrossRef]
123. Lieber, M.R. The FEN-1 family of structure-specific nucleases in eukaryotic DNA replication, recombination and repair. *Bioessays* **1997**, *19*, 233–240. [CrossRef]
124. Bailly, A.P.; Freeman, A.; Hall, J.; Déclais, A.-C.; Alpi, A.; Lilley, D.M.J.; Ahmed, S.; Gartner, A. The *Caenorhabditis elegans* homolog of Gen1/Yen1 resolvases links DNA damage signaling to DNA double-strand break repair. *PLoS Genet.* **2010**, *6*, e1001025. [CrossRef]
125. Yang, Y.; Ishino, S.; Yamagami, T.; Kumamaru, T.; Satoh, H.; Ishino, Y. The OsGEN-L protein from *Oryza sativa* possesses Holliday junction resolvase activity as well as 5′-flap endonuclease activity. *J. Biochem.* **2012**, *151*, 317–327. [CrossRef]
126. Bauknecht, M.; Kobbe, D. AtGEN1 and AtSEND1, two paralogs in Arabidopsis, possess Holliday junction resolvase activity. *Plant Physiol.* **2014**, *166*, 202–216. [CrossRef] [PubMed]
127. Andersen, S.L.; Kuo, H.K.; Savukoski, D.; Brodsky, M.H.; Sekelsky, J. Three structure-selective endonucleases are essential in the absence of BLM helicase in Drosophila. *PLoS Genet.* **2011**, *7*, e1002315. [CrossRef]
128. Lorenz, A.; West, S.C.; Whitby, M.C. The human Holliday junction resolvase GEN1 rescues the meiotic phenotype of a *Schizosaccharomyces pombe* mus81 mutant. *Nucleic Acids Res.* **2010**, *38*, 1866–1873. [CrossRef]
129. Freeman, A.D.J.; Liu, Y.; Déclais, A.-C.; Gartner, A.; Lilley, D.M.J. GEN1 from a thermophilic fungus is functionally closely similar to non-eukaryotic junction-resolving enzymes. *J. Mol. Biol.* **2014**, *426*, 3946–3959. [CrossRef] [PubMed]
130. Shah Punatar, R.; Martin, M.J.; Wyatt, H.D.M.; Chan, Y.W.; West, S.C. Resolution of single and double Holliday junction recombination intermediates by GEN1. *Proc. Natl. Acad. Sci. USA* **2017**, *114*, 443–450. [CrossRef] [PubMed]
131. Rass, U.; Compton, S.A.; Matos, J.; Singleton, M.R.; Ip, S.C.Y.; Blanco, M.G.; Griffith, J.D.; West, S.C. Mechanism of Holliday junction resolution by the human GEN1 protein. *Genes Dev.* **2010**, *24*, 1559–1569. [CrossRef] [PubMed]
132. Chan, Y.W.; West, S. GEN1 promotes Holliday junction resolution by a coordinated nick and counter-nick mechanism. *Nucleic Acids Res.* **2015**, *43*, 10882–10892. [CrossRef] [PubMed]
133. Liu, Y.; Freeman, A.D.J.; Déclais, A.-C.; Wilson, T.J.; Gartner, A.; Lilley, D.M.J. Crystal structure of a eukaryotic GEN1 resolving enzyme bound to DNA. *Cell Rep.* **2015**, *13*, 2565–2575. [CrossRef] [PubMed]
134. Sobhy, M.A.; Bralic, A.; Raducanu, V.-S.; Takahashi, M.; Tehseen, M.; Rashid, F.; Zaher, M.S.; Hamdan, S.M. Resolution of the Holliday junction recombination intermediate by human GEN1 at the single-molecule level. *Nucleic Acids Res.* **2018**, *5*, 282. [CrossRef] [PubMed]
135. Blanco, M.G.; Matos, J.; West, S.C. Dual control of Yen1 nuclease activity and cellular localization by Cdk and Cdc14 prevents genome instability. *Mol. Cell* **2014**, *54*, 94–106. [CrossRef]

136. García-Luis, J.; Clemente-Blanco, A.; Aragón, L.; Machín, F. Cdc14 targets the Holliday junction resolvase Yen1 to the nucleus in early anaphase. *Cell Cycle* **2014**, *13*, 1392–1399. [CrossRef] [PubMed]
137. Kosugi, S.; Hasebe, M.; Tomita, M.; Yanagawa, H. Systematic identification of cell cycle-dependent yeast nucleocytoplasmic shuttling proteins by prediction of composite motifs. *Proc. Natl. Acad. Sci. USA* **2009**, *106*, 10171–10176. [CrossRef] [PubMed]
138. Talhaoui, I.; Bernal, M.; Mullen, J.R.; Dorison, H.; Palancade, B.; Brill, S.J.; Mazón, G. Slx5-Slx8 ubiquitin ligase targets active pools of the Yen1 nuclease to limit crossover formation. *Nat. Commun.* **2018**, *9*, 5016. [CrossRef]
139. Chan, Y.W.; West, S.C. Spatial control of the GEN1 Holliday junction resolvase ensures genome stability. *Nat. Commun.* **2014**, *5*, 4844. [CrossRef] [PubMed]
140. Ait Saada, A.; Lambert, S.A.E.; Carr, A.M. Preserving replication fork integrity and competence via the homologous recombination pathway. *DNA Repair* **2018**, *71*, 135–147. [CrossRef] [PubMed]
141. Branzei, D.; Szakal, B. DNA damage tolerance by recombination: Molecular pathways and DNA structures. *DNA Repair* **2016**, *44*, 68–75. [CrossRef] [PubMed]
142. Agmon, N.; Yovel, M.; Harari, Y.; Liefshitz, B.; Kupiec, M. The role of Holliday junction resolvases in the repair of spontaneous and induced DNA damage. *Nucleic Acids Res.* **2011**, *39*, 7009–7019. [CrossRef] [PubMed]
143. Blanco, M.G.; Matos, J.; Rass, U.; Ip, S.C.Y.; West, S.C. Functional overlap between the structure-specific nucleases Yen1 and Mus81-Mms4 for DNA-damage repair in *S. cerevisiae*. *DNA Repair* **2010**, *9*, 394–402. [CrossRef]
144. Ho, C.K.; Mazón, G.; Lam, A.F.; Symington, L.S. Mus81 and Yen1 promote reciprocal exchange during mitotic recombination to maintain genome integrity in budding yeast. *Mol. Cell* **2010**, *40*, 988–1000. [CrossRef]
145. Tay, Y.D.; Wu, L. Overlapping roles for Yen1 and Mus81 in cellular Holliday junction processing. *J. Biol. Chem.* **2010**, *285*, 11427–11432. [CrossRef] [PubMed]
146. Boddy, M.N.; Lopez-Girona, A.; Shanahan, P.; Interthal, H.; Heyer, W.D.; Russell, P. Damage tolerance protein Mus81 associates with the FHA1 domain of checkpoint kinase Cds1. *Mol. Cell. Biol.* **2000**, *20*, 8758–8766. [CrossRef]
147. García-Luis, J.; Machín, F. Mus81-Mms4 and Yen1 resolve a novel anaphase bridge formed by noncanonical Holliday junctions. *Nat. Commun.* **2014**, *5*, 5652. [CrossRef]
148. Ying, S.; Minocherhomji, S.; Chan, K.-L.; Palmai-Pallag, T.; Chu, W.K.; Wass, T.; Mankouri, H.W.; Liu, Y.; Hickson, I.D. MUS81 promotes common fragile site expression. *Nat. Cell Biol.* **2013**, *15*, 1001–1007. [CrossRef] [PubMed]
149. Naim, V.; Wilhelm, T.; Debatisse, M.; Rosselli, F. ERCC1 and MUS81-EME1 promote sister chromatid separation by processing late replication intermediates at common fragile sites during mitosis. *Nat. Cell Biol.* **2013**, *15*, 1008–1015. [CrossRef]
150. Chan, Y.W.; Fugger, K.; West, S.C. Unresolved recombination intermediates lead to ultra-fine anaphase bridges, chromosome breaks and aberrations. *Nat. Cell Biol.* **2018**, *20*, 92–103. [CrossRef] [PubMed]
151. Eissler, C.L.; Mazón, G.; Powers, B.L.; Savinov, S.N.; Symington, L.S.; Hall, M.C. The Cdk/cDc14 module controls activation of the Yen1 Holliday junction resolvase to promote genome stability. *Mol. Cell* **2014**, *54*, 80–93. [CrossRef]
152. Bizard, A.H.; Hickson, I.D. The dissolution of double Holliday junctions. *Cold Spring Harb. Perspect. Biol.* **2014**, *6*, a016477. [CrossRef] [PubMed]
153. Técher, H.; Koundrioukoff, S.; Carignon, S.; Wilhelm, T.; Millot, G.A.; Lopez, B.S.; Brison, O.; Debatisse, M. Signaling from Mus81-Eme2-dependent DNA damage elicited by Chk1 deficiency modulates replication fork speed and origin usage. *Cell Rep.* **2016**, *14*, 1114–1127. [CrossRef] [PubMed]
154. Forment, J.V.; Blasius, M.; Guerini, I.; Jackson, S.P. Structure-specific DNA endonuclease Mus81/Eme1 generates DNA damage caused by Chk1 inactivation. *PLoS ONE* **2011**, *6*, e23517. [CrossRef] [PubMed]
155. Szmyd, R.; Niska-Blakie, J.; Diril, M.K.; Renck Nunes, P.; Tzelepis, K.; Lacroix, A.; van Hul, N.; Deng, L.-W.; Matos, J.; Dreesen, O.; et al. Premature activation of Cdk1 leads to mitotic events in S phase and embryonic lethality. *Oncogene* **2018**, *448*, 811. [CrossRef] [PubMed]
156. Beck, H.; Nähse, V.; Larsen, M.S.Y.; Groth, P.; Clancy, T.; Lees, M.; Jørgensen, M.; Helleday, T.; Syljuåsen, R.G.; Sørensen, C.S. Regulators of cyclin-dependent kinases are crucial for maintaining genome integrity in S phase. *J. Cell Biol.* **2010**, *188*, 629–638. [CrossRef]

157. Beck, H.; Nähse-Kumpf, V.; Larsen, M.S.Y.; O'Hanlon, K.A.; Patzke, S.; Holmberg, C.; Mejlvang, J.; Groth, A.; Nielsen, O.; Syljuåsen, R.G.; et al. Cyclin-dependent kinase suppression by WEE1 kinase protects the genome through control of replication initiation and nucleotide consumption. *Mol. Cell. Biol.* **2012**, *32*, 4226–4236. [CrossRef]
158. Domínguez-Kelly, R.; Martín, Y.; Koundrioukoff, S.; Tanenbaum, M.E.; Smits, V.A.J.; Medema, R.H.; Debatisse, M.; Freire, R. Wee1 controls genomic stability during replication by regulating the Mus81-Eme1 endonuclease. *J. Cell Biol.* **2011**, *194*, 567–579. [CrossRef]
159. Hanada, K.; Budzowska, M.; Davies, S.L.; van Drunen, E.; Onizawa, H.; Beverloo, H.B.; Maas, A.; Essers, J.; Hickson, I.D.; Kanaar, R. The structure-specific endonuclease Mus81 contributes to replication restart by generating double-strand DNA breaks. *Nat. Struct. Mol. Biol.* **2007**, *14*, 1096–1104. [CrossRef]
160. Hanada, K.; Budzowska, M.; Modesti, M.; Maas, A.; Wyman, C.; Essers, J.; Kanaar, R. The structure-specific endonuclease Mus81-Eme1 promotes conversion of interstrand DNA crosslinks into double-strands breaks. *EMBO J.* **2006**, *25*, 4921–4932. [CrossRef]
161. Kramara, J.; Osia, B.; Malkova, A. Break-induced replication: The where, the why, and the how. *Trends Genet.* **2018**, *34*, 518–531. [CrossRef]
162. Xu, Y.; Ning, S.; Wei, Z.; Xu, R.; Xu, X.; Xing, M.; Guo, R.; Xu, D. 53BP1 and BRCA1 control pathway choice for stalled replication restart. *eLlife* **2017**, *6*, 35897. [CrossRef]
163. Shimura, T.; Torres, M.J.; Martin, M.M.; Rao, V.A.; Pommier, Y.; Katsura, M.; Miyagawa, K.; Aladjem, M.I. Bloom's syndrome helicase and Mus81 are required to induce transient double-strand DNA breaks in response to DNA replication stress. *J. Mol. Biol.* **2008**, *375*, 1152–1164. [CrossRef] [PubMed]
164. Regairaz, M.; Zhang, Y.-W.; Fu, H.; Agama, K.K.; Tata, N.; Agrawal, S.; Aladjem, M.I.; Pommier, Y. Mus81-mediated DNA cleavage resolves replication forks stalled by topoisomerase I-DNA complexes. *J. Cell Biol.* **2011**, *195*, 739–749. [CrossRef] [PubMed]
165. Murfuni, I.; Nicolai, S.; Baldari, S.; Crescenzi, M.; Bignami, M.; Franchitto, A.; Pichierri, P. The WRN and MUS81 proteins limit cell death and genome instability following oncogene activation. *Oncogene* **2013**, *32*, 610–620. [CrossRef] [PubMed]
166. Shimura, T.; Ochiai, Y.; Noma, N.; Oikawa, T.; Sano, Y.; Fukumoto, M. Cyclin D1 overexpression perturbs DNA replication and induces replication-associated DNA double-strand breaks in acquired radioresistant cells. *Cell Cycle* **2013**, *12*, 773–782. [CrossRef]
167. Lai, X.; Broderick, R.; Bergoglio, V.; Zimmer, J.; Badie, S.; Niedzwiedz, W.; Hoffmann, J.-S.; Tarsounas, M. MUS81 nuclease activity is essential for replication stress tolerance and chromosome segregation in BRCA2-deficient cells. *Nat. Commun.* **2017**, *8*, 15983. [CrossRef]
168. Fugger, K.; Chu, W.K.; Haahr, P.; Kousholt, A.N.; Beck, H.; Payne, M.J.; Hanada, K.; Hickson, I.D.; Sørensen, C.S. FBH1 co-operates with MUS81 in inducing DNA double-strand breaks and cell death following replication stress. *Nat. Commun.* **2013**, *4*, 1423. [CrossRef]
169. Kurashima, K.; Sekimoto, T.; Oda, T.; Kawabata, T.; Hanaoka, F.; Yamashita, T. Polη, a Y-family translesion synthesis polymerase, promotes cellular tolerance of Myc-induced replication stress. *J. Cell. Sci.* **2018**, *131*, jcs212183. [CrossRef]
170. Mayle, R.; Campbell, I.M.; Beck, C.R.; Yu, Y.; Wilson, M.; Shaw, C.A.; Bjergbaek, L.; Lupski, J.R.; Ira, G. Mus81 and converging forks limit the mutagenicity of replication fork breakage. *Science* **2015**, *349*, 742–747. [CrossRef] [PubMed]
171. Macheret, M.; Halazonetis, T.D. DNA replication stress as a hallmark of cancer. *Annu. Rev. Pathol.* **2015**, *10*, 425–448. [CrossRef]
172. Chan, Y.W.; West, S.C. A new class of ultrafine anaphase bridges generated by homologous recombination. *Cell Cycle* **2018**, *17*, 2101–2109. [CrossRef] [PubMed]
173. Tiwari, A.; Addis Jones, O.; Chan, K.-L. 53BP1 can limit sister-chromatid rupture and rearrangements driven by a distinct ultrafine DNA bridging-breakage process. *Nat. Commun.* **2018**, *9*, 677. [CrossRef] [PubMed]
174. Chan, K.-L.; Palmai-Pallag, T.; Ying, S.; Hickson, I.D. Replication stress induces sister-chromatid bridging at fragile site loci in mitosis. *Nat. Cell Biol.* **2009**, *11*, 753–760. [CrossRef] [PubMed]
175. Minocherhomji, S.; Ying, S.; Bjerregaard, V.A.; Bursomanno, S.; Aleliunaite, A.; Wu, W.; Mankouri, H.W.; Shen, H.; Liu, Y.; Hickson, I.D. Replication stress activates DNA repair synthesis in mitosis. *Nature* **2015**, *528*, 286–290. [CrossRef]

176. Di Marco, S.; Hasanova, Z.; Kanagaraj, R.; Chappidi, N.; Altmannova, V.; Menon, S.; Sedlackova, H.; Langhoff, J.; Surendranath, K.; Hühn, D.; Bhowmick, R.; Marini, V.; Ferrari, S.; Hickson, I.D.; et al. RECQ5 helicase cooperates with MUS81 endonuclease in processing stalled replication forks at common fragile sites during mitosis. *Mol. Cell* **2017**, *66*, 658–671. [CrossRef]
177. Bhowmick, R.; Minocherhomji, S.; Hickson, I.D. RAD52 facilitates mitotic DNA synthesis following replication stress. *Mol. Cell* **2016**, *64*, 1117–1126. [CrossRef]
178. Downing, B.; Morgan, R.; VanHulle, K.; Deem, A.; Malkova, A. Large inverted repeats in the vicinity of a single double-strand break strongly affect repair in yeast diploids lacking Rad51. *Mutat. Res.* **2008**, *645*, 9–18. [CrossRef]
179. Hastings, P.J.; Ira, G.; Lupski, J.R. A microhomology-mediated break-induced replication model for the origin of human copy number variation. *PLoS Genet.* **2009**, *5*, e1000327. [CrossRef]
180. Ottaviani, D.; LeCain, M.; Sheer, D. The role of microhomology in genomic structural variation. *Trends Genet.* **2014**, *30*, 85–94. [CrossRef] [PubMed]
181. Sakofsky, C.J.; Malkova, A. Break induced replication in eukaryotes: mechanisms, functions, and consequences. *Crit. Rev. Biochem. Mol. Biol.* **2017**, *52*, 395–413. [CrossRef] [PubMed]
182. Özer, Ö.; Bhowmick, R.; Liu, Y.; Hickson, I.D. Human cancer cells utilize mitotic DNA synthesis to resist replication stress at telomeres regardless of their telomere maintenance mechanism. *Oncotarget* **2018**, *9*, 15836–15846. [CrossRef]
183. Budd, M.E.; Tong, A.H.Y.; Polaczek, P.; Peng, X.; Boone, C.; Campbell, J.L. A network of multi-tasking proteins at the DNA replication fork preserves genome stability. *PLoS Genet.* **2005**, *1*, e61. [CrossRef] [PubMed]
184. Falquet, B.; Rass, U. A new role for Holliday junction resolvase Yen1 in processing DNA replication intermediates exposes Dna2 as an accessory replicative helicase. *Microb. Cell* **2017**, *4*, 32–34. [CrossRef] [PubMed]
185. Ölmezer, G.; Levikova, M.; Klein, D.; Falquet, B.; Fontana, G.A.; Cejka, P.; Rass, U. Replication intermediates that escape Dna2 activity are processed by Holliday junction resolvase Yen1. *Nat. Commun.* **2016**, *7*, 13157. [CrossRef]
186. Duxin, J.P.; Dao, B.; Martinsson, P.; Rajala, N.; Guittat, L.; Campbell, J.L.; Spelbrink, J.N.; Stewart, S.A. Human Dna2 is a nuclear and mitochondrial DNA maintenance protein. *Mol. Cell. Biol.* **2009**, *29*, 4274–4282. [CrossRef] [PubMed]
187. Duxin, J.P.; Moore, H.R.; Sidorova, J.; Karanja, K.; Honaker, Y.; Dao, B.; Piwnica-Worms, H.; Campbell, J.L.; Monnat, R.J.; Stewart, S.A. Okazaki fragment processing-independent role for human Dna2 enzyme during DNA replication. *J. Biol. Chem.* **2012**, *287*, 21980–21991. [CrossRef]
188. Thangavel, S.; Berti, M.; Levikova, M.; Pinto, C.; Gomathinayagam, S.; Vujanovic, M.; Zellweger, R.; Moore, H.; Lee, E.H.; Hendrickson, E.A.; et al. DNA2 drives processing and restart of reversed replication forks in human cells. *J. Cell Biol.* **2015**, *208*, 545–562. [CrossRef]
189. Li, Z.; Liu, B.; Jin, W.; Wu, X.; Zhou, M.; Liu, V.Z.; Goel, A.; Shen, Z.; Zheng, L.; Shen, B. hDNA2 nuclease/helicase promotes centromeric DNA replication and genome stability. *EMBO J.* **2018**, e96729. [CrossRef]
190. Michel, A.H.; Hatakeyama, R.; Kimmig, P.; Arter, M.; Peter, M.; Matos, J.; De Virgilio, C.; Kornmann, B. Functional mapping of yeast genomes by saturated transposition. *eLife* **2017**, *6*, E3179. [CrossRef]
191. Alderton, G.K.; Joenje, H.; Varon, R.; Børglum, A.D.; Jeggo, P.A.; O'Driscoll, M. Seckel syndrome exhibits cellular features demonstrating defects in the ATR-signalling pathway. *Hum. Mol. Genet.* **2004**, *13*, 3127–3138. [CrossRef] [PubMed]
192. Shaheen, R.; Faqeih, E.; Ansari, S.; Abdel-Salam, G.; Al-Hassnan, Z.N.; Al-Shidi, T.; Alomar, R.; Sogaty, S.; Alkuraya, F.S. Genomic analysis of primordial dwarfism reveals novel disease genes. *Genome Res.* **2014**, *24*, 291–299. [CrossRef]
193. Peng, G.; Dai, H.; Zhang, W.; Hsieh, H.-J.; Pan, M.-R.; Park, Y.-Y.; Tsai, R.Y.-L.; Bedrosian, I.; Lee, J.-S.; Ira, G.; et al. Human nuclease/helicase DNA2 alleviates replication stress by promoting DNA end resection. *Cancer Res.* **2012**, *72*, 2802–2813. [CrossRef] [PubMed]
194. Strauss, C.; Kornowski, M.; Benvenisty, A.; Shahar, A.; Masury, H.; Ben-Porath, I.; Ravid, T.; Arbel-Eden, A.; Goldberg, M. The DNA2 nuclease/helicase is an estrogen-dependent gene mutated in breast and ovarian cancers. *Oncotarget* **2014**, *5*, 9396–9409. [CrossRef] [PubMed]

195. Neelsen, K.J.; Lopes, M. Replication fork reversal in eukaryotes: from dead end to dynamic response. *Nat. Rev. Mol. Cell Biol.* **2015**, *16*, 207–220. [CrossRef]
196. Lemaçon, D.; Jackson, J.; Quinet, A.; Brickner, J.R.; Li, S.; Yazinski, S.; You, Z.; Ira, G.; Zou, L.; Mosammaparast, N.; et al. MRE11 and EXO1 nucleases degrade reversed forks and elicit MUS81-dependent fork rescue in BRCA2-deficient cells. *Nat. Commun.* **2017**, *8*, 860. [CrossRef] [PubMed]
197. Zellweger, R.; Dalcher, D.; Mutreja, K.; Berti, M.; Schmid, J.A.; Herrador, R.; Vindigni, A.; Lopes, M. Rad51-mediated replication fork reversal is a global response to genotoxic treatments in human cells. *J. Cell Biol.* **2015**, *208*, 563–579. [CrossRef] [PubMed]
198. Quinet, A.; Lemaçon, D.; Vindigni, A. Replication fork reversal: Players and guardians. *Mol. Cell* **2017**, *68*, 830–833. [CrossRef] [PubMed]
199. Ray Chaudhuri, A.; Hashimoto, Y.; Herrador, R.; Neelsen, K.J.; Fachinetti, D.; Bermejo, R.; Cocito, A.; Costanzo, V.; Lopes, M. Topoisomerase I poisoning results in PARP-mediated replication fork reversal. *Nat. Struct. Mol. Biol.* **2012**, *19*, 417–423. [CrossRef]
200. Mutreja, K.; Krietsch, J.; Hess, J.; Ursich, S.; Berti, M.; Roessler, F.K.; Zellweger, R.; Patra, M.; Gasser, G.; Lopes, M. ATR-mediated global fork slowing and reversal assist fork traverse and prevent chromosomal breakage at DNA interstrand cross-links. *Cell Rep.* **2018**, *24*, 2629–2642. [CrossRef]
201. Menin, L.; Ursich, S.; Trovesi, C.; Zellweger, R.; Lopes, M.; Longhese, M.P.; Clerici, M. Tel1/ATM prevents degradation of replication forks that reverse after topoisomerase poisoning. *EMBO Rep.* **2018**, *19*, e45535. [CrossRef]
202. Bhat, K.P.; Krishnamoorthy, A.; Dungrawala, H.; Garcin, E.B.; Modesti, M.; Cortez, D. RADX modulates RAD51 activity to control replication fork protection. *Cell Rep.* **2018**, *24*, 538–545. [CrossRef] [PubMed]
203. Dungrawala, H.; Bhat, K.P.; Le Meur, R.; Chazin, W.J.; Ding, X.; Sharan, S.K.; Wessel, S.R.; Sathe, A.A.; Zhao, R.; Cortez, D. RADX promotes genome stability and modulates chemosensitivity by regulating RAD51 at replication forks. *Mol. Cell* **2017**, *67*, 374–386. [CrossRef]
204. Schlacher, K.; Christ, N.; Siaud, N.; Egashira, A.; Wu, H.; Jasin, M. Double-strand break repair-independent role for BRCA2 in blocking stalled replication fork degradation by MRE11. *Cell* **2011**, *145*, 529–542. [CrossRef]
205. Higgs, M.R.; Reynolds, J.J.; Winczura, A.; Blackford, A.N.; Borel, V.; Miller, E.S.; Zlatanou, A.; Nieminuszczy, J.; Ryan, E.L.; Davies, N.J.; et al. BOD1L is required to suppress deleterious resection of stressed replication forks. *Mol. Cell* **2015**, *59*, 462–477. [CrossRef] [PubMed]
206. Mijic, S.; Zellweger, R.; Chappidi, N.; Berti, M.; Jacobs, K.; Mutreja, K.; Ursich, S.; Ray Chaudhuri, A.; Nussenzweig, A.; Janscak, P.; et al. Replication fork reversal triggers fork degradation in BRCA2-defective cells. *Nat. Commun.* **2017**, *8*, 859. [CrossRef] [PubMed]
207. Przetocka, S.; Porro, A.; Bolck, H.A.; Walker, C.; Lezaja, A.; Trenner, A.; von Aesch, C.; Himmels, S.-F.; D'Andrea, A.D.; Ceccaldi, R.; et al. CtIP-mediated fork protection synergizes with BRCA1 to suppress genomic instability upon DNA replication stress. *Mol. Cell* **2018**, *72*, 568–582. [CrossRef] [PubMed]
208. Berti, M.; Ray Chaudhuri, A.; Thangavel, S.; Gomathinayagam, S.; Kenig, S.; Vujanovic, M.; Odreman, F.; Glatter, T.; Graziano, S.; Mendoza-Maldonado, R.; et al. Human RECQ1 promotes restart of replication forks reversed by DNA topoisomerase I inhibition. *Nat. Struct. Mol. Biol.* **2013**, *20*, 347–354. [CrossRef] [PubMed]
209. Manosas, M.; Perumal, S.K.; Croquette, V.; Benkovic, S.J. Direct observation of stalled fork restart via fork regression in the T4 replication system. *Science* **2012**, *338*, 1217–1220. [CrossRef]
210. Manosas, M.; Perumal, S.K.; Bianco, P.R.; Bianco, P.; Ritort, F.; Benkovic, S.J.; Croquette, V. RecG and UvsW catalyse robust DNA rewinding critical for stalled DNA replication fork rescue. *Nat. Commun.* **2013**, *4*, 2368. [CrossRef]

Chapter 3: The Dna2 Helicase-Nuclease

The Dna2 nuclease-helicase was first identified in yeast[94], is conserved across eukaryotes, and proved to be essential in all organisms tested[95-99]. Over the past 25 years, it has emerged that Dna2 plays key roles in multiple genome maintenance pathways. Recently, *DNA2* has been identified as one of the disease genes in Seckel syndrome[100]. Overexpression of DNA2 is frequent in cancer and associated with poor prognosis[101,102]. A detailed understanding of the molecular processes involving *DNA2* will shed light on mechanisms of genome stability and human disease.

In yeast, Dna2 consists of three domains: (1) a poorly conserved and unstructured N-terminal domain[103]; (2) a central RecB-like nuclease domain with ssDNA-specific endonuclease activity[104]; (3) a C-terminal superfamily 1 helicase domain with 5´-3´ translocation polarity[105]. Cells expressing helicase-defective Dna2 mutants are viable but sensitive to RS[106]. The nuclease activity of Dna2 is essential for cell viability[95,107]. X-ray crystallography of the murine Dna2 has shown how the nuclease and helicase domains cooperate and provided an explanation for the requirement of an accessible ssDNA flap or overhang for Dna2 activity[105,108]. DNA substrates first thread through a tunnel-like structure formed by the nuclease domain, which is too narrow for dsDNA[109]. On exiting the nuclease domain, the DNA reaches helicase domain. This unusual topology of the enzyme places the helicase activity under tight control by the nuclease activity. Consequently, experimental inactivation of the nuclease drastically increases the rate of DNA unwinding by budding yeast Dna2[110]. Similarly in human, the helicase activity of Dna2, which was initially considered weak or absent[111,112], was shown to be potent and processive when the nuclease domain was inhibited [113]. It has been proposed that this unrestrained Dna2 helicase activity is responsible for the toxicity observed upon expression of a nuclease-dead version of Dna2 in yeast[110] and mammals[96,113].

Dna2 resects both 3´ and 5´-ssDNA *in vitro*. However, ssDNA-binding complex RPA stimulates Dna2-mediated cleavage of 5´-ssDNA[114] and directs incision towards the base of 5´-flaps, independently of the Dna2 helicase activity[115]. This suggests that the physiological polarity of the enzyme is 5´-3´[116]. RPA physically interacts with the N-terminal domain of Dna2 in yeast[117]. An interaction that is physiologically important as truncation of the N-terminal portion of Dna2 renders the cells sensitive to high temperature[109,114,117].

Although this section of the protein is poorly conserved, a mouse Dna2 fragment encompassing amino acid residues 1 to 122 also exhibits bimodal interactions with RPA, which

first promotes the recruitment of Dna2 to RPA-coated ssDNA before triggering the disengagement of the N-terminal moiety of RPA from its DNA substrate. In case of 5´-ended ssDNA, this transition reveals a free end that Dna2 can slide onto, leading to end-resection and further eviction of RPA molecules[118]. In case of 3´-terminated ssDNA, removal of the N-terminus of RPA doesn't expose a ssDNA end[109], explaining how RPA modulates the polarity of Dna2 activity.

Early experiments suggested that Dna2 plays a role in late S-phase with temperature-sensitive *dna2* alleles causing an accumulation of cells at the G2/M boundary upon shift to the restrictive temperature[119]. This notion is in line with later work showing nuclear entry of Dna2 during S-phase following a CDK-dependent phosphorylation of a nuclear import signal in budding yeast[120] and a peak in *DNA2* expression in late S/G2 phase[121]. In human cells, the nuclear localization of DNA2 is dependent on the E3 ubiquitine ligase TRAF6 for reasons that are not yet understood[122], and its cell-cycle regulation is less-well defined compared to yeast. The precise functional relationships of Dna2 and DNA replication remain to be fully elucidated. However, there is a growing body of work linking Dna2 to potential functions in Okazaki fragment processing and the recovery of stalled RFs. Moreover, Dna2 mediates DNA end-resection during DBS repair and has an undefined role in mitochondrial DNA maintenance.

Dna2 and DSB repair

DSBs are among the most toxic DNA lesions. Interrupting the continuity of a chromosome creates an acentric fragment that cannot be properly segregated. If left unattended, a single DSB can be lethal for a yeast cell [123]. In eukaryotes, DSBs are principally repaired by two complementary pathways: non-homologuous end-joining (NHEJ), a mechanism for ligating DSB ends to seal the break, and homologous recombination (HR), a process that uses a homologous template to copy any missing genetic information and repair the broken chromosome. DSB repair by HR requires DNA end-resection in order to form a 3´-ssDNA overhang. The central recombinase Rad51 will then polymerize on the ssDNA and initiate homology search and strand invasion into a suitable repair template (reviewed in [124]). An unbroken sister chromatid is the preferred template if available, owing to its physical proximity and sequence identity[125]. HR is generally confined to the S and G2 phases of the cell cycle (reviewed in [126]), which coincides with the entry of Dna2 into the nucleus[120]. Yeast Dna2 is recruited to DSBs upon phosphorylation by Cdk1[127], where it colocalizes with HR factors[128] and participates in DNA end-resection.

In budding yeast, the first step in DNA end-resection is an endonucleolytic incision on the 5´-terminated DNA strand by the MRX-Sae2 (MRN-CtIP in human) complex, which then degrades DNA towards the break end using its 3´-5´ exonuclease activity. This creates a short 3´-overhang that serves as a substrate for the long-range resection machinery, comprised of either the Exo1 (EXO1 in human) nuclease or the helicases Sgs1 (homologue of both BLM and WRN in human) in conjunction with Dna2/DNA2, which extends the length of the 3´-overhangs[129-131]. Dna2 alone cannot process DNA ends that present a 3´-overhang coated with RPA and therefore requires assistance by Sgs1/BLM/WRN to mediate end-resection[132,133]. In contrast to Dna2, Sgs1 is a 3´-5´ helicase. During DNA end-resection, Sgs1 slides along the strand that is not resected to produce a stretch of ssDNA that is subsequently degraded by the coordinated action of the helicase and the nuclease domain of Dna2[113,134,135]. In this process, the Dna2 helicase drives the translocation along ssDNA rather than mediating unwinding of the duplex. In yeast, Sae2 stimulates Dna2 nuclease activity during end-resection while CtIP stimulates BLM and DNA2[136]. On the other hand, Siz2-mediated ubiquitination inhibits the Dna2 nuclease activity *in vivo*, thereby increasing the processivity of the helicase[121], in line with earlier *in vitro* experiments[110]. It has also been reported that CtIP and its interacting partner BRCA1 bind DNA2 to promote its recruitment to DSBs[137], a similar interaction that has been suggested in budding yeast, where MRX is proposed to participate in the recruitment of Dna2 at sites of DNA breaks[138].

Dna2 and Okazaki fragment processing

The 5´-3´ polarity of DNA polymerases and their coordination at the RF during DNA replication result in the continuous replication of the leading strand and discontinuous replication of the lagging strand. The lagging strand is synthesized by Polδ in sections referred to as "Okazaki fragments" (approx. 165 nt in yeast), each initiated by a short RNA-DNA primer laid down by the Pol α/primase complex. When Pol δ reaches the preceding Okazaki fragment, the 5´-terminus is displaced. This creates a 5´-flap that is immediately removed by flap endonuclease Rad27/FEN1 and/or Exo1/EXO1. The rate of DNA synthesis by Pol δ drops dramatically during strand displacement such that rapid incision by the Okazaki fragment processing machinery largely prevents 5´-flaps greater than a few nucleotides and RNA/DNA primer removal proceeds by nick translation[139]. Processed Okazaki fragments are then sealed by DNA ligase Cdc9/LIG1.

Interestingly, several members of the lagging strand synthesis network genetically interact with *DNA2*[106,140,141]. For instance, Dna2 helicase activity becomes essential in the absence of Rad27 flap endonuclease[142]. Conversely, overexpression of Rad27 rescues the viability of temperature

sensitive *dna2* mutants[143]. Furthermore, the two enzymes have been reported to interact physically[140], which has led to the suggestion that Rad27 and Dna2 might form an adaptable Okazaki fragment-processing (OFP) complex[140], where Dna2 processes occasional 5´-flaps escaping the activity of Rad27[144]. In this model, the Polδ subunit Pol32 and the DNA helicase Pif1[145,146] stimulate the processivity of Polδ in such a way that an excessively long flap is created during OFP. Rapid coating by RPA is then thought to preclude cleavage by Rad27 but not by Dna2[147], which can act as the sole nuclease to create ligation-competent DNA fragment *in vitro*[115]. RPA-coated ssDNA is a potent activator of the DNA damage response and its accumulation could cause terminal cell-cycle arrest in absence of Dna2. This model is supported by the observation that deletions of *POL32*, *PIF1*, or DNA damage response mediator *RAD9* suppress the lethality of *dna2*Δ cells[142]. In addition, electron microscopy has provided direct evidence of a Pif1-dependent build-up of ssDNA upon acute depletion of Dna2, which has been interpreted as an accumulation of long 5´-flaps at Okazaki fragments[148].

While its potential role in OFP has become the prevailing explanation for the essential nature of *DNA2*[142,145,148], multiple lines of evidence suggest that Dna2 is not required for OFP *in vivo* or that any involvement in the process is very limited. Depletion of Dna2 alone does not affect the production and size-distribution of ligation-competent Okazaki fragments[149], indicating that Pol δ-mediated strand-displacement DNA synthesis is not excessive and flaps generated during OFP are still efficiently trimmed in the absence of Dna2. Moreover, Okazaki fragment termini in budding yeast are affected by depletion of Pol32, but not in Pif1-depleted cells[150]. This is difficult to reconcile with the genetic interactions between *DNA2*, *PIF1*, and *POL32* on the basis of OFP.

In fission yeast, electron microscopy has been used to detect RFs bearing flaps comprising a few hundred nucleotides of DNA in *dna2* and *rad2* (*fen1*) mutants[151]. These intermediates were suggested to represent Okazaki fragments containing long unprocessed 5´-flaps; however, there were no substantial differences between *dna2* and *rad2* mutants, despite the fact that in contrast to *DNA2* , *RAD2* is non-essential. These observations cast some doubt on the current view that an involvement in OFP is a satisfactory explanation for the essential requirement for Dna2 in cells and it seems plausible that toxic DNA intermediates arise along another Pif1-dependent pathway when Dna2 is absent.

Dna2 and RF recovery

Across species, Dna2-mutant cells are sensitive to RS[97,106] and depletion of Dna2 results in an accumulation of DNA four-way junctions consistent with increased RF reversal[79,148,152]. In

fission yeast, Dna2 is recruited to stalled RFs in a Cds1 kinase-dependent manner[152]. In human, DNA2 promotes replication restart at stalled RFs. This process is stimulated by WRN and thought to involve the degradation of the regressed arm at reversed RFs[79]. U2OS cells, depleted of DNA2, arrest in G2 phase of the cell cycle[153] and display chromosomal aberrations consistent with chromosomal under-replication such as an accumulation of micronuclei, mitotic DNA bridges and aneuploidy. These phenotypes could not be complemented by the expression of FEN1, suggesting that they arise independently of any involvement of DNA2 in OFP (see above)[96].We have shown that a helicase-dead version of Dna2 (Dna2 R1253Q, encoded by *dna2-2*) in budding yeast renders cells sensitive to RS while being fully proficient in cleaving RPA-covered 5´-flaps *in vitro*[154]. These cells arrest at the G2/M transition and accumulate stalled and converged RFs within the rDNA[154,155]. Interestingly, Dna2 helicase-defective cells depend on the activity of Yen1 for viability, suggesting that DNA replication intermediates that are left unprocessed by Dna2 require resolution by this Holliday junction resolvase in mitosis[154]. These observations have established the importance of the Dna2 helicase activity in responding to stalled RFs. Taken together, the available data points to a critical role of Dna2 in RF recovery and replication completion, but it remains to be seen whether this role can explain the essential nature of *DNA2*.

The role of Dna2 in assisting replication is particularly visible at difficult-to-replicate genomic loci. For instance, in budding yeast, Dna2 has been implicated in rDNA replication and telomere homeostasis. Dna2-defective cells display longer telomeres with shorter 3´-overhangs compared to wild-type cells[156,157]. Furthermore, heterozygous *DNA2*-knockout mouse embryonic fibroblasts are viable but the cells display an elevated frequency of telomeric gaps and breaks, characteristic of fragile telomeres. Moreover, *DNA2*-deficient mice have been shown to have noticeably shorter telomeres[98]. Mammalian centromeres are among hard-to-replicate genomic loci proposed to require DNA2's action for the completion of replication. Thus, ChIP-seq assays have revealed that DNA2 is enriched at centromeres, where its helicase and nuclease activities promote RF progression[158]. Finally, RFs have been shown to remain stalled within the rDNA array in budding yeast when the Dna2 helicase is non-functional[154,155]. While locus-specific functions of DNA2 such as for example the resolution of G-quadruplex DNA at telomers[98,159] have been proposed, perhaps the most straightforward explanation for these various phenotypes is that proper RF recovery mediated by *DNA2* is most critical in difficult-to-replicate regions where double-stalling events or lack of fork convergence at telomeres are most likely to jeopardize replication completion.

Checkpoint activation

In yeast, the unstructured[114] N-terminal domain of Dna2 plays a role in activating the central checkpoint kinase Mec1 in S-phase. This role is redundantly shared by other proteins; namely, the 9-1-1 complex and Dpb11[160]. Despite being non-essential, the truncation of the N-terminal portion of Dna2 renders the cells sensitive to high temperature. This might, however, be due to the confounding effect created by the disruption of Dna2-RPA interactions[109,114,117]. It is, therefore, difficult to delineate the contribution of Dna2 to checkpoint activation alone. It is clear, however, that checkpoint activation is not an essential Dna2 role.

Mitochondrial DNA maintenance

In human, DNA2 was initially observed in mitochondria[161] before its presence and role in the nucleus were identified[153]. DNA2 physically interacts with the mitochondrial DNA polymerase Pol γ and may participate in mitochondrial DNA replication[161]. Interestingly, DNA2 forms mitochondrial foci upon mitochondrial RS, induced by oxidative damage or disruption of the mitochondrial replicative helicase TWINKLE[153]. These results are in good agreement with clinical data, linking mitochondrial myopathy with heterozygous mutations of *DNA2*. Patients bearing a defective allele of *DNA2* display symptoms ranging from muscle weakness to cardiac anomalies [162-166], emphasizing the critical role of DNA2 in mitochondrial DNA maintenance.

Chapter 4 : The conserved DNA helicase Pif1

This chapter will review the structure and function of Pif1. As described in more detail below, Pif1 is perhaps best described as an accessory replicative helicase that promotes RF progression and/or recovery in a number of well-described settings. It may therefore come as a surprise that the inactivation of Pif1 suppresses growth defects associated with *DNA2* mutations in budding[142] and fission yeast[167]. This phenotypic suppression is currently thought to relate to an interplay between Pif1 and Dna2 in Okazaki fragment processing, but a number of observations have thrown this view into doubt (see Chapter 3). It is therefore important to take the entire breath of Pif1 functions into account and to consider alternative explanation for the genetic relationship between *DNA2* and *PIF1*.

The Pif1 family of helicases has similarities with prokaryotic RecD helicases[168] and is largely conserved in eukaryotes[169]. While most organisms, including human and fission yeast, contain only one representative of the family, budding yeast possesses two: Pif1 and Rrm3. Pif1 comprises seven conserved helicase motifs[170], a 21 amino acid signature motif characteristic for the Pif1 family[169], and exhibits ssDNA 5´-3´ helicase activity[171]. These characteristics place Pif1 proteins in the helicase superfamily 1B (SF1B), which also comprises Dna2. In marked contrast to Dna2, Pif1 doesn't require the presence of a free 5´-end to unwind dsDNA[172,173] and can act on gapped substrates[174]. However, single-molecule experiments have shown that budding yeast Pif1 binds with higher affinity to ss/dsDNA junctions containing a free 5´-end. Bound at DNA junctions, Pif1 remains stationary while its helicase activity mediates a periodic reeling in of the ssDNA. This unusual mode-of-action could be the basis for several of the functions of Pif1, for example the removal of proteins or RNA from ssDNA[175].

In budding yeast, alternative translation leads to the expression of two isoforms of Pif1. Translation from the first methionine results in inclusion of a mitochondrial targeting signal (MTS) and produces the mitochondrial Pif1 (mt-Pif1), which matures by cleavage of the MTS[172]. Nuclear Pif1 (n-Pif1) is produced by translation from a second methionine codon[176]. When this second start codon is mutated (*pif1-m2* allele), n-Pif1 is depleted while mt-Pif1 functions normally[177]. In human, PIF1 is also present in two isoforms. The shorter PIF1α locates in the nucleus while the slightly longer PIF1β resides in the mitochondria. It is currently unclear whether PIF1β is produced by alternative splicing[178] or translation[179].

Mitochondrial replication

The *PIF1* gene was first identified in the genome of budding yeast through a screen for mutants affecting mitochondrial DNA replication[180]. Disruption of *PIF1* compromises cell viability and mitochondrial DNA maintenance[181], which results in the appearance of small colonies when *pif1*-mutant strains are plated on a non-fermentable carbon source[180]. In fission yeast, Pif1-homologue Pfh1 is essential for cell viability[176,182] due to indispensable mitochondrial and nuclear roles[183]. This is very different in budding yeast, where cells expressing mt-Pif1 (*pif1-m2* allele) exhibit no overt growth defects, suggesting that any vital nuclear functions are redundantly fulfilled by Rrm3. The *pif1-m2* allele thus provides an invaluable analytic tool to interrogate the nuclear actions of Pif1.

Telomere homeostasis

Pif1 regulates telomere length. In budding yeast, depletion of Pif1 induces telomere elongation[177]. This has been explained by the ability of Pif1 to dissociate RNA-DNA hybrids[184,185], allowing the enzyme to disrupt interactions between the RNA moiety of telomerase and telomeric DNA[172,177,186] *in vitro*[174] and *in vivo*[187]. This function is shared by human PIF1[168]. In budding yeast and human, Pif1 is most abundant in late S/G2 phase of the cell cycle, the time when telomerase is active[188,189]. Perhaps surprisingly, mutations in fission yeast Pfh1 decrease – rather than increase – telomere length[176]. Conversely, over-expression of Pfh1 induces telomere lengthening[190]. This, together with the fact that Pfh1 remains essential in fission yeast strain with circular (i.e. telomere-less) chromosomes, points to another essential nuclear function. There may be parallels between Pfh1 and budding yeast Rrm3, which plays a role in facilitating telomere replication through an as-yet unclear mechanism[191].

In budding yeast, Pif1 has been shown to fulfil an important function by controlling telomerase at DSBs[192]. In absence of Pif1 activity, *de novo* telomere addition is frequent at DSBs[177,193]. Ectopic telomere addition can lead to the irreversible truncation of the broken chromosome. How Pif1 differentiates between telomeres and DSBs is not fully understood but telomere-specific protein Cdc13, which is not found at DSBs, appears to control Pif1 activity[194]. In addition, recruitment of budding yeast Pif1 to DSBs is dependent upon phosphorylation of a C-terminal motif (TLSSAES) by Mec1 and Rad53. Pif1 mutants refractory to phosphorylation at this site are proficient in maintaining telomere homeostasis but unable to prevent telomere-addition at DSBs[192] and defective for HR-coupled replication[195] (see below).

Homologous recombination-coupled replication

Pif1 promotes replication restart by HR-dependent mechanisms at arrested and broken RFs. This process has mostly been studied in budding yeast in the context of break-induced replication (BIR) after induction of a site-specific DSB (mimicking a broken RF) or replicative run-off at an induced nick. To assay BIR, a repair template is placed on a different chromosome, which is invaded following end-resection. This results in a displacement loop (D-loop) or "bubble"[196], which moves along the template as Pol δ mediates DNA-repair synthesis. In the process, newly replicated ssDNA is exposed and only later serves as the template for lagging strand synthesis, resulting in conservative DNA replication[197-199]. A similar process termed "recombination-dependent restart" (RDR) mediates the recovery of arrested but unbroken RFs. In this case, reversed forks present a DNA end that can be recognized and resected much like a DSB. This creates a 3´-overhang with perfect homology to the DNA duplex located in front of the perturbed RF. Invasion of the parental duplex then allows resumption of replication, although the replication now proceeds in the context of a D-loop[200]. This model stems from results obtained in fission yeast where replication was halted at a precise location using an inducible RF barrier. Importantly, Pif1/Pfh1 is indispensable for BIR and RDR[201].

The replicative helicase complex MCM2-7 might participate in driving D-loop migration during BIR/RDR[202], but alternatively this role might actually be performed by Pif1. Pif1 recruits to D-loops through interaction with PCNA[203] and promotes bubble migration for hundreds of kilobases[204,205] by unwinding the parental DNA duplex and/or by displacing the newly synthetized strand from the template. In absence of Pif1, BIR efficiency drops sharply and the progression of the D-loop is dramatically reduced[204,205]. Interestingly, the same phosphorylation site that stimulates the recruitment of Pif1 to DBS (see telomere homeostasis, above) is also required for its function in BIR[195].

BIR is a mutagenic process, probably because the long stretches of ssDNA are left exposed during bubble migration, preventing templated repair of any damage incurred. The following step of conservative DNA synthesis will thus be mutagenic[204], which is reflected in patches of mutations near sites of BIR initiation[197]. Due to the high processivity of the D-loop, these mutations can spread over hundreds of kilobases, sometimes reaching the end of chromosomes[197], but their spread is limited by oncoming RFs fusing with the D-loop and by structure-specific endonuclease Mus81, which appears to cleave D-loops to restore more canonical

RFs[206]. These results suggest that, while offering alternative pathways for RF recovery, BIR/RDR reactions may have to be tightly controlled and regulated to maintain genome stability.

Resolution of G-quadruplex DNA

Pif1 seems to play a conserved role in the stability and replication of G-rich DNA sequences. G-rich DNA can give rise to G-quadruplex DNA secondary structures where Hoogsteen base-pairing enables the formation of so-called G-quartets. These structures block DNA synthesis and compromise RF progression, enhancing genome instability (reviewed in[207]). Sequencing efforts in human have revealed that more than 700'000 sites are prone to form G-quadruplexes[208]. These structures are therefore a frequent obstacle that cells have to overcome during DNA replication.

Pif1 preferentially binds G-rich regions and efficiently unwinds ssDNA containing G-quadruplex structures i*n vitro* [209]. This is in line with observations in budding yeast, where Pif1 promotes the stability of sequences prone to form G-quadruplexes during replication[210-212]. This role in unwinding G-quadruplex DNA seems to be conserved from bacteria[209] to human[213]. Whether the absence of Pif1 affects only the fidelity of replication or also RF speed through G-quadruplex DNA is not entirely clear[150]. However, observations of replication at the single-cell level show that the movement of RFs is reduced in absence of Pif1 depending on the ability of the lagging-strand template to form G-quadruplex structures[214]; other helicases may be responsible for unwinding of G-quadruplexes on the leading strand. In addition of its importance in the replication of G-rich regions, it has recently been proposed that, in human, PIF1 promotes DSB repair by assisting the resection machinery in unfolding G-quadruplexes on the resected strand[215].

Eviction of R-loops and transcription-borne obstacles

R-loops are stable RNA-DNA hybrids that are particularly frequent at telomeres, rDNA and tDNA (reviewed in[216]). Pif1 could play a role in the removal of R-loops since it unwinds efficiently RNA-DNA duplexes *in vitro*[185]. Consistent with this notion, depletion of Pfh1 in fission yeast increases RF stalling at tRNA genes[217], while in budding yeast, Pif1 can compensate for the loss of Rrm3 and promote the progression of the RFs through tRNA genes. In absence of Rrm3 and Pif1, RFs stall when replicating tRNA genes, which increases genome instability at these loci[218]. These stalling events have been attributed to the collision of the replication machinery with R-loops. Thus, overexpression of Rnh1, which degrades RNA-DNA hybrids, reduces tDNA instability in *rrm3*Δ-mutant cells[218]. However, this idea is contested by another report, where RF progression was reduced in tRNA genes irrespective of the level of expression of Rnh1 in *pif1*

and/or *rrm3* mutants[150]. It is therefore not clear whether Pif1 and Rrm3 are fully redundant in evicting RNA molecules or the transcription machinery from DNA. More studies are required to understand the exact interplay between the Pif1-helicase family and transcription.

rDNA replication

In budding yeast, Fob1 enforces a unidirectional replication fork barrier (RFB) that prevents head-on collision between the replisome and the transcription machinery. Interestingly, Pif1 promotes the pausing of the RF at sites bound by Fob1. In contrast, Rrm3 promotes RF progression through the RFB[219], as does Pfh1 in fission yeast[220]. The molecular details of Pif1-enforced replication pausing at RFB remain to be elucidated.

Okazaki fragment processing

As mentioned earlier, Pif1 has been suggested to drive strand-displacement DNA synthesis by Pol δ during OFP, unwinding the previous Okazaki fragment thanks to its 5´-3´ helicase activity. This view has evolved from *in vitro* experiments showing that Pif1 stimulates strand-displacement DNA synthesis in a primer extension reaction mediated by Pol δ[145]. This could lead to long 5´-flaps at a small subset of Okazaki fragments[146], but it is unclear whether a "long-flap" pathway for OFP exists as lagging-strand DNA synthesis is intrinsically biased to generate no or very short flaps only[139]. *In vivo,* Rrm3 and Pif1 redundantly stimulate Pol δ during OFP such that loss of Pif1 alone has no effect on Okazaki-fragment size distribution or positioning[150].

Replication termination

DNA replication termination normally takes place when two converging RFs originating from neighboring origins meet. As the replisomes are getting closer to each other, torsional stress builds up between the converging RFs. This tension has to be relaxed by the action of topoisomerases to allow further RF progression. This role performed by topoisomerases has been best characterized *in vitro*, where the replication of plasmids by reconstituted replisomes was greatly enhanced in the presence of TopoII[221]. However, this minimal replisome was unable to fully complete plasmid replication, indicating that termination was problematic unless the reaction was supplemented with Pif1 or Rrm3[222]. These two enzymes also act *in vivo* to finalize plasmid replication in budding yeast[222]. These findings are in good agreement with the observation that in fission yeast, Pfh1 promotes RF merging[220]. Altogether, these results suggest that the helicases of the Pif1 family promote replication termination, which could explain the essential role of Pfh1 and the synthetic-sick relationship between *pif1* and *rrm3*.

RF reversal

As mentioned earlier, RF reversal appears to be a common protective mechanism in the face of RS in metazoans, whereas it could be pathological or very transient in budding yeast. It has been suggested that the checkpoint inhibits Pif1 and Rrm3 by phosphorylating their N-termini. In absence of checkpoint control, electron microscopy inspection revealed an increased in the number of reversed RFs dependent of the presence of Rrm3 and Pif1[223]. Based on these results, it has been proposed that Rrm3 and Pif1 can catalyze RF reversal, even though the action of Pif1 alone appears insufficient to promote RF regression.

Question addressed by my work

During DNA replication, DNA2 employs the interplay between its helicase and nuclease domains to fulfil multiple functions protecting genome integrity across eukaryotes. Interestingly, DNA2 is not required for the completion of bulk DNA synthesis[96,154], although it remains essential for cell viability. Despite its implication in several pathologies (reviewed in [224]), the reason behind the essential nature of DNA2 is still unclear. A better understanding of this key function will help us connect fundamental biological processes with human diseases.

Chapter 5: The role of Dna2 helicase replication stress response

This chapter is based on:

Gizem Ölmezer, Maryna Levikova, Dominique Klein, Benoît Falquet, Gabriele Alessandro Fontana, Petr Cejka, and Ulrich Rass.

Replication intermediates that escape Dna2 activity are processed by Holliday junction resolvase Yen1.

Nat Commun, 2016 vol. 7 p. 13157.

Author contributions:
G.Ö. and UR planned and analyzed the experiments. G.Ö. performed the experiments with the help from D.K. B.F. supported the two dimensional gel analysis and G.F. the microscopic work. M.L. and P.C. purified and analyzed Dna2 *in vitro*. U.R. wrote the paper.

and

Benoît Falquet and Ulrich Rass.

A new role for Holliday junction resolvase Yen1 in processing DNA replication intermediates exposes Dna2 as an accessory replicative helicase.

Microb Cell, 2017 vol. 4 (1) p. 32

Author contributions:
B.F. and U.R. defined the form and content of the paper and wrote the manuscript.

nature COMMUNICATIONS

ARTICLE

Received 12 Jan 2015 | Accepted 8 Sep 2016 | Published 25 Oct 2016

DOI: 10.1038/ncomms13157 OPEN

Replication intermediates that escape Dna2 activity are processed by Holliday junction resolvase Yen1

Gizem Ölmezer[1,2], Maryna Levikova[3,*], Dominique Klein[1,*], Benoît Falquet[1,2], Gabriele Alessandro Fontana[1], Petr Cejka[3] & Ulrich Rass[1]

Cells have evolved mechanisms to protect, restart and repair perturbed replication forks, allowing full genome duplication, even under replication stress. Interrogating the interplay between nuclease-helicase Dna2 and Holliday junction (HJ) resolvase Yen1, we find the Dna2 helicase activity acts parallel to homologous recombination (HR) in promoting DNA replication and chromosome detachment at mitosis after replication fork stalling. Yen1, but not the HJ resolvases Slx1-Slx4 and Mus81-Mms4, safeguards chromosome segregation by removing replication intermediates that escape Dna2. Post-replicative DNA damage checkpoint activation in Dna2 helicase-defective cells causes terminal G2/M arrest by precluding Yen1-dependent repair, whose activation requires progression into anaphase. These findings explain the exquisite replication stress sensitivity of Dna2 helicase-defective cells, and identify a non-canonical role for Yen1 in the processing of replication intermediates that is distinct from HJ resolution. The involvement of Dna2 helicase activity in completing replication may have implications for *DNA2*-associated pathologies, including cancer and Seckel syndrome.

[1] Friedrich Miescher Institute for Biomedical Research, Maulbeerstrasse 66, Basel CH-4058, Switzerland. [2] University of Basel, Petersplatz 10, Basel CH-4003, Switzerland. [3] Institute of Molecular Cancer Research, University of Zurich, Winterthurerstrasse 190, Zurich CH-8057, Switzerland. * These authors contributed equally to this work. Correspondence and requests for materials should be addressed to U.R. (email: ulrich.rass@fmi.ch).

Duplication of the genome requires the passage of DNA replication forks along the entire length of every chromosome. If segments of DNA remain unreplicated, physical links between the nascent sister chromatids persist, which can lead to aberrant chromosome segregation[1]. Replication fork collapse, characterized by replisome inactivation and DNA breakage, induces recombinogenic DNA lesions and gross chromosomal instability[2]. Consistently, replication stress, which increases the risk of replication fork stalling, arrest, and collapse, has been recognized as a driver in cancerogenesis[3]. Cells respond to replication stress by activating the S phase checkpoint, which triggers a cascade of downstream events aimed at preserving the replication machinery at troubled replication forks until DNA synthesis can resume[4]. Replication restart also involves fork remodelling, nucleolytic processing of stalled replication intermediates and homologous recombination (HR) reactions[5–7]. Thus, full genome duplication and proper chromosome segregation is dependent on a complicated network of replication and repair proteins that remains incompletely understood.

A protein implicated in multiple aspects of DNA replication and repair is the conserved nuclease-helicase Dna2. Essential in yeast[8], *DNA2* is required for embryonic development in mice[9], and its downregulation leads to chromosomal instability[10–14]. The enzymatic activities of Dna2 reside in a RecB-like nuclease domain[15] with single-stranded DNA (ssDNA)-specific endonuclease activity[16], and a C-terminal superfamily 1 (SF1) helicase domain[8]; in yeast, Dna2 has an additional, unstructured N-terminal domain that serves a redundant function in S phase checkpoint activation[17].

The nuclease activity of Dna2, in particular, has been linked with a number of molecular pathways. *In vitro*, Dna2 cuts DNA 5′-flaps bound by replication protein A (RPA), and it has been proposed that this activity might facilitate Okazaki fragment maturation by mediating the removal of occasional long 5′-flaps, which might attract RPA and become refractory to cleavage by Rad27 (FEN1 in human)[18,19]. During DNA double-strand break repair, the Dna2 nuclease degrades the 5′-terminated single strand unwound by the Sgs1 helicase (BLM, Bloom syndrome protein in human), promoting DNA end-resection and HR redundantly with Exo1 (ref. 20). Similarly, the Dna2 nuclease has been implicated in *Schizosaccharomyces pombe* in the processing of stalled replication fork intermediates through degradation of the regressed DNA branch emanating from reversed replication forks as the newly synthesized DNA strands become displaced and anneal with one another to form a chicken-foot structure[21,22]. An analogous reaction, mediated by the DNA2 nuclease in conjunction with Werner's syndrome helicase WRN, promotes replication restart in human cells[23], while failure to properly control DNA2-mediated DNA resection at stalled forks leads to excessive DNA degradation and genome instability[24,25].

The physiological role of the Dna2 helicase activity, as opposed to the nuclease activity, has remained unclear. There is currently no evidence that the helicase activity contributes to the degradation/resection of DNA ends at reversed forks or DNA double-strand breaks. Interestingly, a number of Dna2 mutants affected within the conserved SF1 helicase motifs I-VI confer growth defects accompanied by sensitivity to the DNA alkylating agent methyl methanesulfonate (MMS)[14,26]. This phenotype is not generally shared with mutants affected in the N-terminal domain[26] or nuclease domain[27], indicating that Dna2 helicase-specific functions in the repair of DNA damage or in the response to damage-induced replication stress exist.

Intriguingly, a genetic screen[28] uncovered a synthetic sick interaction, characterized by slow growth, between *dna2-2*, an allele that encodes a Dna2 variant with a single amino acid change (R1253Q) in the helicase domain[14], and structure-specific *RAD2/XPG* superfamily nuclease *YEN1*, indicating a potential functional interplay. Yen1, and its human orthologue GEN1, are Holliday junction (HJ) resolvases[29]. These enzymes are best known for their role in processing late HR intermediates, such as fully double-stranded DNA (dsDNA) four-way HJ junctions[30]. Eukaryotes use three conserved HJ resolvases, Yen1/GEN1, Mus81-Mms4/human MUS81-EME1 and Slx1-Slx4/human SLX1-FANCP to remove recombination intermediates that form during replication-associated DNA repair processes in mitotic cells[31]. Mounting evidence suggests that Mus81-Mms4/MUS81-EME1 also targets unproductive replication intermediates, effectively breaking stalled replication forks to allow HR-dependent replication restart or repair[32]. In human cells, MUS81-EME1 promotes the expression of chromosomal fragile sites, which is thought to represent controlled breakage of underreplicated DNA at the time of mitosis to limit sister chromatid non-disjunction[33,34]. At present, there is no evidence for a similar role of Yen1/GEN1 in targeting replication—rather than recombination—intermediates.

Here, we analyse the interplay between Dna2 and Yen1 to reveal new aspects of the cellular response to replication stress. We find that the Dna2 helicase activity acts on replication fork stalling, promoting full genome duplication along a pathway parallel to HR-mediated replication fork recovery. If the Dna2 helicase fails to respond properly to stalled replication forks, replication intermediates remain and give rise to post-replicative chromosomal DNA links that preclude chromosome segregation. Resolution is uniquely dependent on the actions of Yen1, which identifies a first non-redundant function of Yen1 in protecting cells from mitotic catastrophe after replication stress.

Results

Dna2^{R1253Q} is helicase defective and nuclease proficient. Using budding yeast, Campbell and colleagues have conducted a large-scale genetic screen[28] using *dna2-2* (R1253Q) and nuclease-defective allele *dna2-1* (P504S)[14], which identified 37 synthetic sick/synthetic lethal interactions, predominantly with genes involved in DNA replication and repair. Many interactions were shared between *dna2-2* and *dna2-1*, but a synthetic sick interaction with *YEN1* was unique to *dna2-2*. Dna2^{R1253Q} is affected at an invariant arginine in helicase motif IV of the SF1 helicase domain, suggesting that the Dna2 helicase and Yen1 may function in related pathways. However, since single amino acid changes in Dna2 have been described that impact both the nuclease and ATPase/helicase activities[35], and because Dna2^{R1253Q} has never been isolated and analysed biochemically, we first assessed directly the mutant protein's ATPase/helicase and nuclease activities. Dna2^{R1253Q} was purified to near-homogeneity following overexpression in *Saccharomyces cerevisiae* (Fig. 1a,b), and tested alongside wild-type Dna2, and well-established[35] nuclease-dead and helicase-dead variants, Dna2^{E675A} and Dna2^{K1080E}, respectively.

When wild-type Dna2 was incubated with 5′-tailed DNA, the activity of the ATPase/helicase domain was readily detected, before the potent Dna2 nuclease degraded the ssDNA tails, so that the ATPase was no longer stimulated and ATP hydrolysis subsided; the nuclease-dead variant Dna2^{E675A} exhibited persistent ATPase activity[35,36] (Fig. 1c). In contrast to wild-type and Dna2^{E675A}, Dna2^{R1253Q} showed no ATPase activity, and was indistinguishable from previously characterized[35,36] ATPase/helicase-dead variant Dna2^{K1080E} (Fig. 1c and Supplementary Fig. 1). *In vitro*, Dna2 exhibits ssDNA-specific nuclease activity on 5′-tailed or 3′-tailed DNA substrates, while RPA stimulates its nuclease and enforces 5′-3′ directionality,

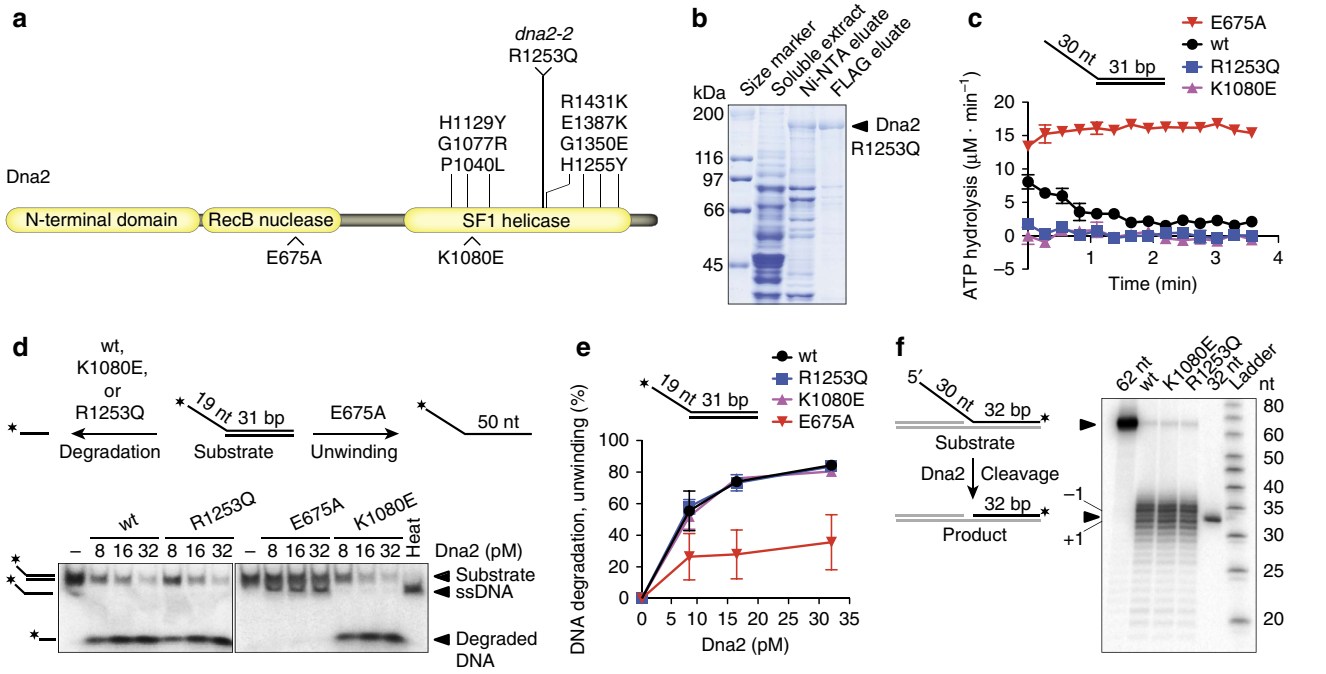

Figure 1 | Biochemical analysis of Dna2 variant R1253Q. (**a**) Domain structure of *Saccharomyces cerevisiae* nuclease-helicase Dna2. *Above*, single amino acid changes within the helicase domain of Dna2 that result in MMS sensitivity, including R1253Q, encoded by *dna2-2*. *Below*, position of mutations E675A and K1080E, which have been shown to inactivate the Dna2 nuclease or helicase activity, respectively. (**b**) $Dna2^{R1253Q}$ carrying 6 × His and FLAG tags was expressed in *S. cerevisiae* and purified by affinity chromatography using nickel-nitrilotriacetic acid (Ni-NTA)-agarose and anti-FLAG affinity gel. Fractions were analysed by polyacrylamide gel electrophoresis followed by Coomassie blue staining. (**c**) Kinetics of ATP hydrolysis by wild-type (wt) Dna2 and indicated variants (all 4 nM) in the presence of a 5′-tailed DNA substrate (1 μM nucleotides). Data are presented as mean values ± s.e.m. ($n = 2$). (**d**) Processing of 5′-tailed DNA by Dna2. The panel shows a representative 10% polyacrylamide gel with reaction products after incubation of the DNA substrate with the indicated DNA2 variants and RPA (16.8 nM). *, position of the ^{32}P-label on the DNA. Heat, heat-denatured DNA substrate. (**e**) Quantification of experiments such as those shown in **d**. Data are presented as mean values ± s.e.m. ($n = 2$). (**f**) 5′-flap cleavage by Dna2 variants (all 2 nM) in the presence of RPA (30 nM). Reaction products were separated on a 20% polyacrylamide denaturing urea gel. Cleavage at the base of the flap produces a radiolabelled fragment of 32 nt.

which is likely the relevant polarity *in vivo*[20]. In the presence of RPA, $Dna2^{R1253Q}$ degraded 5′-tailed DNA in a manner similar to wild-type Dna2, showing that the R1253Q mutation does not interfere with the nuclease activity (Fig. 1d). In line with the observed lack of ATPase activity, we did not find evidence of DNA unwinding by $Dna2^{R1253Q}$, an activity that was readily detected for nuclease-deficient mutant $Dna2^{E675A}$ (Fig. 1d). Quantification of the nuclease/helicase assays showed that $Dna2^{R1253Q}$ was as efficient as wild-type and Dna2 helicase mutant K1080E in degrading 5′-tailed DNA (Fig. 1e). Finally, and in accord with previous studies using other Dna2 helicase mutants[37,38], $Dna2^{R1253Q}$ was fully proficient in removing 5′-flaps from dsDNA by cleavage at the flap base, in a reaction that mimics the potential role of Dna2 in Okazaki fragment processing (Fig. 1f). These results show that the *dna2-2* allele confers a helicase-specific defect and does not impinge on the activity of the Dna2 nuclease.

Checkpoint activation and loss of *YEN1* impair *dna2-2* cells. Having established that the R1253Q mutation selectively inactivates the helicase activity of Dna2, we introduced the *dna2-2* allele into cells to investigate the effect of Dna2 helicase deficiency *in vivo*. While Dna2 protein levels were unaffected (Supplementary Fig. 2a), the R1253Q mutation caused MMS sensitivity, as expected for *dna2-2* cells[14] (Supplementary Fig. 2b). Under unperturbed conditions, the *dna2-2* strain exhibited a plating efficiency similar to wild-type. In contrast, viability dropped sharply for the *dna2-2 yen1*Δ double mutant to ∼35% of wild-type levels (Fig. 2a). Doubling time measurements revealed that the *dna2-2* mutation was associated with a mild slow growth phenotype, extending doubling times by ∼10 min (103 min versus 92 min for wild-type). On deletion of *YEN1*, the growth phenotype was much more severe, with an increase in doubling time of ∼50 min for the double mutant (143.5 min). Consistent with previous results[28], we did not observe a synthetic growth defect when *YEN1* was deleted in Dna2 nuclease-mutant *dna2-1* cells (data not shown), indicating that the genetic interaction between *YEN1* and *DNA2* relates specifically to the Dna2 helicase activity. Contrary to a reported temperature-dependent lethal interaction between *YEN1* and *DNA2* (ref. 28), we found double mutant cells were viable at elevated temperature (37 °C) (Supplementary Fig. 2c), although doubling times for *dna2-2* and *dna2-2 yen1*Δ were further increased by ∼20 and ∼5 min, respectively.

Microscopic inspection of exponentially growing *dna2-2* cultures revealed an accumulation of cells in G2/M phase of the cell cycle, and this effect was further accentuated on deletion of *YEN1*. Morphological examination showed that *dna2-2* cultures contained ∼4% large dumbbell-shaped cells. In *dna2-2 yen1*Δ cultures, this sub-fraction was more extensive, accounting for ∼8% of cells, and ∼5% of cells exhibited morphological changes such as bud elongation and the formation of short chains of elongated cells (Fig. 2b). Finally, the vast majority of G2/M cells within the *dna2-2* and *dna2-2 yen1*Δ cultures (≥70%), but not within wild-type or *yen1*Δ cultures, contained unsegregated nuclear DNA positioned near the bud neck (Fig. 2b).

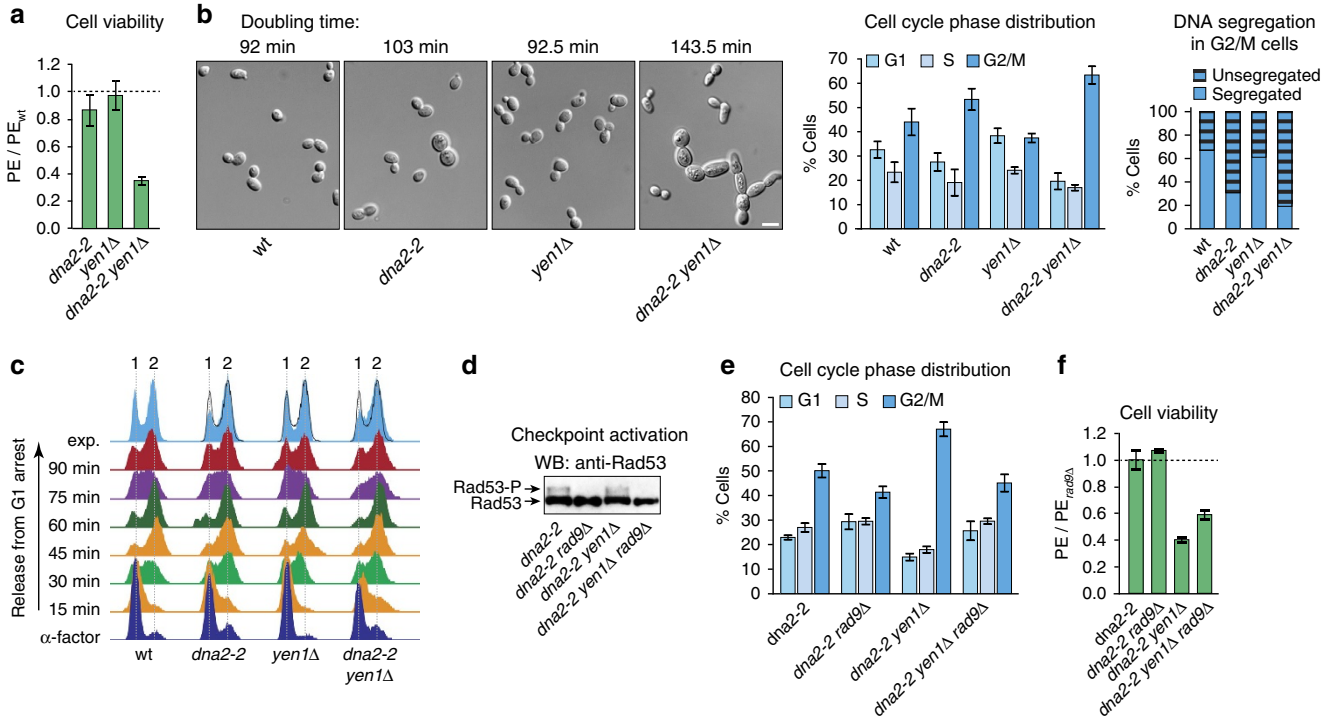

Figure 2 | Dna2 helicase-defective cells suffer dual growth inhibition by checkpoint activation and loss of *YEN1*. (**a**) Cell viability of the indicated strains assessed by colony outgrowth. The mean plating efficiency (PE) ± s.e.m. ($n=3$) is presented relative to wild-type. (**b**) Microscopic analysis of the indicated strains growing exponentially in rich medium. *Left*, representative images (DIC) showing morphological changes associated with Dna2 helicase dysfunction and loss of Yen1. Average doubling times are given ($n=3$). Scale bar, 5 μm. *Centre*, mean distribution of G1, S, and G2/M cells ± s.e.m. ($n=4$). *Right*, DNA segregation in G2/M cells as determined by DAPI-staining. An average of 200 cells were scored per strain. (**c**) Flow cytometric analysis of the indicated strains synchronized in G1 using α-factor and released into YPAD. The position of cells with 1 and 2 N DNA content is indicated. Topmost tracks are asynchronous cultures overlaid with the outline of the wild-type profile, showing that Dna2 helicase-defective strains accumulate cells with a 2 N content over time. (**d**) Western blot analysis showing chronic low-level DNA damage checkpoint activation in Dna2 helicase-defective cells as indicated by Rad53 phosphorylation (Rad53-P). (**e**) Effect of DNA damage checkpoint disruption by deletion of *RAD9* on the distribution of G1, S, and G2/M cells in exponentially growing cultures of the indicated strains. Data presented as mean distribution ± s.e.m. ($n=3$). (**f**) Cell viability of the indicated strains assessed by colony outgrowth. The mean plating efficiency ± s.e.m. ($n=3$) is presented relative to a *rad9*Δ control.

While an accumulation of G2/M cells occurred during exponential growth, analysis by flow cytometry showed that *dna2-2* and *dna2-2 yen1*Δ cells progressed through a single cell cycle with apparently normal kinetics on synchronous release into S phase after α-factor pheromone-induced G1 arrest (Fig. 2c). This indicates that the helicase activity of Dna2 is largely dispensable for bulk DNA synthesis, but that Dna2 helicase-deficient cells have a tendency to arrest at the G2/M transition, as noted previously[14]. Importantly, replication and the G2/M transition phenotype were unaffected by the presence or absence of Yen1. The accumulation of G2/M cells may result from elevated levels of stochastic DNA damage, since we detected low-level phosphorylation of the checkpoint kinase Rad53 in *dna2-2* and *dna2-2 yen1*Δ cells in unperturbed conditions, which was suppressed on deletion of the DNA damage checkpoint mediator *RAD9* (Fig. 2d). Moreover, the levels of G2/M cells in either strain were much reduced in the absence of *RAD9*, and bud-elongation and cell-chain formation was no longer observed (Fig. 2e and data not shown). The extended doubling times for the *dna2-2* and *dna2-2 yen1*Δ strains were reduced on *RAD9* deletion, albeit not to wild-type levels (96 and 122 min, respectively). Significantly, the viability of both *dna2-2* and *dna2-2 rad9*Δ cells was indistinguishable from the *rad9*Δ control, whereas the severe reduction of viability we had observed on loss of *YEN1* in the *dna2-2* background was only mildly suppressed by *RAD9* deletion (Fig. 2f). Together these data suggest that growth defects in *dna2-2 yen1*Δ cells arise from two separate sources: (1) Dna2 helicase dysfunction causes cells to accumulate DNA lesions during unperturbed growth, triggering Rad9-dependent DNA damage checkpoint activation and a delay at the G2/M transition. (2) Yen1 cannot prevent these defects, so that they manifest themselves similarly in *dna2-2 yen1*Δ double mutant and *dna2-2* single mutant cells. Yet, the absence of Yen1 is toxic to *dna2-2* cells, indicating that Yen1 acts downstream, resolving a catastrophic DNA metabolic event that ensues when the Dna2 helicase is non-functional.

Yen1 is critical in *dna2-2* cells under replication stress. Dna2 helicase deficiency sensitizes cells to DNA alkylating agent MMS[14,26] (Supplementary Fig. 2b). To test whether loss of Yen1 has an additional effect on the MMS sensitivity of Dna2 helicase-defective cells, we exposed *dna2-2 yen1*Δ cells to increasing amounts of the drug. As expected[39], loss of *YEN1* alone did not result in overt MMS sensitivity. In contrast, *dna2-2 yen1*Δ cells proved to be several orders of magnitude more sensitive than *dna2-2* cells in drop assays (Fig. 3a). This phenotype was not restricted to MMS, and similar results were obtained with topoisomerase I poison camptothecin (CPT) and ribonucleotide reductase inhibitor hydroxyurea (HU). These drugs have disparate mechanisms of action, but their effects (DNA damage, accumulation of trapped Top1 cleavage complexes throughout the genome and nucleotide depletion, respectively) all inhibit the progression of replication forks,

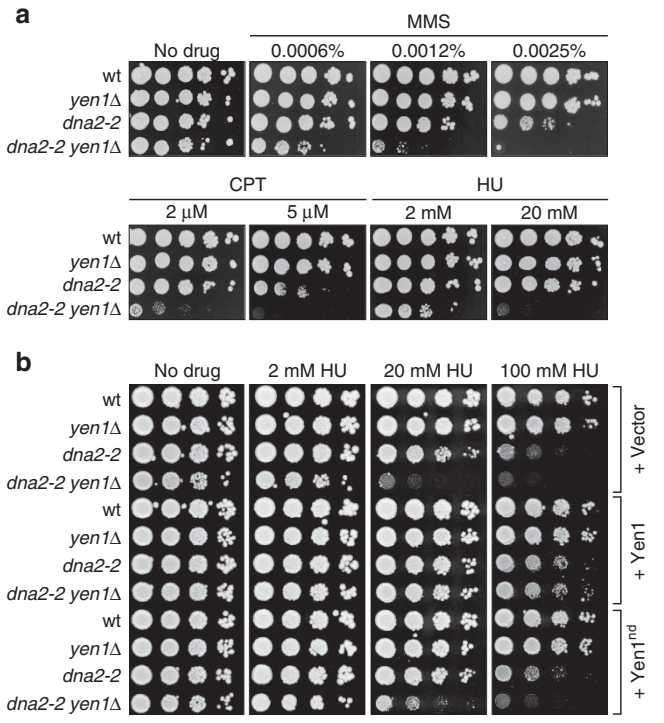

Figure 3 | Dna2 helicase dysfunction and loss of Yen1 nuclease activity synergistically sensitize cells to exogenous replication stress. (**a**) Drop assays to determine the drug-sensitivity of the indicated strains were done by spotting normalized tenfold serial dilutions of exponentially growing cells onto YPAD plates containing the indicated amounts of MMS, CPT or HU. (**b**) Analysis of the effects of Yen1 overexpression. Cells of the indicated strains were transformed with empty vector, or derivatives encoding wild-type or nuclease-deficient (Yen1nd) versions of Yen1, and plated on YPAD medium in the presence or absence of HU.

suggesting that the functional overlap of Dna2 and Yen1 relates to replication fork stalling. This also suggests that endogenous replication problems are responsible for the growth defects of *dna2-2* and *dna2-2 yen1*Δ cells in unperturbed conditions.

Plasmid-based expression of Yen1 suppressed the HU sensitivity phenotype of *dna2-2 yen1*Δ cells. This suppression was strictly dependent on the nuclease activity of Yen1, demonstrating that Yen1 protects *dna2-2* cells through nucleolytic cleavage of otherwise toxic DNA intermediates (Fig. 3b).

DNA damage follows acute replication stress in *dna2-2* cells. To investigate the immediate effects of replication stress on Dna2 helicase-defective cells, we next performed mitotic time-course experiments (Fig. 4). Synchronized *dna2-2* and *dna2-2 yen1*Δ cells were released into S phase under mild replication stress conditions in the presence of 50 mM HU, which impairs, but does not block, replication. After 2 h, cells were shifted back to drug-free medium. DNA synthesis was monitored by flow cytometry, while DNA replication/DNA damage checkpoint activation was assessed by Western blot analysis of the phosphorylation status of Rad53. As expected, wild-type and *yen1*Δ cells exhibited slowed replication progression in the presence of HU. Interestingly, *dna2-2* and *dna2-2 yen1*Δ cells progressed through S phase at a pace similar to wild-type. As shown in Fig. 4a, all strains showed S phase checkpoint activation in the presence of HU, and S phase checkpoint silencing occurred with normal kinetics across strains, followed by completion of bulk DNA synthesis in drug-free medium. One hundred twenty minutes after removal of HU, wild-type and *yen1*Δ cells underwent cell division. In contrast, *dna2-2* and *dna2-2 yen1*Δ cells exhibited a reemergence of Rad53 phosphorylation and remained in G2/M with a 2 N DNA content. This biphasic Rad53 phosphorylation pattern, with an unexpected second wave of checkpoint activation in G2/M phase, required both the presence of the *dna2-2* allele and replication stress in the preceding S phase (that is, it was not discernible above background in control experiments without HU; Supplementary Fig. 3). One interpretation of these observations is that the Dna2 helicase is involved in an immediate response to replication fork stalling, preventing the emergence of DNA structures that signal DNA damage in G2/M.

The presence of Yen1 could not protect Dna2 helicase-defective cells from G2/M checkpoint activation and cell cycle arrest after acute replication stress. However, in the presence of Yen1, the G2/M arrest proved more transient. Thus, G1 cells with a 1 N DNA content started to appear 240 min after removal of HU, and continued to appear through overnight incubation in the *dna2-2* culture, while the *dna2-2 yen1*Δ strain produced very few G1 cells, as judged by flow cytometry (Fig. 4a). Microscopic analysis showed that within the *dna2-2 yen1*Δ culture ~11% of cells had segregated their nuclear DNA, while the *dna2-2* culture contained a significantly higher number of cells, ~32%, with segregated DNA after overnight incubation (Fig. 4b). This correlated with a significantly lower lethality scored for *dna2-2* mutants (~28% viability compared to wild-type) than for the *dna2-2 yen1*Δ double mutant (<1% viability compared to wild-type) (Fig. 4c). We conclude that Yen1 promotes mitotic exit with viable chromosome segregation in Dna2 helicase-defective cells recovering from acute replication stress.

Yen1 resolves *dna2-2* post-replicative chromosome links. A potential explanation for the apparent slow recovery of *dna2-2* cells from G2/M checkpoint arrest relates to recent work showing that Yen1 activity is cell cycle-regulated, with cyclin-dependent kinase (CDK)-mediated phosphorylation lowering its catalytic activity and inhibiting access to the nucleus in S and G2 phase[40]. Upon anaphase onset, Cdc14-dependent dephosphorylation activates Yen1 and allows the protein to accumulate inside the nucleus during mitosis. To test whether Yen1 cell cycle control is manifest in Dna2 helicase-defective cells recovering from acute replication stress, we expressed and monitored a functional (Supplementary Fig. 4a) version of Yen1, tagged with enhanced green fluorescent protein (EGFP), in *dna2-2* and wild-type cells. The expected bi-phasic checkpoint activation of *dna2-2* cells in response to acute HU treatment was recapitulated in the presence of Yen1-EGFP (Supplementary Fig. 4b), and the fusion protein exhibited the characteristic cell cycle-dependent subcellular localization reported for Yen1 (Fig. 5a)[40]. Importantly, when cells accumulated as large-budded G2/M cells after HU wash-out, a subset of cells was double-nucleated with a nuclear Yen1-EGFP signal, indicating that mitotic entry had occurred. This subset of cells was markedly larger in case of the wild-type strain after 2 h in drug-free medium (Fig. 5b). After 4 h in drug-free medium, the fraction of wild-type G2/M cells diminished as cells underwent mitosis. In contrast, *dna2-2* cells remained mostly in G2/M, with Yen1-EGFP in the cytoplasm and a single nucleus at the bud neck, as expected for DNA damage checkpoint-mediated pre-anaphase arrest. Thus, targeting of Yen1 to the nucleus through the actions of Cdc14 (ref. 40) remained largely blocked, showing that unscheduled DNA damage checkpoint signalling in *dna2-2* cells is associated with retention of Yen1 in the cytoplasm, and that this may

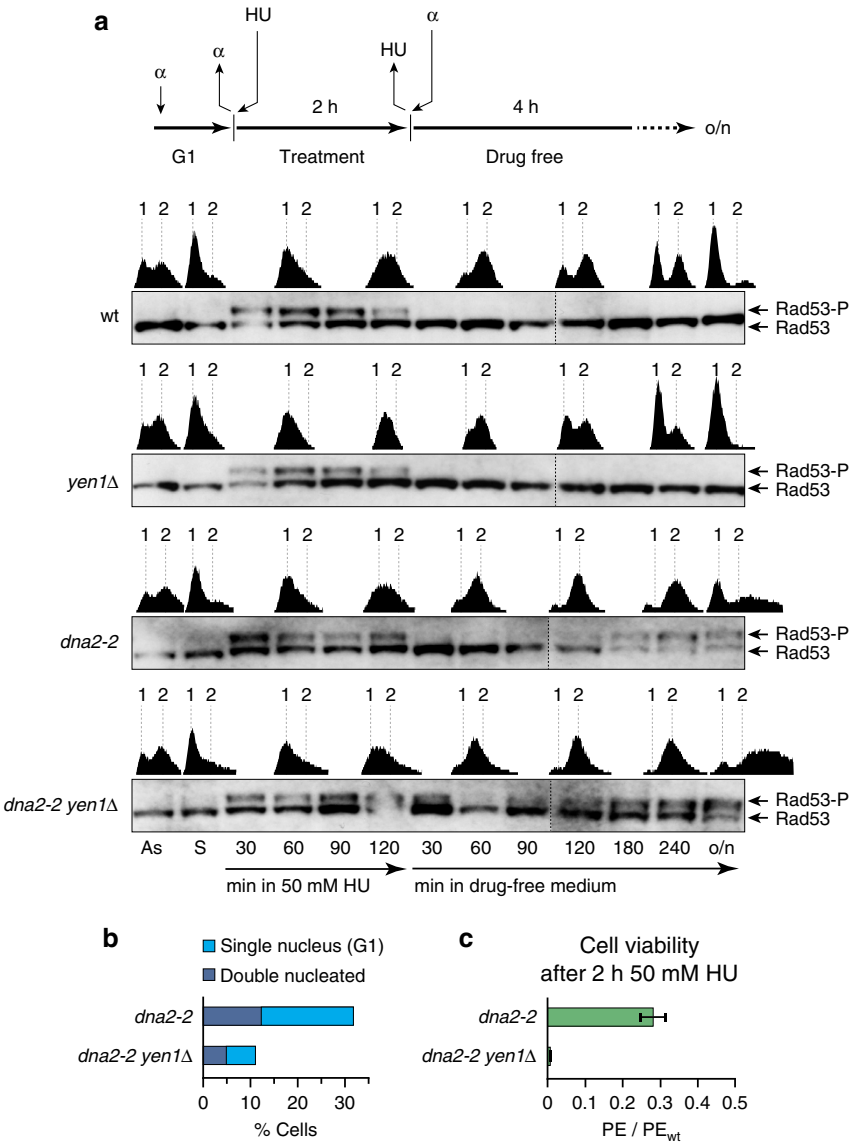

Figure 4 | Dna2 helicase-defective cells are defective in the response to acute replication stress and require Yen1 for subsequent growth. (**a**) Mitotic time-courses were performed as indicated. Cells, synchronized in G1, were released into acute replication stress in medium containing 50 mM HU for 2 h, followed by drug wash-out and incubation in drug-free medium with α-factor. Checkpoint activation and the progression of DNA replication were monitored by Western blot analysis of Rad53 phosphorylation (Rad53-P) and flow cytometry (1 and 2 N DNA content indicated). As, asynchronous; S, synchronous; o/n, overnight. (**b**) Quantification of single-nucleated G1 cells and double-nucleated G2/M cells in the indicated overnight yeast cultures shown in **a**. Two hundred cells per strain were analysed by microscopic inspection. (**c**) Viability of the indicated strains after acute replication stress. Cells were plated on drug-free YPAD medium and colony formation was quantified. The mean plating efficiency (PE) ± s.e.m. ($n = 3$) is presented relative to wild-type.

represent a major impediment to the recovery of Dna2 helicase-defective cells from replication stress.

To test this idea further, we next disrupted the G2/M DNA damage checkpoint by deletion of *RAD9*, allowing unrestrained anaphase entry, and thus Yen1 activation, in Dna2 helicase-defective cells. Upon acute replication stress treatment, checkpoint activation during S phase occurred normally in the absence of Rad9, consistent with signalling in response to replication fork stalling, rather than DNA damage, through the intact Mec1-Ddc2/Mrc1/Rad53-dependent pathway. In contrast, unscheduled Rad53 phosphorylation in G2/M phase after HU wash-out was abolished in *dna2-2 rad9*Δ and *dna2-2 yen1*Δ *rad9*Δ cells (Fig. 5c). Dna2 helicase-defective cells now progressed to cell division with kinetics similar to those exhibited by the *rad9*Δ control strain, and we were able to study the effects of Yen1 by microscopic inspection. This revealed two important phenotypes associated with concomitant loss of Dna2 helicase function and Yen1. Sixty minutes after the removal of HU, *dna2-2 yen1*Δ *rad9*Δ samples contained roughly threefold higher levels of early anaphase cells characterized by an elongated nucleus stretched through the bud neck, as compared to *dna2-2 rad9*Δ and *rad9*Δ samples. Concomitantly, there was a delay in the appearance of G1 cells containing a single nucleus (Fig. 5d). This suggests that chromosome segregation and cytokinesis were physically impeded in the absence of Yen1. Consistently, and exclusively in *dna2-2 yen1*Δ *rad9*Δ cells, we observed prominent chromosomal DNA bridges that span the bud neck and connect the segregating masses of nuclear DNA (13.6 and 8% of the double-nucleated cells affected 180 and 240 min after HU wash-out, respectively) (Fig. 5e). In some instances this phenotype could be seen in cells approaching abscission, as indicated by a narrowing bud neck.

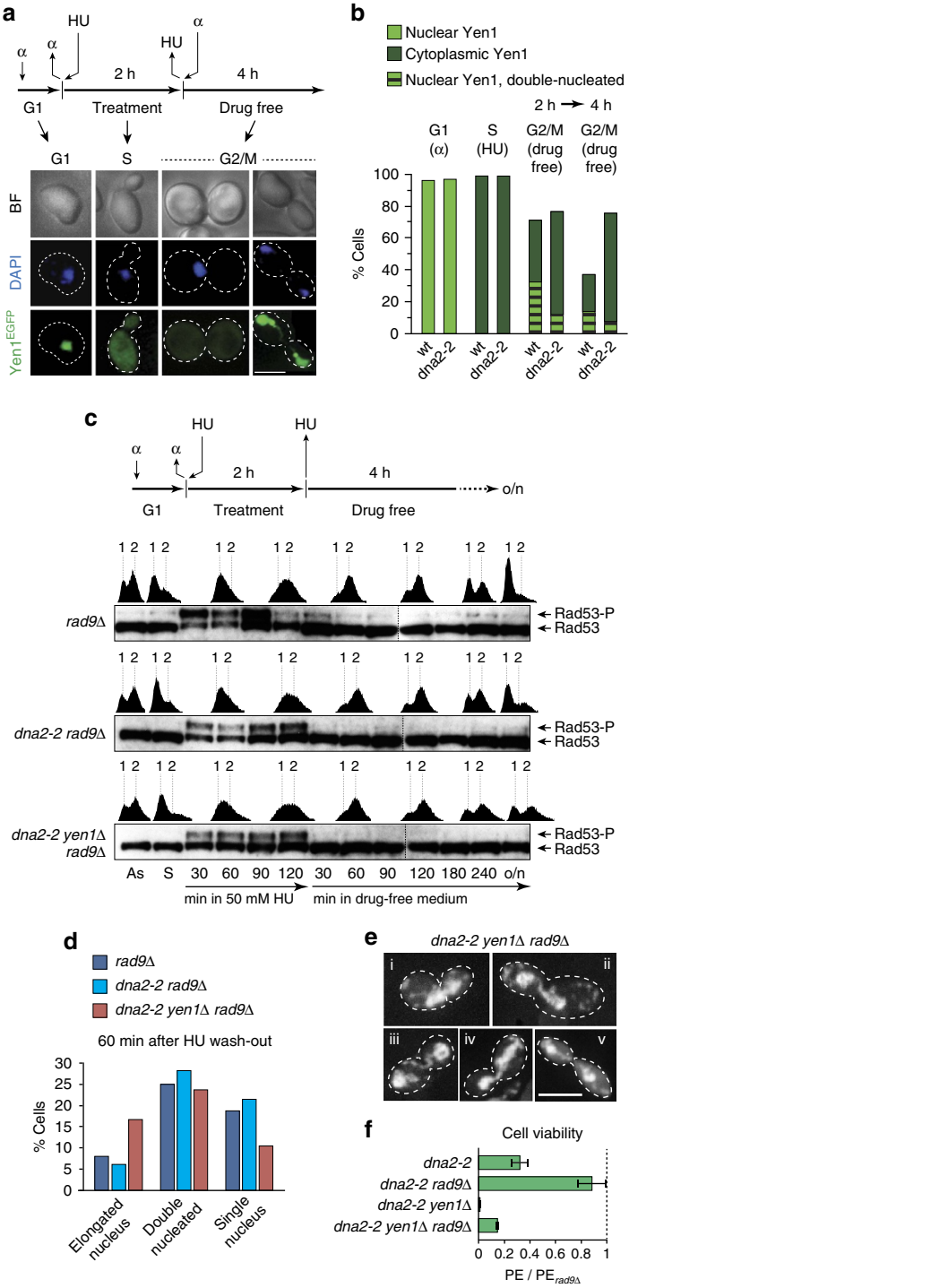

Figure 5 | Post-replicative chromosomal links in Dna2 helicase-defective cells and mitotic resolution by Yen1. (**a**) Subcellular localization of Yen1 in *dna2-2* cells exposed to acute replication stress. Mitotic time-courses were performed as indicated with wild-type and *dna2-2* cells expressing Yen1-EGFP. Samples were analysed for nuclear and cytoplasmic localization of Yen1-EGFP following α-factor arrest, 1 h after release into HU-containing medium, and 2 and 4 h after drug wash-out. Representative images are shown. Scale bar, 5 μm. (**b**) Quantitative view of Yen1-EGFP localization as determined in experiments such as those shown in **a** (≥100 cells scored for G1 and S phase per strain; ≥200 cells 2 and 4 h after drug wash-out). (**c**) Mitotic time-course experiment with DNA damage checkpoint-disrupted strains, performed as indicated and analysed as described for Fig. 4a. (**d**) Relative distribution of cells in early anaphase (elongated nucleus), late anaphase (double-nucleated) and post-cytokinesis (single-nucleated), as determined by microscopic inspection of samples from **c**, 60 min after HU wash-out (≥100 cells scored per strain). (**e**) Representative microscopic images showing an early anaphase cell with elongated nucleus spanning the bud neck (i), and late anaphase cells with chromosomal DNA bridges between the segregated masses of nuclear DNA (ii-v), a phenotype exclusively observed in *dna2-2 yen1Δ rad9Δ* cells. Cells treated as described for **c**. Scale bar, 5 μm. (**f**) Cell viability of the indicated strains, treated as in **c**, assessed by colony outgrowth. The mean plating efficiency (PE) ± s.e.m. ($n = 3$) is presented relative to *rad9Δ*.

When we determined the effect of checkpoint disruption on cell viability, we found that deletion of *RAD9* increased the viability of Dna2 helicase-defective cells after acute replication stress treatment threefold, reaching levels very similar to those observed for the *rad9*Δ control strain. In the absence of *YEN1*, viability was also improved, but did not reach more than ~14% of the viability of the *rad9*Δ control (Fig. 5f). Checkpoint activation in Dna2 helicase-defective cells after acute replication stress therefore appears futile, and eliminating the G2/M checkpoint enabled a highly effective Yen1-dependent survival pathway, while allowing a small subset of cells to survive in a Yen1-independent manner. As expected, checkpoint disruption had no beneficial effect when cells were exposed to chronic replication stress (Supplementary Fig. 5), consistent with improved survival being linked specifically to allowing Yen1 access to post-replicative lesions in Dna2 helicase-defective cells after acute replication stress. These observations resonate with previous findings showing that the lethality of some temperature-sensitive *dna2* alleles, and of *dna2*Δ, can be suppressed by deleting *RAD9* (refs 14,41,42), linking this phenomenon, at least for the Dna2 helicase-defective *dna2-2* allele, to the removal of the inhibitory effect of the G2/M DNA damage checkpoint on Yen1 activation.

To test whether Yen1 activation, not mitotic entry *per se*, is sufficient for Yen1 to resolve aberrant DNA intermediates that arise in Dna2 helicase-defective cells, we used a constitutively active form of Yen1, referred to as Yen1^{on} (Supplementary Fig. 6a). Yen1^{on} is not controlled by CDK and therefore permanently active and nuclear[43]. We expressed Yen1^{on} from a galactose-inducible promoter in G2/M in *dna2-2 yen1*Δ cells recovering from acute, HU-induced replication stress in the presence of nocodazole. Strikingly, Yen1^{on}-expressing cells did not exhibit unscheduled DNA damage checkpoint activation during nocodazole-induced G2/M arrest (Supplementary Fig. 6b). Furthermore, transient expression of Yen1^{on} in *dna2-2* cells recovering from acute HU treatment led to a significant increase in cell viability (~3.3-fold ± 0.24 s.e.m., $n = 2$), as determined by colony outgrowth.

Collectively, these results suggest that Dna2 helicase-defective cells fail to respond adequately to replication stress, leading to post-replicative DNA damage signalling and chromosome entanglements. Upon anaphase entry, Yen1 promotes the survival of Dna2 helicase-defective cells by resolving post-replicative chromosomal DNA links, allowing proper chromosome segregation.

Yen1 acts distinct from HJ resolution in *dna2-2* cells. Yen1 is known for its role in removing persistent HJ DNA structures that accumulate as Rad52-dependent HR intermediates. Previous findings also suggest an increased requirement for Rad52-dependent DNA repair by HR in Dna2 helicase-defective cells. Thus, *dna2-2 rad52*Δ cells without overt growth defect at 30 °C, but temperature sensitivity at a restrictive temperature of 37 °C, have been described[44]. We generated *dna2-2 rad52*Δ cells and found that compared to *dna2-2* (103 min) and *rad52*Δ (112 min), double mutant cells grew slowly, even at 30 °C, with a doubling time of 144 min. Furthermore, loss of Rad52 led to pronounced synthetic hypersensitivity of *dna2-2* cells to HU (Fig. 6a). Finally, we observed a significant increase of spontaneous Rad52 foci, indicative of HR[45], in *dna2-2* cells in unperturbed conditions (Fig. 6b), whereas Dna2 focus formation is elevated in *rad52*Δ cells[46]. This suggests that Dna2 and Rad52-dependent HR represent parallel and compensatory pathways in the response to replication stress.

Elevated levels of HR repair could explain why loss of Yen1 is detrimental to *dna2-2* cells. If so, *dna2-2 mus81*Δ cells should exhibit an even stronger growth defect than *dna2-2 yen1*Δ cells, given that Mus81-Mms4 is activated, in a CDK-dependent manner, prior to Yen1 activation at anaphase onset. Reaching an activity peak in its hyperphosphorylated state in G2/M, Mus81-Mms4 is thus the major nuclease in removing HR intermediates in budding yeast[40]. Notwithstanding, we found that in contrast to loss of Yen1, disruption of Mus81-Mms4, or the Slx1-Slx4 HJ resolvase, did not increase the doubling time of *dna2-2* cells in unperturbed conditions. In the presence of HU or MMS, deletion of *SLX1* had no effect on the sensitivity of Dna2 helicase-defective cells. Deletion of *MUS81*, which in itself results in replication stress sensitivity, added to their sensitivity (Fig. 6c and data not shown), consistent with a requirement for Mus81-Mms4 in the resolution of excessive HR intermediates in *dna2-2* cells. However, *dna2-2 yen1*Δ cells were significantly more sensitive to HU or MMS than *dna2-2 mus81*Δ cells (0.2 versus 45% cell survival at 20 mM HU as determined by colony outgrowth) (Fig. 6c,d and data not shown), despite the fact that defects related to HJ resolution as a consequence of Yen1 loss have been shown to transpire only in the absence of a functional Mus81-Mms4 resolvase[39]. Therefore, there is a pathway, distinct from canonical HJ resolution, which uniquely requires Yen1 for the removal of DNA intermediates that are apparently not amenable to cleavage by Mus81-Mms4, in *dna2-2* cells. Indeed, the toxicity caused by loss of Yen1 cannot be explained by an accumulation of HR intermediates alone, as we found that the synthetic sick relationship between *DNA2* and *YEN1* is maintained in cells deleted for *RAD52*, which cannot engage in HR reactions. In fact, we were unable to generate a *dna2-2 rad52*Δ *yen1*Δ triple mutant by tetrad dissection (data not shown), and have confirmed an essential requirement for Yen1 in *dna2-2 rad52*Δ cells using a plasmid-based assay (Fig. 6e). These results contrast with an epistatic relationship that exists between *RAD52* and the HJ resolution pathway defined by *MUS81-MMS4* and *YEN1* (refs 39,47), and imply that the structures that are targeted by Yen1 in order to maintain the viability of Dna2 helicase-defective cells derive from perturbed replication intermediates in a HR-independent manner.

Yen1 resolves DNA replication intermediates in *dna2-2* cells. To address the question whether replication fork stalling in Dna2 helicase-defective cells gives rise to an accumulation of DNA intermediates that might become targets for Yen1, we turned to the natural replication fork barrier (RFB)[48] within the ribosomal DNA (rDNA) on chromosome XII. We compared rDNA from actively replicating wild-type and *dna2-2* mutant cells by two-dimensional (2D) gel electrophoresis and monitored the disappearance of replication intermediates as cells progressed from S phase to nocodazole-induced G2/M arrest. In S phase, Dna2 helicase-defective cells showed a pattern of replication intermediates very similar to wild-type (Fig. 6f). As expected, replication intermediate levels dropped significantly when cells accumulated in G2/M during nocodazole arrest. However, the resolution of replication intermediates, in particular of RFB-stalled and converged forks, was less efficient in *dna2-2* cells, leading to a ~2 and ~3-fold less prominent decrease compared to wild-type, respectively. These results are in good agreement with previous observations of accumulating stalled and converged fork intermediates within the rDNA of *dna2-2* cells[49], and corroborate the notion of an aberrant response to replication fork stalling in Dna2 helicase-defective cells. To see if Yen1 targets aberrant replication intermediates that persist in Dna2 helicase-defective cells, we expressed, in asynchronous *dna2-2* cultures, constitutively active Yen1^{on} (Fig. 6g), allowing us to monitor Yen1 actions prior to the activation of endogenous Yen1 and chromosome segregation in M phase. Similar to staged S phase cells, 2D gel electrophoresis of exponentially growing

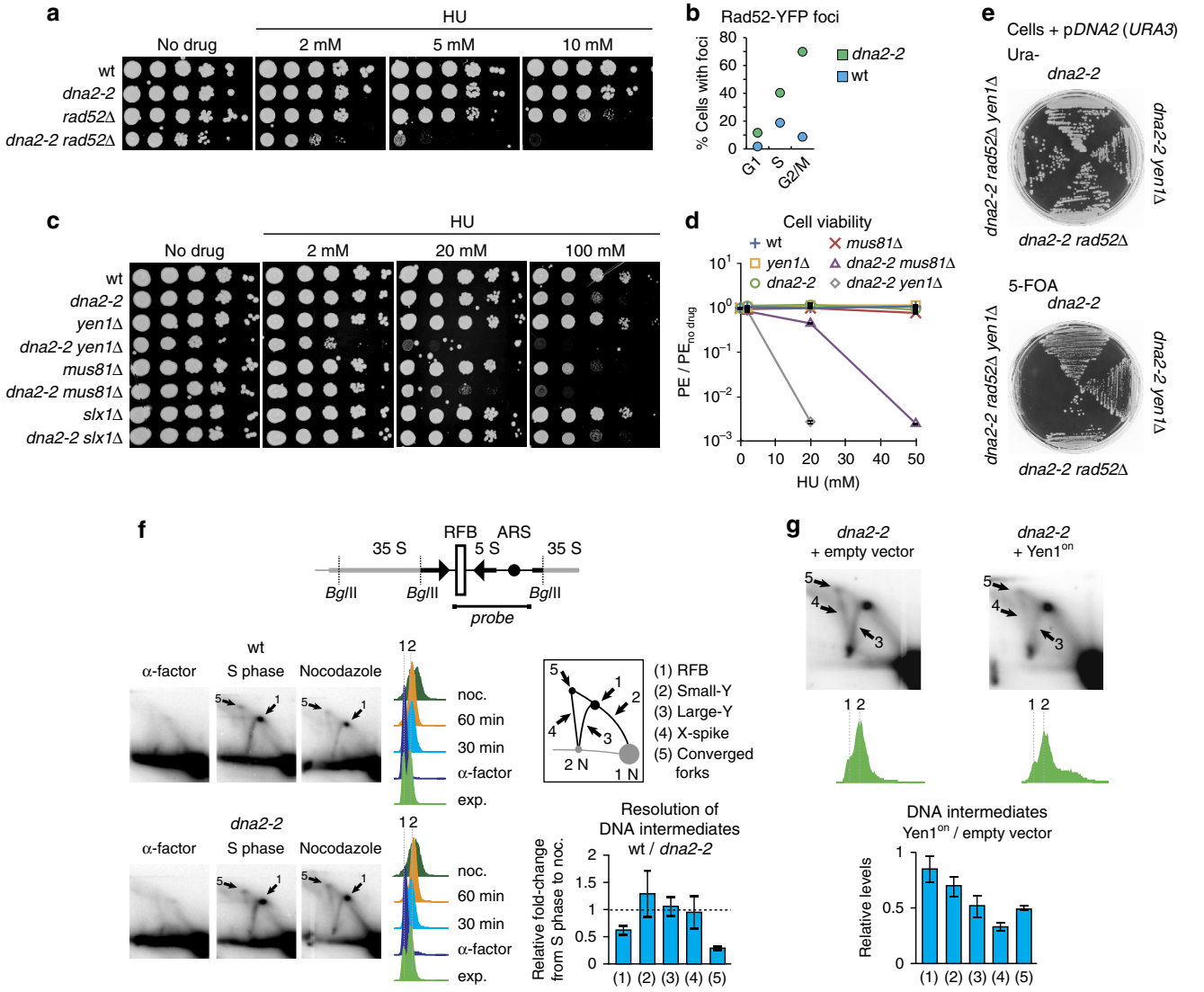

Figure 6 | Yen1 uniquely resolves toxic DNA intermediates in Dna2 helicase-defective cells along a pathway distinct from canonical HJ resolution. (**a**) Synergistic defects in the resistance to replication stress in homologous recombination-deficient *dna2-2 rad52Δ* cells. Drop assay performed as in Fig. 3a. (**b**) Spontaneous Rad52-YFP foci in wild-type and *dna2-2* cells in different cell cycle stages, determined by microscopic analysis (≥180 cells scored per strain). (**c**) Genetic interactions of *dna2-2* with HJ resolvases *YEN1*, *MUS81-MMS4* and *SLX1-SLX4*. Drop assays performed as in Fig. 3a. (**d**) Mean plating efficiency (PE) ± s.e.m. ($n=3$) of the indicated strains assessed by colony outgrowth in the presence of increasing amounts of HU, relative to no-drug conditions. (**e**) Interaction between *dna2-2*, *RAD52* and *YEN1*. Cells of the indicated genotypes and containing a plasmid expressing wild-type *DNA2* (p*DNA2*) were grown under uracil selection to ensure retention of the p*DNA2*, or on medium containing 5-FOA to select against the plasmid. Failure to grow on 5-FOA is indicative of an inviable genotype. (**f**) Analysis of replication and recombination intermediates in the rDNA of wild-type and *dna2-2* cells traversing S phase into nocodazole-induced G2/M arrest. Genomic DNA was digested with *Bgl*II and subjected to 2D gel electrophoresis. The fragment probed by Southern hybridization contained the rDNA autonomously replicating sequence (ARS), the 5S transcriptional unit, and the RFB in its centre, as indicated. DNA structures chosen for quantification included RFB-arrested forks (1), Y-arc structures containing a replication fork at varying positions outside the RFB (2,3), the X-spike indicative of four-way branched DNAs containing Holliday junctions or hemicatenanes (4), and forks converging at the RFB (5). Representative autoradiographies are marked for RFB-stalled (1) and converged replication fork intermediates (5), which were resolved less efficiently in *dna2-2* cells compared to wild-type following S phase. Three independent experiments were quantified and the data are presented as mean values ± s.e.m. (**g**) 2 D analysis as in **f**, but using exponentially growing *dna2-2* cells expressing or not Yen1^{on}. Intermediates that were reduced upon Yen1^{on} expression are indicated. Three independent experiments were quantified and the data are presented as mean values ± s.e.m.

dna2-2 cells showed the expected rDNA replication intermediates and, in addition, a more prominent signal indicative of recombination intermediates (X-spike), consistent with an accumulation of G2/M cells with increased rates of HR[49]. Yen1^{on} did not affect the RFB signal, suggesting that replication forks arrested at the barrier are not immediately susceptible to Yen1 nuclease activity. In contrast, and consistent with the ability of Yen1 to resolve recombination intermediates, moderate constitutive Yen1^{on} expression markedly reduced the X-spike signal. Importantly, single fork intermediates (Y structures) and converged forks were also decreased on Yen1^{on} expression, showing that Yen1, in addition to resolving four-way X-DNA, is able to remove replication intermediates that accumulate in Dna2 helicase-defective cells. These results suggest that endogenous Yen1, activated on anaphase entry, uniquely resolves persistent replication fork/converging fork structures to disentangle

underreplicated nascent sister chromatids when Dna2 helicase-defective cells enter mitosis, thereby safeguarding chromosome segregation and enabling viable mitotic exit.

Discussion

Our analyses of the interplay between Dna2, HJ resolvase Yen1 and the DNA damage checkpoint allows us to define important functions of the Dna2 helicase activity and the Yen1 nuclease in the replication stress response. We propose a model, where the Dna2 helicase activity represents a HR-independent replication stress response pathway that helps to ensure full replication of the genome. Replication intermediates that escape the attention of Dna2 persist and impair sister chromatid separation, unless they are resolved by Yen1 in mitosis. Thus, the actions of Yen1, which has so far only been known to target HR intermediates, allow viable chromosome segregation along a novel pathway, distinct from canonical HJ resolution (Fig. 7).

The precise constitution of the DNA structures that threaten chromosome segregation in Dna2 helicase-defective cells remains to be determined. However, the fact that Yen1 can detoxify them indicates that these DNA intermediates conform to the substrate spectrum of Yen1, which includes 5′-flaps and fully double-stranded DNA three-way and four-way junctions[29,43]. As $Dna2^{R1253Q}$ retains 5′-flap endonuclease activity (Fig. 1f), this activity of Yen1, which could potentially support the proposed role of Dna2 in Okazaki fragment processing[18,19], is unlikely to explain the requirement for Yen1 in Dna2 helicase-defective cells. Consistently, we find no genetic indication that Yen1 might support functions of the major Okazaki fragment processing nuclease Rad27 *in vivo* (Supplementary Fig. 7). We thus favour the possibility that the capacity of Yen1 to target branched dsDNA intermediates is relevant for the protection of *dna2-2* cells. This ability distinguishes Yen1, Mus81-Mms4 and Slx1-Slx4 from other structure-specific nucleases, and allows them to resolve HR-dependent HJs, but also analogues of replication forks, and presumably reversed fork intermediates, which are structurally equivalent to four-way HJs[30,32,50]. DNA intermediates that require detoxification by Yen1 arise in Dna2 helicase-defective cells in the absence of Rad52 (Fig. 6e), and in the presence of Mus81-Mms4, which we find in the active, hyperphosphorylated[40] form in post-replicative *dna2-2* cells (Supplementary Fig. 8). Therefore, Yen1 appears not to be primarily required to remove HR intermediates in *dna2-2* cells, but instead for removing persistent replication intermediates, such as arrested forks or converged forks that fail to fuse (Fig. 6f,g). Of note, a similar activity of MUS81-EME1 towards late replication intermediates has been shown to avoid sister chromatid non-disjunction in human cells[33,34]. Thus, Yen1 and other HJ resolving enzymes might function in complementary fashion, rather than redundantly, in targeting dead-end replication intermediates to protect chromosome segregation.

Persistent replication intermediates could explain chromosome non-disjunction in Dna2 helicase-defective cells (Fig. 5e), and it is tempting to speculate that the Dna2 helicase activity may be involved in replication fork remodelling reactions that facilitate fork recovery. This would be conceptually similar to the role of the Dna2 nuclease in replication restart at reversed forks through degradation of the regressed DNA branch[21–23]. A particularly attractive possibility is that fork reversal might occur and/or persist as a consequence of Dna2 helicase dysfunction. The resulting chicken-foot structure, which effectively contains a single-ended DNA double-strand break at the tip of the regressed DNA branch, could account for DNA damage checkpoint activation[51], which we observe in Dna2 helicase-defective cells (Figs 2d,4a and 5c). A four-way chicken-foot DNA intermediate would also be amenable to resolution by Yen1; perhaps more so than by Mus81-Mms4, which is greatly stimulated by pre-existing nicks within DNA junctions, such as those that may be present in HR-dependent joint molecules and maturing HJs prior to a final ligation step[29,30,43]. Importantly, and regardless of their exact structural features, the intermediates resolved by Yen1 in Dna2 helicase-defective cells constitute a first DNA target that is uniquely processed by Yen1. This demonstrates greater complexity in the uses of HJ resolvases in cells, and could explain the evolutionary conservation of Yen1/GEN1.

Intriguingly, Dna2 and Yen1 are both subject to CDK1-regulated nucleocytoplasmic shuttling[52] (Fig. 7b). During S phase, phosphorylation of Yen1 mediates nuclear exclusion, whereas phospho-Dna2 accumulates inside the nucleus. Thus, Dna2 can access sites of impaired DNA replication, and, consistently, has been found to form discrete nuclear foci during HU-induced replication arrest[53]. Dna2 helicase dysfunction gives rise to lesions that require Yen1 for resolution, but also triggers G2/M checkpoint activation, precluding dephosphorylation-dependent Yen1 activation and translocation to the nucleus on anaphase entry (Fig. 5a). Paradoxical though it may seem, this likely reflects a trade-off between the need to protect chromosomes from the DNA de-branching activities of Yen1 during S phase, while exploiting its unique biochemical properties to remove persistent chromosomal DNA links in M phase. Indeed, $Yen1^{on}$ expression in G2/M allows resolution of toxic DNA intermediates in *dna2-2* cells (Supplementary Fig. 6), but constitutive expression is associated with MMS sensitivity, and tight control over the activities of HJ resolvases has been shown to limit sister chromatid exchange and the risk of loss of heterozygosity[40,54–56]. Despite the risk of terminal G2/M arrest, Yen1 effectively maintains the viability of Dna2 helicase-defective cells in unperturbed conditions (Fig. 2a), indicating its late activation as an elegant failsafe mechanism that allows Yen1 to act indiscriminately on DNA structures that resemble normal replication intermediates, identified as aberrant only by their presence at the wrong time in the cell cycle. In future, it will be interesting to see whether Yen1 represents a more general surveillance nuclease for aberrant replication intermediates that persist into anaphase. Strong G2/M checkpoint signalling and terminal arrest at the G2/M boundary might have precluded the detection of Yen1 functions downstream of repair and replication factors other than *DNA2* in large-scale screening efforts thus far.

Loss and overexpression of DNA2 has been observed in human cancers and cancer cell lines[12,57,58], while haploinsufficiency promotes cancer formation in heterozygous *DNA2*-knockout mice[9]. This suggests a complex role in cancer, where genome instability caused by impaired DNA2 function may drive tumorigenesis, whereas upregulation of *DNA2* may help cancer cells to survive continuous DNA replication stress. Interestingly, a homozygous mutation in *DNA2* has recently been identified in patients with Seckel syndrome[59], a disease associated with a compromised response to replication fork stalling on the cellular level[60]. Depletion of DNA2 in mammalian cells recapitulates many of the phenotypes seen in Dna2-defective yeast, including sensitivity to replication stress, elevated DNA damage, chromosome instability and G2/M cell cycle delay[9–12], indicating functional conservation. Our results implicate the elusive Dna2 helicase in replication fork recovery. Yen1 provides a downstream survival pathway, along which toxic DNA intermediates that arise when the Dna2 helicase activity fails to respond adequately to replication fork stalling are resolved. Similar two-tiered mechanisms may contribute to the aetiology of human pathologies involving *DNA2*.

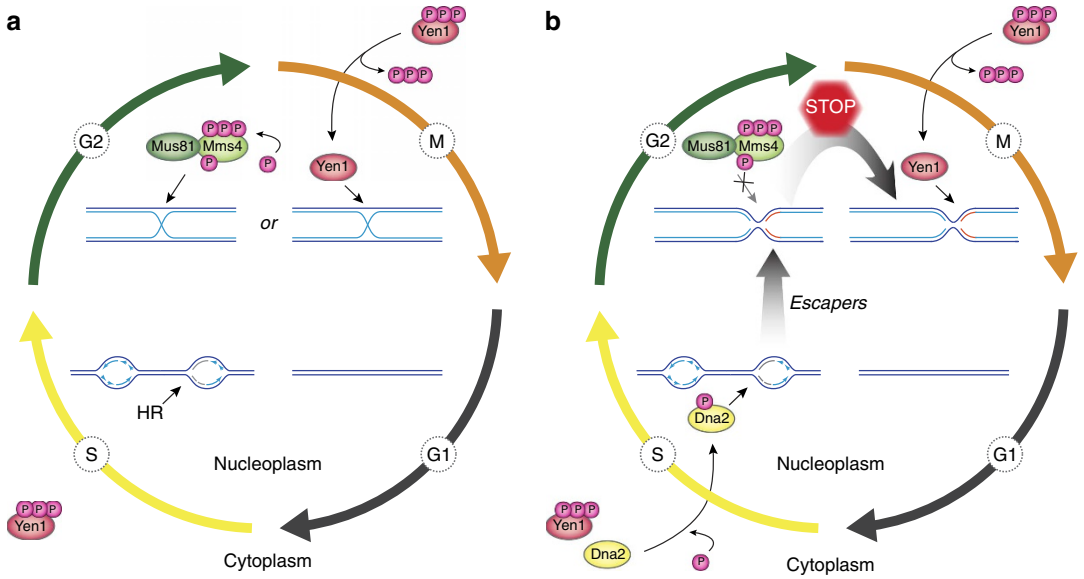

Figure 7 | Model for a two-tiered response to replication stress by Dna2 and Yen1. (**a**) Canonical role of Yen1 in the resolution of HR intermediates that arise during HR-mediated recovery of stalled replication forks. Mus81-Mms4 is activated by hyperphosphorylation in G2/M, prior to activation and nuclear import of Yen1 upon anaphase onset. Thus, HR intermediates are predominantly cleaved by Mus81-Mms4, with Yen1 acting as a catchall in M phase to remove persistent recombination structures in time for chromosome segregation. (**b**) Parallel to HR, the Dna2 helicase is tending to stalled replication forks. Replication intermediates that escape the attention of Dna2 give rise to toxic structures that are sensed by the DNA damage checkpoint, but which are refractory to processing by Mus81-Mms4. At anaphase entry, Yen1 is activated and uniquely resolves persistent replication intermediates, averting mitotic catastrophe. See text for details.

Methods

Recombinant proteins. Wild-type Dna2, Dna2^{R1253Q}, Dna2^{E675A} and Dna2^{K1080E} were expressed from a modified p*GAL:DNA2* vector, adding N-terminal FLAG and HA tags and a C-terminal 6× His tag, and purified as described previously[36,37]. RPA protein was expressed and purified as described[61].

Nuclease/helicase and ATPase assays. Experiments were carried out and analysed as described[36,37]. In brief, we used an assay that couples ATP hydrolysis to oxidation of NADH to determine the rate of ATP hydrolysis by Dna2 variants by following the decrease in optical absorbance by NADH at 340 nm over time. Kinetic plots of ATP hydrolysis were derived by calculating the amount of ATP hydrolysed per time interval. Fifteen microlitres reactions contained 25 mM Tris-acetate (pH 7.5), 2 mM magnesium acetate, 1 mM ATP, 1 mM dithiothreitol, 0.1 mg ml^{-1} bovine serum albumin, 1 mM phosphoenolpyruvate, 16 U ml^{-1} pyruvate kinase, 1 nM DNA substrate, 16.8 nM RPA and Dna2 proteins as indicated. Nuclease assays were incubated at 30 °C for 30 min. For analysis by denaturing polyacrylamide electrophoresis, samples were heat-denatured in formamide. DNA substrates were assembled using oligonucleotides X12-3 and X12-4SC, and PC 92 and X12-4SC for the 19 and 30 nt 5′-tailed DNA substrates, respectively[36,37]; the 5′-flapped DNA substrate consisted of oligonucleotides X12-4NC, Flap 19 X12-4C, and 292, as described[37]. Where indicated, oligonucleotides were ^{32}P-labelled at the 5′-end using [γ-^{32}P] ATP and T4 polynucleotide kinase (New England Biolabs). Unincorporated nucleotides were removed using MicroSpin G25 columns (GE Healthcare) before annealing the respective DNA substrates.

Yeast strains and plasmids. *S. cerevisiae* strains (Supplementary Table 1) were derived from BY4741 (ref. 62) using standard methods. The *dna2-2* allele was generated using pop-in/pop-out mutagenesis[63], and the DNA damage sensitivity of the resulting strain could be complemented with plasmid-borne wild-type *DNA2* cloned into vector pAG416GPD-ccdB (p*DNA2*) (Supplementary Fig. 2b). For constitutive expression, *YEN1* was cloned into vector pAG416GPD-ccdB or pAG416GPD-ccdB-EGFP[64], and site-directed mutagenesis was performed to generate a catalytically inactive form of Yen1 bearing the mutations E193A and E195A. Yellow fluorescent protein (YFP)-tagged Rad52 was expressed from its endogenous promoter using centromeric plasmid pWJ1213 (ref. 65). If not stated otherwise, all strains were cultured at 30 °C using YPAD media. *YEN1*^{on} was cloned into vector pAG416GPD-ccdB, or pYES-DEST52 (Invitrogen) for expression from a *GAL1* promoter in YPLG medium with 2% (w/v) galactose and 1% (w/v) raffinose. Antibodies used to monitor the expression of tagged proteins were Abcam mouse monoclonal anti-V5 antibody ab27671, and Sigma mouse monoclonal anti-Myc antibody 9E10. Santa Cruz Biotechnology goat polyclonal anti-Mcm2 antibody yN-19 was routinely used to ensure gel lanes were equally loaded for total protein.

Cell viability and drug sensitivity assays. Doubling times were determined as described[66] and averaged over at least three independent experiments. For microscopic determination of cell cycle stage (budding index), an average of 400 cells per strain and replicate were scored. Plating efficiency as a measure of strain viability was determined by colony outgrowth after plating a defined number of cells. The number of colonies formed after 3–4 days at 30 °C was divided by the number of cells plated as quantified in haemocytometer counts. For drop assays, exponentially growing cells were normalized to 10^7 cells ml^{-1}, and 2 µl drops of tenfold serial dilutions were spotted onto the appropriate medium with or without MMS, HU or CPT. If not stated otherwise, plates were incubated for 3–4 days at 30 °C. For liquid survival assays, overnight cultures were diluted to OD_{600} = 0.1–0.2 and grown for 4 h, then synchronized with α-factor in G1 and released into YPAD containing 50 mM HU for 120 min. Relevant dilutions were plated onto YPAD plates and colonies were counted after 3–4 days.

Mitotic time-courses. For time-course experiments, cells were grown exponentially (OD_{600} = 0.4–0.6) and synchronized by addition of α-factor (routinely >95% unbudded cells for wild-type, ≥90% for Dna2 helicase-defective strains). Cells were then harvested, washed and released into YPAD containing 50 mM HU for 2 h. After HU wash-out, cells were cultured in drug-free medium. Aliquots for flow cytometry, Western blot analysis and microscopy were withdrawn at regular intervals. Where indicated, α-factor or nocodazole (15 µg ml^{-1}) was added during and/or after treatment.

Analysis of Rad53-phosphorylation. TCA-precipitated proteins were separated by SDS-PAGE using precast gels (Invitrogen), and blotted onto polyvinylidene difluoride membranes using a Bio-Rad Turbo blot system. Rad53 protein was detected using a custom-made mouse monoclonal antibody[67]. Uncropped immunoblots are shown in Supplementary Fig. 9.

Flow cytometry. Cells were fixed overnight in 70% ethanol at 4 °C with rotation and processed as described[68]. Cells were then washed and resuspended using 50 mM Na-citrate (pH 7). After brief sonication, RNase A was added (0.25 mg ml^{-1}), and cells were incubated overnight at 37 °C, washed, and resuspended in 50 mM Na-citrate (pH 7) containing 16 µg ml^{-1} propidium iodide. Measurements of DNA content were done using a BD LSR II flow cytometer

(Becton Dickinson) operated with BD FACSDiva software. Data was processed with FlowJo (TreeStar).

Microscopy. DIC images were obtained using a Zeiss Axio Imager Z1 with a Plan-Apochromat 63 ×/1.4 DIC oil objective (Zeiss) and an AxioCam camera controlled by ZEN Blue 2012 software. To analyse nuclear DNA and chromosome segregation, cells were fixed with 70% ethanol for 5 min at room temperature and stained with 4,6-diamidino-2-phenylindole (DAPI) (50 ng ml^{-1}). For Yen1-EGFP and Rad52-YFP analyses, cells were fixed in 4% paraformaldehyde for 3 min at room temperature and stained with DAPI. Confocal images were collected using a Zeiss Axio Imager M1/Yokogawa CSU-X1 scanhead multipoint confocal microscope with a Plan-Neofluar 100 ×/1.45 oil objective and EM-CCD Cascade II camera (Photometrics) controlled by Metamorph 7.7.2 software (Molecular Devices), or a Rolera Thunder Back Illuminated EM-CCD camera (Q Imaging) controlled by VisiView software (Visitron Systems). Stacks of >20 optical slices separated by 200 nm were collected, and images of two-dimensional projections were prepared with ImageJ software (Fiji).

Analysis of rDNA replication by 2D gel electrophoresis. Synchronized or exponentially growing cells were harvested by centrifugation, and genomic DNA was purified using G-20 columns (Qiagen) before digestion with *Bgl*II. For S phase samples, aliquots were withdrawn every 10 min for 60 min on release from α-factor-induced G1 arrest, and pooled before preparing genomic DNA. Ethanol-purified DNA digests (2.5 μg) were subjected to 2D gel analysis as described[69], with minor modifications. The first dimension gel (0.4% agarose in TBE) was run at 1 V cm^{-1} at room temperature for 16 h. The second dimension gel (1.5% in TBE containing 0.3 g ml^{-1} ethidium bromide) was run at 5 V cm^{-1} at 4 °C in circulating TBE buffer for 5 h. The DNA was then blotted onto Hybond XL membrane (Amersham) by capillary transfer in 0.4 N NaOH. After UV-crosslinking, the membrane was blocked with ssDNA, probed for rDNA, and washed according to instructions by the manufacturer. A DNA template for the Southern probe was prepared by PCR from genomic DNA using primers 5′-GCCATTTACAAAAACATAACG and 5′-GGGC CTAGTTTAGAGAGAAGT[49]. The radiolabelled probe was then synthesized in the presence of [α-^{32}P] dCTP and [α-^{32}P] dATP using Klenow fragment polymerization (New England Biolabs/Bioconcept). Radioactive Southern blots were imaged using a phosphorimager screen (Kodak) and a Typhoon^{TM} 9400 system (GE Healthcare), and quantified using ImageQuant TL v2005 software as described[70]. In brief, the signal intensities for individual image objects were normalized to the intensity of the 1 N spot after background correction. The fold change was calculated by dividing the normalized signal intensity of each intermediate in G2 phase by the corresponding signal in S phase. For the experiment with Yen1^{on} expression in *dna2-2* cells, the normalized signal intensity for each scrutinized DNA intermediate in the strain harbouring the Yen1^{on} construct was divided by the corresponding signal in the strain with empty vector.

Data availability. The authors declare that all data supporting the findings of this study are available within the article and its Supplementary Information, or from the corresponding author on request.

References

1. Torres-Rosell, J. *et al.* Anaphase onset before complete DNA replication with intact checkpoint responses. *Science* **315,** 1411–1415 (2007).
2. Aguilera, A. & Gómez-González, B. Genome instability: a mechanistic view of its causes and consequences. *Nat. Rev. Genet.* **9,** 204–217 (2008).
3. Halazonetis, T. D., Gorgoulis, V. G. & Bartek, J. An oncogene-induced DNA damage model for cancer development. *Science* **319,** 1352–1355 (2008).
4. Hustedt, N., Gasser, S. & Shimada, K. Replication checkpoint: tuning and coordination of replication forks in S phase. *Genes* **4,** 388–434 (2013).
5. Lambert, S., Froget, B. & Carr, A. M. Arrested replication fork processing: interplay between checkpoints and recombination. *DNA Repair (Amst.)* **6,** 1042–1061 (2007).
6. Atkinson, J. & McGlynn, P. Replication fork reversal and the maintenance of genome stability. *Nucleic Acids Res.* **37,** 3475–3492 (2009).
7. Petermann, E. & Helleday, T. Pathways of mammalian replication fork restart. *Nat. Rev. Mol. Cell Biol.* **11,** 683–687 (2010).
8. Budd, M. E. & Campbell, J. L. A yeast gene required for DNA replication encodes a protein with homology to DNA helicases. *Proc. Natl Acad. Sci. USA* **92,** 7642–7646 (1995).
9. Lin, W. *et al.* Mammalian DNA2 helicase/nuclease cleaves G-quadruplex DNA and is required for telomere integrity. *EMBO J.* **32,** 1425–1439 (2013).
10. Duxin, J. P. *et al.* Okazaki fragment processing-independent role for human Dna2 enzyme during DNA replication. *J. Biol. Chem.* **287,** 21980–21991 (2012).
11. Duxin, J. P. *et al.* Human Dna2 is a nuclear and mitochondrial DNA maintenance protein. *Mol. Cell Biol.* **29,** 4274–4282 (2009).
12. Peng, G. *et al.* Human nuclease/helicase DNA2 alleviates replication stress by promoting DNA end resection. *Cancer Res.* **72,** 2802–2813 (2012).
13. Cheng, E. *et al.* Genome rearrangements caused by depletion of essential DNA replication proteins in *Saccharomyces cerevisiae*. *Genetics* **192,** 147–160 (2012).
14. Formosa, T. & Nittis, T. Dna2 mutants reveal interactions with Dna polymerase alpha and Ctf4, a Pol alpha accessory factor, and show that full Dna2 helicase activity is not essential for growth. *Genetics* **151,** 1459–1470 (1999).
15. Aravind, L., Walker, D. R. & Koonin, E. V. Conserved domains in DNA repair proteins and evolution of repair systems. *Nucleic Acids Res.* **27,** 1223–1242 (1999).
16. Bae, S. H. *et al.* Dna2 of *Saccharomyces cerevisiae* possesses a single-stranded DNA-specific endonuclease activity that is able to act on double-stranded DNA in the presence of ATP. *J. Biol. Chem.* **273,** 26880–26890 (1998).
17. Kumar, S. & Burgers, P. M. Lagging strand maturation factor Dna2 is a component of the replication checkpoint initiation machinery. *Genes Dev.* **27,** 313–321 (2013).
18. Bae, S. H., Bae, K. H., Kim, J. A. & Seo, Y. S. RPA governs endonuclease switching during processing of Okazaki fragments in eukaryotes. *Nature* **412,** 456–461 (2001).
19. Bae, S. H. & Seo, Y. S. Characterization of the enzymatic properties of the yeast Dna2 helicase/endonuclease suggests a new model for Okazaki fragment processing. *J. Biol. Chem.* **275,** 38022–38031 (2000).
20. Cejka, P. DNA end resection: nucleases team up with the right partners to initiate homologous recombination. *J. Biol. Chem.* **19,** 169–175 (2014).
21. Hu, J. *et al.* The intra-S phase checkpoint targets Dna2 to prevent stalled replication forks from reversing. *Cell* **149,** 1221–1232 (2012).
22. Lai, M. S. & Foiani, M. Dna2 offers support for stalled forks. *Cell* **149,** 1181–1183 (2012).
23. Thangavel, S. *et al.* DNA2 drives processing and restart of reversed replication forks in human cells. *J. Cell Biol.* **208,** 545–562 (2015).
24. Karanja, K. K., Lee, E. H., Hendrickson, E. A. & Campbell, J. L. Preventing over-resection by DNA2 helicase/nuclease suppresses repair defects in Fanconi anemia cells. *Cell Cycle* **13,** 1540–1550 (2014).
25. Higgs, M. R. *et al.* BOD1L is required to suppress deleterious resection of stressed replication forks. *Mol. Cell* **59,** 462–477 (2015).
26. Araki, Y., Kawasaki, Y., Sasanuma, H., Tye, B. K. & Sugino, A. Budding yeast *mcm10/dna43* mutant requires a novel repair pathway for viability. *Genes Cells* **8,** 465–480 (2003).
27. Lee, K. H. *et al.* The endonuclease activity of the yeast Dna2 enzyme is essential *in vivo*. *Nucleic Acids Res.* **28,** 2873–2881 (2000).
28. Budd, M. E. *et al.* A network of multi-tasking proteins at the DNA replication fork preserves genome stability. *PLoS Genet.* **1,** e61 (2005).
29. Ip, S. C. Y. *et al.* Identification of Holliday junction resolvases from humans and yeast. *Nature* **456,** 357–361 (2008).
30. Schwartz, E. K. & Heyer, W.-D. Processing of joint molecule intermediates by structure-selective endonucleases during homologous recombination in eukaryotes. *Chromosoma* **120,** 109–127 (2011).
31. Sarbajna, S. & West, S. C. Holliday junction processing enzymes as guardians of genome stability. *Trends Biochem. Sci.* **39,** 409–419 (2014).
32. Rass, U. Resolving branched DNA intermediates with structure-specific nucleases during replication in eukaryotes. *Chromosoma* **122,** 499–515 (2013).
33. Naim, V., Wilhelm, T., Debatisse, M. & Rosselli, F. ERCC1 and MUS81–EME1 promote sister chromatid separation by processing late replication intermediates at common fragile sites during mitosis. *Nat. Cell Biol.* **15,** 1008–1015 (2013).
34. Ying, S. *et al.* MUS81 promotes common fragile site expression. *Nat. Cell Biol.* **15,** 1001–1007 (2013).
35. Budd, M. E., Choe, W.-C. & Campbell, J. L. The nuclease activity of the yeast Dna2 protein, which is related to the RecB-like nucleases, is essential *in vivo*. *J. Biol. Chem.* **275,** 16518–16529 (2000).
36. Levikova, M., Klaue, D., Seidel, R. & Cejka, P. Nuclease activity of *Saccharomyces cerevisiae* Dna2 inhibits its potent DNA helicase activity. *Proc. Natl Acad. Sci. USA* **110,** E1992–E2001 (2013).
37. Levikova, M. & Cejka, P. The *Saccharomyces cerevisiae* Dna2 can function as a sole nuclease in the processing of Okazaki fragments in DNA replication. *Nucleic Acids Res.* **43,** 7888–7897 (2015).
38. Bae, S. H. *et al.* Coupling of DNA helicase and endonuclease activities of yeast Dna2 facilitates Okazaki fragment processing. *J. Biol. Chem.* **277,** 26632–26641 (2002).
39. Blanco, M. G., Matos, J., Rass, U., Ip, S. C. Y. & West, S. C. Functional overlap between the structure-specific nucleases Yen1 and Mus81-Mms4 for DNA-damage repair in *S. cerevisiae*. *DNA Repair (Amst.)* **9,** 394–402 (2010).
40. West, S. C. *et al.* Resolution of recombination intermediates: mechanisms and regulation. *Cold Spring Harb. Symp. Quant. Biol.* **80,** 103–109 (2015).

41. Fiorentino, D. F. & Crabtree, G. R. Characterization of *Saccharomyces cerevisiae dna2* mutants suggests a role for the helicase late in S phase. *Mol. Biol. Cell* **8,** 2519–2537 (1997).
42. Budd, M. E., Antoshechkin, I. A., Reis, C., Wold, B. J. & Campbell, J. L. Inviability of a *DNA2* deletion mutant is due to the DNA damage checkpoint. *Cell Cycle* **10,** 1690–1698 (2011).
43. Blanco, M. G., Matos, J. & West, S. C. Dual control of Yen1 nuclease activity and cellular localization by Cdk and Cdc14 prevents genome instability. *Mol. Cell* **54,** 94–106 (2014).
44. Budd, M. E. & Campbell, J. L. The pattern of sensitivity of yeast *dna2* mutants to DNA damaging agents suggests a role in DSB and postreplication repair pathways. *Mutat. Res.* **459,** 173–186 (2000).
45. Lisby, M., Rothstein, R. & Mortensen, U. H. Rad52 forms DNA repair and recombination centers during S phase. *Proc. Natl Acad. Sci. USA* **98,** 8276–8282 (2001).
46. Yimit, A., Riffle, M. & Brown, G. W. Genetic regulation of Dna2 localization during the DNA damage response. *G3 (Bethesda)* **5,** 1937–1944 (2015).
47. Ho, C. K., Mazón, G., Lam, A. F. & Symington, L. S. Mus81 and Yen1 promote reciprocal exchange during mitotic recombination to maintain genome integrity in budding yeast. *Mol. Cell* **40,** 988–1000 (2010).
48. Brewer, B. J. & Fangman, W. L. A replication fork barrier at the 3′ end of yeast ribosomal RNA genes. *Cell* **55,** 637–643 (1988).
49. Weitao, T., Budd, M., Hoopes, L. L. M. & Campbell, J. L. Dna2 helicase/nuclease causes replicative fork stalling and double-strand breaks in the ribosomal DNA of *Saccharomyces cerevisiae*. *J. Biol. Chem.* **278,** 22513–22522 (2003).
50. Neelsen, K. J. & Lopes, M. Replication fork reversal in eukaryotes: from dead end to dynamic response. *Nat. Rev. Mol. Cell Biol.* **16,** 207–220 (2015).
51. Fugger, K. *et al.* FBH1 catalyzes regression of stalled replication forks. *Cell Rep.* **10,** 1749–1757 (2015).
52. Kosugi, S., Hasebe, M., Tomita, M. & Yanagawa, H. Systematic identification of cell cycle-dependent yeast nucleocytoplasmic shuttling proteins by prediction of composite motifs. *Proc. Natl Acad. Sci. USA* **106,** 10171–10176 (2009).
53. Tkach, J. M. *et al.* Dissecting DNA damage response pathways by analysing protein localization and abundance changes during DNA replication stress. *Nat. Cell Biol.* **14,** 966–976 (2012).
54. Szakal, B. & Branzei, D. Premature Cdk1/Cdc5/Mus81 pathway activation induces aberrant replication and deleterious crossover. *EMBO J.* **32,** 1155–1167 (2013).
55. Matos, J., Blanco, M. G. & West, S. C. Cell-cycle kinases coordinate the resolution of recombination intermediates with chromosome segregation. *Cell Rep.* **4,** 76–86 (2013).
56. Chan, Y. W. & West, S. C. Spatial control of the GEN1 Holliday junction resolvase ensures genome stability. *Nat. Commun.* **5,** 4844 (2014).
57. Lee, S. H., Kim, Y. R., Yoo, N. J. & Lee, S. H. Mutation and expression of *DNA2* gene in gastric and colorectal carcinomas. *Korean J. Pathol.* **44,** 354–349 (2010).
58. Strauss, C. *et al.* The *DNA2* nuclease/helicase is an estrogen-dependent gene mutated in breast and ovarian cancers. *Oncotarget* **5,** 9396–9409 (2014).
59. Shaheen, R. *et al.* Genomic analysis of primordial dwarfism reveals novel disease genes. *Genome Res.* **24,** 291–299 (2014).
60. Alderton, G. K. *et al.* Seckel syndrome exhibits cellular features demonstrating defects in the ATR-signalling pathway. *Hum. Mol. Genet.* **13,** 3127–3138 (2004).
61. Kantake, N., Sugiyama, T., Kolodner, R. D. & Kowalczykowski, S. C. The recombination-deficient mutant RPA (rfa1-t11) is displaced slowly from single-stranded DNA by Rad51 protein. *J. Biol. Chem.* **278,** 23410–23417 (2003).
62. Brachmann, C. *et al.* Designer deletion strains derived from *Saccharomyces cerevisiae* S288C: a useful set of strains and plasmids for PCR-mediated gene disruption and other applications. *Yeast* **14,** 115–132 (1998).
63. Scherer, S. & Davis, R. W. Replacement of chromosome segments with altered DNA sequences constructed *in vitro*. *Proc. Natl Acad. Sci. USA* **76,** 4951–4955 (1979).
64. Alberti, S., Gitler, A. D. & Lindquist, S. A suite of Gateway cloning vectors for high-throughput genetic analysis in *Saccharomyces cerevisiae*. *Yeast* **24,** 913–919 (2007).
65. Feng, Q. *et al.* Rad52 and Rad59 exhibit both overlapping and distinct functions. *DNA Repair (Amst.)* **6,** 27–37 (2007).
66. Bernstein, K. A. *et al.* Sgs1 function in the repair of DNA replication intermediates is separable from its role in homologous recombinational repair. *EMBO J.* **28,** 915–925 (2009).
67. Seeber, A., Dion, V. & Gasser, S. M. Checkpoint kinases and the INO80 nucleosome remodeling complex enhance global chromatin mobility in response to DNA damage. *Genes Dev.* **27,** 1999–2008 (2013).
68. Nash, G. B., Jones, J. G., Mikita, J. & Dormandy, J. A. Methods and theory for analysis of flow of white cell subpopulations through micropore filters. *Br. J. Haematol.* **70,** 165–170 (1988).
69. Huberman, J. A., Spotila, L. D., Nawotka, K. A., El-Assouli, S. M. & Davis, L. R. The *in vivo* replication origin of the yeast 2 microns plasmid. *Cell* **51,** 473–481 (1987).
70. Fumasoni, M., Zwicky, K., Vanoli, F., Lopes, M. & Branzei, D. Error-free DNA damage tolerance and sister chromatid proximity during DNA replication rely on the Polα/Primase/Ctf4 complex. *Mol. Cell* **57,** 812–823 (2015).

Acknowledgements

We are indebted to S. Gasser, K. Shimada and A. Seeber for their generous technical help and reagents. We thank our colleagues S. Gasser, N. Thomä, and members of the Gasser and Rass laboratories for critical reading of the manuscript and helpful discussions. S. West and M. Blanco kindly provided the Yen1^{on} construct. We are grateful for the assistance of H. Kohler from the Cell Sorting platform, and L. Gelman and S. Bourke from the Facility for Advanced Imaging and Microscopy at the Friedrich Miescher Institute. Work in the laboratory of P.C. is supported by Swiss National Science Foundation Professorship PP00P3 133636, and work in the laboratory of U.R. by the Swiss Cancer League & Swiss Cancer Research and the Novartis Research Foundation.

Author contributions

G.Ö. and U.R. planned and analysed the experiments. G.Ö. performed the experiments with help from D.K. B.F. supported the two-dimensional gel analyses, and G.A.F. imaging and microscopy. M.L. and P.C. purified and analysed Dna2 *in vitro*. U.R. wrote the paper.

Additional information

Supplementary Information accompanies this paper at http://www.nature.com/naturecommunications

Competing financial interests: The authors declare no competing financial interests.

Reprints and permission information is available at http://npg.nature.com/reprintsandpermissions/

How to cite this article: Ölmezer, G. *et al.* Replication intermediates that escape Dna2 activity are processed by Holliday junction resolvase Yen1. *Nat. Commun.* **7,** 13157 doi: 10.1038/ncomms13157 (2016).

Supplementary Information

Supplementary Figures

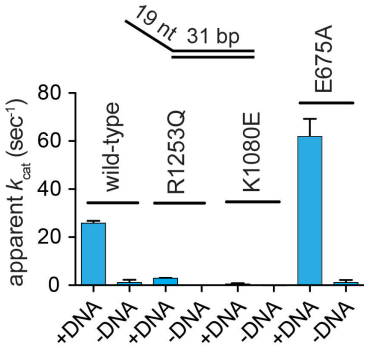

Supplementary Figure 1 | Apparent ATP turnover number of Dna2 proteins. Apparent k_{cat} values were calculated from the initial rate of ATP hydrolysis in experiments such as those shown in Fig. 1 c, containing a 5'-tailed DNA substrate, but with 3 nM Dna2 variants. Data presented as mean values ±s.e.m. (*n* = 2).

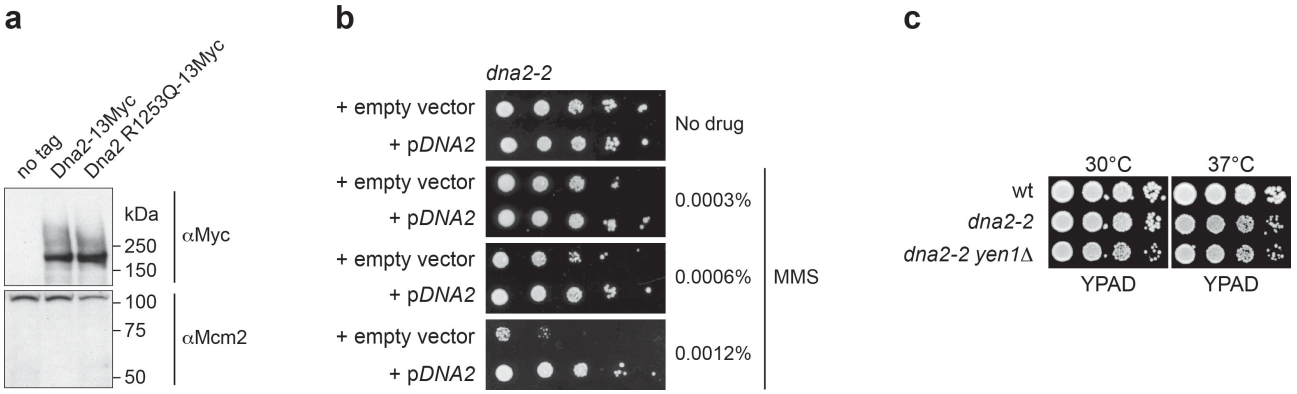

Supplementary Figure 2 | Assessment of Dna2 helicase-defective *dna2-2* cells. (**a**) Western blot analysis showing that the R1253Q mutation within the helicase domain of Dna2 does not alter protein expression or protein stability. Whole cell extracts were prepared from logarithmically growing cultures and resolved on a NuPAGE 7% Tris-acetate gel (Life Technologies). The upper part of the membrane was probed for wild-type and mutant Dna2 tagged with 13 x Myc at the C-terminus and expressed from the endogenous *DNA2* locus. The lower part of the membrane was probed for Mcm2, which served as loading control. The positions of size-markers are indicated. (**b**) Drop assay, performed as described for Fig. 3, showing that *dna2-2* cells are sensitive to MMS, and that expression of *DNA2* from a low-copy number plasmid with a GPD promoter restores resistance. (**c**) Drop assay showing that *dna2-2 yen1*Δ cells are viable at elevated temperature.

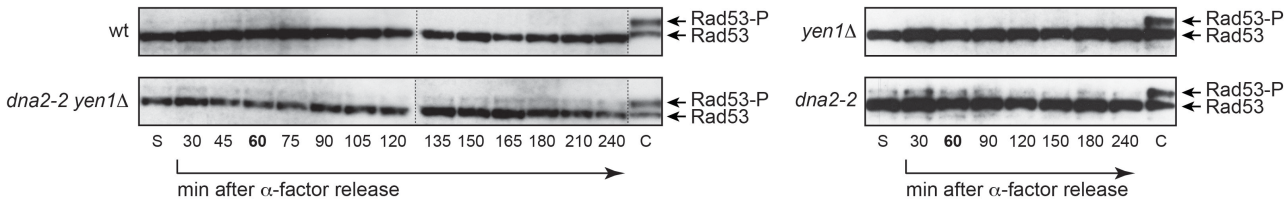

Supplementary Figure 3 | Unscheduled post-replicative checkpoint activation in Dna2 helicase-defective cells is not discernible in unperturbed conditions. The indicated strains were synchronized in G1, released into YPAD medium without HU, and monitored by Western blot analysis for phosphorylation of Rad53 over a period of 4 h. Under these conditions, cells routinely completed bulk DNA synthesis within 60 min of α-factor release (see Fig. 2c). S, synchronous; C, control samples showing Rad53 phosphorylation (Rad53-P) after exposure of the respective strains to HU.

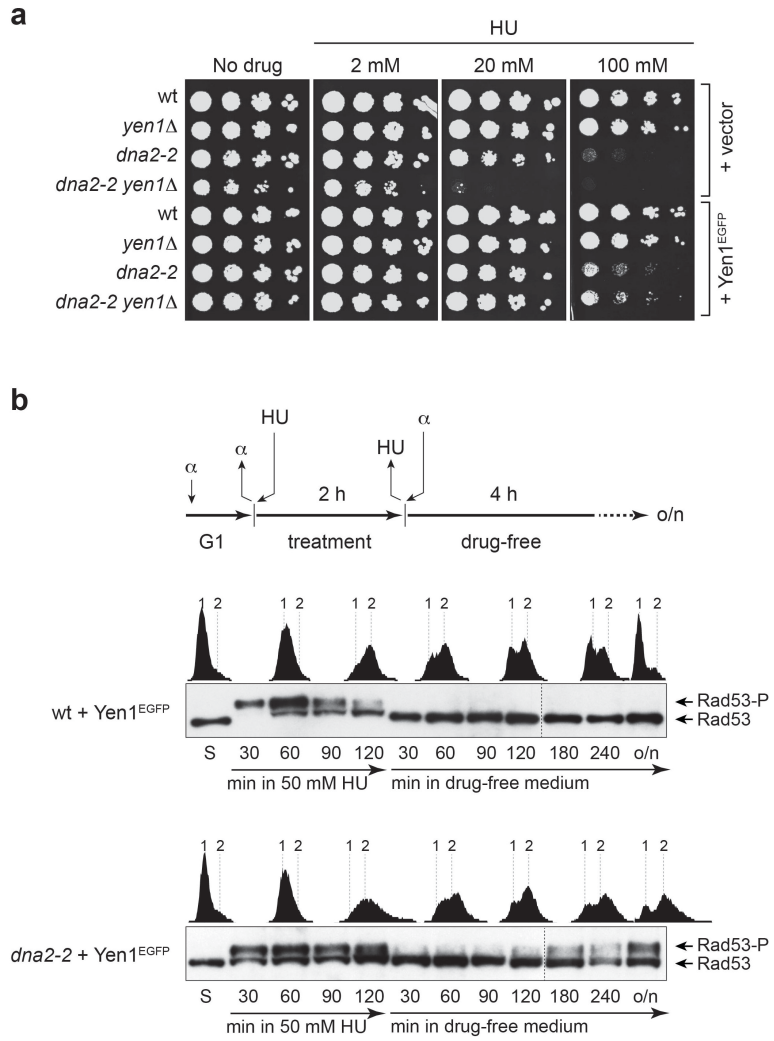

Supplementary Figure 4 | Green fluorescent protein-tagged Yen1-EGFP is functional. (**a**) Drop assay, performed as described for Fig. 3, showing that Yen1-EGFP suppresses the severe HU sensitivity of *dna2-2 yen1*Δ cells, which demonstrates that the tag does not interfere with Yen1 function. (**b**) Biphasic checkpoint activation in response to acute replication stress is maintained in Dna2 helicase-defective cells expressing Yen1-EGFP. Mitotic time-course experiments performed as described for Fig. 4. Checkpoint activation and replication progression were monitored by analyzing Rad53 phosphorylation (Rad53-P) and DNA content (1N and 2N indicated), respectively. S, synchronous; o/n, overnight.

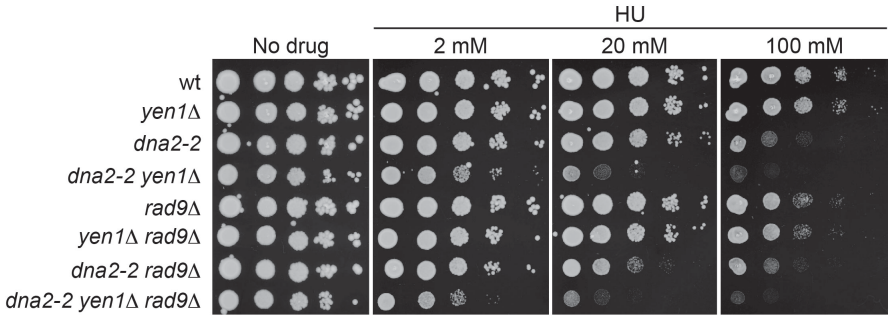

Supplementary Figure 5 | Disruption of the DNA damage checkpoint does not suppress the sensitivity of Dna2 helicase-defective cells to chronic replication stress. Drop assays of the indicated strains on plates containing increasing amounts of HU, performed as described for Fig. 3.

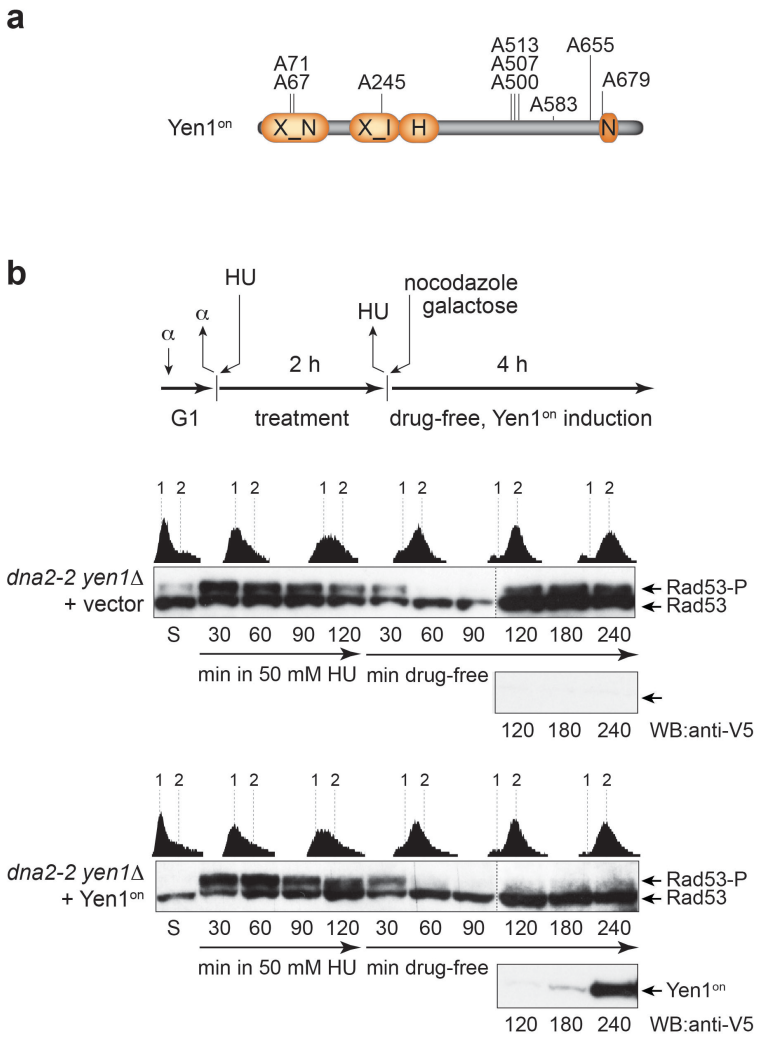

Supplementary Figure 6 | Constitutively active Yen1^{on} suppresses post-replicative DNA damage checkpoint activation in Dna2 helicase-defective cells recovering from acute replication stress. (**a**) Yen1^{on} is mutated at all CDK consensus sites (serine to alanine substitutions), as indicated. This eliminates CDK-dependent control, allowing the active enzyme into the nucleus at all cell cycle stages. (**b**) Mitotic time-courses with *dna2-2 yen1*Δ cells harboring an empty vector control or a vector for the expression of YEN1^{on} under control of a galactose-inducible promoter. Cells were synchronized in G1, released into acute replication stress in the presence of 50 mM HU for 2 h, and then shifted to medium containing galactose to induce Yen1^{on} expression, and nocodazole to block cells in G2. Checkpoint activation and replication progression were monitored by assessing Rad53 phosphorylation (Rad53-P) and DNA content (1N and 2N indicated), respectively. Insets show the expression of Yen1^{on}, detected using an anti-V5 antibody.

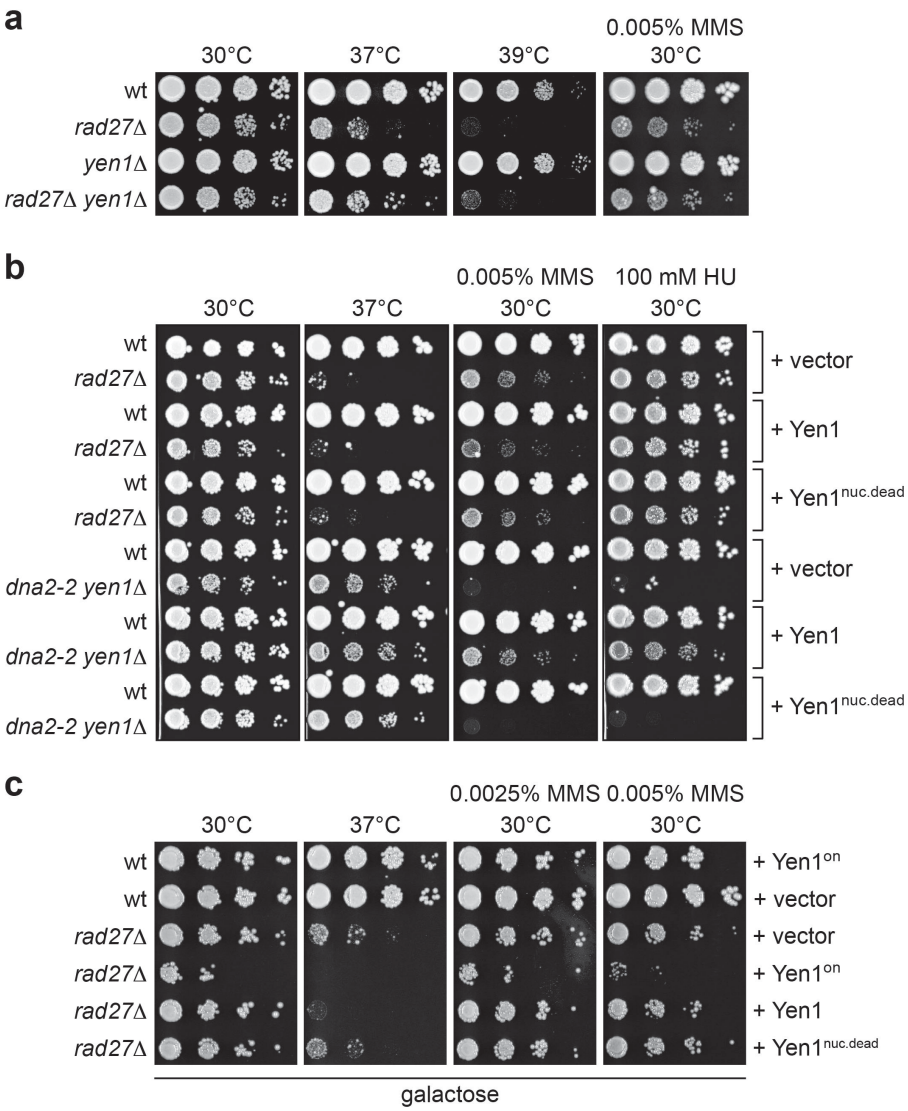

Supplementary Figure 7 | Genetic analysis of the relationship between Yen1 and Rad27. (**a**) A deletion of *YEN1* does not aggravate the temperature or MMS sensitivity of *rad27*Δ cells. (**b**) Constitutive or (**c**) galactose-induced expression of Yen1 or Yen1^{on} does not alleviate the temperature or MMS sensitivity of *rad27*Δ cells. Note how Yen1^{on} expression even attenuates growth in *rad27*Δ mutants under all conditions. In contrast, wild-type cells are inhibited by Yen1^{on} only in the presence of MMS. Drop assays were performed as described for Fig. 3 and plates were imaged after 2 to 3 days.

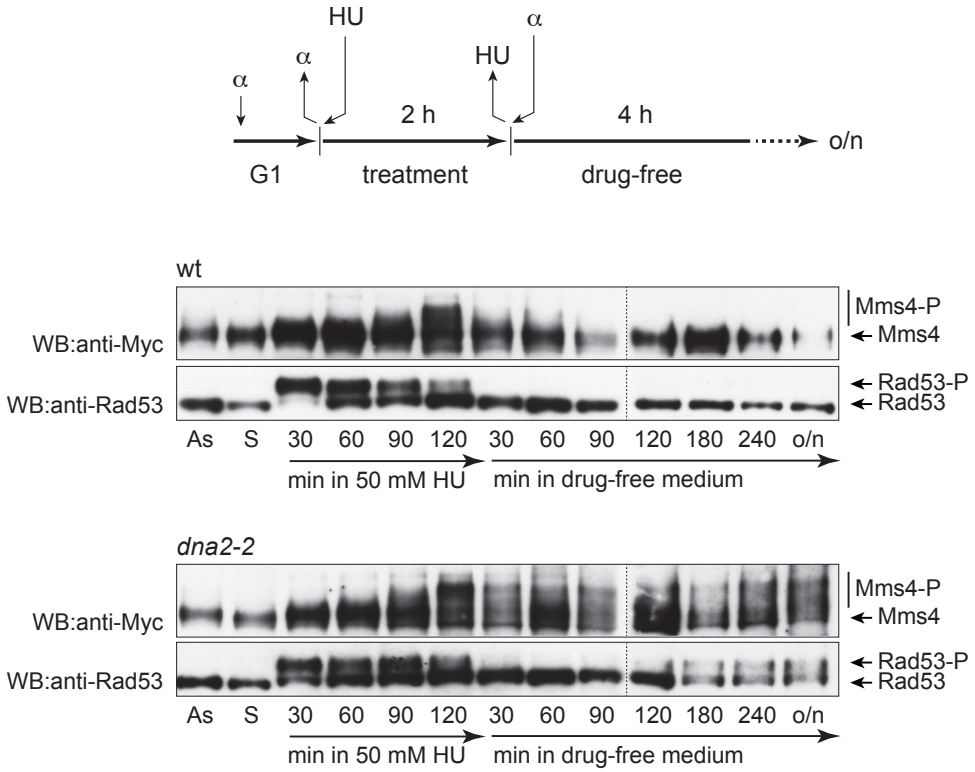

Supplementary Figure 8 | Mus81-Mms4 is hyperphosphorylated in Dna2 helicase-defective cells after replication stress. Mitotic time-courses with wild-type and *dna2-2* cells with an endogenously 13 x Myc-tagged version of Mms4, performed as described for Fig. 4. Phosphorylation of Rad53 (Rad53-P) indicates checkpoint activation. Western blot analysis with an anti-Myc antibody reveals an upshift in the Mms4 signal caused by G2/M-specific hyperphosphorylation (Mms4-P). Hyperphosphorylation of Mms4 is transient in the wild-type, but persistent in *dna2-2* cells, which recover slowly from acute HU treatment and delay at the G2/M boundary (see also Fig. 4a). As, asynchronous; S, synchronous; o/n, overnight.

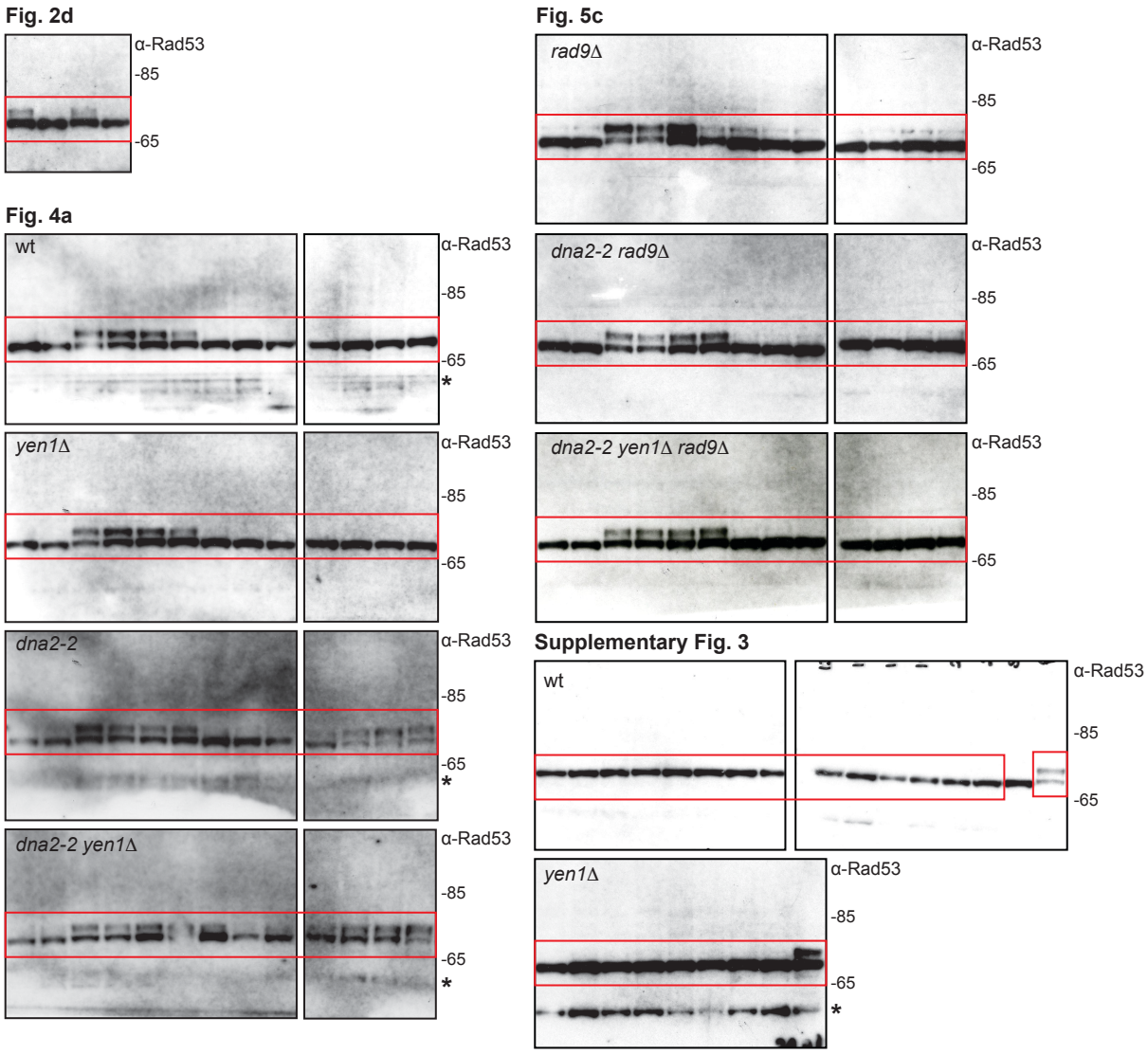

Supplementary Figure 9 | Uncropped immunoblots. Boxed areas correspond to images presented in the indicated main text and supplementary figures. Size markers (kDa) are indicated. *, denotes unspecific bands.

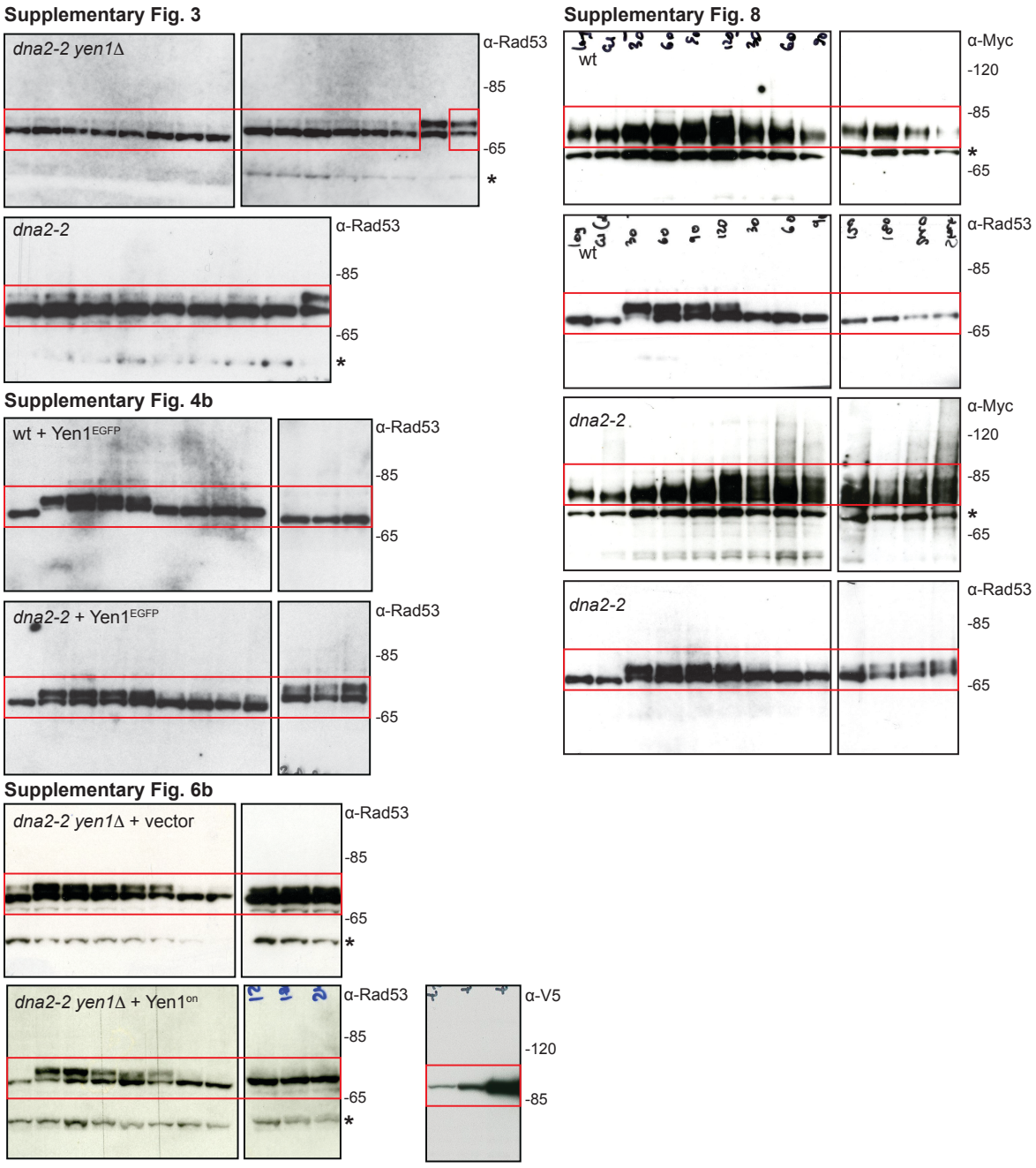

Supplementary Figure 9 | Uncropped immunoblots. Boxed areas correspond to images presented in the indicated main text and supplementary figures. Size markers (kDa) are indicated. *, denotes unspecific bands.

Supplementary Tables

Supplementary Table 1 | *S. cerevisiae* strains used in this study.

Strain	Relevant genotype	Source
BY4741 (wild-type)	*MAT***a** *his3Δ1 leu2Δ0 met15Δ0 ura3Δ0*	GE Healthcare
clone ID 174	BY4741 *yen1*Δ::*KanMX4*	GE Healthcare
clone ID 540	BY4741 *rad52*Δ::*KanMX4*	GE Healthcare
clone ID 3368	BY4741 *slx1*Δ::*KanMX4*	GE Healthcare
YRL31	BY4741 *DNA2-13myc:: KanMX4*	this study
YRL33	BY4741 *dna2-2-13myc:: KanMX4*	this study
YRL96	BY4741 *dna2-2*	this study
YRL97	BY4741 *dna2-2 yen1*Δ::*KanMX4*	this study
YRL98	BY4741 *dna2-2 mus81*Δ::*URA3*	this study
YRL99	BY4741 *dna2-2 slx1*Δ::*KanMX4*	this study
YRL129	BY4741 *dna2-2 rad52*Δ::*URA3*	this study
YRL133	BY4741 *rad9*Δ::*URA3*	this study
YRL134	BY4741 *yen1*Δ::*KanMX4 rad9*Δ::*URA3*	this study
YRL136	BY4741 *dna2-2 rad9*Δ::*URA3*	this study
YRL138	BY4741 *dna2-2 yen1*Δ::*KanMX4 rad9*Δ::*URA3*	this study
YRL241	BY4741 *MMS4-13myc::URA3*	this study
YRL243	BY4741 *dna2-2 MMS4-13myc::URA3*	this study
YRL249	BY4741 *rad27*Δ::*HIS3*	this study
YRL250	BY4741 *rad27*Δ::*HIS3 yen1*Δ::*KanMX4*	this study
YRL268	BY4741 *dna2-2 yen1*Δ::*KanMX4 rad52*Δ::*HIS3* p*DNA2* (*URA3*)	this study
YRL272	BY4741 *dna2-2 rad52*Δ::*HIS3* p*DNA2* (*URA3*)	this study
YWL169	BY4741 *mus81*Δ::*HIS3*	reference 1

Supplementary References

1. Blanco, M. G., Matos, J., Rass, U., Ip, S. C. Y. & West, S. C. Functional overlap between the structure-specific nucleases Yen1 and Mus81-Mms4 for DNA-damage repair in S. cerevisiae. *DNA Repair (Amst.)* **9,** 394–402 (2010).

microbial cell

Microreview

www.microbialcell.com

A new role for Holliday junction resolvase Yen1 in processing DNA replication intermediates exposes Dna2 as an accessory replicative helicase

Benoît Falquet[1,2] and Ulrich Rass[1,*]

[1] Friedrich Miescher Institute for Biomedical Research, Maulbeerstrasse 66, CH-4058 Basel, Switzerland.
[2] University of Basel, Petersplatz 10, CH-4003 Basel, Switzerland.
* Corresponding Author:
Ulrich Rass, Tel: +41 61 696 17 30; E-mail: ulrich.rass@fmi.ch

DNA replication is mediated by a multi-protein complex known as the replisome. With the hexameric MCM (minichromosome maintenance) replicative helicase at its core, the replisome splits the parental DNA strands, forming replication forks (RFs), where it catalyses coupled leading and lagging strand DNA synthesis. While replication is a highly effective process, intrinsic and oncogene-induced replication stress impedes the progression of replisomes along chromosomes. As a consequence, RFs stall, arrest, and collapse, jeopardizing genome stability. In these instances, accessory fork progression and repair factors, orchestrated by the replication checkpoint, promote RF recovery, ensuring the chromosomes are fully replicated and can be safely segregated at cell division. Homologous recombination (HR) proteins play key roles in negotiating replication stress, binding at stalled RFs and shielding them from inappropriate processing. In addition, HR-mediated strand exchange reactions restart stalled or collapsed RFs and mediate error-free post-replicative repair. DNA transactions at stalled RFs further involve various DNA editing factors, notably helicases and nucleases. A study by Ölmezer *et al*. (2016) has recently identified a role for the structure-specific nuclease Yen1 (GEN1 in human) in the resolution of dead-end DNA replication intermediates after RF arrest. This new function of Yen1 is distinct from its previously known role as a Holliday junction resolvase, mediating the removal of branched HR intermediates, and it becomes essential for viable chromosome segregation in cells with a defective Dna2 helicase. These findings have revealed greater complexity in the tasks mediated by Yen1 and expose a replicative role for the elusive helicase activity of the conserved Dna2 nuclease-helicase.

The Dna2 nuclease-helicase has emerged as a multifunctional mediator of genome stability. Other labs have shown that Dna2's nuclease activity is involved in DNA end-resection, facilitating HR-mediated DNA double-strand break repair and the resetting of reversed RFs. The Dna2 helicase activity appears to be dispensable for these processes and its function *in vivo* has remained enigmatic. In *Saccharomyces cerevisiae*, cells harboring various different point mutations within the Dna2 helicase domain share a common sensitivity to the DNA alkylating agent methyl methane sulfonate (MMS). Ölmezer *et al*. (2016) now provide evidence that this phenotype relates to a critical role of the Dna2 helicase at stalled RFs. Key for elucidating this function was a synthetic sick phenotype that arises when the Holliday junction resolvase *YEN1* is deleted in cells expressing Dna2 R1253Q. Ölmezer and co-workers first demonstrated that Dna2 R1253Q, encoded by mutant allele *dna2-2* and bearing the R to Q amino acid substitution in an ATP binding loop between the characteristic RecA lobes of the Dna2 superfamily 1 helicase domain, is indeed helicase-dead but retains full nuclease activity. Cells expressing Dna2 R1253Q exhibit chronic checkpoint activation and a delay in G2/M phase of the cell cycle. Nevertheless, cell viability remained high in Dna2 R1253Q cells, dropping significantly when *YEN1* was deleted, while the kinetics of bulk DNA synthesis during S phase were indistinguishable from wild-type in Dna2 R1253Q cells in the presence or absence of Yen1.

MICROREVIEW on: Ölmezer G, Levikova M, Klein D, Falquet B, Fontana GA, Cejka P, and Rass U (2016). Replication intermediates that escape Dna2 activity are processed by Holliday junction resolvase Yen1. Nat Commun 7:13157. doi: 10.1038/ncomms13157

doi: *10.15698/mic2017.01.554*
Received *16.12.2016,* ***Accepted*** *20.12.2016,* ***Published*** *02.01.2017.*
Keywords*: replication stress, DNA repair, genome stability, replication fork restart, anaphase bridges, chromosome non-disjunction, structure-specific nucleases.*

Analysis during a single cell cycle showed that Dna2 R1253Q cells exhibit an unusual, biphasic checkpoint activation pattern in response to mild, acute replication stress induced through nucleotide depletion by hydroxyurea (HU). Like wild-type cells, Dna2 R1253Q and Dna2 R1253Q *yen1*Δ cells activated the replication checkpoint in the presence of HU, followed by checkpoint silencing and completion of bulk DNA synthesis after removal of the drug. However, in contrast to wild-type cells, Dna2 helicase-defective cells failed to divide, and instead exhibited reemerging checkpoint signaling, elicited by the G2/M DNA damage checkpoint. Yen1 was unable to suppress this unscheduled G2/M checkpoint activation. This may seem counter-intuitive, given that Yen1 is the factor maintaining viability in Dna2 helicase-defective cells. However, considering that Yen1 is tightly controlled, so that accumulation within the nucleus occurs only after cells make the G2-M transition and enter anaphase, the inability to prevent Dna2-related DNA lesions during the course of S and G2/M phase is perhaps not surprising. Indeed, Yen1 remained cytoplasmic in Dna2 R1253Q cells for extended periods of time while the G2/M arrest was maintained. When cells made the transition into M phase after experiencing replication stress, Yen1 became nuclear and cell survival was then fully dependent upon the nuclease activity of Yen1, which suppressed toxic chromosome entanglements detected as anaphase bridges. One implication of these findings is that Dna2 helicase activity is needed at stalled RFs, ensuring that the genome is fully replicated and chromosomes are no longer attached to one another at segregation.

DNA synthesis is not globally affected in Dna2 R1253Q cells, suggesting the Dna2 helicase is only needed at a subset of troubled RFs to promote replication restart or fork stability, helping to ensure full genome duplication either by reinitiating DNA synthesis or by maintaining arrested forks in a conformation favorable for subsequent fork fusion with an oncoming, active fork (Figure 1; pathways indicated by green arrows). A role in replication termination is consistent with an accumulation of converged yet unresolved RFs in Dna2 helicase-defective cells, which were detected by two-dimensional gel electrophoresis of replication intermediates at the natural replication fork pausing site in the rDNA. Further clues as to the actions of Dna2 come from the biphasic checkpoint activation pattern seen in Dna2 R1253Q cells upon exposure to acute replication stress. The gap in checkpoint signaling that was ob-

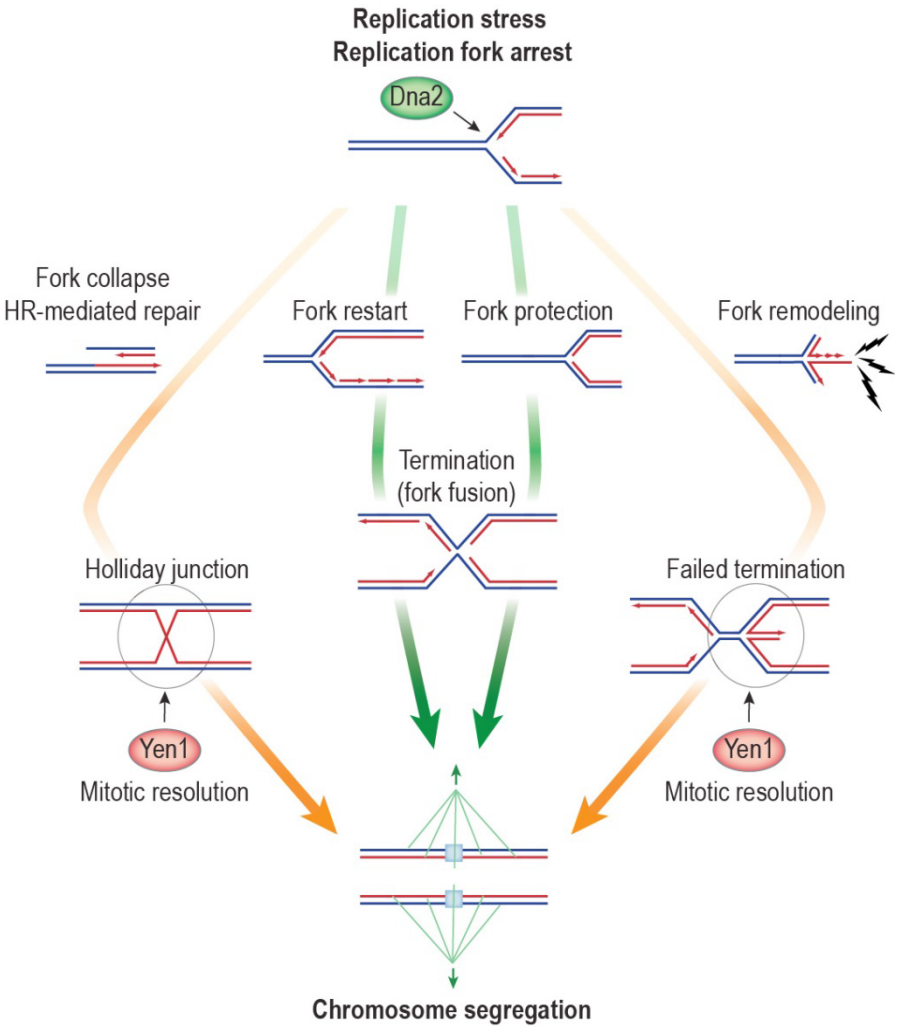

FIGURE 1: Dna2 helicase activity promotes the recovery of stalled DNA replication intermediates. Dna2 acts as an accessory replicative helicase, suppressing toxic replication intermediates and chromosome non-disjunction after RF arrest. This suggests that the Dna2 helicase activity facilitates fork restart or fork protection (green arrows), promoting full genome replication and/or fork fusion during replication termination. Arrested RFs that escape the attention of Dna2 may collapse, triggering HR-mediated restart. Alternatively, unscheduled fork remodeling may occur with the resulting chicken foot structure constituting a potential source for DNA damage checkpoint signaling (lightning bolts) in Dna2 helicase-defective cells, and a possible obstruction to replication termination. These pathways (orange arrows) lead to chromosome entanglements that are resolved by Yen1 in anaphase, ensuring viable chromosome segregation.

served after replication checkpoint silencing and before DNA damage checkpoint activation suggests that replication intermediates that escape the attention of Dna2 are not at first detected by the DNA damage checkpoint. This could be explained if the sensitivity of the DNA damage checkpoint increases over time such that initially checkpoint-blind replicative lesions can be detected as cells approach G2/M phase. We favor a different explanation, namely that an initial checkpoint-blind DNA structure is subsequently converted into a detectable lesion, and that Dna2 either prevents or counteracts this process. An attractive possibility is that fork reversal is involved, a well-described phenomenon in response to replication stress that entails annealing of the nascent DNA strands. As a result, three-way RFs are converted into a so-called chicken foot structure with four DNA branches similar to a HJ. Importantly, the tip of the newly extruded branch is indistinguishable from a DNA double-strand break, a structure that elicits a strong DNA damage checkpoint response (Figure 1). RF conversion into a chicken foot intermediate is also consistent with the unique requirement for Yen1 in Dna2 helicase-defective cells. Yen1 possesses the rare ability to recognize and resolve DNA four-way junctions through coordinated incisions on either side of the branch point and is therefore perfectly suited to remove dead-end fork-reversal intermediates upon its activation in anaphase, just prior to chromosome segregation. Consistent with this notion, Ölmezer *at al*. (2016) showed, for the first time, that Yen1 is capable of removing persistent dead-end replication intermediates – detected by two-dimensional gel electrophoresis – in Dna2 helicase-defective cells. Yen1 is thus a versatile mitotic DNA de-branching nuclease whose actions are not restricted to canonical Holliday junction resolution downstream of HR-mediated strand exchange. Given the specificity of *DNA2*'s genetic interaction with *YEN1*, which was found not to extend to the other Holliday junction resolvases *MUS81-MMS4* and *SLX1-SLX4*, Yen1's activity towards dead-end replication intermediates, as opposed to HR structures, appears most relevant to maintain viability in Dna2 helicase-defective cells.

This is consistent with the finding that the requirement for Yen1 in Dna2 helicase-defective cells cannot be suppressed by eliminating HR. Nonetheless, we expect that Yen1 (in this case redundantly with Mus81-Mms4) contributes to the resolution of HR intermediates in Dna2 helicase-defective cells, which exhibit elevated levels of HR, likely due to compensatory RF recovery by HR and/or HR-dependent repair of Yen1-induced DNA breaks at troubled RFs. Indeed, the repair events that take place downstream of Yen1-mediated resolution of dead-end replication intermediates have not been addressed and remain to be elucidated. It is remarkable that the cleavage of post-replicative sister chromatid entanglements by Yen1 in anaphase does not appear to interfere with mitosis. Ölmezer and co-workers showed that disruption of the G2/M checkpoint restored normal mitotic progression and full viability in Dna2 R1253Q cells after acute replication stress, provided Yen1 was functional. This suggests that Yen1-dependent repair is either straightforward and simple enough to be completed in anaphase, or that Yen1-dependent repair intermediates can be safely transmitted to daughter cells for processing in the next cell cycle. Either way, Yen1 provides efficient protection against anaphase bridges and mitotic catastrophe; it will be interesting to assess whether there is a price to pay for this last-minute intervention by Yen1 with regard to genetic stability.

A key point of the study by Ölmezer *et al.* (2016) is that it demonstrates how intimately the Dna2 helicase activity is linked to replication. It is worth pointing out that loss of Yen1, which in itself does not lead to any overt phenotype, strongly compromises growth in Dna2 helicase-defective cells, indicating that post-replicative chromosome entanglements and chromosome non-disjunction occur even in unperturbed conditions. This highlights the so-far underestimated importance of the Dna2 helicase in ameliorating the consequences of endogenous RF stalling and avoiding underreplication. We think the Dna2 helicase is best described as an accessory replicative helicase.

Replication stress and RF demise is an important driver of genome instability and cancer formation. A better understanding of the molecular choreography at stalled RFs therefore has direct biomedical implications. *DNA2* has been linked to a number of human disease syndromes and is frequently overexpressed in cancer, suggesting that cancer cells may use the activities of DNA2 to overcome excessive levels of RF stalling. Inhibiting the DNA2 helicase could in principle provide a therapeutic avenue aimed at killing cancer cells by stress-overload.

ACKNOWLEDGMENTS

We thank Gizem Ölmezer for fruitful discussions. The study discussed herein was supported by the Novartis Research Foundation.

CONFLICT OF INTEREST

The authors declare that no competing interest exists.

Please cite this article as: Benoît Falquet and Ulrich Rass (2016). A new role for Holliday junction resolvase Yen1 in processing DNA replication intermediates exposes Dna2 as an accessory replicative helicase. **Microbial Cell** 4(1): 32-34. doi: 10.15698/mic2017.01.554

Chapter 6: Disease-associated DNA2 nuclease-helicase protects cells from lethal chromosome under-replication

This chapter is based on a manuscript in preparation

Benoît Falquet, Gizem Ölmezer, Franz Enkner, Dominique Klein, Kiran Challa, Susan M. Gasser and Ulrich Rass

Provisory title: Disease-associated Dna2 nuclease-helicase protects cells from lethal chromosome underreplication

Author Contributions:

U.R. and B.F. planned and analysed the experiments with input from G.Ö. who made initial genetic observations. B.F. performed the experiments with help from D.K., G.Ö., and F.E. K.C performed SIM experiments. S.M.G. supervised B.F. and K.C. U.R. wrote the paper with input from all authors.

Disease-associated *DNA2* nuclease-helicase protects cells from lethal chromosome under-replication

Benoît Falquet[1,2], Gizem Ölmezer[1,2], Franz Enkner[1], Dominique Klein[1], Kiran Challa[1], Susan M. Gasser[1,2] & Ulrich Rass[1,3]

[1]Friedrich Miescher Institute for Biomedical Research, Maulbeerstrasse 66, CH-4058 Basel, Switzerland.

[2]University of Basel, Faculty of Natural Sciences, Klingelbergstrasse 70, CH-4058 Basel, Switzerland.

[3]Genome Damage and Stability Centre, School of Life Sciences, University of Sussex, Falmer, Brighton, BN1 9RQ, United Kingdom.

Correspondence and requests for materials should be addressed to U.R. (U.W.Rass@sussex.ac.uk).

SUMMARY

DNA2 is an essential nuclease-helicase mediating multiple genome-maintenance pathways including Okazaki fragment ligation and replication fork (RF) recovery. In *Saccharomyces cerevisiae*, *dna2*Δ inviability is reversed by concomitant *PIF1* helicase or *RAD9* checkpoint-mediator deletion. To establish why *dna2*Δ is inviable, we examined the relationship between *DNA2*, *PIF1*, *RAD9*, and Holliday junction resolvase *YEN1*. We show that DNA replication is not faithfully completed in *dna2*Δ *pif1* cells, leading to chromosome entanglements that are lethal unless removed by Yen1. Using a *dna2* hypomorphic background, we reveal that Pif1 drives unscheduled DNA damage-checkpoint activation in response to RF-stalling. This activity maps to Pif1's ability to promote recombination-coupled DNA synthesis. We propose that Dna2 controls the fate of stalled RFs, promoting RF recovery and replication completion, while suppressing Pif1-mediated recombination-dependent replication (RDR) restart. In *dna2*Δ cells, inappropriate RDR generates DNA intermediates that elicit Rad9-dependent cell-cycle arrest. Thus, controlling RF recovery is an essential Dna2 function.

Keywords: Replication stress, replication fork arrest, homologous recombination, chromosome stability, cell cycle checkpoint, structure-specific nucleases, Seckel syndrome, microcephalic primordial dwarfism, cancer

INTRODUCTION

Dna2 is a conserved enzyme of DNA metabolism that comprises a nuclease domain with single-stranded DNA (ssDNA)-specific endonuclease activity fused to a superfamily 1 helicase domain with 5´-to-3´ translocation polarity[1-3]. *DNA2* is essential for cell proliferation and embryonic development[2,4-6]. Mutations within *DNA2* are associated with sensitivity to DNA replication stress (RS), genome instability, mitochondrial myopathy, and the primordial dwarfism disorder Seckel syndrome[7-10]. Overexpression of *DNA2* is frequent in cancer cells and has been linked to poor patient prognosis[11,12]. Mechanistically, *DNA2* has been implicated in DNA double-strand break (DSB) repair, checkpoint activation, Okazaki fragment processing, telomere homeostasis, centromeric DNA replication, and the recovery of stalled replication forks (RFs)[6,13-20]. Pinpointing which of its genome stability roles are indispensable for cell proliferation is an important step in rationalizing the molecular pathologies associated with *DNA2*.

In *S. cerevisiae*, the lethality caused by disruption of Dna2 is suppressed by concomitant loss of either the conserved DNA helicase Pif1[21] or the DNA damage checkpoint-mediator Rad9[22]. This indicates that Pif1 mediates the formation of DNA structures that elicit a Rad9-dependent checkpoint response in Dna2-defective cells, which in turn triggers cell-cycle arrest and *dna2*Δ inviability. Pif1 is known to remove obstacles to RF progression, including G-quadruplex structures, RNA-DNA hybrids (such as transcription-associated R-loops), and DNA-binding proteins[23,24]. Moreover, Pif1 promotes homologous recombination (HR)-dependent DNA damage bypass[25] and replication restart at arrested or broken RFs by recombination-dependent replication (RDR) and break-induced replication (BIR), respectively[26,27]. Pif1-toxicity in Dna2-defective cells has been attributed to its participation in strand-displacement DNA synthesis by DNA polymerase δ (Pol δ), a reaction that Pif1 stimulates *in vitro*[28]. During lagging strand synthesis, Pol δ extends the 3´-end of each Okazaki fragment such that the 5´-end of preceding Okazaki fragments is displaced and the RNA/initiator-DNA primer can be nucleolytically removed before ligation. It is proposed that extensive strand displacement, promoted by Pif1, could lead to long flaps bound by ssDNA-binding protein RPA, a potent checkpoint-activating

intermediate[29]. While the 5´-flap endonuclease Rad27 (FEN1 in human) is thought to deal with the majority of Okazaki fragments, its activity is inhibited by RPA. In contrast, Dna2 is able to cleave RPA-covered DNA flaps *in vitro*[30,31]. Thus, Dna2 is thought to play an essential housekeeping role by policing Okazaki fragment maturation, preventing a build-up of RPA-ssDNA and checkpoint-mediated cell-cycle arrest[22].

This Okazaki fragment processing model is not without caveats. Reconstitution experiments and the analysis of Okazaki fragments synthesized in budding yeast *in vivo* have indicated that the role of Dna2 in Okazaki fragment maturation is likely to be very limited[32-34]. First, the size of the strand-displacement DNA synthesis patch on the lagging strand is largely unaffected by loss of Dna2 or Pif1[34,35]. There is also no evidence that DNA2 contributes to Okazaki fragment processing in human cells[9]. Biochemically, nascent DNA flaps inhibit nucleotide incorporation by Pol δ, which favours instantaneous incision and flap removal by Rad27 once single-nucleotide or very short flaps are formed[36]. This ensures that Okazaki fragment maturation proceeds by nick translation without long flap intermediates[36]. Polymerase idling, whereby Pol δ uses its 3´-5´ exonuclease activity to backtrack if flap removal by Rad27 is delayed, further limits the extensive growth of DNA flaps during Okazaki fragment processing[37]. These observations collectively argue that Dna2 may ensure cell survival by processing DNA structures other than 5´-flaps at Okazaki fragments.

From yeast to human, loss of Dna2 results in the accumulation of reversed RFs[6,20,38]. These DNA four-way junctions arise at stalled and arrested RFs by the dissociation of the nascent leading and lagging strands from the parental template and their annealing with one another[39]. Dna2 interacts dynamically with the DNA replication machinery at RFs via Ctf4 (And-1 in vertebrates)[9,40,41]. In *Schizosaccharomyces pombe*, phosphorylation by the S-phase checkpoint kinase Cds1 ensures the presence of Dna2 at hydroxyurea (HU)-stalled RFs, where it is thought to counteract RF reversal by degrading the nascent DNA strands[6,18]. Similarly, human DNA2 has been shown to degrade stalled RFs in conjunction with Werner syndrome helicase WRN, thereby facilitating the direct resumption of replication[20]. In budding yeast, Dna2 accumulates in microscopically-visible nuclear foci in response

to RS[42] and the helicase activity of Dna2 contributes to the processing of stalled replication intermediates, preventing post-replicative chromosome entanglements that impair sister chromatid separation unless they are cleaved by Holliday junction resolvase Yen1 in mitosis[19]. These findings have established a physiologically-relevant contribution of Dna2 to the completion of DNA replication that involves the processing of stalled RFs. Whether failed RF processing and recovery is sufficient to explain the inviability of cells in the absence of Dna2 is currently unclear. It is also unknown if and how a Pif1 and Rad9-dependent checkpoint activation might arise from stalled RFs that have escaped the actions of Dna2.

Here we show that RF-stalling leads to incomplete chromosome replication in the absence of Dna2. This exposes cells to Pif1-driven checkpoint activation, elicited by DNA intermediates that arise in a manner dependent on Pif1's ability to promote HR-coupled DNA synthesis. We suggest that the essential requirement for Dna2 in cells results from a dual role in DNA replication: First, Dna2 mediates the recovery of stalled RFs, promoting replication completion. Secondly, the actions of Dna2 suppress the promiscuous use of RDR for replication restart, thereby preventing checkpoint-activating RDR by-products that lead to cell-cycle arrest.

RESULTS

Dna2 and Yen1 provide vital protection from RS

Cell death in absence of Dna2 is mediated by Pif1[21,43]. We characterized *dna2*Δ cells whose viability was restored by replacing *PIF1* with the *pif1-m2* allele[21,43], which depletes cells of nuclear Pif1 while maintaining normal cell growth by expressing the mitochondrial form of Pif1. While control *pif1-m2* cells behaved like wild-type, a subset of *dna2*Δ *pif1-m2* cells grew into large, dumbbell-shaped cells, indicative of cell-cycle arrest at the G2/M boundary, in unperturbed conditions (**Fig. 1a**, **b**). Consistently, *dna2*Δ *pif1-m2* cultures exhibited chronic DNA damage-checkpoint activation detected by Rad9-dependent Rad53 checkpoint-kinase phosphorylation (**Fig. 1c**). Deletion of *RAD9* corrected the dumbbell phenotype of *dna2*Δ *pif1-m2* cells and accelerated cell-cycle progression (**Fig. 1b**, **d**).

However, the reduced viability that characterizes *dna2*Δ *pif1-m2* cells compared to wild-type was only partially suppressed by deletion of *RAD9* (**Fig. 1e**). This suggests that deleterious DNA intermediates arise in *dna2*Δ cells independently of nuclear Pif1, and that these intermediates negatively affect cell viability independently of Rad9-mediated checkpoint signalling.

To gain insight into the nature of the DNA intermediates that cause growth defects and reduced viability in *dna2*Δ *pif1-m2* cells, we investigated the role of Holliday junction resolvase Yen1 in these cells. Yen1 accumulates in the nucleus in its nucleolytically-active form in mitosis[44,45] and is best known for its role in removing branched HR intermediates[46]. Previously, we have shown that Yen1 resolves post-replicative chromosomal DNA-links derived from stalled RFs that haven't been properly processed by Dna2[19]. This non-canonical Yen1 function of cleaving persistent replication intermediates facilitates chromosome segregation in hypomorphic *dna2* cells exposed to RS[19]. Testing the requirement for Yen1 in complete absence of Dna2, we found that Yen1 became indispensable for cell survival in *dna2*Δ *pif1-m2* cells, even in unperturbed conditions. Cell viability was not restored by the additional deletion of *RAD9* (**Fig. 1f** and **Supplementary Fig. 1a**). In contrast to deleting *YEN1*, disrupting another Holliday junction resolvase capable of cleaving branched HR intermediates, Mus81-Mms4[46], did not lead to lethality in the *dna2*Δ *pif1-m2* background (**Fig. 1f**). Yen1 is therefore uniquely required to maintain cell viability in the absence of Dna2.

Next, we exposed *dna2*Δ *pif1-m2* cells to chronic RS to induce increased RF-stalling. Consistent with previous reports[21], we observed that loss of Dna2 rendered *dna2*Δ *pif1-m2* cells highly sensitive to RS induced by HU (**Fig. 1g**) or methyl methanesulfonate (MMS) (**Supplementary Fig. 1b**). This sensitivity was markedly improved by concomitant *RAD9* deletion. The deleterious effect of RS in *dna2*Δ *pif1-m2*, which is independent of nuclear Pif1 in the *pif1-m2* background, is therefore partially dependent on checkpoint-mediator Rad9. Rad9-dependent checkpoint activation in *dna2*Δ cells results in cell-cycle arrest at the G2/M boundary, a time when Yen1 is inactive[44,45]. To test whether Yen1 can mitigate Dna2-dysfunction if it is experimentally manipulated to act throughout the cell cycle, we expressed Yen1^{ON}, a constitutively nuclear and active variant of Yen1[45]. Yen1^{ON} expression

alleviated growth defects and the RS-sensitivity of *dna2*Δ *pif1-m2* cells (**Fig. 1h**). This indicated that ectopic Yen1 activity in S phase can counteract deleterious – and Pif1-independent – DNA structures, which otherwise accumulate in cells lacking Dna2.

Considering the possibility that the observed RS-sensitivity of *dna2Δ pif1-m2* cells could be due to residual Pif1 in the nucleus, we replaced the *pif1-m2* allele with a full deletion of *PIF1*. While complete loss of Pif1 (nuclear and mitochondrial isoforms) leads to moderate growth impairment, *dna2Δ pif1Δ* cells clearly recapitulated the elevated RS-sensitivity seen in *dna2Δ pif1-m2* cells when exposed to elevated temperature (**Supplementary Fig. 1c**) or HU (**Supplementary Fig. 1d**), and exhibited chronic DNA damage-checkpoint activation (**Supplementary Fig. 1e**). Deleterious DNA intermediates therefore accumulate in *dna2Δ* cells due to RF-stalling in complete absence of Pif1, as in cells harbouring the *pif1-m2* allele.

We conclude that Yen1 provides essential protection from the consequences of RF-stalling in the absence of Dna2. Protection by Yen1 is exerted along a pathway that is unrelated to policing Okazaki fragment maturation for extended DNA flaps downstream of Pif1-stimulated strand-displacement DNA synthesis. Taken together, these results strongly suggested that DNA replication remains unfinished in the absence of Dna2, leading to mitotic chromosome entanglements that must be resolved by Yen1 in order to uphold cell viability.

Replication remains incomplete in the absence of Dna2

To address the inability of *dna2Δ pif1-m2* cells to faithfully complete replication directly, we visualized chromosomes before and after a single round of DNA replication by pulsed-field gel electrophoresis (PFGE). This technique gel-resolves fully replicated, linear chromosomes as discrete bands, while incompletely replicated chromosomes containing branched DNA intermediates remain in the wells of the gel. Cells were synchronized in G1 phase of the cell cycle using α-factor and released into S phase in medium containing nocodazole to prevent cells from undergoing mitosis. Ethidium bromide staining after PFGE showed a weaker increase of gel-resolved chromosomal DNA for *dna2Δ pif1-m2* cells

passing through S phase compared to *pif1-m2* cells (**Fig. 2a**). The effect was most obvious for chromosome XII containing the rDNA array. Quantitative Southern blot analysis of chromosome XII showed full recovery of gel-resolved chromosomal DNA – indicative of complete replication – between 60 and 80 min after release of *pif1-m2* cells into S phase. In contrast, genomic DNA of *dna2*Δ *pif1-m2* cells contained a much smaller fraction of gel-resolved material, indicating chromosome XII replication remained incomplete even 2 h after release into S phase (**Fig. 2b**, **c**). Chromosome XII harbours several hundred repeats of the ribosomal DNA (rDNA), which is replicated unidirectionally and therefore at increased risk of remaining incompletely replicated when RF recovery is impaired[47,48]. Importantly, bulk DNA synthesis progressed similarly in *dna2Δ pif1-m2* cells and *pif1-m2* control cells, with cells reaching a 2N DNA content approx. 40 min after release into S phase (**Fig. 2d**). Together, these data reveal a severe problem with driving chromosome replication to completion in *dna2Δ pif1-m2* cells.

To provide further evidence that it is a dysfunctional response to stalled RFs that results in incomplete chromosome replication in the absence of Dna2, we transiently exposed *dna2Δ pif1-m2* cells to exogenous RS. Cells were synchronized in G1 using α-factor and released into S phase in the presence of 200 mM HU to arrest RF progression. After 2 h, HU was removed to allow cells to continue replication while nocodazole was added to the medium to prevent mitosis. Genomic DNA of cells arrested in G1 phase and released into S phase for increasing amounts of time was analysed by PFGE. Compared to non-RS conditions, replication completion in the absence of Dna2 was more dramatically impaired across all chromosomes (**Fig. 2e**), despite *dna2*Δ *pif1-m2* cells progressing through bulk DNA synthesis with kinetics similar to *pif1-m2* control cells (**Fig. 2f**). Quantitative Southern blot analysis revealed a pronounced reduction in gel-resolved chromosome XII (**Fig. 2h**), showing that *dna2*Δ *pif1-m2* cells cannot complete the replication of the difficult-to-replicate, rDNA-bearing chromosome XII after acute RS-exposure. Probing another chromosome, XIII, which lacks rDNA repeats, we detected a less dramatic, but still marked shortfall in gel-resolved material for *dna2*Δ *pif1-m2* cells compared to the *pif1-m2* control (**Fig. 2i**, **j**). These findings are consistent with a genome-wide replication problem that renders chromosomes incompletely replicated after bulk DNA synthesis has taken place in Dna2-

deficient cells. To rule out that this chromosome under-replication phenotype was mediated by residual nuclear Pif1 in *dna2*Δ *pif1-m2* cells, we analysed genomic DNA from *dna2*Δ *pif1*Δ cells after acute RS-exposure by PFGE. We observed significant chromosomal under-replication in complete absence of Dna2 and Pif1, confirming that Dna2 acts fully independently of the actions of Pif1 to promote replication completion following RF-stalling (**Supplementary Fig. 2a**, **b**).

A failure to complete chromosome replication in absence of Dna2 would predict that *dna2*Δ *pif1-m2* cells should lose viability within one cell cycle following transient exposure to 200 mM HU. Consistent with this notion, we found that G1-synchronized *dna2*Δ *pif1-m2* cells released into S phase in the presence of 200 mM HU for 2 h and then allowed to recover in drug-free medium, accumulated at the G2/M boundary with a 2N DNA content (**Fig. 2k**) and cell viability dropped dramatically (**Fig. 2l**). Compared to the *pif1-m2* control, the number of single-nucleated G1 cells and double-nucleated, mitotic *dna2Δ pif1-m2* cells dropped after RS-exposure. Concomitantly, the number of single-nucleated, G2-arrested cells and cells with elongated nuclei spanning the bud neck – indicative of physical impediments to segregation – increased for the *dna2Δ pif1-m2* mutant (**Fig. 2m**, **n**).

These results provide direct evidence that Dna2 contributes to DNA replication in an essential manner after transiently induced RF-stalling, ensuring complete chromosome replication and cell survival. This activity of Dna2 is unrelated to housekeeping roles downstream of Pif1 in Okazaki fragment processing.

Yen1 resolves incompletely replicated chromosomes

Having found that Dna2 is required to drive chromosome replication to completion, and that Yen1 becomes essential in the absence of Dna2, we used super-resolution structured illumination microscopy (SIM) to analyse Yen1 dynamics. We monitored a fully functional version of endogenous Yen1[19,45] tagged with enhanced green-fluorescent protein (EGFP). Yen1 enters the cell nucleus in mitosis[44,45], and we detected Yen1-EGFP in discrete foci and as a diffuse signal tracing the segregating nuclei and the tube-like structure that connects them in anaphase (**Fig. 3a**, **b**). We observed that cells

tend to form a greater number of Yen1 foci when Dna2 is absent (average number of Yen1-EGFP foci of 2.7 ± 0.5 for *dna2*Δ *pif1-m2* cells compared to 1.7 ± 0.3 for *pif1-m2* control cells), although this increase was not statistically significant in unperturbed conditions (**Fig. 3c**). Treatment with 200 mM HU in the preceding S phase led to a marked increase of Yen1 foci in anaphase in both *pif1-m2* control and *dna2*Δ *pif1-m2* cells. This indicates a build-up of structures bound by Yen1 following RS. Importantly, under RS-conditions, the absence of Dna2 correlated with a significant increase in Yen1-EGFP foci compared to control (average number of Yen1-EGFP foci of 6.4 ± 0.8 for *dna2*Δ *pif1-m2* cells compared to 3.6 ± 0.4 for *pif1-m2* control cells, $p < 0.001$). While Yen1 foci mainly localized to the bulk of the separating masses of DNA in *pif1-m2* control cells, there was a marked increase of foci along the bridge connecting them in *dna2*Δ *pif1-m2* cells, in particular after HU-treatment (average number of Yen1-EGFP foci on bridges of 1.6 ± 0.1 for *dna2*Δ *pif1-m2* cells compared to 0.5 ± 0.3 for *pif1-m2* control cells, $p < 0.001$) (**Fig. 3d**).

In some cases, Yen1-EGFP assembled into foci on circular structures that emanated from the bridge between the separating nuclei (**Fig. 3b**). These structures were suggestive of rDNA-loops[49,50]. 1We thus expressed nucleolar protein Nop1[51] tagged with RFP and found that the majority of Yen1 foci colocalized with, or bordered, Nop1-marked rDNA (73 ± 4% of Yen1 foci in *pif1-m2* and 58 ± 2% in *dna2*Δ *pif1-m2* cells) (**Fig. 3e, f**). A more dispersed localization of Yen1 foci away from the rDNA in *dna2*Δ *pif1-m2* compared to *pif1-m2* cells is in good agreement with our PFGE analyses showing a genome-wide replication defect in the absence of Dna2 that is not restricted to the rDNA.

These findings are consistent with the notion that Yen1 fulfils its essential function in Dna2-deficient cells by resolving persistent replication intermediates arising at stalled RFs that would normally be processed by Dna2, thus enabling viable chromosome segregation.

Pif1-toxicity results from incomplete replication

The failure of *dna2*Δ *pif1-m2* and *dna2*Δ *pif1*Δ cells to complete chromosome replication begged the question whether Pif1/Rad9-dependent toxicity might arise as a consequence of the improper

response to stalled RFs in in Dna2-defective cells. To address this, we turned to a *dna2* hypomorphic background harbouring the *dna2-2* allele[52]. This allele, R1253Q, encodes a Dna2 that is nuclease-proficient and helicase-deficient[19], and will henceforth be referred to as *dna2-HD,* for helicase-dead. While *dna2-HD* cells are RS-sensitive and accumulate unresolved replication intermediates that require processing by Yen1[19], they tolerate the presence of nuclear Pif1. This is likely due to the intact nuclease activity of this helicase-dead Dna2[19], which provides partial protection from RS even in the absence of helicase activity (**Supplementary Fig. 3a**). Thus, *dna2-HD* allowed us to compare the response to RS in Dna2-defective cells in the presence and absence of Pif1.

Dna2 helicase-defective cells exhibit a number of growth defects and fail to progress properly through the cell cycle, even in unperturbed conditions[19]. These phenotypes are exacerbated by the deletion of *YEN1,* but we found them to be strongly suppressed upon nuclear depletion of Pif1. Thus, the *pif1-m2* mutation reduced the doubling times of *dna2-HD* and *dna2-HD yen1*Δ cells, which were ~15 and ~55 min above wild-type times, respectively, to only ~7 and ~10 min above wild-type, for *dna2-HD pif1-m2* and *dna2-HD yen1*Δ *pif1-m2* cells, respectively (**Supplementary Fig. 3b**). Furthermore, *pif1-m2* increased the viability of *dna2-HD* and *dna2-HD yen1*Δ cultures, restoring wild-type levels of viability to *dna2-HD pif1-m2* and *dna2-HD yen1*Δ *pif1-m2* cells (**Supplementary Fig. 3c**). Finally, the delayed cell-cycle progression at the G2/M boundary, chronic DNA damage-checkpoint activation, and an accumulation of G2/M-arrested cells with a large-budded morphology observed for *dna2-HD* and *dna2-HD yen1*Δ cultures, were all abolished in the presence of the *pif1-m2* allele (**Supplementary Fig. 3d-f**). Under RS-conditions, we observed that depletion of nuclear Pif1 conferred increased RS-resistance in *dna2-HD pif1-m2* and *dna2-HD yen1*Δ *pif1-m2* cells (**Fig. 4a**), which is in line with previous findings[21].

Size measurements of colonies formed on medium containing HU revealed that *dna2-HD pif1-m2* and, to a greater extent, *dna2-HD yen1*Δ *pif1-m2* cells retain residual RS-sensitivity (**Supplementary Fig. 3g**, **h**), consistent with the Pif1-independent requirement of Dna2 for RF

recovery, which is partially dependent on an intact Dna2 helicase activity. Nonetheless, these findings demonstrate that Pif1 is responsible for most of the toxicity found in the hypomorphic *dna2-HD* cells.

We have shown previously that the accumulation of unresolved replication intermediates in Dna2 helicase-defective cells is accompanied by unscheduled DNA damage-checkpoint activation that manifests itself as a direct response to transient RF-stalling[19]. Thus, replicating *dna2-HD* and *dna2-HD yen1*Δ cells reach a 2N DNA content after transient exposure to 50 mM HU with kinetics similar to wild-type, but, unlike the wild-type, arrest at the G2/M boundary in a Rad9-dependent manner with phosphorylated Rad53[19]. To address a potential involvement of Pif1 in this detrimental response to RF-stalling, we performed mitotic time-course experiments. G1-synchronized cells were released into S phase in the presence of 50 mM HU for 2 h, before removing HU from the medium and incubating the cells for a further 4 h. Under these conditions, cells can complete one cell cycle and are held in the next G1 phase by addition of α-factor to the growth medium. As expected[19], *dna2-HD* and *dna2-HD yen1*Δ cultures showed a normal response to HU by activating the S-phase checkpoint, which was silenced again upon removal of HU (**Fig. 4b**). Then, as cultures reached the end of bulk DNA synthesis, indicated by a 2N cellular DNA content, wild-type cells started to divide approximately 2 h after HU-removal. In contrast, *dna2-HD* and *dna2-HD yen1*Δ cells arrested at the G2/M boundary and exhibited renewed Rad53 phosphorylation (**Fig. 4b**). Strikingly, depletion of nuclear Pif1 abolished this unscheduled G2/M checkpoint response in *dna2-HD pif1-m2* and *dna2-HD yen1*Δ *pif1-m2* cells and progression through mitosis was no longer delayed (**Fig. 4b**). In *dna2-HD* cells, Pif1 therefore drives unscheduled G2/M checkpoint activation provoked by transient RS in the preceding S phase. Collectively, these results suggest that stalled RFs that fail to be resolved by Dna2 become converted into DNA damage checkpoint-activating DNA structures in a Pif1-dependent manner, leading to the cell-cycle arrest of Dna2-defective cells.

Pif1-toxicity relates to RDR

To gain insight into how Pif1 mediates the conversion of stalled replication intermediates, which were improperly processed by Dna2, into structures that elicit a Rad9-dependent checkpoint response, we analysed the effect of well-characterized Pif1 mutants (**Fig. 5a**). First, we disrupted the catalytic activity of Pif1, comparing *dna2-HD pif1-m2* cells expressing wild-type Pif1 or helicase-dead variant Pif1 K264A (*pif1-HD*)[53]. As expected, only the expression of catalytically active Pif1 sensitized the cells to RS (**Fig. 5b**), showing that Pif1's helicase activity is required for the toxicity induced upon RF-stalling in cells with compromised Dna2 activity.

Next, we targeted an interaction between Pif1 and the replicative sliding clamp PCNA[27]. This interaction is required for Pif1 to promote HR-coupled DNA synthesis[54]. Structure-function analyses have shown that a Pif1-R3E mutant (with point mutations I817R, M820R, L821R, and R823E) loses the ability to bind PCNA, to co-localize with HR-mediator Rad52 following RS, and to mediate BIR[25,54]. Strikingly, introduction of the *pif1-R3E* allele into the endogenous *PIF1* locus rendered *dna2-HD* cells markedly more resistant to RS (**Fig. 5c**). The phenotypic suppression was similar to that achieved by depletion of nuclear Pif1 (see **Fig. 4a**). These observations implicate Pif1-PCNA interactions and HR-coupled replication in the toxicity arising in Dna2-defective cells on HU.

HR-coupled replication has been shown to also depend on a TLSSAES phosphorylation motif within the C-terminal domain of Pif1[55]. Disruption of TLSSAES by exchanging all phosphorylatable threonine and serine residues for alanine (Pif1-4A mutant with T763A, S765A, S766A, and S769A) renders Pif1 unable to be recruited to DNA lesions and defective for BIR, while other cellular functions of Pif1 are preserved[55,56]. Introduction of the *pif1-4A* mutation into the endogenous *PIF1* locus resulted in a strong suppression of the RS-sensitivity observed for *dna2-HD* and *dna2-HD yen1*Δ cells (**Fig. 5d**). Importantly, disruption of the TLSSAES motif also suppressed the unscheduled DNA damage-checkpoint response and G2/M arrest exhibited by *dna2-HD* cells in response to RF-stalling (see **Fig. 4b**) in *dna2-HD pif1-4A* cells (**Fig. 5e**).

Together, these results suggest that Pif1-dependent, HR-coupled replication restart at stalled RFs that haven’t been properly processed by Dna2 leads to toxic, checkpoint-activating DNA

structures. This implies that the lethality caused by Pif1 and Rad9 in *dna2*Δ cells is a consequence of unfaithful RF recovery in Dna2-defective cells.

Discussion

It is not known precisely why *DNA2* is an essential gene. Based on work in budding yeast, it has been proposed that the essential function of Dna2 relates to its role in removing long RPA-covered flaps derived from strand-displacement DNA synthesis during Okazaki fragment maturation. Here, we identify RF recovery as an essential function of Dna2. We further speculate that impaired Okazaki fragment processing may not be the cause of inviability in Dna2-deficient cells.

Previously, we showed that the structure-specific nuclease Yen1 resolves persistent DNA replication intermediates that escape resolution by Dna2. Yen1 therefore becomes critical for survival following mild HU-treatment in a *dna2* hypomorphic background[19]. Using nuclear depletion of Pif1 to restore viability to *DNA2*-deleted cells, we now find that Yen1 becomes essential for cell survival in the absence of Dna2, even in unstressed conditions (**Fig. 1**). We interpret our data to suggest equivalence between the response induced by exogenous RS in *dna2* hypomorphic cells and the response to intrinsic replication perturbations in *dna2*Δ cells. We propose that, in unstressed Dna2-deficient cells, dysfunctional RF recovery at stochastically stalled RFs results in unfaithful chromosome replication and a significant burden of unresolved replication intermediates (**Fig. 2**). These are carried over into mitosis and require resolution by Yen1 to promote survival.

We provide evidence that Yen1 localizes to DNA structures arising from RS. DNA replication in *dna2*□ cells was accompanied by an increase of Yen1 foci on mitotic nuclei (**Fig. 3**). Consistent with previous findings[57], we found that Yen1 foci predominantly associated with the rDNA in Dna2-proficient cells. However, in the absence of Dna2, Yen1 foci formed with similar frequency in the rDNA and elsewhere in the genome. This indicates that Yen1 mostly responds to rDNA replication errors in wild-type cells but tends to sites of mis-replication outside of the rDNA context when RF recovery is compromised by the loss of Dna2. Importantly, in absence of Dna2, Yen1 foci were strongly increased

on chromatin bridges connecting the segregating nuclear masses. We propose this is a manifestation of Yen1's engagement with DNA structures that impair chromosome segregation, and which result from dysfunctional RF recovery (**Fig. 3**).

These observations corroborate a critical role of Dna2-mediated RF recovery in completing DNA replication. This can explain the rescue of *dna2*⍰ inviability by concomitant deletion of *RAD9*: when the DNA damage checkpoint is activated by as-yet unknown replication structures, Yen1 is kept inactive and cells are terminally arrested in G2, unable to resolve persistent replication intermediates following activation of Yen1 in mitosis. Disruption of the checkpoint mediator *RAD9* allows progression into mitosis and the resolution of potentially lethal chromosome entanglements by Yen1.

Why is Pif1 toxic in cells lacking Dna2?

Pif1 is required for the majority of the toxicity when Dna2 helicase-defective cells are exposed to chronic RS (**Fig 4a)** and we show that, in response to transient HU-treatment, Pif1 is responsible for the unscheduled DNA damage-checkpoint activation that occurs in G2 phase following recovery from RS (**Fig. 4b**). These findings place Pif1-mediated toxicity downstream of RF-stalling, and our mutational analysis of Pif1 (**Fig. 5**) strongly implicates the resumption of DNA synthesis by HR-dependent mechanisms such as BIR and RDR[58] in this toxicity. At broken RFs, where there is a single-ended DSB, HR proteins assemble at the DSB and catalyse strand-invasion of an intact chromosome to prime DNA synthesis within a displacement loop (D-loop). BIR then proceeds by bubble-migration with uncoupled leading and lagging-strand synthesis. A similar process, RDR, occurs at arrested but unbroken RFs[59-61]. In this case, it is likely that the regressed arm of reversed RFs provides the HR substrate, which is used for invasion of the parental duplex ahead of the site of fork reversal with subsequent D-loop DNA synthesis. Pif1 is essential to drive DNA synthesis in the context of a D-loop, which often covers many thousands of nucleotides[26,27,62]. At D-loops, Pif1 binds PCNA, and loss of PCNA interactions renders Pif1 BIR-defective[54]. It has been shown that the localization of Pif1 to sites of RS-induced HR reactions and its ability to promote BIR depend on a DNA damage-responsive TLSSAES phosphorylation

site[55,56,63]. Here we find that, like BIR/RDR, RS-sensitivity and RS-induced G2/M-checkpoint activation in Dna2 helicase-defective cells requires the catalytic activity of Pif1, its interaction with PCNA, and the TLSSAES phosphorylation motif (**Fig. 5**).

Reversed RFs accumulate in Dna2-depleted cells[6,20,38]. This may lead to increased RDR instead of direct replication resumption mediated by Dna2 at stalled RF when the replication impediment is resolved or removed. On the one hand, RDR could mitigate under-replication problems caused by the absence of Dna2. On the other hand, promiscuous use of RDR may entail the formation of toxic DNA intermediates. We suggest that this is because D-loop progression during BIR and RDR is unstable and the nascent DNA strand undergoes frequent cycles of dissociation and re-annealing with the template[64-67]. Excessive RDR may thus become a significant source of checkpoint-activating intermediates by way of D-loop collapse, potentially leaving nascent strands of extended length permanently exposed as ssDNA in Dna2-deficient cells. Regardless of the precise nature of the checkpoint-activating DNA intermediates in Dna2-mutant cells, our findings demonstrate that Dna2-mediated RF recovery is essential for cell survival, and we propose that Dna2 acts as a gatekeeper at stalled RFs. The essential requirement for Dna2 would result from a dual function at sites of stochastic RF-stalling: Dna2 would promote fork recovery and replication completion while at the same time suppressing inappropriate replication restart by RDR.

Does Dna2 have an essential role in Okazaki fragment processing?

A recent study has evaluated aberrant DNA intermediates after acute depletion of Dna2 by electron microscopy in the presence and absence of nuclear Pif1[38]. As expected, reversed RFs accumulated after depletion of Dna2. In line with findings in fission yeast[68], RF structures bearing DNA flaps of a few hundred nucleotides, which could conform to Okazaki fragments with unprocessed flaps, were also identified, but these occurred at low frequency[38]. The vast majority of Pif1-dependent intermediates consisted of linear dsDNA with a single ssDNA branch ranging from ~1000 to ~5000 nucleotides, with some exceeding 10000 nucleotides[38]. Given that the strength of the DNA damage-

checkpoint response is quantitatively related to the amount of RPA-bound ssDNA present in cells[69], these observations have pinpointed the most likely source of toxic checkpoint signalling and cell-cycle arrest in cells devoid of Dna2. The molecular processes that generate these dsDNA intermediates with very long ssDNA segments are therefore key to understanding the essential role of Dna2 in cells.

One explanation is that in absence of Dna2, extensive DNA strand-displacement synthesis occurs on the lagging strand due to improper flap-control during Okazaki fragment maturation[38]. This results in dsDNA with very long ssDNA branches. Arguing against this model is the fact that lagging-strand replication is intrinsically biased against the formation of DNA flaps greater than a few nucleotides[34,36,37] and that Pol δ has a limited ability to penetrate nucleosomes[70,71], even in the presence of Pif1 and a second Pol δ-processivity factor, the Pif1-related helicase Rrm3[35]. Nascent chromatin on the lagging strand is therefore expected to stifle any extended strand-displacement synthesis, raising the possibility that another process accounts for the dsDNA molecules with ssDNA segments of up to ~15000 nucleotides observed after depletion of Dna2[38].

On the basis of our results, we suggest an alternative – but not necessarily mutually exclusive – model to explain these Pif1-dependent intermediates. We propose that dsDNA molecules with extensive ssDNA segments can be derived from excessive RDR at stalled RFs. Pol δ-mediated RDR can generate thousands of nucleotides worth of DNA[58] by D-loop migration, covering the range of ssDNA segments seen emanating from dsDNA after depletion of Dna2[38]. During this process, D-loops are unstable, and we envision that passage of an oncoming RF and subsequent RF fusion may render nascent RDR strands permanently disengaged. In an attempt to reconcile the available data, we have included these molecular steps in a model of events at stalled RFs in the presence or absence of Dna2 (**Fig. 6**).

We note that our model resolves a previously observed inconsistency in the Okazaki fragment processing-based model for the essential requirement of Dna2 downstream of the actions of Pif1[35]. Pol δ-processivity on the lagging strand is redundantly stimulated by Pif1 and Rrm3 *in vivo*[35]. This functional redundancy argues that if Pif1 is removed in a Rrm3-proficient background, this should not

reverse the lethality of *dna2*Δ cells if this lethality resulted from strand-displacement DNA synthesis during Okazaki fragment maturation[35]. In contrast, Pif1's role in stimulating Pol δ-mediated DNA synthesis in the context of a D-loop during HR-coupled replication restart is non-redundant with Rrm3[27]. A reduction of RDR and toxic RDR by-products afforded by stopping Pif1 acting in the HR-coupled restart of stalled RFs therefore provides a consistent explanation for the restoration of viability to Dna2-deficient cells by concomitant mutation of *PIF1*.

Implication for disease

Mutations in *DNA2* that result in strongly reduced protein levels and/or dysfunction of DNA2's helicase activity have been identified in patients with Seckel syndrome and microcephalic primordial dwarfism[7,10]. A number of Seckel syndrome disease genes including *ATR*, *ATRIP*, *DONSON*, and *TRAIP* have well-established roles in the response to RF-stalling[72-76]. Their dysfunction provides an explanation for intrauterine and postnatal growth defects in Seckel syndrome based on incomplete chromosome replication, cell-cycle arrest, and a general defect in cell proliferation during development[77]. Collectively, our results suggest that *DNA2* falls into the same category of Seckel syndrome genes with mutations leading to an inappropriate response to stalled RFs that ultimately results in reduced cell numbers and global growth failure. This is consistent with the lack of evidence for an Okazaki fragment processing role of DNA2 in human cells[9], while human DNA2 has been shown to facilitate RF recovery and replication completion[20]. Given the higher complexity of the human genome compared to yeast, its role in RF recovery may be sufficient to explain the essential role of *DNA2*. However, it will be interesting to explore whether a switch to inappropriate replication restart pathways contributes to the demise of human cells when DNA2 activity is perturbed.

The frequent overexpression of *DNA2* in cancer likely reflects an adaptation to increased levels of intrinsic RS, which is prominent in cancer cells[78]. Its central role in RF recovery described herein supports *DNA2* as a therapeutic target[79,80], whose inhibition might be exploited to generate

clinical synthetic lethality in settings with elevated RS, selectively eliminating cancer cells by stress-overload.

Methods

Yeast strains and plasmids. *S. cerevisiae* strains were derived from BY4741[81], and are listed in **Supplementary Table 1**. If not stated otherwise, strains were cultured in YPAD medium at 30°C. The *pif1-m2* allele was generated using pop-in/pop-out mutagenesis[82]. The replication stress sensitivity of the *dna2*Δ *pif1-m2* strain was complemented with plasmid-borne *DNA2* cloned into vector pAG416GPD-ccbd (Addgene). The replication stress sensitivity of *dna2-HD* cells harbouring the *pif1-m2* allele was restored by expressing the sequence coding for the nuclear form of Pif1 (starting at amino acid residue M40) from a pYES-DEST52 vector (Invitrogen). Site-directed mutagenesis was used to generate the *HD* version of *PIF1* (K264A). The *pif1-R3E* (I817R, M820R, L821R, R823E) and *pif1-4a* (T763A, S765A, S766A, S769A) alleles were introduced into the endogenous *PIF1* locus by Cas9-mediated mutagenesis[83].

For complementation of Yen1-deficiency, *YEN1* was cloned into vector pAG416GPD-ccbd (Addgene). *YEN1^{ON}* was expressed from a pYES-DEST52 vector (Invitrogen). For microscopy, *YEN1* was cloned into pAG415GPD-ccbd-EGFP and NOP1-dsRED was expressed from pWJ1321[84].

Cell viability, growth, and drug-sensitivity assays. Doubling times[85] were averaged over three independent experiments. Microscopic cell-cycle stage determination was performed by examining at least 300 cells per strain in each experiment. Plating efficiency as a measure of strain viability was determined from five experiments, dividing the number of colonies formed after 3-4 days at 30 °C by the number of cells plated, as determined in haemocytometer counts. For drop assays, exponentially growing cells were normalized to 10^7 cells ml^{-1} and tenfold serial dilutions were applied onto plates of YPAD or synthetic complete medium, with or without replication stress-inducing agents (HU, MMS), using a replica-plater (Sigma-Aldrich). Photographs were taken following 2-3 days of incubation at

30°C. For liquid survival assays, overnight cultures were diluted to OD_{600} = 0.1-0.2, grown for 4 h in YPAD, synchronized in G1 using α-factor mating pheromone, washed, and then treated or not with 200 mM HU for 2 h in YPAD. Relevant dilutions were plated onto YPAD plates and colonies were counted after 3-4 days. For colony size measurements, exponentially growing cells were plated on YPAD with or without HU. Plates were incubated 2 or 3 days at 30°C before photographs were acquired for analysis.

Mitotic time-course experiment. Exponentially growing yeast cells were harvested and diluted to OD_{600} = 0.4 in YPAD with addition of 1 µg ml^{-1} α-factor for G1-synchronization. After 2.5 h of incubation, synchronized cells were harvested, washed in ddH_2O, and released into YPAD containing 50 or 200 mM HU (Sigma) for 2 h to induce RS. After HU wash-out, cells were cultured in YPAD containing 1 µg ml^{-1} α-factor to prevent re-entry into S-phase, or 15 µg ml^{-1} nocodazole (Sigma) and 1% (v/v) DMSO to block entry into mitosis.

Flow cytometry. 10^7 cells where harvested, fixed overnight at 4°C in 70% ethanol, resuspended in 50 mM sodium citrate solution, and de-clumped by sonication. Sonicated cells were resuspended in sodium citrate solution containing 0.25 mg ml^{-1} RNAse A (Roche). After 1 h of incubation at 50°C, cells were washed and resuspended in sodium citrate containing 16 µg ml^{-1} propidium iodide (Sigma) for 30 min. FACS analysis was performed using a BD LSRII-1 device and BD FACSDiva software.

Analysis of Rad53-phosphorylation. Cells were harvested and protein samples were prepared by trichloroacetic acid (Sigma) precipitation. Samples were resuspended in 100 µl Nu-PAGE sample buffer (Invitrogen), supplemented with 250 mM DTT, and boiled. After SDS-PAGE, proteins were transferred onto PVDF membrane (Merck Millipore) by semi-dry transfer (25 V / 1.0 A, 30 min) using a Trans-Blot Turbo Transfer System (BioRad). Membranes were blocked by incubation in 5% non-fat dried milk (Sigma): TEN-T (150 mM NaCl, 1 mM EDTA , 40 mM Tris-HCl pH 7.5, 0.05% Tween-20) and probed

overnight with a custom-made anti-Rad53 antibody[86], followed by incubation with a HRP-conjugated anti-mouse antibody for 1 h. Protein bands were visualized using enhanced chemiluminescence (GE healthcare).

Microscopy. For differential interference contrast images (DIC), yeast in exponential growth phase were harvested, fixed 5 min in 4% paraformaldehyde, washed 3 times in PBS (1 mM KH_2PO_4, 3 mM Na_2HPO_4, 150 mM NaCl), and attached to glass coverslips using Concanavalin A (Sigma). Images were acquired with a Z1 Zeiss microscope, an AxioCam 506 mono camera, a Plan-APOCHROMAT 63x/1.4 DIC microscope oil objective, and Zen Blue 2012 software. For the observation of Yen1 foci, live cells were transferred in µ-Slides 4 Well imaging chambers (ibidi) coated with ibidi polymer, placed under an Olympus IX81 spinning disk confocal microscope equipped with an EM-CCD cascade II camera (Photometrics), a Yokogawa CSU-X1 scan head and an ASI MS-2000 Z-piezo stage. The fluorophores were excited sequentially at 561nm (dsRED) and 491nm (EGFP) and the emitted light filtered with Semrock FF01-617/73-25 (dsRED) and Semrock FF01-525/40-25 (EGFP). The images were acquired using an oil-immersed PlanApo 100x/1.45 objective and Visiview software. For SIM experiments, cells were fixed in 4% paraformaldehyde, washed with PBS, and attached to a thin SIM-grade Zeiss 1.5 glass coverslip using concanavalin A. Image acquisitions were performed on a super resolution-SIM Elyra S.1 microscope (Zeiss) with a Plan-Apochromat 63x/1.4 NA objective lens, an EM-CCD camera iXon 885 (Andor Technology), and the ZEN software (Zeiss). Cells were fully sectioned into 60 slices at 0.1-nm intervals, with images taken at 60-ms exposures per slice with five rotations of the illumination grid. Image processing was performed with ZEN Black with the automatic settings and the “Raw scale” option selected.

Pulsed field gel electrophoresis (PFGE) and Southern blotting. Chromosomal DNA was analysed by PFGE[87]. Yeast cells were harvested by centrifugation and washed in ice-cold 0.5 M EDTA. Cell pellets were suspended in Zymolyase buffer (50 mM NaH_2PO_4, 50 mM EDTA, 1 mM DTT) and embedded in

1% pulsed field-certified agarose (Bio-Rad) to form a plug. Plugs were treated 1 h at 37°C with 0.4 mg ml^{-1} Zymolyase (USBiological), overnight at 50°C with proteinase K (Eurobio) in 10 mM Tris-HCl, 50 mM EDTA, 1% N-lauroylsarcosinate (Sigma), and then washed with ddH_2O. Genomic DNA was migrated through 1% agarose in 0.5x TBE (89 mM Tris-HCl, 89 mM boric acid, 2mM EDTA) in a CHEF-DR II PFGE system (BioRad) maintained at 14°C, 6 V/cm, 60 s switch time for 15 h, followed by 90 s switch time for 9h. Ethidium bromide-stained DNA was visualized using a GE Typhoon 9400 system. The DNA was then depurinated in 125 mM HCl solution, blotted onto Hybond-XL membrane (Amersham) by capillary transfer in NaOH, and fixed by baking at 80°C for 2 h. Membranes were blocked 1 h at 65°C with 20 ng ml^{-1} heat-denatured DNA (Sigma) in Church buffer (0.5 M sodium phosphate buffer, pH 7.5, 10 mM EDTA, 7% SDS) and probed overnight at 65°C for the chromosome of interest by Southern hybridization with sequence-specific, heat-denatured, radiolabelled DNA probes. After washing of the membranes, signals were recorded on phosphor-screens (Kodak) and visualized using a GE Typhoon 9400 system for quantification (see below). Radiolabelled probes were generated by Klenow reaction: 200 ng of heat-denatured DNA template in labelling solution (50 mM Tris-HCl, 5 mM $MgCl_2$, 0.2 M HEPES, pH 6.6, 150 µg ml^{-1} heat-denatured random hexadeoxyribonucleotides, 400 µg ml^{-1} bovine serum albumin, 25 µM GTP, 25 µM TTP, 0.3 µM [α-^{32}P]ATP, 0.3 µM [α-^{32}P]CTP) were incubated for 1 h at 37°C in presence of 5 U DNA Polymerase I Large Klenow Fragment (NEB). Radiolabelled DNA was purified on G-25 MicroSpin columns (GE healthcare).

Quantification and statistical analysis

Microscopy. Images were deconvolved using Huygens professional and the classic maximum-likelihood estimate algorithm with a signal-to-noise ratio of 5, automatic background estimation and 40 iterations. Thresholding and foci analysis were performed using the Fiji image processing package. Data were plotted using RStudio and the violin plot R package version 0.3.2 (https://github.com/TomKellyGenetics/vioplot). On violin plots, the black dot and the error bars

represent the mean and the standard deviation of three independent biological replicates, respectively.

Quantification of Southern blots. Intensity calculations for Southern blots were performed using the Fiji image processing package. Signals for gel-resolved chromosomal DNA and DNA retained in the well were determined and background signal subtracted. The fraction of gel-resolved chromosomal DNA was calculated within each lane by dividing the signal for gel-resolved DNA by total DNA signal. For each experimental series, the migrating fraction of DNA following a single round of replication was expressed relative to the migrating fraction either in the respective G1 (maximal migration = 1) and HU samples (minimal migration = 0) or in the respective G1 (maximal migration = 1) and 40 min samples (minimal migration = 0) for the unperturbed S-phase progression.

Colony size measurements. Thresholding was applied using Fiji to exclude plate imperfections and fused colonies from the analysis. Colony area was evaluated using the Fiji image processing package. Data were plotted using RStudio. Individual data points corresponding to single colonies are represented in a boxplot displaying the median value (black rectangle), the limits of the first and third quartile (lower and upper limits of the box), the most extreme data points that are less than 1.5x IQR from the limits of the first and third quartiles (whisker), and an approximation of the 95% confidence interval of the median (notches, median ± 1.57 x IQR / sqrt(n)).

Acknowledgements

We thank Kenji Shimada, Andrew Seeber, and all members of the Gasser and Rass laboratories for stimulating discussions and technical help. We are grateful to Tony Carr for critical reading of the manuscript and insightful comments. We are obliged to Hubertus Kohler from the Cell Sorting Platform, and Laurent Gelman and Steven Bourke from the Facility for Advanced Imaging and Microscopy at the Friedrich Miescher Institute for their assistance. Work in the laboratory of U.R. was

supported by the Swiss Cancer League and the Novartis Research Foundation. Research in the Gasser laboratory is funded by the Swiss National Science Foundation through grant 31003A_176286. We dedicate this paper to the memory of our dear friend Franz Enkner.

Author Contributions

U.R. and B.F. planned and analysed the experiments with input from G.Ö. who made initial genetic observations. B.F. performed the experiments with help from D.K., G.Ö., and F.E. K.C performed SIM experiments. S.M.G. supervised B.F. and K.C. U.R. wrote the paper with input from all authors.

Legends

Fig. 1 Dna2 and Yen1 protect cells from RS. **a** Microscopic inspection of wild-type (WT) and the indicated mutant strains grown exponentially in rich medium. Representative images showing cell-morphological changes in the absence of Dna2 and nuclear Pif1. Scale bar, 5 µm. **b** Cell-cycle phase distribution of the indicated strains grown as in panel **a**, based on cell morphology determined by microscopic inspection. Data represent mean percentages of cells in G1, S, and G2/M ± SD (n = 3 independent experiments). **c** Representative anti-Rad53 Western blot from whole-cell extracts of the indicated strains grown exponentially. Hyperphosphorylation of Rad53 (black arrowhead) indicates checkpoint activation. **d** Cell-cycle progression analysed by flow cytometry of the indicated strains synchronized in G1 using α-factor and released into rich medium. **e** Cell viability for the indicated strains, assessed by plating efficiency (PE). Data represent mean values ± SD (n = 3 independent experiments), relative to WT. **f** Plasmid-shuffle experiments assessing whether *YEN1* or *MUS81* are essential for viability in *dna2*Δ *pif1-m2* cells. Cells of the indicated genotypes contained a plasmid expressing Yen1 (*pYEN1*) that can be selected for (Ura-) or against (5-FOA). Failure to grow on 5-FOA indicates an inviable genotype. **g** Drop assays of serial dilutions of the indicated strains on drug-free and HU-containing plates for an assessment of growth and RS-sensitivity. **h** Drop assays of serial dilutions of the indicated strains on drug-free and HU-containing plates of cells expressing Yen1^{ON} (*pYEN1*^{ON}) or containing an empty vector.

Fig. 2 Dna2 is required for the completion of chromosome replication. **a** Representative PFGE experiments with the indicated strains, DNA stained by ethidium bromide. Gel-resolved DNA is labelled with chromosome numbers. G1-synchronized cells were released into S phase in medium containing nocodazole to arrest cells prior to mitosis. At the indicated experimental stages, genomic DNA was analysed for fully replicated (gel-resolved) chromosomes by PFGE. **b** Southern blot analysis of the gel shown in panel **a**, probing for chromosome XII. **c** Quantification of Southern blots as shown in panel **b** to determine the fraction of gel-resolved chromosome XII. Data represent mean values ±

SEM (n = 3 independent experiments). **d** Cell-cycle progression analysis by flow cytometry of cells collected as in panel **a**. **e** Representative PFGE of the indicated strains treated with HU, DNA stained by ethidium bromide. Gel-resolved DNA is labelled with chromosome numbers. G1-synchronized cells were released into medium containing 200 mM HU for 2 h, followed by drug wash-out and incubation in HU-free medium, which contained nocodazole to prevent mitosis. At the indicated stages, genomic DNA was analysed for fully replicated (gel-resolved) chromosomes by PFGE. **f** Cell-cycle progression analysis by flow cytometry of cells collected in panel **e**. **g** Southern blot analysis of a gel obtained as in panel **e**, probing for chromosome XII. **h** Quantification of Southern blots as shown in panel **g** to determine the fraction of gel-resolved chromosome XII. Data represent mean values ± SEM (n = 3 independent experiments). **i** Southern blot analysis of a gel obtained as in panel **e**, probed for chromosome XIII. **j** Quantification of Southern blots as shown in panel **i** to determine the fraction of gel-resolved chromosome XIII. Data represent mean values ± SEM (n = 3 independent experiments). **k** Cell-cycle progression analysis of cells of the indicated strains synchronized in G1, treated with 200 mM HU for 2 h and released for 4 h into a drug-free medium. **l** Cell viability of the indicated strains, assessed by plating efficiency (PE) after synchronization in G1, removal of α-factor, and treatment or not with 200 mM HU for 2 h. Data expressed relative to *pif1-m2* cells as mean values ± SD (n = 3 independent experiments). **m** Representative images of cells treated as in panel **k** showing single-nucleated cells (I), a double-nucleated cell in G2 (II), a G2 cell with a nucleus at the bud neck (III), and an early anaphase cell with an elongated nucleus spanning the bud neck (IV). **n** Quantification of cells (n ≥ 110 cells per strain) observed as in panel **m.**

Fig. 3 Yen1 focus formation on DNA in response to unfaithful chromosome replication caused by the absence of Dna2. **a** Representative SIM image of an anaphase cell expressing Yen1-EGFP (green). Scale bar, 5µm. **b** Representative images of Yen1-EGFP-expressing cells in anaphase used to score Yen1 foci. *Right*, representative images with Yen1 foci located on a loop-like structure indicative of rDNA (white arrows). Scale bar, 5µm. **c** Quantification of the number of Yen1-EGFP foci per anaphase cell in the

indicated strains. Unperturbed samples were collected from exponentially growing cultures. For HU samples, cells were synchronized in G1, treated with 200 mM HU for 2 h and released into a drug-free medium. All data are represented as violin plot, with the mean ± SD (n=3 independent experiments, ≥ 99 cells observed per strain and condition). For statistical analysis, one-way analysis of variance (Anova) and a post-hoc Tukey multiple comparison test was performed, (n.s., non-significant; **, P<0.01; ***, P<0.001). **d** Quantification as in **c** but focused only on foci formed between two segregating masses of DNA. **e** Representative images of cells expressing Yen1-EGFP (green) and the nucleolar marker Nop1-dsRED (magenta), on separating DNA masses (top panel, white arrows) and within the anaphase tube connecting them (bottom panel, white arrows). Scale bar, 5µm. **f** Quantification of the co-localization between Yen1 and Nop1 in the indicated strains, determined as shown in **e**. Data are represented as mean values ± SD (n = 3 independent experiments, ≥ 61 cells scored per strain and condition).

Fig. 4 Pif1-toxicity in absence of Dna2 results from incomplete replication. **a** Drop assays of serial dilutions of the indicated strains on drug-free and HU-containing plates to assess growth and RS-sensitivity. **b** Mitotic time-courses with transient RS-treatment were performed with the indicated strains. Cells, synchronized in G1, were released into medium containing 50 mM HU for 2 h, followed by drug wash-out and incubation in drug-free medium with α-factor to prevent entry into a second S phase. Checkpoint activation was monitored by Western blot analysis of whole-cell extracts for Rad53 hyperphosphorylation (black arrowheads). The progression of DNA replication was monitored by flow cytometry (1 and 2 N DNA content indicated).

Fig. 5 Pif1-toxicity in Dna2-defective cells involves RDR. **a** Schematic representation of Pif1 showing the bi-partite helicase domain (grey), a TLSSAES phosphorylation site required for BIR, and the PCNA-interacting peptide (PIP). Mutations introduced into these domains are denoted below, see text for details. **b** Drop assays of serial dilutions on drug-free and HU-containing medium of the indicated

675 strains expressing wild-type Pif1 (+*pPIF1*), a helicase-dead version of Pif1 (+*pPIF1-HD*), or containing
676 the empty vector. **c** Drop assays of serial dilutions of the indicated strains on drug-free and HU-
677 containing medium assessing growth and sensitivity to RS in the presence or absence of the *pif1-R3E*
678 allele at the endogenous *PIF1* locus in multiple independently created strains. **d** Drop assays as in
679 panel **c**, assessing multiple independently created strains harbouring the *pif1-4a* allele. **e** *dna2-HD*
680 *pif1-4a* cells treated as in **Fig. 4**, panel **b**, were assessed for unscheduled G2/M checkpoint activation
681 following transient exposure to RS. The progression of DNA replication was monitored by flow
682 cytometry (1 and 2 N DNA content indicated).
683
684 **Fig. 6** Dna2 gatekeeper model: Dna2 controls the fate of stalled RFs by promoting RF recovery and
685 suppressing inappropriate restart by RDR. **a** Dna2 counteracts RF reversal (I) at stalled RFs by
686 degrading the regressed arm[6,20] (II). This enables direct resumption of RF progression (III) and
687 promotes the completion of chromosome duplication (IV). **b** Reversed RFs left unprocessed by Dna2
688 (I) are subject to alternative restart by RDR (II), leading to the formation of a D-loop (III). Pif1 promotes
689 RDR by binding PCNA and stimulating DNA synthesis in the context of a D-loop[54] (IV). RDR can facilitate
690 replication completion as indicated by the arrow. However, migrating D-loops are characterized by
691 frequent nascent strand dissociation (V). D-loop collapse and passage of a conventional RF may cause
692 the nascent RDR strand to become permanently exposed as ssDNA. The resulting dsDNA intermediate
693 with a long ssDNA branch (VI) conforms to Pif1-dependent intermediates that have been observed in
694 Dna2-depleted cells[38]. This explains why Dna2 is essential: In the absence of Dna2, excessive RDR
695 results in toxic levels of RPA-covered ssDNA, causing DNA damage-checkpoint activation and cell-cycle
696 arrest. Because RDR is dependent on Pif1[26,27], *dna2*Δ inviability is reversed by concomitant disruption
697 of *PIF1*. **c** In the absence of Dna2 and Pif1, replication remains incomplete, but because stalled RFs are
698 prevented from undergoing excessive RDR, the DNA damage checkpoint remains silent and cells enter
699 mitosis. This activates Yen1, enabling it to resolve chromosome entanglements at persistent
700 replication intermediates and maintain cell viability (I). The DNA repair steps downstream of Yen1-

cleavage (II) remain to be determined. It is conceivable that arrival of a converging RF (III) facilitates replication of the unbroken sister chromatid and DSB repair on the sister chromatid cut by Yen1 (IV), thereby mediating replication completion (V).

Supplementary Fig. 1 relates to Fig. 1. **a** *YEN1* is essential for cell viability in *dna2*Δ *rad9*Δ cells. Cells contained a plasmid expressing *YEN1* (*pYEN1*) that can be selected for (Ura-) or against (5-FOA). Failure to grow on 5-FOA indicates an inviable genotype. **b** Drop assays of serial dilutions of the indicated strains on drug-free and MMS-containing medium demonstrate the sensitivity of *dna2*Δ mutants to RS, even in absence of nuclear Pif1 or Rad9. **c** Drop assays of serial dilutions of the indicated *pif1-m2* and *pif1*Δ mutant strains incubated at different temperatures. **d** Drop assays of serial dilutions of the indicated strains on drug-free and HU-containing medium demonstrate the RS-sensitivity of *dna2*Δ cells, even in complete absence of Pif1. **e** Representative anti-Rad53 Western blots from whole-cell extracts of exponentially growing cultures of the indicated strains. Hyperphosphorylation of Rad53 (black arrowhead) indicates checkpoint activation.

Supplementary Fig. 2 relates to Fig. 2. **a** Dna2 is essential for replication completion in a *pif1*Δ background **a** Representative PFGE of the indicated strains, DNA stained by ethidium bromide. Gel-resolved DNA is labelled with chromosome numbers. G1-synchronized cells were released into medium containing 200 mM HU for 2 h, followed by drug wash-out and incubation in HU-free medium, which contained nocodazole to prevent mitosis. At the indicated experimental stages, genomic DNA was analysed for fully replicated chromosomes resolved by PFGE. **b** Southern blot analysis of a gel obtained as in panel **a**, probing for chromosome XII. A distinct shortfall in gel-resolved chromosome XII following transient RS-exposure is detected for the *dna2*Δ *pif1*Δ strain.

Supplementary Fig. 3 relates to Fig. 4. **a** The Dna2 nuclease activity protects Dna2 helicase-defective cells from RS. Drop assays of serial dilutions of the indicated strains bearing different mutation alleles

of *DNA2* in a *pif1-m2* background. *dna2-HD*, Dna2 R1253Q; *dna2-ND/HD*, nuclease/helicase-dead Dna2 with mutations D657A and R1253Q. **b** Doubling time measurements of the indicated strains presented as mean values ± SD (n = 3 independent experiments). **c** Cell viability of the indicated strains, assessed by plating efficiency (PE). Data represent mean values ± SD (n = 5 replicates), relative to wild-type (WT). **d** Cell-cycle phase distribution of the indicated strains, assessed by microscopic inspection of cell morphology, represented as mean percentage of cells in G1, S, and G2/M ± SD (n = 3 independent experiments). **e** Depletion of nuclear Pif1 suppresses chronic checkpoint activation in *dna2-HD* cells. Representative anti-Rad53 Western blots from whole-cell extracts of exponentially growing cultures of the indicated strains. Hyperphosphorylation of Rad53 (black arrowhead) indicates checkpoint activation. **f** Representative DIC images showing the cell morphologies observed for the indicated strains. Scale bar, 10 µm. **g** Colony-size measurements of cells grown on medium with or without 150 mM HU for two days, or **h** three days, with representative images. Scale bar, 5 mm. Box plots represent individual data points corresponding to single colonies (n > 250), median values (black rectangles), and the limits of the first and third quartile (lower and upper limits of the box, respectively).

Supplementary Table 1 List of *S. cerevisiae* strains used in this study.

Strain	Relevant genotype	Source
YRL19	*Mata, hisΔ3, leu2Δ0, met15Δ0, ura3Δ0 (BY4741)*	GE Healthcare
CloneID 174	*YRL19, yen1::KAN*	GE Healthcare
YRL300	*YRL19, pif1::pif1-m2*	This study
YRL301	*YRL19, pif1::pif1-m2, yen1::KAN*	This study
YRL29	*YRL19, dna2::dna2-HD*	Ref. 19
YRL302	*YRL19, dna2::dna2-HD, pif1::pif1-m2*	This study
YRL97	*YRL19, dna2::dna2-HD, yen1::KAN*	Ref. 19
YRL303	*YRL19, dna2::dna2-HD, pif1::pif1-m2, yen1::KAN*	This study
YRL304	*YRL19, pif1::pif1-m2, pYES-DEST52 PIF1*	This study
YRL305	*YRL19, pif1::pif1-m2, pYES-DEST52 pif1-HD*	This study
YRL306	*YRL19, pif1::pif1-m2, pYES-DEST52 ccdB*	This study
YRL307	*YRL19, dna2::dna2-HD, pif1::pif1-m2, pYES-DEST52 PIF1*	This study
YRL308	*YRL19, dna2::dna2-HD, pif1::pif1-m2, pYES-DEST52 pif1-HD*	This study

YRL309	*YRL19, dna2::dna2-HD, pif1::pif1-m2, pYES-DEST52 ccdB*	This study
YRL310	*YRL19, dna2::HIS, pif1::pif1-m2*	This study
YRL311	*YRL19, dna2::HIS, pif1::pif1-m2, rad9::KAN*	This study
YRL316	*YRL19, dna2::HIS, pif1::pif1-m2, pAG416 GPD YEN1*	This study
YRL317	*YRL19, dna2::HIS, pif1::pif1-m2, mus81::NAT, pAG416 GPD YEN1*	This study
YRL318	*YRL19, dna2::HIS, pif1::pif1-m2, yen1::NAT, pAG416 GPD YEN1*	This study
YRL325	*YRL19, rad9::KAN*	This study
YRL326	*YRL19, dna2::HIS, rad9::KAN*	This study
YRL327	*YRL19, dna2::HIS, rad9::KAN, pAG416 YEN1*	This study
YRL328	*YRL19, dna2::HIS, rad9::KAN, yen1::NAT, pAG416 GPD YEN1*	This study
YRL330	*YRL19, dna2::dna2-ND/HD, pif1::pif1-m2*	This study
YRL334	*YRL19, pif1::pif1-R3E*	This study
YRL335	*YRL19, dna2::dna2-HD, pif1::pif1-R3E*	This study
YRL378	*YRL19, pif1::pif1-m2, rad9::KAN*	This study
YRL382	*YRL19, pif1::pif1-m2, pAG415 GPD YEN1-EGFP*	This study
YRL383	*YRL19, dna2 ::HIS, pif1::pif1-m2, pAG415 GPD YEN1-EGFP*	This study
YRL386	*YRL19, pif1::pif1-m2, pAG415 GPD YEN1-EGFP, pWJ1322 NOP1-dsRED*	This study
YRL387	*YRL19, dna2::HIS, pif1::pif1-m2, pAG415 GPD YEN1-EGFP, pWJ1322 NOP1-dsRED*	This study
YRL405	*YRL19, pif1::HIS*	This study
YRL408	*YRL19, dna2::NAT, pif1::HIS*	This study
YRL411	*YRL19, pif1::pif1-m2 pYES-DEST YEN1^{ON}*	This study
YRL412	*YRL19, dna2::HIS pif1::pif1-m2 pYES-DEST YEN1^{ON}*	This study
YRL439	*YRL19, dna2::dna2-HD, pif1::pif1-4a*	This study
YRL442	*YRL19, dna2::dna2-HD, pif1::pif1-4a yen1::HIS*	This study
YRL444	*YRL19, dna2::HIS, mus81::NAT, pif1::pif1-m2*	This study

References

1. Bae, S. H. *et al.* Dna2 of Saccharomyces cerevisiae possesses a single-stranded DNA-specific endonuclease activity that is able to act on double-stranded DNA in the presence of ATP. *J. Biol. Chem.* **273**, 26880–26890 (1998).
2. Budd, M. E. & Campbell, J. L. A yeast gene required for DNA replication encodes a protein with homology to DNA helicases. *Proc. Natl. Acad. Sci. USA* **92**, 7642–7646 (1995).
3. Pinto, C., Kasaciunaite, K., Seidel, R. & Cejka, P. Human DNA2 possesses a cryptic DNA unwinding activity that functionally integrates with BLM or WRN helicases. *Elife* **5**, 3006 (2016).
4. Lin, W. *et al.* Mammalian DNA2 helicase/nuclease cleaves G-quadruplex DNA and is required for telomere integrity. *EMBO J.* **32**, 1425–1439 (2013).
5. Hoa, N. N. *et al.* BRCA1 and CtIP Are Both Required to Recruit Dna2 at Double-Strand Breaks in Homologous Recombination. *PLoS One* **10**, e0124495 (2015).

6. Hu, J. *et al.* The intra-S phase checkpoint targets Dna2 to prevent stalled replication forks from reversing. *Cell* **149**, 1221–1232 (2012).

7. Shaheen, R. *et al.* Genomic analysis of primordial dwarfism reveals novel disease genes. *Genome Res.* **24**, 291–299 (2014).

8. Ronchi, D. *et al.* Mutations in DNA2 link progressive myopathy to mitochondrial DNA instability. *Am. J. Hum. Genet.* **92**, 293–300 (2013).

9. Duxin, J. P. *et al.* Okazaki fragment processing-independent role for human Dna2 enzyme during DNA replication. *J. Biol. Chem.* **287**, 21980–21991 (2012).

10. Tarnauskaitė, Ž. *et al.* Biallelic variants in DNA2 cause microcephalic primordial dwarfism. *Hum. Mutat.* **40**, 1063–1070 (2019).

11. Peng, G. *et al.* Human nuclease/helicase DNA2 alleviates replication stress by promoting DNA end resection. *Cancer Res.* **72**, 2802–2813 (2012).

12. Strauss, C. *et al.* The DNA2 nuclease/helicase is an estrogen-dependent gene mutated in breast and ovarian cancers. *Oncotarget* **5**, 9396–9409 (2014).

13. Wanrooij, P. H. & Burgers, P. M. Yet another job for Dna2: Checkpoint activation. *DNA Repair (Amst.)* **32**, 17–23 (2015).

14. Cejka, P. DNA End Resection: Nucleases Team Up with the Right Partners to Initiate Homologous Recombination. *J. Biol. Chem.* **290,** 22931–22938 (2015).

15. Markiewicz-Potoczny, M., Lisby, M. & Lydall, D. A Critical Role for Dna2 at Unwound Telomeres. *Genetics* **209**, 129–141 (2018).

16. Li, Z. *et al.* hDNA2 nuclease/helicase promotes centromeric DNA replication and genome stability. *EMBO J.* **37**, e96729 (2018).

17. Berti, M. & Vindigni, A. Replication stress: getting back on track. *Nat. Struct. Mol. Biol.* **23**, 103–109 (2016).

18. Lai, M. S. & Foiani, M. Dna2 offers support for stalled forks. *Cell* **149**, 1181–1183 (2012).

19. Ölmezer, G. *et al.* Replication intermediates that escape Dna2 activity are processed by Holliday junction resolvase Yen1. *Nat. Commun.* **7**, 13157 (2016).

20. Thangavel, S. *et al.* DNA2 drives processing and restart of reversed replication forks in human cells. *J. Cell Biol.* **208**, 545–562 (2015).

21. Budd, M. E., Reis, C. C., Smith, S., Myung, K. & Campbell, J. L. Evidence suggesting that Pif1 helicase functions in DNA replication with the Dna2 helicase/nuclease and DNA polymerase delta. *Mol. Cell. Biol.* **26**, 2490–2500 (2006).

22. Budd, M. E., Antoshechkin, I. A., Reis, C., Wold, B. J. & Campbell, J. L. Inviability of a DNA2 deletion mutant is due to the DNA damage checkpoint. *Cell Cycle* **10**, 1690–1698 (2011).

23. Pohl, T. J. & Zakian, V. A. Pif1 family DNA helicases: A helpmate to RNase H? *DNA Repair (Amst.)* 102633 (2019). doi:10.1016/j.dnarep.2019.06.004

24. Chistol, G. & Walter, J. Molecular watchdogs on genome patrol. *Elife* **3**, e02854 (2014).

25. García-Rodríguez, N., Wong, R. P. & Ulrich, H. D. The helicase Pif1 functions in the template switching pathway of DNA damage bypass. *Nucleic Acids Res.* **46**, 8347–8356 (2018).

26. Jalan, M., Oehler, J., Morrow, C. A., Osman, F. & Whitby, M. C. Factors affecting template switch recombination associated with restarted DNA replication. *Elife* **8**, e41697 (2019).

27. Wilson, M. A. *et al.* Pif1 helicase and Polδ promote recombination-coupled DNA synthesis via bubble migration. *Nature* **502**, 393–396 (2013).

28. Rossi, M. L. *et al.* Pif1 helicase directs eukaryotic Okazaki fragments toward the two-nuclease cleavage pathway for primer removal. *J. Biol. Chem.* **283**, 27483–27493 (2008).

29. Zou, L. & Elledge, S. J. Sensing DNA damage through ATRIP recognition of RPA-ssDNA complexes. *Science* **300**, 1542–1548 (2003).

30. Bae, S. H., Bae, K. H., Kim, J. A. & Seo, Y. S. RPA governs endonuclease switching during processing of Okazaki fragments in eukaryotes. *Nature* **412**, 456–461 (2001).

31. Balakrishnan, L. & Bambara, R. A. Okazaki fragment metabolism. *Cold Spring Harb. Perspect. Biol.* **5**, a010173–a010173 (2013).

32. Ayyagari, R., Gomes, X. V., Gordenin, D. A. & Burgers, P. M. J. Okazaki fragment maturation in yeast. I. Distribution of functions between FEN1 and DNA2. *J. Biol. Chem.* **278**, 1618–1625 (2003).

33. Pike, J. E., Burgers, P. M. J., Campbell, J. L. & Bambara, R. A. Pif1 helicase lengthens some Okazaki fragment flaps necessitating Dna2 nuclease/helicase action in the two-nuclease processing pathway. *J. Biol. Chem.* **284**, 25170–25180 (2009).

34. Kahli, M., Osmundson, J. S., Yeung, R. & Smith, D. J. Processing of eukaryotic Okazaki fragments by redundant nucleases can be uncoupled from ongoing DNA replication in vivo. *Nucleic Acids Res.* **47**, 1814–1822 (2018).

35. Osmundson, J. S., Kumar, J., Yeung, R. & Smith, D. J. Pif1-family helicases cooperatively suppress widespread replication-fork arrest at tRNA genes. *Nat. Struct. Mol. Biol.* **24**, 162–170 (2017).

36. Stodola, J. L. & Burgers, P. M. Resolving individual steps of Okazaki-fragment maturation at a millisecond timescale. *Nat. Struct. Mol. Biol.* **23**, 402–408 (2016).

37. Garg, P., Stith, C. M., Sabouri, N., Johansson, E. & Burgers, P. M. Idling by DNA polymerase delta maintains a ligatable nick during lagging-strand DNA replication. *Genes Dev.* **18**, 2764–2773 (2004).

38. Rossi, S. E., Foiani, M. & Giannattasio, M. Dna2 processes behind the fork long ssDNA flaps generated by Pif1 and replication-dependent strand displacement. *Nat. Commun.* **9**, 4830 (2018).

39. Neelsen, K. J. & Lopes, M. Replication fork reversal in eukaryotes: from dead end to dynamic response. *Nat. Rev. Mol. Cell Biol.* **16**, 207–220 (2015).

40. Wawrousek, K. E. *et al.* Xenopus DNA2 is a helicase/nuclease that is found in complexes with replication proteins And-1/Ctf4 and Mcm10 and DSB response proteins Nbs1 and ATM. *Cell Cycle* **9**, 1156–1166 (2010).

41. Villa, F. *et al.* Ctf4 Is a Hub in the Eukaryotic Replisome that Links Multiple CIP-Box Proteins to the CMG Helicase. *Mol. Cell* **63**, 385–396 (2016).

42. Tkach, J. M. *et al.* Dissecting DNA damage response pathways by analysing protein localization and abundance changes during DNA replication stress. *Nat. Cell Biol.* **14**, 966–976 (2012).

43. Schulz, V. P. & Zakian, V. A. The saccharomyces PIF1 DNA helicase inhibits telomere elongation and de novo telomere formation. *Cell* **76**, 145–155 (1994).

44. García-Luis, J., Clemente-Blanco, A., Aragón, L. & Machín, F. Cdc14 targets the Holliday junction resolvase Yen1 to the nucleus in early anaphase. *Cell Cycle* **13**, 1392–1399 (2014).

45. Blanco, M. G., Matos, J. & West, S. C. Dual control of Yen1 nuclease activity and cellular localization by Cdk and Cdc14 prevents genome instability. *Mol. Cell* **54**, 94–106 (2014).

46. West, S. C. *et al.* Resolution of Recombination Intermediates: Mechanisms and Regulation. *Cold Spring Harb. Symp. Quant. Biol.* **80**, 103–109 (2015).

47. Brewer, B. J. & Fangman, W. L. A replication fork barrier at the 3' end of yeast ribosomal RNA genes. *Cell* **55**, 637–643 (1988).

48. Linskens, M. H. & Huberman, J. A. Organization of replication of ribosomal DNA in Saccharomyces cerevisiae. *Mol. Cell. Biol.* **8**, 4927–4935 (1988).

49. Guacci, V., Koshland, D. & Strunnikov, A. A direct link between sister chromatid cohesion and chromosome condensation revealed through the analysis of MCD1 in S. cerevisiae. *Cell* **91**, 47–57 (1997).

50. Guacci, V., Hogan, E. & Koshland, D. Chromosome condensation and sister chromatid pairing in budding yeast. *J. Cell Biol.* **125**, 517–530 (1994).

51. Schimmang, T., Tollervey, D., Kern, H., Frank, R. & Hurt, E. C. A yeast nucleolar protein related to mammalian fibrillarin is associated with small nucleolar RNA and is essential for viability. *EMBO J.* **8**, 4015–4024 (1989).

52. Formosa, T. & Nittis, T. Dna2 Mutants Reveal Interactions with Dna Polymerase α and Ctf4, a Pol α Accessory Factor, and Show That Full Dna2 Helicase Activity Is Not Essential for Growth. *Genetics* **151**, 1459–1470 (1999).

53. Zhou, J., Monson, E. K., Teng, S. C., Schulz, V. P. & Zakian, V. A. Pif1p helicase, a catalytic inhibitor of telomerase in yeast. *Science* **289**, 771–774 (2000).

54. Buzovetsky, O. *et al.* Role of the Pif1-PCNA Complex in Pol δ-Dependent Strand Displacement DNA Synthesis and Break-Induced Replication. *Cell Rep.* **21**, 1707–1714 (2017).

55. Makovets, S. & Blackburn, E. H. DNA damage signalling prevents deleterious telomere addition at DNA breaks. *Nat. Cell Biol.* **11**, 1383–1386 (2009).

56. Vasianovich, Y., Harrington, L. A. & Makovets, S. Break-Induced Replication Requires DNA Damage-Induced Phosphorylation of Pif1 and Leads to Telomere Lengthening. *PLoS Genet.* **10**, e1004679 (2014).

57. Talhaoui, I. *et al.* Slx5-Slx8 ubiquitin ligase targets active pools of the Yen1 nuclease to limit crossover formation. *Nat. Commun.* **9**, 5016 (2018).

58. Ait Saada, A., Lambert, S. A. E. & Carr, A. M. Preserving replication fork integrity and competence via the homologous recombination pathway. *DNA Repair (Amst.)* **71**, 135–147 (2018).

59. Lambert, S., Watson, A., Sheedy, D. M., Martin, B. & Carr, A. M. Gross chromosomal rearrangements and elevated recombination at an inducible site-specific replication fork barrier. *Cell* **121**, 689–702 (2005).

60. Lambert, S. *et al.* Homologous recombination restarts blocked replication forks at the expense of genome rearrangements by template exchange. *Mol. Cell* **39**, 346–359 (2010).

61. Nguyen, M. O., Jalan, M., Morrow, C. A., Osman, F. & Whitby, M. C. Recombination occurs within minutes of replication blockage by RTS1 producing restarted forks that are prone to collapse. *Elife* **4**, e04539 (2015).

62. Saini, N. *et al.* Migrating bubble during break-induced replication drives conservative DNA synthesis. *Nature* **502**, 389–392 (2013).

63. García-Rodríguez, N., Morawska, M., Wong, R. P., Daigaku, Y. & Ulrich, H. D. Spatial separation between replisome- and template-induced replication stress signaling. *EMBO J.* **37**, e98369 (2018).

64. Iraqui, I. *et al.* Recovery of arrested replication forks by homologous recombination is error-prone. *PLoS Genet.* **8**, e1002976 (2012).

65. Mizuno, K., Miyabe, I., Schalbetter, S. A., Carr, A. M. & Murray, J. M. Recombination-restarted replication makes inverted chromosome fusions at inverted repeats. *Nature* **493**, 246–249 (2013).

66. Smith, C. E., Llorente, B. & Symington, L. S. Template switching during break-induced replication. *Nature* **447**, 102–105 (2007).

67. Mayle, R. *et al.* DNA REPAIR. Mus81 and converging forks limit the mutagenicity of replication fork breakage. *Science* **349**, 742–747 (2015).

68. Liu, B., Hu, J., Wang, J. & Kong, D. Direct Visualization of RNA-DNA Primer Removal from Okazaki Fragments Provides Support for Flap Cleavage and Exonucleolytic Pathways in Eukaryotic Cells. **292**, 4777–4788 (2017).

69. Bantele, S. C. S., Lisby, M. & Pfander, B. Quantitative sensing and signalling of single-stranded DNA during the DNA damage response. *Nat. Commun.* **10**, 944–12 (2019).

70. Smith, D. J. & Whitehouse, I. Intrinsic coupling of lagging-strand synthesis to chromatin assembly. *Nature* **483**, 434–438 (2012).

71. Devbhandari, S., Jiang, J., Kumar, C., Whitehouse, I. & Remus, D. Chromatin Constrains the Initiation and Elongation of DNA Replication. *Mol. Cell* **65**, 131–141 (2017).

72. O'Driscoll, M., Ruiz-Perez, V. L., Woods, C. G., Jeggo, P. A. & Goodship, J. A. A splicing mutation affecting expression of ataxia-telangiectasia and Rad3-related protein (ATR) results in Seckel syndrome. *Nat. Genet.* **33**, 497–501 (2003).

73. Ogi, T. *et al.* Identification of the first ATRIP-deficient patient and novel mutations in ATR define a clinical spectrum for ATR-ATRIP Seckel Syndrome. *PLoS Genet.* **8**, e1002945 (2012).

74. Reynolds, J. J. *et al.* Mutations in DONSON disrupt replication fork stability and cause microcephalic dwarfism. *Nat. Genet.* **49**, 537–549 (2017).

75. Harley, M. E. *et al.* TRAIP promotes DNA damage response during genome replication and is mutated in primordial dwarfism. *Nat. Genet.* **48**, 36–43 (2016).

76. Deng, L. *et al.* Mitotic CDK Promotes Replisome Disassembly, Fork Breakage, and Complex DNA Rearrangements. *Mol. Cell* **73**, 915–929 (2019).

77. Klingseisen, A. & Jackson, A. P. Mechanisms and pathways of growth failure in primordial dwarfism. *Genes Dev.* **25,** 2011–2024 (2011).

78. Macheret, M. & Halazonetis, T. D. DNA replication stress as a hallmark of cancer. *Annu. Rev. Pathol.* **10**, 425–448 (2015).

79. Liu, W. *et al.* A Selective Small Molecule DNA2 Inhibitor for Sensitization of Human Cancer Cells to Chemotherapy. *EBioMedicine.* **6**, 73–86 (2016).

80. Kumar, S. *et al.* Inhibition of DNA2 nuclease as a therapeutic strategy targeting replication stress in cancer cells. *Oncogenesis* **6**, e319 (2017).

81. Brachmann, C. B. *et al.* Designer deletion strains derived from Saccharomyces cerevisiae S288C: a useful set of strains and plasmids for PCR-mediated gene disruption and other applications. *Yeast* **14**, 115–132 (1998).

82. Scherer, S. & Davis, R. W. Replacement of chromosome segments with altered DNA sequences constructed in vitro. *Proc. Natl. Acad. Sci. USA* **76**, 4951–4955 (1979).

83. Anand, R., Memisoglu, G. & Haber, J. Cas9-mediated gene editing in Saccharomyces cerevisiae. (2017). *Protoc. Exch.* doi:10.1038/protex.2017.021a (2017).

84. Torres-Rosell, J. *et al.* The Smc5-Smc6 complex and SUMO modification of Rad52 regulates recombinational repair at the ribosomal gene locus. *Nat. Cell Biol.* **9**, 923–931 (2007).

85. Bernstein, K. A. *et al.* Sgs1 function in the repair of DNA replication intermediates is separable from its role in homologous recombinational repair. *EMBO J.* **28**, 915–925 (2009).

86. Seeber, A., Dion, V. & Gasser, S. M. Checkpoint kinases and the INO80 nucleosome remodeling complex enhance global chromatin mobility in response to DNA damage. *Genes Dev.* **27**, 1999–2008 (2013).

87. Hage, A. E. & Houseley, J. Resolution of Budding Yeast Chromosomes Using Pulsed-Field Gel Electrophoresis. In: Makovets S. (Ed.) DNA Electrophoresis (Humana Press). *Methods Mol. Biol.* **1054**, 195–207 (2013).

Falquet et al. Fig. 1

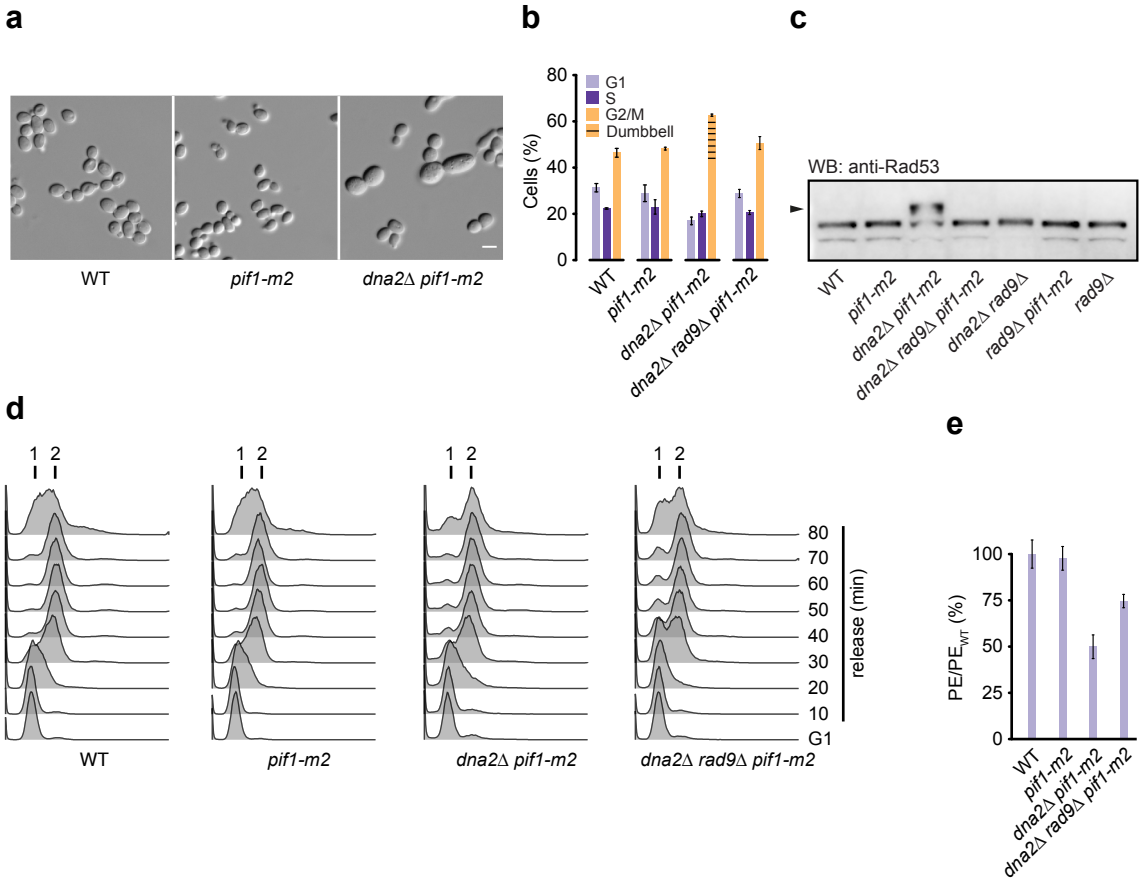

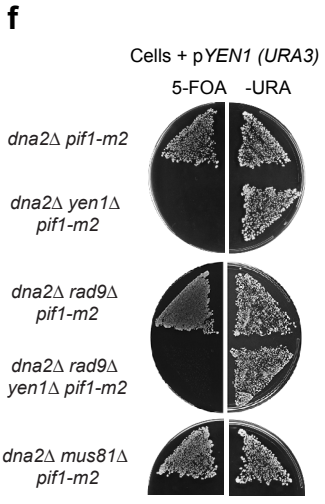

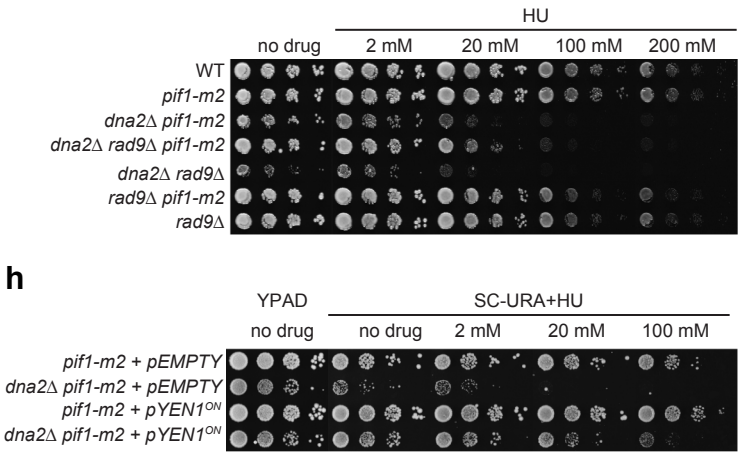

Falquet et al. Fig. 2

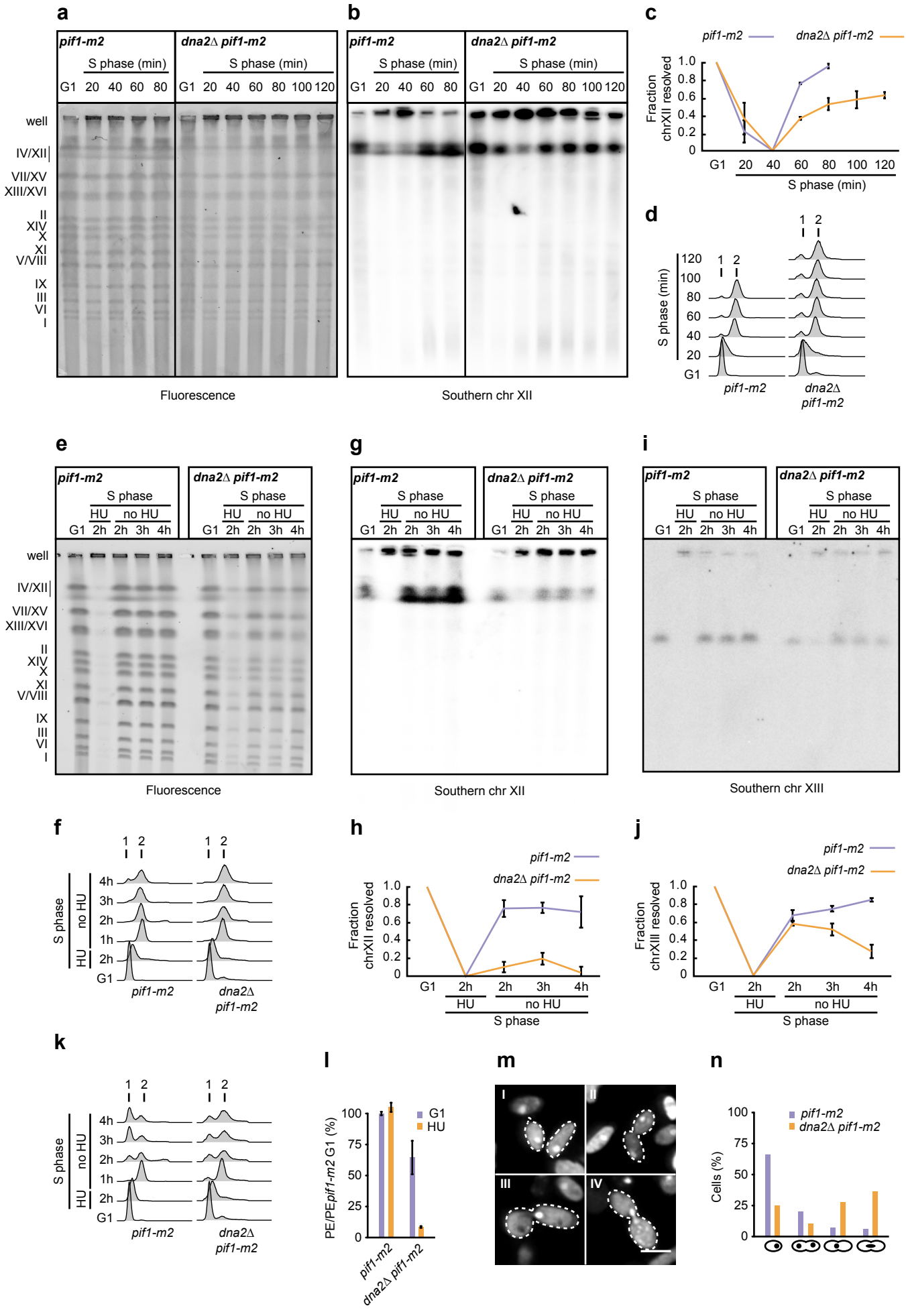

Falquet et al. Fig. 3

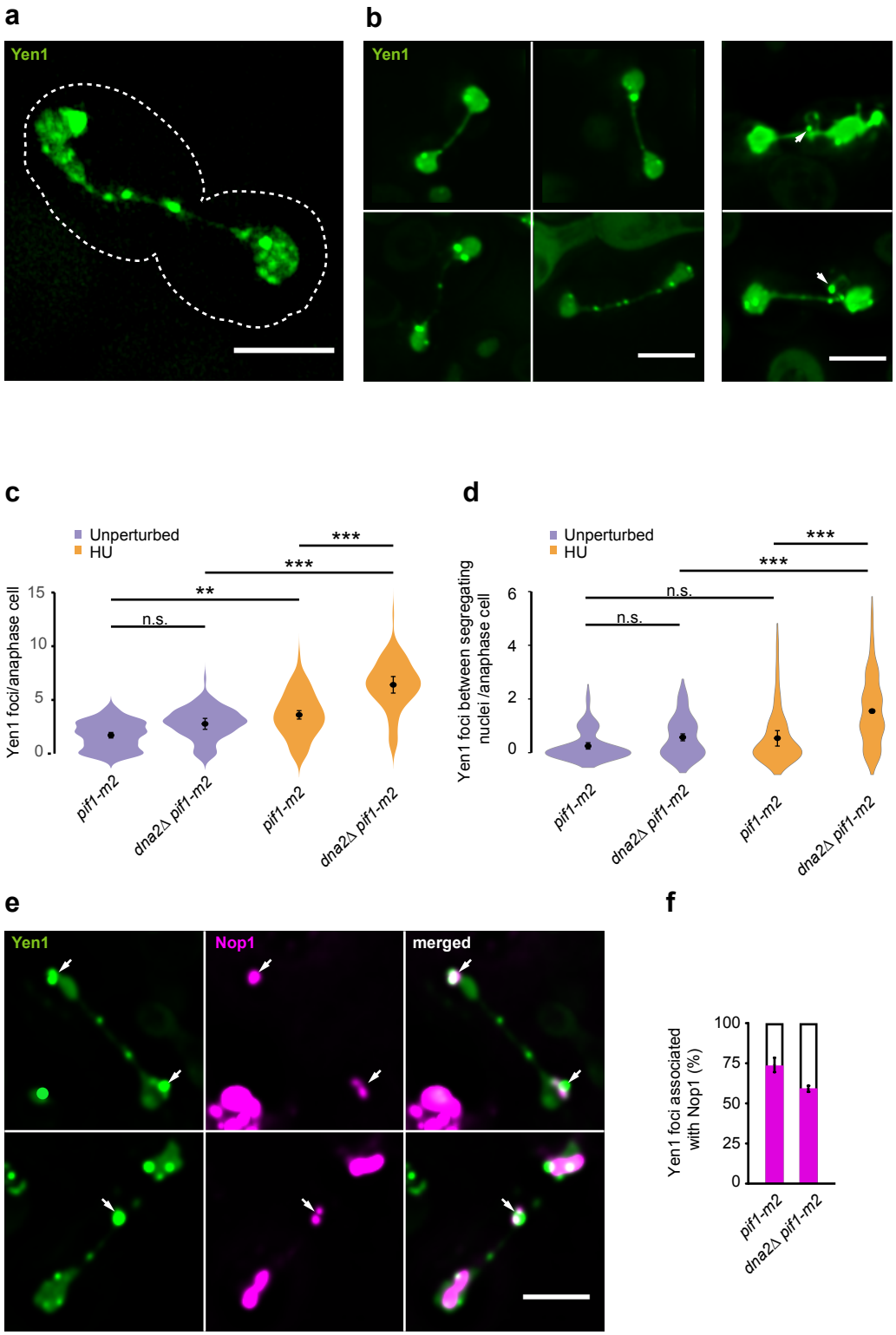

Falquet et al. Fig. 4

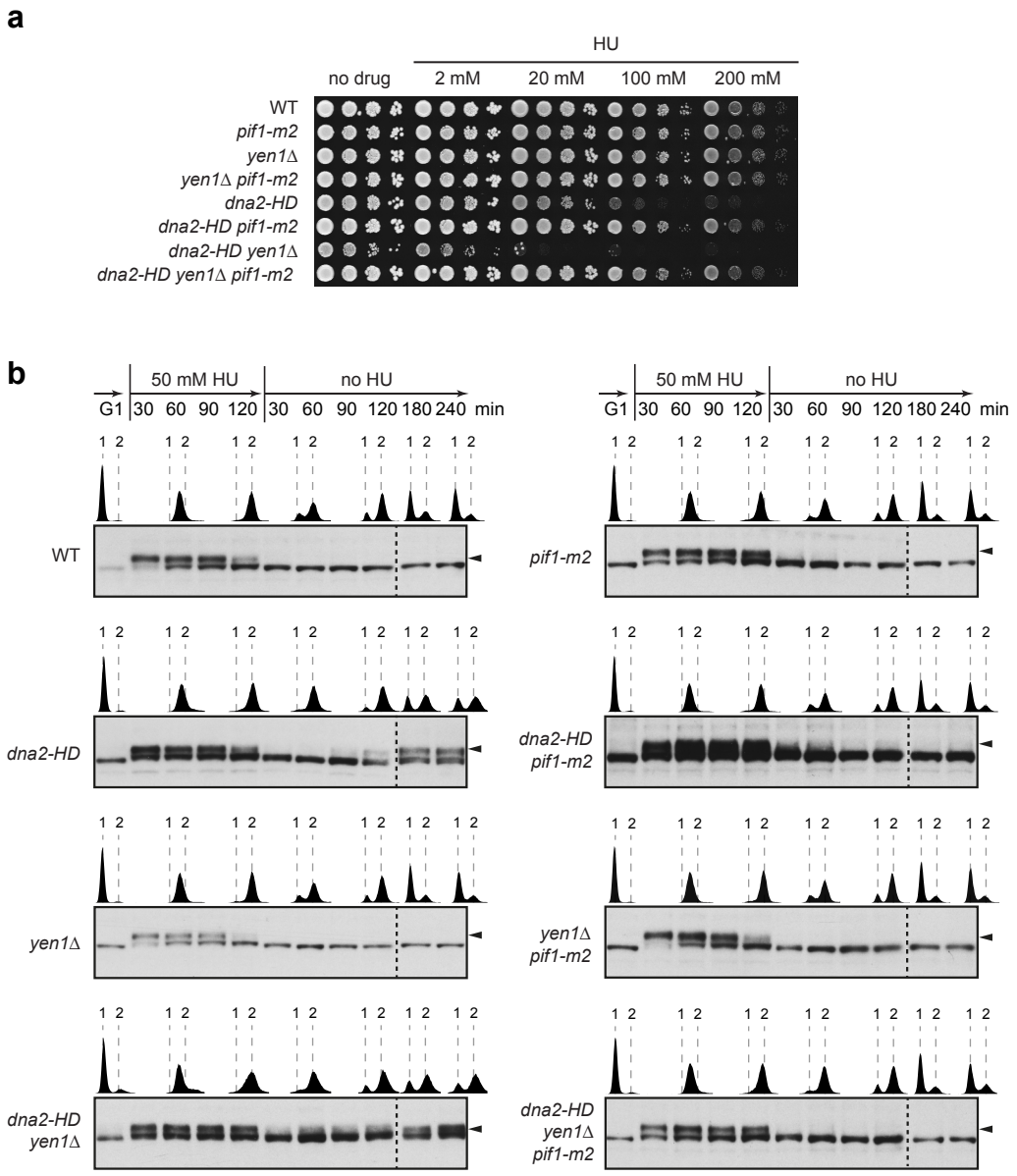

Falquet et al. Fig. 5

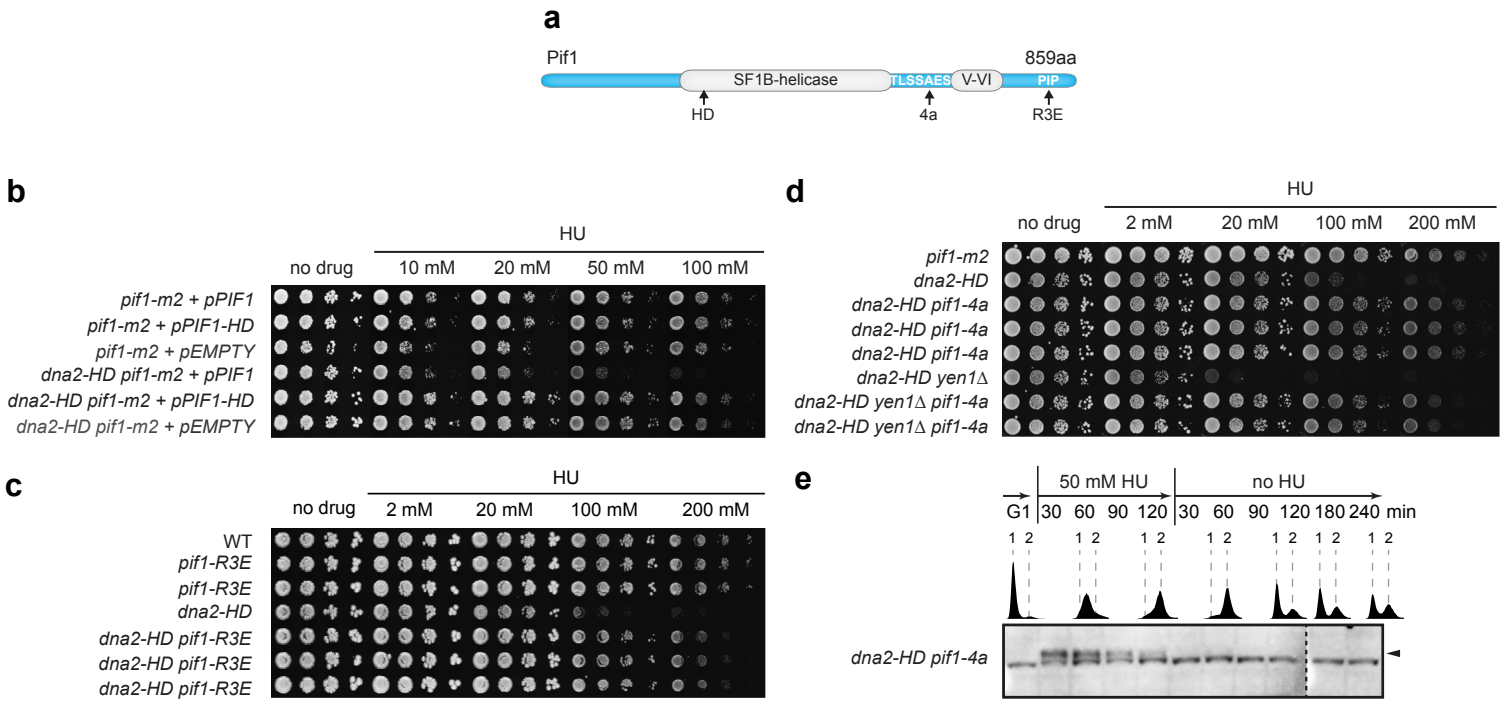

Falquet et al. Fig. 6

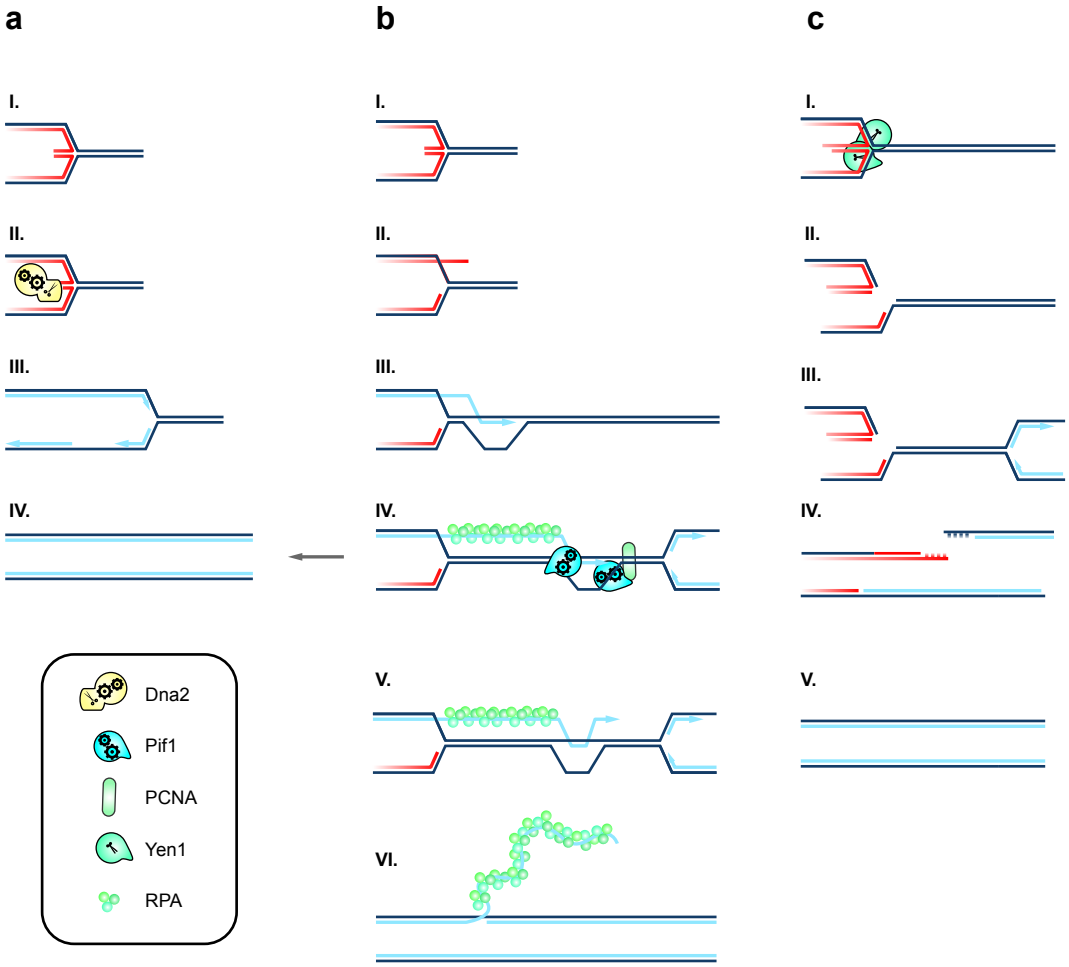

Falquet et al. Supplementary Fig. 1 (relates to Fig.1)

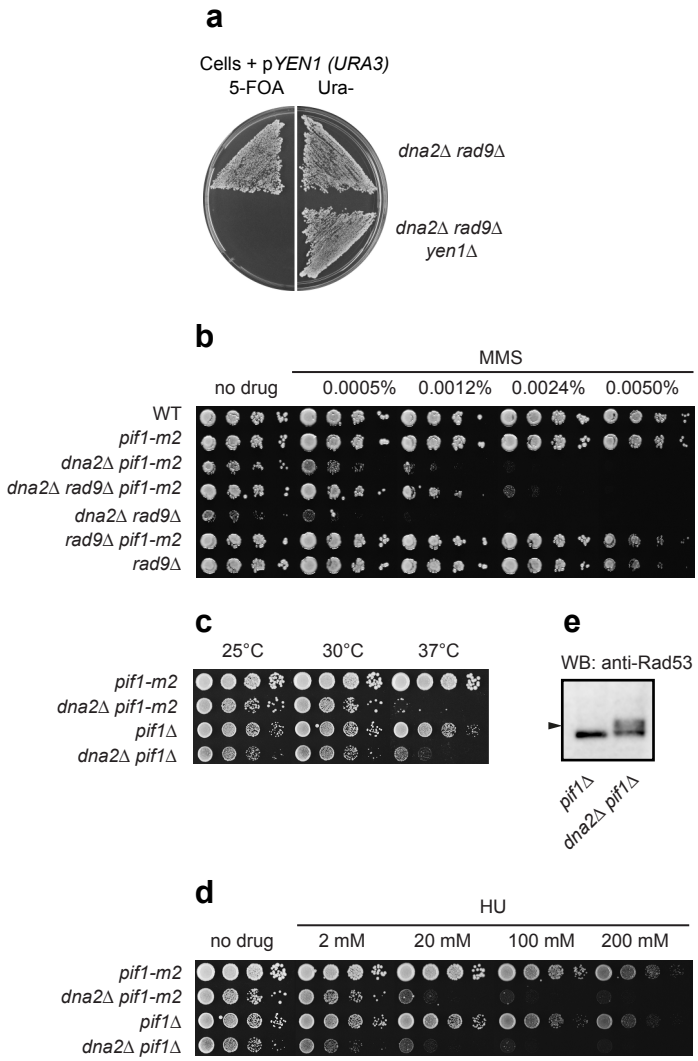

Falquet et al. Supplementary Fig. 2 (relates to Fig.2)

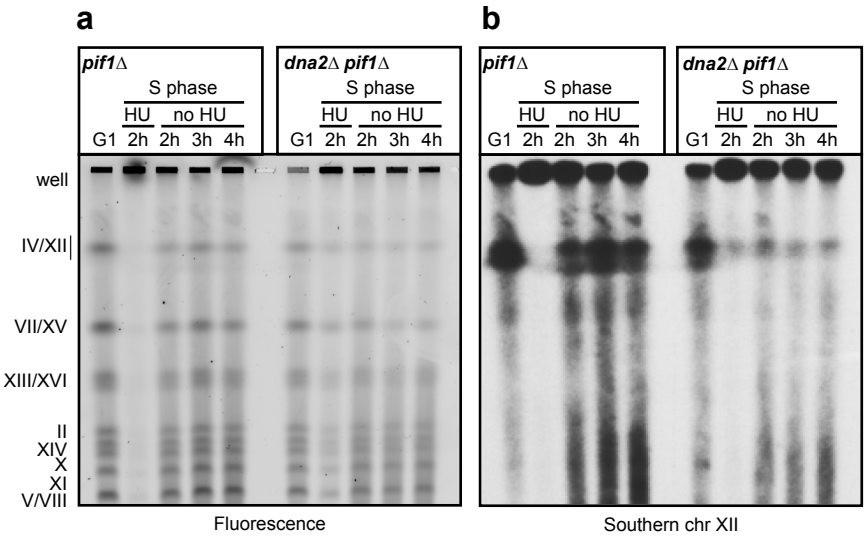

Falquet et al. Supplementary Fig. 3 (relates to Fig. 4)

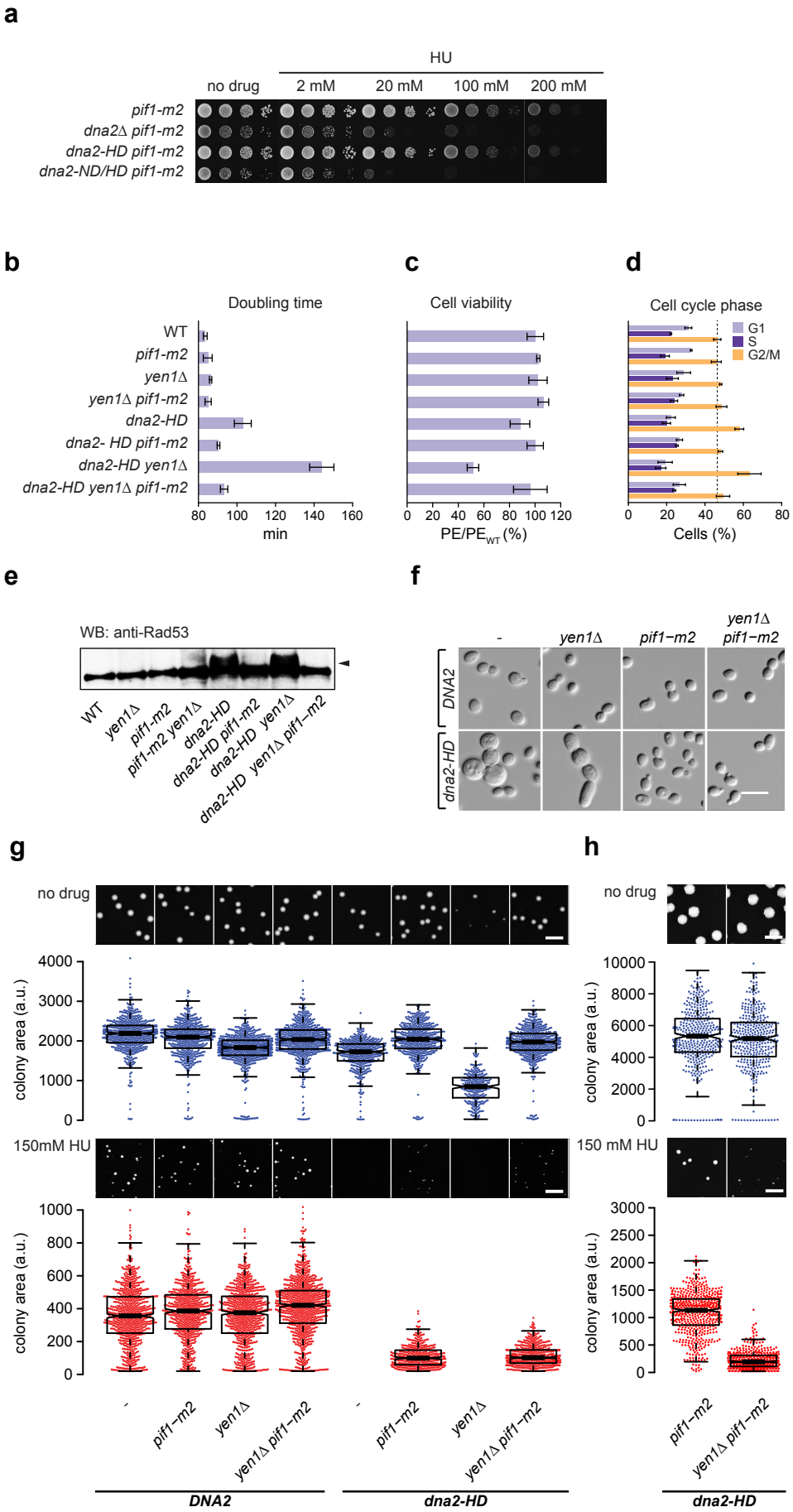

Chapter 7: Additional results

The DNA structures recognized by Yen1 are largely devoid of ssDNA

We show that Yen1 resolves post-replicative chromosomal links arising in Dna2-defective cells[154] (Falquet et al., Manuscript in revision). The exact nature of these intermediates remains to be determined. In a bid to characterize the DNA structures resolved by Yen1 during mitosis further, we turned to microscopy and observed *pif1-m2* and *dna2*Δ *pif1-m2* cells expressing a GFP-tagged version of Yen1 and an RFP-tagged version of Rfa1, a subunit of the ssDNA-binding RPA complex. The cells where synchronized in G1 with α-factor, exposed to 200 mM HU for 2 h and released into drug-free medium before live-cell imaging by microscopy (**Fig. 1a**).

In good agreement with previous experiments, *dna2*Δ *pif1-m2* displayed more Yen1 foci than *pif1-m2* cells (5.9 vs. 3.5 foci per cell on average). Consistent with published data[156], *dna2*Δ *pif1-m2* also presented more Rfa1 foci compared to *pif1-m2* (2.1 vs 0.4 foci per cell on average) (**Fig. 1b**). Although Yen1-Rfa1 colocalization was considerably increased in *dna2*Δ *pif1-m2* relative to *pif1-m2* (14% vs 2% of colocalization) (**Fig. 1c**), the majority of the sites marked by Yen1 were devoid of detectable Rfa1, suggesting that Yen1 binds mostly double stranded DNA structures.

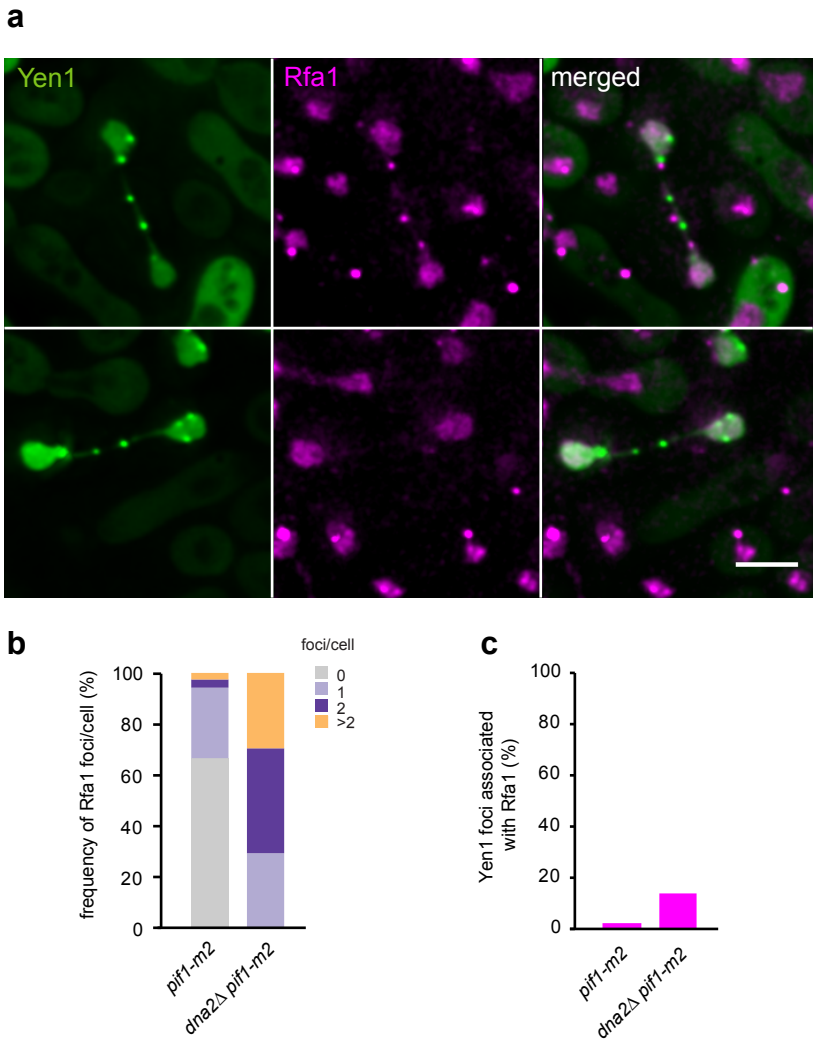

Figure 1: a) Representative image of *dna2Δ pif-m2* (top row) or *pif1-m2* (bottom row) cells expressing Yen1-EGFP (green) and Rfa1-RFP (magenta), during anaphase following a 2 h-treatment with 200 mM HU. Scale bar = 5µm. b) Relative frequency of Rfa1 foci in the indicated strains during anaphase, as observed in panel a. c) Proportion of Yen1 foci colocalizing with Rfa1 foci in the indicated strains during anaphase, as observed in panel a (n>30 cells).

A nuclease-dead version of Dna2 is cell-lethal

We identified the nuclease activity of Dna2 as a major player in the resistance to RS (Falquet et al., Manuscript in revision). Thus, *dna2*Δ *pif1-m2* cells are much more sensitive to HU than *dna2-HD pif1-m2* with the only difference between these cells being the lack of Dna2 nuclease activity. We decided to study the impact of a nuclease-dead Dna2 version (*dna2-ND* allele).

Plasmid shuffle experiments revealed that the expression of *dna2-ND* is lethal in *dna2*Δ *pif1-m2*, yet tolerated when a wild type copy of *DNA2* is present (**Fig. 2**). This precluded the study

of the effects of the Dna2 nuclease activity in isolation in any more detail. Nonetheless, we can surmise that this synthetic lethality is probably due to the fact that in absence of Dna2 nuclease activity, the helicase domain of Dna2 becomes hyperactive and detrimental[110].

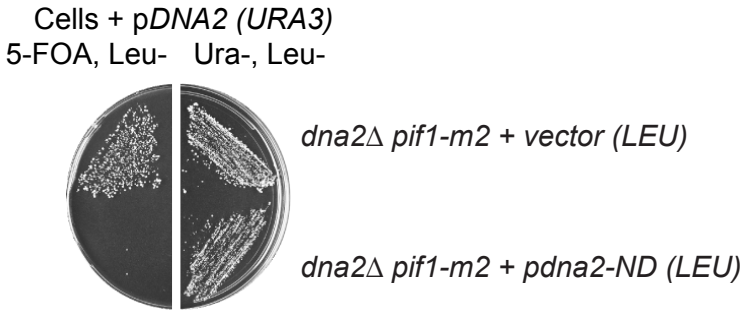

Figure 2: Plasmid shuffle assay using the indicated strains. The inability to grow on 5-FOA, Leu- identifies lethality generated by a nuclease-dead version of Dna2 in absence of wild-type *DNA2*.

A Pol32 C-terminal truncation suppresses defects in Dna2 helicase-defective cells

The function of the Dna2 helicase in the RS response can be compensated by the nucleolytic action of Yen1[154]. We sought to identify suppressors of the RS sensitivity of *yen1*Δ *dna2-HD* to elucidate molecular determinants of RS sensitivity in this strain. We routinely observed a small number of colonies of *yen1*Δ *dna2-HD* suppressors arising on a dose of MMS lethal for *yen1*Δ *dna2-HD*. So far, all clones isolated in this way bore a mutation in the *PIF1* gene affecting its helicase domain either by truncation of point mutation. Interestingly, we also isolated a *yen1*Δ *dna2-HD* suppressor on lethal doses of HU. This clone was resistant to high doses of HU (**Fig. 3a**). Sequencing of candidate genes implicated in suppression of *dna2-HD* defects revealed that in this clone, a nonsense mutation was affecting the *POL32* allele, leading to the production of a truncated protein (Pol32 E237X, hereafter referred to as Pol32ΔC) (**Fig. 3a**).

First, we confirmed that the truncated protein was stable by immunoblotting. The expression of the *pol32*Δ*C* protein was similar to wild-type Pol32 (**Fig**. **3b**). To confirm the observation that truncating the C-terminus of Pol32 results in the suppression of dna2-HD sensitivity we observed a range of phenotypes associated with a defective Dna2-helicase activity. *pol32*Δ*C* effectively reduced the doubling time (**Fig**. **3c**), increased cell viability (**Fig. 3d**), and diminished G2/M cell accumulation (**Fig. 3e**) of *dna2-HD* and *dna2-HD yen1*Δ cells. The morphological defects of these mutants were also corrected upon Pol32 truncation (**Fig. 3f**) as the

chronic checkpoint activation observed in *dna2-HD* was suppressed (**Fig. 3g**). Finally, we assessed the impact of the *pol32*Δ*C* mutation on RS sensitivity. While the *pol32*Δ*C* allele alone did not cause any visible phenotype, it considerably increased the resistance to HU in the *dna2-HD* and *dna2-HD yen1*Δ strains, although not to the level of wild-type (**Fig. 3h**).

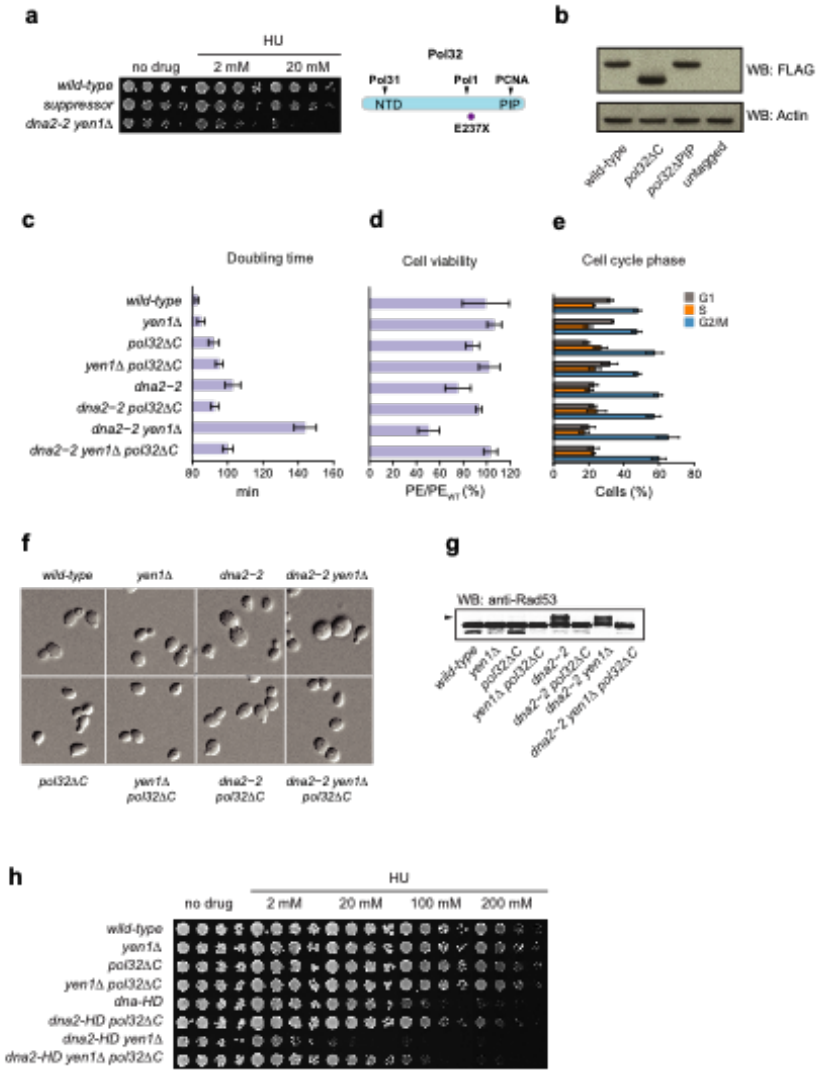

Figure 3: a) Drop assay of the indicated strains on HU and control plates confirms the resistance of the suppressor, whose mutation is indicated on a schematic representation of the Pol32 protein. Potential interacting proteins are indicated above. b) Immunoblotting of Flag-tagged mutants of Pol32. c) doubling time of the indicated strains ± SD (n = 3 independent experiments). d) Cell viability ± SD relative to wild-type (n = 5 technical replicas). e) Budding index ± SD of the indicated strains (n = 3 independent experiments). f) Representative DIC image of the indicated strains showing cell morphology. Scale bar = 5µm. g) Rad53 blot of the indicated strains in exponential growth phase. Checkpoint activation is detected by the appearance of a phosphorylated form of Rad53 migrating slower (black arrowhead). h) Drop assay of the indicated strain on HU and control plates assessing the level of RS sensitivity.

To the best of our knowledge, no catalytical activity has been ascribed to Pol32 alone, but the protein forms a stable complex with Pol31 through its N-terminal portion. In addition, the C-terminal PIP box of Pol32 interacts with PCNA[225], while Pol1 has been reported to bind a conserved motif in the central part of the protein[225]. We hypothesize that interaction between Pol32 and one of its interacting factors might be responsible for the RS sensitivity of *dna2* mutants.

Complete deletion of *POL32* rendered cells sensitive to HU (**Fig. 4a**) and moderately increased the resistance of *dna2-HD yen1*Δ to HU. Truncation of the PIP box (*pol32*Δ*PIP*) on the other hand did not induce HU sensitivity and slightly increased *dna2-HD yen1*Δ viability on HU (**Fig. 4ab**). Similar to *pol32*Δ*PIP*, *pol32*Δ*C* mutation, did not cause RS sensitivity indicating that the protein is still partially functional (**Fig. 4a**). As observed previously, *pol32*Δ*C* greatly enhanced the fitness of *dna2-HD yen1*Δ on HU (**Fig. 4a,b**)

To get better insight into the mechanisms of *pol32*Δ*C*-mediated suppression of *dna2-HD* sensitivity to HU, we performed a mitotic time course experiment where cells synchronized in G1 where exposed to acute RS by the addition 50 mM HU for 2 h and subsequently released in a media containing α-factor to prevent the entry into the next cell cycle. The status of the checkpoint was followed by monitoring the phosphorylation level of the Rad53-kinase. *pol32*Δ*C* and *pol32*Δ suppressed the second wave of checkpoint activation observed in *dna2-HD (***Fig. 4c**) even if *pol32*Δ induced a prolongated checkpoint activation following the HU treatment (**Fig. 4c**), probably reflecting its role in S-phase.

Mutation of either Pif1 or Pol32 is sufficient to suppress checkpoint activation in *dna2-HD* cells, suggesting that these proteins could cooperate in the same pathway. To test this hypothesis, we turned to *dna2*Δ *pif1-m2*, as *dna2-HD* phenotypes are almost completely suppressed by Pif1 depletion from the nucleus. Truncation of Pol32 slightly improved the viability of *dna2*Δ *pif1-m2* on HU but not to the level of *pif1-m2*. Altogether, the primary interpretation of these experiments is that Pol32 and Pif1 act along the same pathway to generate RS sensitivity in a *dna2*Δ mutant. (**Fig. 4d**). Regardless, these results show once again that the Dna2 plays a role independently in RS response independently of Pif1 and Pol32. More research is needed to understand the exact role on Pol32 in this context.

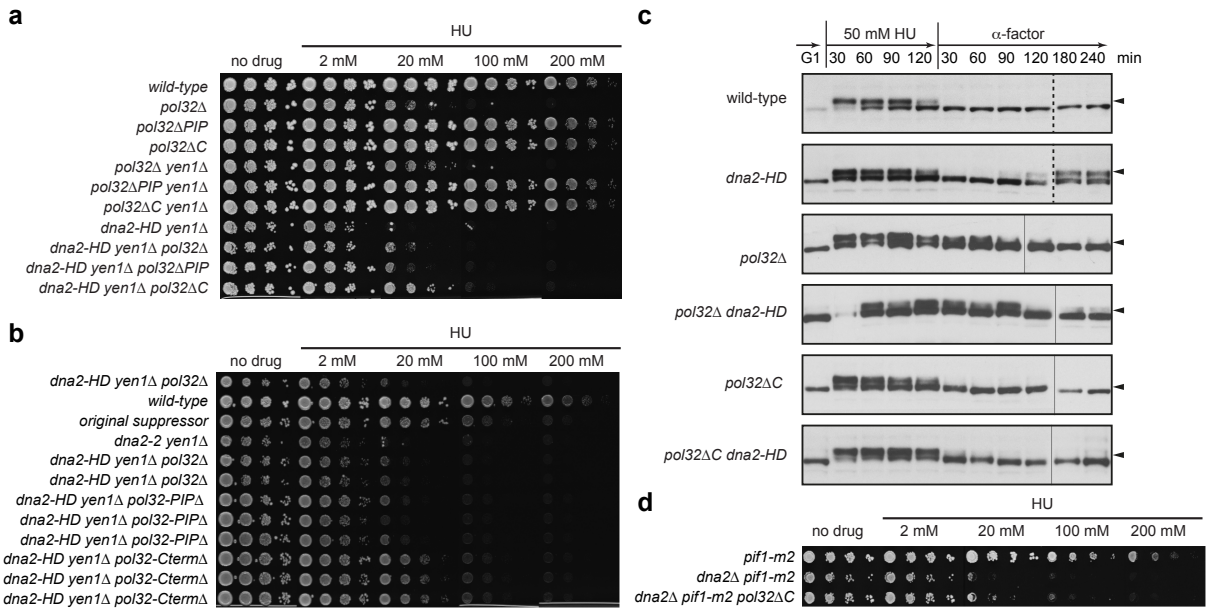

Figure 4: a & b) Drop assay of the indicated strains on HU and control plates. c) Mitotic time course experiments. The indicated strains were arrested in G1, treated with 200 mM HU for 2 h and released into α-factor. Checkpoint activation is monitored by following the upward shift of Rad53 (black arrowhead) by immunoblotting. d) Drop assay of the indicated strains on HU and control plates.

The synthetic lethality of *dna2* with *sgs1* and *rrm3* is suppressed by *pif1*-m2

Dna2 helicase-defective cells are inviable in absence of Sgs1, but the reasons behind this synthetic lethality are unclear. We managed to suppress this lethality by introducing the *pif1-m2* mutation. *dna2-HD pif1-m2 sgs1*Δ cells are sensitive to RS, but not much more than *sgs1*Δ or *pif1-m2 sgs1*Δ cells (**Fig. 5a**). This suggests that the essential function performed by Sgs1 in *dna2-HD* cells is no longer required when nuclear Pif1 is depleted. In other words, Pif1 generates a toxic DNA structure that may be counteracted by Sgs1 in *dna2-HD* mutants.

Sgs1 plays several roles in genome maintenance ranging from DSB end-resection to RF maintenance (reviewed in [226]). In metazoans, other RecQ helicases have been shown to participate in RF reversal (reviewed in [74]) Interestingly, Sgs1 has been implicated in the inhibition of BIR, as this repair pathway is increased in *sgs1*Δ cells[227-229]. One could therefore envision a model where Sgs1 counteracts toxic BIR/RDR reactions promoted by Pif1 in *dna2* mutants (Falquet et al., Manuscript in revision).

Finally, we decided to evaluate the effect of Pif1 depletion on the synthetic lethal interaction between *dna2-HD* and rrm3Δ[155]. As reported elsewhere, *pif1-m2 rrm3*Δ cells are sick,

probably due to a defect in replication termination[222]. This strain grew slowly and arrested in G2/M phase (**Fig. 5b,c**), but was not sensitive to HU (**Fig. 5d**). Pif1 depletion suppressed the lethality of *dna2-HD rrm3*Δ, but the strain was slow-growing and cells accumulated in G2/M phase. However, cells were still able to form colonies on high doses of HU (**Fig. 5d**).

What is the functional overlap between Rrm3 and Dna2? The contrasting genetic interactions of *PIF1* and *RRM3* with *DNA2* suggest that the function of Rrm3 that is essential for *dna2* mutants is not shared by Pif1. Since the lethality of *dna2-HD rrm3*Δ is rescued by the deletion of neither *RAD51* nor *FOB1*[106], one should also exclude an aberrant recombination process or a problem specific to rDNA. The reason for this interaction therefore remains unclear, but Rrm3 might remove protein blocks in front of the RF, alleviating the need for RF recovery by Dna2.

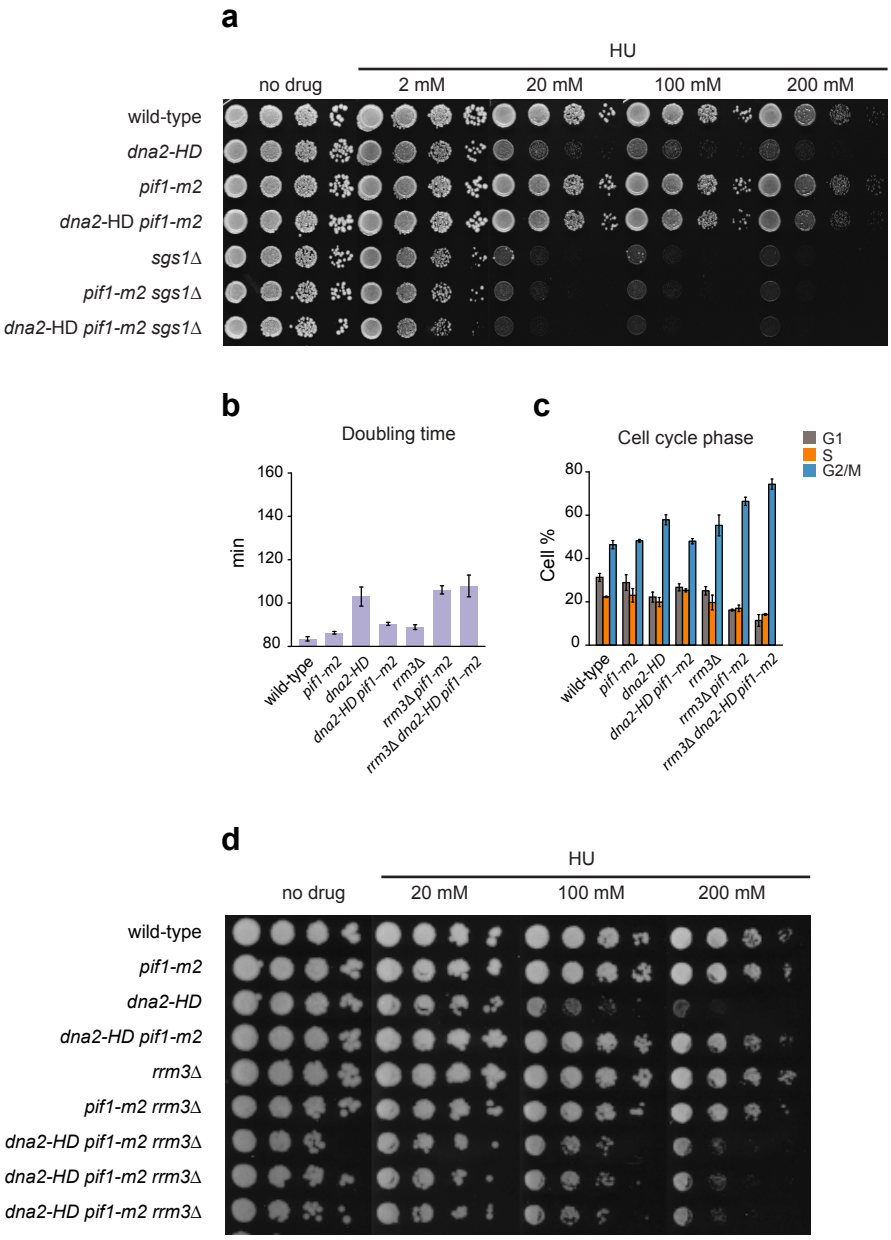

Figure 5: a) Drop assay of the indicated strains on HU. b) Doubling time of the indicated strains ± SD (n = 3 independent experiments). c) Budding index ± SD of the indicated strains (n = 3 independent experiments). d) Drop assay of the indicated strain on HU.

Materials and methods

Yeast strain

S. cerevisiae strains were derived from BY4741[230], and are listed in **Table 1**. Strain were grown in YPAD at 30°C except for microscopy where synthetic complete media were used.

Cell viability, growth, and drug-sensitivity assays.

Doubling time, budding index and cell viability were determined as described[154]. For drop assays, exponentially growing cells were normalized to 10^7 cells ml^{-1}, and tenfold serial dilutions applied onto YPAD plates with or without HU. Pictures were taken after 2-3 days of growth at 30°C.

Mitotic time course experiment

Mitotic time course experiments were performed as previously described[154]. Briefly, exponentially growing yeast cells were synchronized in G1 with addition of 1 μg ml^{-1} of α-factor. After 2.5 h of incubation, synchronized cells were harvested, washed in ddH_2O, and released into YPAD containing 50 mM HU (Sigma) for 2 h to expose them to RS during S phase. After HU removal, cells were cultured in YPAD containing 1 μg ml^{-1} α-factor to prevent re-entry into S-phase. Samples were taken at the indicated timepoints and used for immunoblotting as previously described[154].

Microscopy

For differential interference contrast images (DIC) and fluorescence microscopy, images were aquired as previously describes (Falquet et al. Manuscript in revision). Briefly, cell were grown in synthetic complete media, immobilized in an imaging chambers coated with ibidi polymer and pictures were acquired using a Olympus IX81 spinning disk confocal microscope.

Supplementary Table 2 List of *S. cerevisiae* strains used in this study.

Strain	Relevant genotype	Source
YRL19	*Mata, hisΔ3, leu2Δ0, met15Δ0, ura3Δ0 (BY4741)*	GE Healthcare
CloneID 174	*YRL19, yen1::KAN*	GE Healthcare
YRL300	*YRL19, pif1::pif1-m2*	This study
YRL301	*YRL19, pif1::pif1-m2, yen1::KAN*	This study
YRL29	*YRL19, dna2::dna2-HD*	Ölmezer et al 2016
YRL302	*YRL19, dna2::dna2-HD, pif1::pif1-m2*	This study
YRL97	*YRL19, dna2::dna2-HD, yen1::KAN*	Ölmezer et al 2016
YRL303	*YRL19, dna2::dna2-HD, pif1::pif1-m2, yen1::KAN*	This study
YRL310	*YRL19, dna2::HIS, pif1::pif1-m2*	This study
YRL319	*YRL19, dna2::HIS, pif1::pif1-m2, pAG415 GPD ccdB, pAG416 GPD DNA2*	This study
YRL320	*YRL19, dna2::HIS, pif1::pif1-m2, pAG415GPD dna2-ND, pAG416 GPD DNA2*	This study
YRL338	*YRL19, sgs1::HIS*	This study
YRL339	*YRL19, pif1::pif1-m2, sgs1::HIS*	This study
YRL340	*YRL19, dna2::dna2-HD, pif1::pif1-m2, sgs1::HIS*	This study
YRL338	*YRL19, rrm3::HIS*	This study
YRL339	*YRL19, pif1::pif1-m2, rrm3::HIS*	This study
YRL339	*YRL19, dna2::dna2-HD, pif1::pif1-m2, rrm3::HIS*	This study
YRL349	*YRL19, pol32::HIS*	This study
YRL350	*YRL19, dna2::dna2-HD, pol32::HIS*	This study
YRL351	*YRL19, pol32::HIS, yen1::KAN*	This study
YRL352	*YRL19, dna2::dna2-HD, pol32::HIS, yen1::KAN*	This study
YRL353	*YRL19, pol32::pol32ΔC HIS*	This study
YRL354	*YRL19, dna2::dna2-HD, pol32::pol32ΔC HIS*	This study
YRL355	*YRL19, pol32::pol32ΔC HIS, yen1::KAN*	This study
YRL356	*YRL19, dna2::dna2-HD, pol32::pol32ΔC HIS, yen1::KAN*	This study
YRL357	*YRL19, pol32::pol32ΔPIP HIS*	This study
YRL358	*YRL19, dna2::dna2-HD, pol32::pol32PIP HIS*	This study
YRL359	*YRL19, pol32::pol32ΔPIP HIS, yen1::KAN*	This study

YRL360	*YRL19, dna2::dna2-HD, pol32::pol32ΔPIP HIS, yen1::KAN*	This study
YRL361	*YRL19, pol32::POL32-6His-3Flag KAN*	This study
YRL362	*YRL19, pol32::pol32ΔC-6His-3Flag KAN*	This study
YRL363	*YRL19, pol32::pol32ΔPIP-6His-3Flag KAN*	This study
YRL469	*YRL19, dna2::HIS, pif1::pif1-m2, rfa1::rfa1-RFP, pAG415 GPD YEN1-EGFP*	This study
YRL470	*YRL19, pif1::pif1-m2, rfa1::rfa1-RFP, pAG415 GPD YEN1-EGFP*	This study
YRL471	*YRL19, dna2::HIS, pif1::pif1-m2, pol32::pol32ΔC KAN*	This study

Chapter 8: Conclusion and outlook

In the time it took the author to write this thesis, a mammalian cell would have had the time to "write" roughly 100 billion characters in the language of life. Although this comparison doesn't flatter the human writer, one should not forget that the process of DNA replication has been refined by natural selection for billions of years to reach its astonishing efficiency.

Among the enzyme contributing to DNA replication across eukaryotes is the conserved Dna2 nuclease-helicase. Although Dna2 has been implicated in multiple processes, the reason for its essentiality had remained unknown. My work addresses the molecular roles of Dna2.

To shed light on Dna2 in DNA replication, we used budding yeast as a model. First, we investigated the role of the poorly understood helicase activity of Dna2, using its genetic interaction with the Holliday junction resolvase Yen1 as an entry point. We first observed that *dna2-HD* cells can survive RS due to the compensatory mitotic action of Yen1. This role of Yen1 was independent of Rad52, indicating that Yen1 fulfils a function different from its canonical activity in cleaving DNA intermediates arising from HR. In absence of Yen1, *dna2-HD* cells reaching mitosis displayed DNA bridges characteristic of chromosomal entanglement. Moreover, we showed that at the rDNA locus, *dna2-HD* cells accumulate stalled and converging RFs and that these DNA structures could be removed *in vivo* by the actions of Yen1. Altogether these data demonstrated that Yen1 processes replication-borne DNA intermediates to promote viable mitotic exit. These results also revealed that the Dna2 helicase plays a previously undescribed role in the completion of DNA replication[154].

In support of this idea, we observed that following exposure to HU during S-phase, *dna2-HD* cells activate the DNA-damage checkpoint at the time when wild-type cells enter mitosis. This indicates that remnants from perturbed RFs, left unprocessed in absence of the Dna2 helicase activity, are recognized as damage late in the cell cycle, ultimately causing terminal cell-cycle arrest in a large proportion of Dna2 helicase-defective cells[154].

This first study led to an important question: what are the molecular determinants leading to the formation of these checkpoint-activating DNA structures? Sequencing of suppressors revealed that Pif1 was the major factor generating RS sensitivity in *dna2-HD yen1*Δ mutant cells (G. Ölmezer, personal communication). We then elucidated that loss of Dna2 results in significant DNA underreplication independently of Pif1 (i.e. in *dna2*Δ *pif1-m2* and *dna2*Δ *pif1*Δ double mutant

cells). Cells can escape lethality at this stage as long as RF stalling is limited and Yen1 is present. However, When Pif1 is present, toxic DNA intermediates are formed at unprocessed RFs.

Since Pif1 is a multifunctional enzyme, we decided to test mutants with well-described functional defects. Mutating motifs essential for HR-coupled replication restart (BIR) greatly improved the resistance of *dna2* mutants to RS and suppressed unscheduled DNA damage-checkpoint activation in response to RS. A similar effect was observed when Pol32, another protein implicated in BIR, was mutated. Based on these finding, we propose that in absence of Dna2, stalled RFs become susceptible to excessive Pif1-dependent restart by RDR. We thus envision Dna2 as a gatekeeper at stalled RFs that mediates RF restart and suppresses alternative RF recovery by RDR. This gatekeeper model provides an alternative explanation to the prevailing Okazaki fragment processing model as a basis for the essential requirement of Dna2 in cells (Falquet et al., Manuscript in revision).

But why is excessive RDR toxic for cells? First, since leading and lagging strand replication are uncoupled when DNA synthesis takes place in the context of a D-loop, nascent ssDNA is exposed[197]. Bound by RPA, this ssDNA could contribute to unscheduled checkpoint activation. However, we further suggest that the unstable nature of D-loops during RDR results in permanently displaced nascent ssDNA upon passage of an oncoming RF, especially when HR-dependent replication restart is used promiscuously. We believe that this provides a viable explanation for dsDNA with ssDNA branches comprising up to 15'000 nucleotides observed upon acute depletion of Dna2 in budding yeast[148].

We have provided a new framework to rationalize the molecular functions of Dna2. However, the way in which Dna2 operates at stalled RFs is still uncertain. It seems plausible that Dna2 resects reversed RFs to promote the restoration of a cannonical RF, a model that is consistent with the activity of the DNA2 human enzyme[79] and the accumulation of four-way junctions upon loss of Dna2 across organisms[79,148,152]. Interestingly, these structures fit the substrate specificity of Yen1, which we know processes DNA intermediates persisting in absence of Dna2. A future goal will be to identify the precise nature of these DNA intermediates, elucidate where they originate, and determine which factors are working with Yen1 in their resolution.

Concerning the mode of operation of Yen1, we observed that it forms foci in the "anaphase tube", probably marking sites of DNA cleavage. This situation is reminiscent of the

LEM-3 nuclease in *C. elegans*. During mitosis, LEM-3 cleaves chromatin bridges once it is recruited to the midbody by the AIR-2 an Aurora B kinase[231,232]. In budding yeast, the Aurora kinase Ipl1 also localizes to the site of abscission and delays cytokinesis until the chromosomes separate[233], a mechanism that promotes resistance to RS[234]. It is tempting to speculate that this pathway may be involved in the recruitment of Yen1. Investigating how Yen1 recognizes its target could offer an opportunity to better understand links between chromosome segregation and cell cycle control, a crucial aspect of genome stability.

Dna2, Pif1, and Yen1 are all conserved in human. It will be interesting to see how far their interplay is also mechanistically conserved. As mentioned earlier, Dna2 is essential in all eukaryotes[95-99]. In human, reduced DNA2 abundance caused by faulty spicing[100] or inactivation of the DNA2 helicase domain by a point mutation[235] causes microcephalic primordial dwarfism (Seckel syndrome). This pathology can be caused by a failure to respond properly to RS, leading to cell death during development and resulting in an hypocellular phenotype (reviewed in [236]). These observations are consistent with our proposal of an essential function of DNA2 as a gatekeeper at stalled RFs. It will be interesting to address the question whether failed RF restart in the context of a more complex human genome alone explains the lethality associated with loss of DNA2, or whether excessive replication restart along alternative pathways contributes, as seen in yeast.

DNA2 is also implicated in cancer development. Several mutations clustering in the helicase or the nuclease domain of DNA2 were identified in breast and ovarian cancer cells[102]. While these alternations may impair the function of the enzyme, DNA2 was also found to be upregulated in cancerous cells[101,102] and depletion of DNA2 reduced tumor growth in these cells[102]. These findings can be rationalized if we consider that mutations of *DNA2* in precancerous lesions may increase genomic instability and drive cancer evolution, while, at a later stage, DNA2 could be upregulated to cope with the high level of RS that is intrinsic to cancer cells[237].

Its vital role in the RS response makes DNA2 an attractive target for cancer therapy, and several inhibitors of DNA2 have been developed based on *in-silico* screening[238,239]. Yeast could offer a powerful platform for *in vivo* screening. Indeed, large-scale humanization of yeast genes suggests that human *DNA2* can complement the function of the yeast gene[240]. If this result is confirmed, one could envision to screen compounds killing specifically *dna2::hDNA2* but not *dna2::hDNA2 pif1-m2* mutant strains and identify, through this procedure, specific inhibitors of human DNA2.

These efforts should be complemented by further mechanistic studies in the human system informed by our latest results in the yeast system.

Overall, I hope my work has shed important new light on key players and events during DNA replication, contributing to our understanding of this rather marvelous process.

References

1. Bleichert, F., Botchan, M. R. & Berger, J. M. Mechanisms for initiating cellular DNA replication. *Science* **355,** eaah6317 (2017).
2. Siddiqui, K., On, K. F. & Diffley, J. F. X. Regulating DNA replication in eukarya. *Cold Spring Harb. Perspect. Biol.* **5,** a012930–a012930 (2013).
3. Hartwell, L. H. & Weinert, T. A. Checkpoints: controls that ensure the order of cell cycle events. *Science* **246,** 629–634 (1989).
4. Morgan, D. O. Cyclin-dependent kinases: engines, clocks, and microprocessors. *Annu. Rev. Cell Dev. Biol.* **13,** 261–291 (1997).
5. Donovan, S., Harwood, J., Drury, L. S. & Diffley, J. F. Cdc6p-dependent loading of Mcm proteins onto pre-replicative chromatin in budding yeast. *Proc. Natl. Acad. Sci. U.S.A.* **94,** 5611–5616 (1997).
6. Hustedt, N., Gasser, S. & Shimada, K. Replication Checkpoint: Tuning and Coordination of Replication Forks in S Phase. *Genes* **4,** 388–434 (2013).
7. Nigg, E. A. Mitotic kinases as regulators of cell division and its checkpoints. *Nat. Rev. Mol. Cell Biol.* **2,** 21–32 (2001).
8. Alberts, B. *et al. Molecular Biology of the Cell.* (Garland Science, 2002).
9. Ganier, O., Prorok, P., Akerman, I. & Méchali, M. Metazoan DNA replication origins. *Curr. Opin. Cell Biol.* **58,** 134–141 (2019).
10. Yekezare, M., Gómez-González, B. & Diffley, J. F. X. Controlling DNA replication origins in response to DNA damage - inhibit globally, activate locally. *J. Cell. Sci.* **126,** 1297–1306 (2013).
11. Yeeles, J. T. P., Janska, A., Early, A. & Diffley, J. F. X. How the Eukaryotic Replisome Achieves Rapid and Efficient DNA Replication. *Mol. Cell* **65,** 105–116 (2017).
12. Ciccia, A. & Elledge, S. J. The DNA damage response: making it safe to play with knives. *Mol. Cell* **40,** 179–204 (2010).
13. Zeman, M. K. & Cimprich, K. A. Causes and consequences of replication stress. *Nat. Cell Biol.* **16,** 2–9 (2014).
14. Amin, A. D., Vishnoi, N. & Prochasson, P. A global requirement for the HIR complex in the assembly of chromatin. *Biochim. Biophys. Acta* **1819,** 264–276 (2013).
15. Jaeger, S., Barends, S., Giegé, R., Eriani, G. & Martin, F. Expression of metazoan replication-dependent histone genes. *Biochimie* **87,** 827–834 (2005).
16. Aguilera, A. & García-Muse, T. R loops: from transcription byproducts to threats to genome stability. *Mol. Cell* **46,** 115–124 (2012).

17. Kobayashi, T. The replication fork barrier site forms a unique structure with Fob1p and inhibits the replication fork. *Mol. Cell. Biol.* **23,** 9178–9188 (2003).
18. Makovets, S., Herskowitz, I. & Blackburn, E. H. Anatomy and dynamics of DNA replication fork movement in yeast telomeric regions. *Mol. Cell. Biol.* **24,** 4019–4031 (2004).
19. Greenfeder, S. A. & Newlon, C. S. Replication forks pause at yeast centromeres. *Mol. Cell. Biol.* **12,** 4056–4066 (1992).
20. Gadaleta, M. C. & Noguchi, E. Regulation of DNA Replication through Natural Impediments in the Eukaryotic Geno me. *Genes* **8,** 98 (2017).
21. Magdalou, I., Lopez, B. S., Pasero, P. & Lambert, S. A. E. The causes of replication stress and their consequences on genome stability and cell fate. *Semin. Cell Dev. Biol.* **30,** 154–164 (2014).
22. Glover, T. W., Wilson, T. E. & Arlt, M. F. Fragile sites in cancer: more than meets the eye. *Nature Reviews Cancer* **17,** 489–501 (2017).
23. Petermann, E., Orta, M. L., Issaeva, N., Schultz, N. & Helleday, T. Hydroxyurea-stalled replication forks become progressively inactivated and require two different RAD51-mediated pathways for restart and repair. *Mol. Cell* **37,** 492–502 (2010).
24. Rivera-Mulia, J. C. & Gilbert, D. M. Replicating Large Genomes: Divide and Conquer. *Mol. Cell* **62,** 756–765 (2016).
25. Kaykov, A. & Nurse, P. The spatial and temporal organization of origin firing during the S-phase of fission yeast. *Genome Res.* **25,** 391–401 (2015).
26. Syljuåsen, R. G. *et al.* Inhibition of human Chk1 causes increased initiation of DNA replication, phosphorylation of ATR targets, and DNA breakage. *Mol. Cell. Biol.* **25,** 3553–3562 (2005).
27. Toledo, L. I. *et al.* ATR prohibits replication catastrophe by preventing global exhaustion of RPA. *Cell* **155,** 1088–1103 (2013).
28. Toledo, L., Neelsen, K. J. & Lukas, J. Replication Catastrophe: When a Checkpoint Fails because of Exhaustion. *Mol. Cell* **66,** 735–749 (2017).
29. Ge, X. Q., Jackson, D. A. & Blow, J. J. Dormant origins licensed by excess Mcm2-7 are required for human cells to survive replicative stress. *Genes Dev.* **21,** 3331–3341 (2007).
30. Woodward, A. M. *et al.* Excess Mcm2-7 license dormant origins of replication that can be used under conditions of replicative stress. *J. Cell Biol.* **173,** 673–683 (2006).

31. Ibarra, A., Schwob, E. & Mendez, J. Excess MCM proteins protect human cells from replicative stress by licensing backup origins of replication. *Proc. Natl. Acad. Sci. U.S.A.* **105,** 8956–8961 (2008).
32. Zimmerman, K. M., Jones, R. M., Petermann, E. & Jeggo, P. A. Diminished origin-licensing capacity specifically sensitizes tumor cells to replication stress. *Mol. Cancer Res.* **11,** 370–380 (2013).
33. Shima, N. *et al.* A viable allele of Mcm4 causes chromosome instability and mammary adenocarcinomas in mice. *Nat. Genet.* **39,** 93–98 (2007).
34. Kawabata, T. *et al.* Stalled fork rescue via dormant replication origins in unchallenged S phase promotes proper chromosome segregation and tumor suppression. *Mol. Cell* **41,** 543–553 (2011).
35. Lengronne, A. & Schwob, E. The yeast CDK inhibitor Sic1 prevents genomic instability by promoting replication origin licensing in late G(1). *Mol. Cell* **9,** 1067–1078 (2002).
36. Tanaka, S. & Diffley, J. F. X. Deregulated G1-cyclin expression induces genomic instability by preventing efficient pre-RC formation. *Genes Dev.* **16,** 2639–2649 (2002).
37. Newman, T. J., Mamun, M. A., Nieduszynski, C. A. & Blow, J. J. Replisome stall events have shaped the distribution of replication origins in the genomes of yeasts. *Nucleic Acids Res.* **41,** 9705–9718 (2013).
38. Mamun, Al, M. *et al.* Inevitability and containment of replication errors for eukaryotic genome lengths spanning megabase to gigabase. *Proc. Natl. Acad. Sci. U.S.A.* **113,** E5765–74 (2016).
39. Brown, E. J. & Baltimore, D. ATR disruption leads to chromosomal fragmentation and early embryonic lethality. *Genes Dev.* **14,** 397–402 (2000).
40. de Klein, A. *et al.* Targeted disruption of the cell-cycle checkpoint gene ATR leads to early embryonic lethality in mice. *Curr. Biol.* **10,** 479–482 (2000).
41. O'Driscoll, M., Ruiz-Perez, V. L., Woods, C. G., Jeggo, P. A. & Goodship, J. A. A splicing mutation affecting expression of ataxia-telangiectasia and Rad3-related protein (ATR) results in Seckel syndrome. *Nat. Genet.* **33,** 497–501 (2003).
42. Alani, E., Thresher, R., Griffith, J. D. & Kolodner, R. D. Characterization of DNA-binding and strand-exchange stimulation properties of y-RPA, a yeast single-strand-DNA-binding protein. *J. Mol. Biol.* **227,** 54–71 (1992).
43. Zou, L. & Elledge, S. J. Sensing DNA damage through ATRIP recognition of RPA-ssDNA complexes. *Science* **300,** 1542–1548 (2003).

44. Deshpande, I. *et al.* Structural Basis of Mec1-Ddc2-RPA Assembly and Activation on Single-Stranded DNA at Sites of Damage. *Mol. Cell* **68,** 431–445.e5 (2017).
45. Majka, J., Niedziela-Majka, A. & Burgers, P. M. J. The checkpoint clamp activates Mec1 kinase during initiation of the DNA damage checkpoint. *Mol. Cell* **24,** 891–901 (2006).
46. MacDougall, C. A., Byun, T. S., Van, C., Yee, M.-C. & Cimprich, K. A. The structural determinants of checkpoint activation. *Genes Dev.* **21,** 898–903 (2007).
47. Kumagai, A., Lee, J., Yoo, H. Y. & Dunphy, W. G. TopBP1 activates the ATR-ATRIP complex. *Cell* **124,** 943–955 (2006).
48. Puddu, F. *et al.* Phosphorylation of the budding yeast 9-1-1 complex is required for Dpb11 function in the full activation of the UV-induced DNA damage checkpoint. *Mol. Cell. Biol.* **28,** 4782–4793 (2008).
49. Nakada, D., Matsumoto, K. & Sugimoto, K. ATM-related Tel1 associates with double-strand breaks through an Xrs2-dependent mechanism. *Genes Dev.* **17,** 1957–1962 (2003).
50. Hustedt, N. *et al.* Yeast PP4 interacts with ATR homolog Ddc2-Mec1 and regulates checkpoint signaling. *Mol. Cell* **57,** 273–289 (2015).
51. Alcasabas, A. A. *et al.* Mrc1 transduces signals of DNA replication stress to activate Rad53. *Nat. Cell Biol.* **3,** 958–965 (2001).
52. Weinert, T. A. & Hartwell, L. H. The RAD9 gene controls the cell cycle response to DNA damage in Saccharomyces cerevisiae. *Science* **241,** 317–322 (1988).
53. Gilbert, C. S., Green, C. M. & Lowndes, N. F. Budding yeast Rad9 is an ATP-dependent Rad53 activating machine. *Mol. Cell* **8,** 129–136 (2001).
54. Sanchez, Y. *et al.* Control of the DNA Damage Checkpoint by Chk1 and Rad53 Protein Kinases Through Distinct Mechanisms. *Science* **286,** 1166–1171 (1999).
55. Desany, B. A., Alcasabas, A. A., Bachant, J. B. & Elledge, S. J. Recovery from DNA replicational stress is the essential function of the S-phase checkpoint pathway. *Genes Dev.* **12,** 2956–2970 (1998).
56. Zhao, X., Muller, E. G. & Rothstein, R. A suppressor of two essential checkpoint genes identifies a novel protein that negatively affects dNTP pools. *Mol. Cell* **2,** 329–340 (1998).
57. Ge, X. Q. & Blow, J. J. Chk1 inhibits replication factory activation but allows dormant origin firing in existing factories. *J. Cell Biol.* **191,** 1285–1297 (2010).
58. Rybak, P., Waligórska, A., Bujnowicz, Ł., Hoang, A. & Dobrucki, J. W. Activation of new replication foci under conditions of replication stress. *Cell Cycle* **14,** 2634–2647 (2015).

59. Can, G., Kauerhof, A. C., Macak, D. & Zegerman, P. Helicase Subunit Cdc45 Targets the Checkpoint Kinase Rad53 to Both Replication Initiation and Elongation Complexes after Fork Stalling. *Mol. Cell* **73,** 562–573.e3 (2019).
60. Lopez-Mosqueda, J. *et al.* Damage-induced phosphorylation of Sld3 is important to block late origin firing. *Nature* **467,** 479–483 (2010).
61. Zegerman, P. & Diffley, J. F. X. Checkpoint-dependent inhibition of DNA replication initiation by Sld3 and Dbf4 phosphorylation. *Nature* **467,** 474–478 (2010).
62. Boos, D. *et al.* Regulation of DNA replication through Sld3-Dpb11 interaction is conserved from yeast to humans. *Curr. Biol.* **21,** 1152–1157 (2011).
63. Lee, A. Y.-L. *et al.* Dbf4 is direct downstream target of ataxia telangiectasia mutated (ATM) and ataxia telangiectasia and Rad3-related (ATR) protein to regulate intra-S-phase checkpoint. **287,** 2531–2543 (2012).
64. Tercero, J. A. & Diffley, J. F. Regulation of DNA replication fork progression through damaged DNA by the Mec1/Rad53 checkpoint. *Nature* **412,** 553–557 (2001).
65. Segurado, M. & Diffley, J. F. X. Separate roles for the DNA damage checkpoint protein kinases in stabilizing DNA replication forks. *Genes Dev.* **22,** 1816–1827 (2008).
66. Lopes, M. *et al.* The DNA replication checkpoint response stabilizes stalled replication forks. *Nature* **412,** 557–561 (2001).
67. Paulovich, A. G. & Hartwell, L. H. A checkpoint regulates the rate of progression through S phase in S. cerevisiae in response to DNA damage. *Cell* **82,** 841–847 (1995).
68. Ragland, R. L. *et al.* RNF4 and PLK1 are required for replication fork collapse in ATR-deficient cells. *Genes Dev.* **27,** 2259–2273 (2013).
69. El-Shemerly, M., Hess, D., Pyakurel, A. K., Moselhy, S. & Ferrari, S. ATR-dependent pathways control hEXO1 stability in response to stalled forks. *Nucleic Acids Res.* **36,** 511–519 (2008).
70. Cotta-Ramusino, C. *et al.* Exo1 Processes Stalled Replication Forks and Counteracts Fork Reversal in Checkpoint-Defective Cells. *Mol. Cell* **17,** 153–159 (2005).
71. Gan, H. *et al.* Checkpoint Kinase Rad53 Couples Leading- and Lagging-Strand DNA Synthesis under Replication Stress. *Mol. Cell* **68,** 446–455.e3 (2017).
72. Sogo, J. M., Lopes, M. & Foiani, M. Fork reversal and ssDNA accumulation at stalled replication forks owing to checkpoint defects. *Science* **297,** 599–602 (2002).
73. Buisson, R., Boisvert, J. L., Benes, C. H. & Zou, L. Distinct but Concerted Roles of ATR, DNA-PK, and Chk1 in Countering Replication Stress during S Phase. *Mol. Cell* **59,** 1011–1024 (2015).

74. Quinet, A., Lemaçon, D. & Vindigni, A. Replication Fork Reversal: Players and Guardians. *Mol. Cell* **68,** 830–833 (2017).
75. Meng, X. & Zhao, X. Replication fork regression and its regulation. *FEMS Yeast Res.* **17,** fow110 (2017).
76. Ray Chaudhuri, A. *et al.* Topoisomerase I poisoning results in PARP-mediated replication fork reversal. *Nat. Struc. Mol. Biol.* **19,** 417–423 (2012).
77. Zellweger, R. *et al.* Rad51-mediated replication fork reversal is a global response to genotoxic treatments in human cells. *J. Cell Biol.* **208,** 563–579 (2015).
78. Berti, M. *et al.* Human RECQ1 promotes restart of replication forks reversed by DNA topoisomerase I inhibition. *Nat. Struc. Mol. Biol.* **20,** 347–354 (2013).
79. Thangavel, S. *et al.* DNA2 drives processing and restart of reversed replication forks in human cells. *J. Cell Biol.* **208,** 545–562 (2015).
80. Mutreja, K. *et al.* ATR-Mediated Global Fork Slowing and Reversal Assist Fork Traverse and Prevent Chromosomal Breakage at DNA Interstrand Cross-Links. *Cell Rep.* **24,** 2629–2642.e5 (2018).
81. Saldivar, J. C. *et al.* An intrinsic S/G2 checkpoint enforced by ATR. *Science* **361,** 806–810 (2018).
82. Lemmens, B. *et al.* DNA Replication Determines Timing of Mitosis by Restricting CDK1 and PLK1 Activation. *Mol. Cell* **71,** 117–128.e3 (2018).
83. Torres-Rosell, J. *et al.* Anaphase onset before complete DNA replication with intact checkpoint responses. *Science* **315,** 1411–1415 (2007).
84. Chan, K.-L., North, P. S. & Hickson, I. D. BLM is required for faithful chromosome segregation and its localization defines a class of ultrafine anaphase bridges. *EMBO J.* **26,** 3397–3409 (2007).
85. Baumann, C., Körner, R., Hofmann, K. & Nigg, E. A. PICH, a centromere-associated SNF2 family ATPase, is regulated by Plk1 and required for the spindle checkpoint. *Cell* **128,** 101–114 (2007).
86. Chan, K.-L., Palmai-Pallag, T., Ying, S. & Hickson, I. D. Replication stress induces sister-chromatid bridging at fragile site loci in mitosis. *Nat. Cell Biol.* **11,** 753–760 (2009).
87. Nielsen, C. F. *et al.* PICH promotes sister chromatid disjunction and co-operates with topoisomerase II in mitosis. *Nat. Commun.* **6,** 8962 (2015).
88. Nielsen, C. F. & Hickson, I. D. PICH promotes mitotic chromosome segregation: Identification of a novel role in rDNA disjunction. *Cell Cycle* **15,** 2704–2711 (2016).

89. d'Alcontres, M. S., Palacios, J. A., Mejias, D. & Blasco, M. A. TopoIIα prevents telomere fragility and formation of ultra thin DNA bridges during mitosis through TRF1-dependent binding to telomeres. *Cell Cycle* **13,** 1463–1481 (2014).
90. Barefield, C. & Karlseder, J. The BLM helicase contributes to telomere maintenance through processing of late-replicating intermediate structures. *Nucleic Acids Res.* **40,** 7358–7367 (2012).
91. Fernández-Casañas, M. & Chan, K.-L. The Unresolved Problem of DNA Bridging. *Genes* **9,** 623 (2018).
92. Lukas, C. *et al.* 53BP1 nuclear bodies form around DNA lesions generated by mitotic transmission of chromosomes under replication stress. *Nat. Cell Biol.* **13,** 243–253 (2011).
93. Halazonetis, T. D., Gorgoulis, V. G. & Bartek, J. An Oncogene-Induced DNA Damage Model for Cancer Development. *Science* **319,** 1352–1355 (2008).
94. Budd, M. E., Choe, W. C. & Campbell, J. L. DNA2 encodes a DNA helicase essential for replication of eukaryotic chromosomes. *J. Biol. Chem.* **270,** 26766–26769 (1995).
95. Budd, M. E., Choe, W. C. & Campbell, J. L. The nuclease activity of the yeast DNA2 protein, which is related to the RecB-like nucleases, is essential in vivo. *J. Biol. Chem.* **275,** 16518–16529 (2000).
96. Duxin, J. P. *et al.* Okazaki fragment processing-independent role for human Dna2 enzyme during DNA replication. **287,** 21980–21991 (2012).
97. Kang, H.-Y. *et al.* Genetic Analyses of Schizosaccharomyces pombe dna2+ Reveal That Dna2 Plays an Essential Role in Okazaki Fragment Metabolism. *Genetics* **155,** 1055–1067 (2000).
98. Lin, W. *et al.* Mammalian DNA2 helicase/nuclease cleaves G-quadruplex DNA and is required for telomere integrity. *EMBO J.* **32,** 1425–1439 (2013).
99. Kim, D.-H. *et al.* Enzymatic properties of the Caenorhabditis elegans Dna2 endonuclease/helicase and a species-specific interaction between RPA and Dna2. *Nucleic Acids Res.* **33,** 1372–1383 (2005).
100. Shaheen, R. *et al.* Genomic analysis of primordial dwarfism reveals novel disease genes. *Genome Res.* **24,** 291–299 (2014).
101. Peng, G. *et al.* Human nuclease/helicase DNA2 alleviates replication stress by promoting DNA end resection. *Cancer Res.* **72,** 2802–2813 (2012).
102. Strauss, C. *et al.* The DNA2 nuclease/helicase is an estrogen-dependent gene mutated in breast and ovarian cancers. *Oncotarget* **5,** 9396–9409 (2014).

103. Wanrooij, P. H. & Burgers, P. M. Yet another job for Dna2: Checkpoint activation. *DNA Repair (Amst.)* **32,** 17–23 (2015).

104. Aravind, L., Walker, D. R. & Koonin, E. V. Conserved domains in DNA repair proteins and evolution of repair systems. *Nucleic Acids Res.* **27,** 1223–1242 (1999).

105. Bae, S. H. & Seo, Y. S. Characterization of the enzymatic properties of the yeast dna2 Helicase/endonuclease suggests a new model for Okazaki fragment processing. **275,** 38022–38031 (2000).

106. Budd, M. E. *et al.* A network of multi-tasking proteins at the DNA replication fork preserves genome stability. *PLoS Genet.* **1,** e61 (2005).

107. Lee, K. H. *et al.* The endonuclease activity of the yeast Dna2 enzyme is essential in vivo. *Nucleic Acids Res.* **28,** 2873–2881 (2000).

108. Kao, H.-I., Campbell, J. L. & Bambara, R. A. Dna2p helicase/nuclease is a tracking protein, like FEN1, for flap cleavage during Okazaki fragment maturation. **279,** 50840–50849 (2004).

109. Zhou, C., Pourmal, S. & Pavletich, N. P. Dna2 nuclease-helicase structure, mechanism and regulation by Rpa. *Elife* **4,** 213 (2015).

110. Levikova, M., Klaue, D., Seidel, R. & Cejka, P. Nuclease activity of Saccharomyces cerevisiae Dna2 inhibits its potent DNA helicase activity. *Proc. Natl. Acad. Sci. U.S.A.* **110,** E1992–2001 (2013).

111. Kim, J.-H. *et al.* Isolation of human Dna2 endonuclease and characterization of its enzymatic properties. *Nucleic Acids Res.* **34,** 1854–1864 (2006).

112. Masuda-Sasa, T., Imamura, O. & Campbell, J. L. Biochemical analysis of human Dna2. *Nucleic Acids Res.* **34,** 1865–1875 (2006).

113. Pinto, C., Kasaciunaite, K., Seidel, R. & Cejka, P. Human DNA2 possesses a cryptic DNA unwinding activity that functionally integrates with BLM or WRN helicases. *Elife* **5,** 3006 (2016).

114. Bae, S. H., Bae, K. H., Kim, J. A. & Seo, Y. S. RPA governs endonuclease switching during processing of Okazaki fragments in eukaryotes. *Nature* **412,** 456–461 (2001).

115. Levikova, M. & Cejka, P. The Saccharomyces cerevisiae Dna2 can function as a sole nuclease in the processing of Okazaki fragments in DNA replication. *Nucleic Acids Res.* gkv710 (2015). doi:10.1093/nar/gkv710

116. Cejka, P. *et al.* DNA end resection by Dna2-Sgs1-RPA and its stimulation by Top3-Rmi1 and Mre11-Rad50-Xrs2. *Nature* **467,** 112–116 (2010).

117. Bae, K.-H. *et al.* Bimodal interaction between replication-protein A and Dna2 is critical for Dna2 function both in vivo and in vitro. *Nucleic Acids Res.* **31,** 3006–3015 (2003).

118. Stewart, J. A., Miller, A. S., Campbell, J. L. & Bambara, R. A. Dynamic removal of replication protein A by Dna2 facilitates primer cleavage during Okazaki fragment processing in Saccharomyces cerevisiae. **283,** 31356–31365 (2008).

119. Fiorentino, D. F. & Crabtree, G. R. Characterization of Saccharomyces cerevisiae dna2 mutants suggests a role for the helicase late in S phase. *Mol. Biol. Cell.* **8,** 2519–2537 (1997).

120. Kosugi, S., Hasebe, M., Tomita, M. & Yanagawa, H. Systematic identification of cell cycle-dependent yeast nucleocytoplasmic shuttling proteins by prediction of composite motifs. *Proc. Natl. Acad. Sci. U.S.A.* **106,** 10171–10176 (2009).

121. Ranjha, L., Levikova, M., Altmannova, V., Krejci, L. & Cejka, P. Sumoylation regulates the stability and nuclease activity of Saccharomyces cerevisiae Dna2. *Commun Biol* **2,** 174–12 (2019).

122. Meng, Y. *et al.* TRAF6 mediates human DNA2 polyubiquitination and nuclear localization to maintain nuclear genome integrity. *Nucleic Acids Res.* **71,** 333 (2019).

123. Bennett, C. B., Lewis, A. L., Baldwin, K. K. & Resnick, M. A. Lethality induced by a single site-specific double-strand break in a dispensable yeast plasmid. *Proc. Natl. Acad. Sci. U.S.A.* **90,** 5613–5617 (1993).

124. Ranjha, L., Howard, S. M. & Cejka, P. Main steps in DNA double-strand break repair: an introduction to homologous recombination and related processes. *Chromosoma* **127,** 187–214 (2018).

125. Johnson, R. D. & Jasin, M. Sister chromatid gene conversion is a prominent double-strand break repair pathway in mammalian cells. *EMBO J.* **19,** 3398–3407 (2000).

126. Panier, S. & Durocher, D. Push back to respond better: regulatory inhibition of the DNA double-strand break response. *Nat. Rev. Mol. Cell Biol.* **14,** 661–672 (2013).

127. Chen, X. *et al.* Cell cycle regulation of DNA double-strand break end resection by Cdk1-dependent Dna2 phosphorylation. *Nat. Struc. Mol. Biol.* **18,** 1015–1019 (2011).

128. Yimit, A., Riffle, M. & Brown, G. W. Genetic Regulation of Dna2 Localization During the DNA Damage Response. *G3 (Bethesda)* g3.115.019208 (2015). doi:10.1534/g3.115.019208

129. Gravel, S., Chapman, J. R., Magill, C. & Jackson, S. P. DNA helicases Sgs1 and BLM promote DNA double-strand break resection. *Genes Dev.* **22,** 2767–2772 (2008).

130. Zhu, Z., Chung, W.-H., Shim, E. Y., Lee, S. E. & Ira, G. Sgs1 helicase and two nucleases Dna2 and Exo1 resect DNA double-strand break ends. *Cell* **134,** 981–994 (2008).
131. Mimitou, E. P. & Symington, L. S. Sae2, Exo1 and Sgs1 collaborate in DNA double-strand break processing. *Nature* **455,** 770–774 (2008).
132. Nimonkar, A. V. *et al.* BLM-DNA2-RPA-MRN and EXO1-BLM-RPA-MRN constitute two DNA end resection machineries for human DNA break repair. *Genes Dev.* **25,** 350–362 (2011).
133. Sturzenegger, A. *et al.* DNA2 cooperates with the WRN and BLM RecQ helicases to mediate long-range DNA end resection in human cells. **289,** 27314–27326 (2014).
134. Levikova, M., Pinto, C. & Cejka, P. The motor activity of DNA2 functions as an ssDNA translocase to promote DNA end resection. *Genes Dev.* **31,** 493–502 (2017).
135. Kasaciunaite, K. *et al.* Competing interaction partners modulate the activity of Sgs1 helicase during DNA end resection. *EMBO J.* **38,** (2019).
136. Daley, J. M. *et al.* Enhancement of BLM-DNA2-Mediated Long-Range DNA End Resection by CtIP. *Cell Rep.* **21,** 324–332 (2017).
137. Hoa, N. N. *et al.* BRCA1 and CtIP Are Both Required to Recruit Dna2 at Double-Strand Breaks in Homologous Recombination. *PLoS One* **10,** e0124495 (2015).
138. Shim, E. Y. *et al.* Saccharomyces cerevisiae Mre11/Rad50/Xrs2 and Ku proteins regulate association of Exo1 and Dna2 with DNA breaks. *EMBO J.* **29,** 3370–3380 (2010).
139. Stodola, J. L. & Burgers, P. M. Resolving individual steps of Okazaki-fragment maturation at a millisecond timescale. *Nat. Struc. Mol. Biol.* **23,** 402–408 (2016).
140. Budd, M. E. & Campbell, J. L. A yeast replicative helicase, Dna2 helicase, interacts with yeast FEN-1 nuclease in carrying out its essential function. *Mol. Cell. Biol.* **17,** 2136–2142 (1997).
141. Formosa, T. & Nittis, T. Dna2 Mutants Reveal Interactions with Dna Polymerase α and Ctf4, a Pol α Accessory Factor, and Show That Full Dna2 Helicase Activity Is Not Essential for Growth. *Genetics* **151,** 1459–1470 (1999).
142. Budd, M. E., Reis, C. C., Smith, S., Myung, K. & Campbell, J. L. Evidence suggesting that Pif1 helicase functions in DNA replication with the Dna2 helicase/nuclease and DNA polymerase delta. *Mol. Cell. Biol.* **26,** 2490–2500 (2006).
143. Munashingha, P. R. *et al.* The Trans-autostimulatory Activity of Rad27 Suppresses dna2 Defects in Okazaki Fragment Processing. **287,** 8675–8687 (2012).

144. Budd, M. E., Antoshechkin, I. A., Reis, C., Wold, B. J. & Campbell, J. L. Inviability of a DNA2 deletion mutant is due to the DNA damage checkpoint. *Cell Cycle* **10,** 1690–1698 (2011).

145. Pike, J. E., Burgers, P. M. J., Campbell, J. L. & Bambara, R. A. Pif1 helicase lengthens some Okazaki fragment flaps necessitating Dna2 nuclease/helicase action in the two-nuclease processing pathway. **284,** 25170–25180 (2009).

146. Rossi, M. L. *et al.* Pif1 helicase directs eukaryotic Okazaki fragments toward the two-nuclease cleavage pathway for primer removal. **283,** 27483–27493 (2008).

147. Kao, H.-I., Veeraraghavan, J., Polaczek, P., Campbell, J. L. & Bambara, R. A. On the roles of Saccharomyces cerevisiae Dna2p and Flap endonuclease 1 in Okazaki fragment processing. **279,** 15014–15024 (2004).

148. Rossi, S. E., Foiani, M. & Giannattasio, M. Dna2 processes behind the fork long ssDNA flaps generated by Pif1 and replication-dependent strand displacement. *Nat. Commun.* **9,** 4830 (2018).

149. Kahli, M., Osmundson, J. S., Yeung, R. & Smith, D. J. Processing of eukaryotic Okazaki fragments by redundant nucleases can be uncoupled from ongoing DNA replication in vivo. *Nucleic Acids Res.* **284,** 4041 (2018).

150. Osmundson, J. S., Kumar, J., Yeung, R. & Smith, D. J. Pif1-family helicases cooperatively suppress widespread replication-fork arrest at tRNA genes. *Nat. Struc. Mol. Biol.* **24,** 162–170 (2017).

151. Liu, B., Hu, J., Wang, J. & Kong, D. Direct Visualization of RNA-DNA Primer Removal from Okazaki Fragments Provides Support for Flap Cleavage and Exonucleolytic Pathways in Eukaryotic Cells. **292,** 4777–4788 (2017).

152. Hu, J. *et al.* The intra-S phase checkpoint targets Dna2 to prevent stalled replication forks from reversing. *Cell* **149,** 1221–1232 (2012).

153. Duxin, J. P. *et al.* Human Dna2 is a nuclear and mitochondrial DNA maintenance protein. *Mol. Cell. Biol.* **29,** 4274–4282 (2009).

154. Ölmezer, G. *et al.* Replication intermediates that escape Dna2 activity are processed by Holliday junction resolvase Yen1. *Nat. Commun.* **7,** 13157 (2016).

155. Weitao, T., Budd, M., Hoopes, L. L. M. & Campbell, J. L. Dna2 helicase/nuclease causes replicative fork stalling and double-strand breaks in the ribosomal DNA of Saccharomyces cerevisiae. *J. Biol. Chem.* **278,** 22513–22522 (2003).

156. Markiewicz-Potoczny, M., Lisby, M. & Lydall, D. A Critical Role for Dna2 at Unwound Telomeres. *Genetics* **209,** 129–141 (2018).

157. Budd, M. E. & Campbell, J. L. Dna2 is involved in CA strand resection and nascent lagging strand completion at native yeast telomeres. **288,** 29414–29429 (2013).

158. Li, Z. *et al.* hDNA2 nuclease/helicase promotes centromeric DNA replication and genome stability. *EMBO J.* e96729 (2018). doi:10.15252/embj.201796729

159. Masuda-Sasa, T., Polaczek, P., Peng, X. P., Chen, L. & Campbell, J. L. Processing of G4 DNA by Dna2 helicase/nuclease and replication protein A (RPA) provides insights into the mechanism of Dna2/RPA substrate recognition. **283,** 24359–24373 (2008).

160. Kumar, S. & Burgers, P. M. Lagging strand maturation factor Dna2 is a component of the replication checkpoint initiation machinery. *Genes Dev.* **27,** 313–321 (2013).

161. Zheng, L. *et al.* Human DNA2 is a mitochondrial nuclease/helicase for efficient processing of DNA replication and repair intermediates. *Mol. Cell* **32,** 325–336 (2008).

162. Ronchi, D. *et al.* Mutations in DNA2 link progressive myopathy to mitochondrial DNA instability. *Am. J. Hum. Genet.* **92,** 293–300 (2013).

163. Ronchi, D. *et al.* Novel mutations in DNA2 associated with myopathy and mtDNA instability. *Ann Clin Transl Neurol* **16,** 18054 (2019).

164. Chae, J. H. *et al.* Utility of next generation sequencing in genetic diagnosis of early onset neuromuscular disorders. *Journal of Medical Genetics* **52,** 208–216 (2015).

165. Phowthongkum, P. & Sun, A. Novel truncating variant in DNA2-related congenital onset myopathy and ptosis suggests genotype-phenotype correlation. *Neuromuscul. Disord.* **27,** 616–618 (2017).

166. del Angel, A. G., Fernandez-Valverde, F., Rucheton, B., Jardel, C. & Malfatti, E. A novel frameshift mutation in DNA2 causes early onset myopathy with velopharyngeal weakness and cardiac arrhythmias (P5.4-010). *Neurology* **92,** P5.4–010 (2019).

167. Ryu, G.-H. *et al.* Genetic and biochemical analyses of Pfh1 DNA helicase function in fission yeast. *Nucleic Acids Res.* **32,** 4205–4216 (2004).

168. Zhang, D.-H., Zhou, B., Huang, Y., Xu, L.-X. & Zhou, J.-Q. The human Pif1 helicase, a potential Escherichia coli RecD homologue, inhibits telomerase activity. *Nucleic Acids Res.* **34,** 1393–1404 (2006).

169. Bochman, M. L., Sabouri, N. & Zakian, V. A. Unwinding the functions of the Pif1 family helicases. *DNA Repair (Amst.)* **9,** 237–249 (2010).

170. Fairman-Williams, M. E., Guenther, U.-P. & Jankowsky, E. SF1 and SF2 helicases: family matters. *Curr. Opin. Struct. Biol.* **20,** 313–324 (2010).

171. Lahaye, A., Stahl, H., Sempoux, D. T. & Foury, F. PIF1: a DNA helicase in yeast mitochondria. *EMBO J.* **10,** 997–1007 (1991).

172. Zhou, J., Monson, E. K., Teng, S. C., Schulz, V. P. & Zakian, V. A. Pif1p helicase, a catalytic inhibitor of telomerase in yeast. *Science* **289,** 771–774 (2000).

173. Lahaye, A., Leterme, S. & Foury, F. PIF1 DNA helicase from Saccharomyces cerevisiae. Biochemical characterization of the enzyme. **268,** 26155–26161 (1993).

174. Li, J. R. *et al.* Pif1 regulates telomere length by preferentially removing telomerase from long telomere ends. *Nucleic Acids Res.* **42,** 8527–8536 (2014).

175. Zhou, R., Zhang, J., Bochman, M. L., Zakian, V. A. & Ha, T. Periodic DNA patrolling underlies diverse functions of Pif1 on R-loops and G-rich DNA. *Elife* **3,** e02190 (2014).

176. Zhou, J.-Q. *et al.* Schizosaccharomyces pombe pfh1+ encodes an essential 5‘ to 3’ DNA helicase that is a member of the PIF1 subfamily of DNA helicases. *Mol. Biol. Cell.* **13,** 2180–2191 (2002).

177. Schulz, V. P. & Zakian, V. A. The saccharomyces PIF1 DNA helicase inhibits telomere elongation and de novo telomere formation. *Cell* **76,** 145–155 (1994).

178. Futami, K., Shimamoto, A. & Furuichi, Y. Mitochondrial and nuclear localization of human Pif1 helicase. *Biol. Pharm. Bull.* **30,** 1685–1692 (2007).

179. Kazak, L. *et al.* Alternative translation initiation augments the human mitochondrial proteome. *Nucleic Acids Res.* **41,** 2354–2369 (2013).

180. Foury, F. & Kolodynski, J. pif mutation blocks recombination between mitochondrial rho+ and rho- genomes having tandemly arrayed repeat units in Saccharomyces cerevisiae. *Proc. Natl. Acad. Sci. U.S.A.* **80,** 5345–5349 (1983).

181. Van Dyck, E., Foury, F., Stillman, B. & Brill, S. J. A single-stranded DNA binding protein required for mitochondrial DNA replication in S. cerevisiae is homologous to E. coli SSB. *EMBO J.* **11,** 3421–3430 (1992).

182. Tanaka, H. *et al.* The fission yeast pfh1(+) gene encodes an essential 5‘ to 3’ DNA helicase required for the completion of S-phase. *Nucleic Acids Res.* **30,** 4728–4739 (2002).

183. Pinter, S. F., Aubert, S. D. & Zakian, V. A. The Schizosaccharomyces pombe Pfh1p DNA helicase is essential for the maintenance of nuclear and mitochondrial DNA. *Mol. Cell. Biol.* **28,** 6594–6608 (2008).

184. Chib, S., Byrd, A. K. & Raney, K. D. Yeast Helicase Pif1 Unwinds RNA:DNA Hybrids with Higher Processivity than DNA:DNA Duplexes. **291,** 5889–5901 (2016).

185. Boulé, J.-B. & Zakian, V. A. The yeast Pif1p DNA helicase preferentially unwinds RNA DNA substrates. *Nucleic Acids Res.* **35,** 5809–5818 (2007).

186. Boulé, J.-B., Vega, L. R. & Zakian, V. A. The yeast Pif1p helicase removes telomerase from telomeric DNA. *Nature* **438,** 57–61 (2005).

187. Phillips, J. A., Chan, A., Paeschke, K. & Zakian, V. A. The pif1 helicase, a negative regulator of telomerase, acts preferentially at long telomeres. *PLoS Genet.* **11,** e1005186 (2015).

188. Vega, L. R. *et al.* Sensitivity of yeast strains with long G-tails to levels of telomere-bound telomerase. *PLoS Genet.* **3,** e105 (2007).

189. Mateyak, M. K. & Zakian, V. A. Human PIF helicase is cell cycle regulated and associates with telomerase. *Cell Cycle* **5,** 2796–2804 (2006).

190. McDonald, K. R., Sabouri, N., Webb, C. J. & Zakian, V. A. The Pif1 family helicase Pfh1 facilitates telomere replication and has an RPA-dependent role during telomere lengthening. *DNA Repair (Amst.)* **24,** 80–86 (2014).

191. Ivessa, A. S. *et al.* The Saccharomyces cerevisiae helicase Rrm3p facilitates replication past nonhistone protein-DNA complexes. *Mol. Cell* **12,** 1525–1536 (2003).

192. Makovets, S. & Blackburn, E. H. DNA damage signalling prevents deleterious telomere addition at DNA breaks. *Nat. Cell Biol.* **11,** 1383–1386 (2009).

193. Myung, K., Chen, C. & Kolodner, R. D. Multiple pathways cooperate in the suppression of genome instability in Saccharomyces cerevisiae. *Nature* **411,** 1073–1076 (2001).

194. Strecker, J. *et al.* A sharp Pif1-dependent threshold separates DNA double-strand breaks from critically short telomeres. *Elife* **6,** 2251 (2017).

195. Vasianovich, Y., Harrington, L. A. & Makovets, S. Break-Induced Replication Requires DNA Damage-Induced Phosphorylation of Pif1 and Leads to Telomere Lengthening. *PLoS Genet.* **10,** e1004679 (2014).

196. Sakofsky, C. J. & Malkova, A. Break induced replication in eukaryotes: mechanisms, functions, and consequences. *Crit. Rev. Biochem. Mol. Biol.* **52,** 395–413 (2017).

197. Sakofsky, C. J. *et al.* Break-induced replication is a source of mutation clusters underlying kataegis. *Cell Rep.* **7,** 1640–1648 (2014).

198. Donnianni, R. A. & Symington, L. S. Break-induced replication occurs by conservative DNA synthesis. *Proc. Natl. Acad. Sci. U.S.A.* **110,** 13475–13480 (2013).

199. Saini, N. *et al.* Migrating bubble during break-induced replication drives conservative DNA synthesis. *Nature* **502,** 389–392 (2013).

200. Ait Saada, A., Lambert, S. A. E. & Carr, A. M. Preserving replication fork integrity and competence via the homologous recombination pathway. *DNA Repair (Amst.)* **71,** 135–147 (2018).

201. Jalan, M., Oehler, J., Morrow, C. A., Osman, F. & Whitby, M. C. Factors affecting template switch recombination associated with restarted DNA replication. *Elife* **8,** 1 (2019).

202. Lydeard, J. R. *et al.* Break-induced replication requires all essential DNA replication factors except those specific for pre-RC assembly. *Genes Dev.* **24,** 1133–1144 (2010).
203. Buzovetsky, O. *et al.* Role of the Pif1-PCNA Complex in Pol δ-Dependent Strand Displacement DNA Synthesis and Break-Induced Replication. *Cell Rep.* **21,** 1707–1714 (2017).
204. Saini, N. *et al.* Migrating bubble during break-induced replication drives conservative DNA synthesis. *Nature* **502,** 389–392 (2013).
205. Wilson, M. A. *et al.* Pif1 helicase and Polδ promote recombination-coupled DNA synthesis via bubble migration. *Nature* **502,** 393–396 (2013).
206. Mayle, R. *et al.* DNA REPAIR. Mus81 and converging forks limit the mutagenicity of replication fork breakage. *Science* **349,** 742–747 (2015).
207. Lerner, L. K. & Sale, J. E. Replication of G Quadruplex DNA. *Genes* **10,** 95 (2019).
208. Chambers, V. S. *et al.* High-throughput sequencing of DNA G-quadruplex structures in the human genome. *Nat. Biotechnol.* **33,** 877–881 (2015).
209. Paeschke, K. *et al.* Pif1 family helicases suppress genome instability at G-quadruplex motifs. *Nature* **497,** 458–462 (2013).
210. Ribeyre, C. *et al.* The yeast Pif1 helicase prevents genomic instability caused by G-quadruplex-forming CEB1 sequences in vivo. *PLoS Genet.* **5,** e1000475 (2009).
211. Paeschke, K., Capra, J. A. & Zakian, V. A. DNA Replication through G-Quadruplex Motifs Is Promoted by the Saccharomyces cerevisiae Pif1 DNA Helicase. *Cell* **145,** 678–691 (2011).
212. Lopes, J. *et al.* G-quadruplex-induced instability during leading-strand replication. *EMBO J.* **30,** 4033–4046 (2011).
213. Sanders, C. M. Human Pif1 helicase is a G-quadruplex DNA-binding protein with G-quadruplex DNA-unwinding activity. *Biochem. J.* **430,** 119–128 (2010).
214. Dahan, D. *et al.* Pif1 is essential for efficient replisome progression through lagging strand G-quadruplex DNA secondary structures. *Nucleic Acids Res.* **46,** 11847–11857 (2018).
215. Jimeno, S. *et al.* The Helicase PIF1 Facilitates Resection over Sequences Prone to Forming G4 Structures. *Cell Rep.* **25,** 3543 (2018).
216. Santos-Pereira, J. M. & Aguilera, A. R loops: new modulators of genome dynamics and function. *Nat. Rev. Genet.* **16,** 583–597 (2015).
217. Sabouri, N., McDonald, K. R., Webb, C. J., Cristea, I. M. & Zakian, V. A. DNA replication through hard-to-replicate sites, including both highly transcribed RNA Pol II and Pol III genes, requires the S. pombe Pfh1 helicase. *Genes Dev.* **26,** 581–593 (2012).

218. Tran, P. L. T. *et al.* PIF1 family DNA helicases suppress R-loop mediated genome instability at tRNA genes. *Nat. Commun.* **8,** 15025 (2017).

219. Ivessa, A. S., Zhou, J.-Q. & Zakian, V. A. The Saccharomyces Pif1p DNA Helicase and the Highly Related Rrm3p Have Opposite Effects on Replication Fork Progression in Ribosomal DNA. *Cell* **100,** 479–489 (2000).

220. Steinacher, R., Osman, F., Dalgaard, J. Z., Lorenz, A. & Whitby, M. C. The DNA helicase Pfh1 promotes fork merging at replication termination sites to ensure genome stability. *Genes Dev.* **26,** 594–602 (2012).

221. Yeeles, J. T. P., Deegan, T. D., Janska, A., Early, A. & Diffley, J. F. X. Regulated eukaryotic DNA replication origin firing with purified proteins. *Nature* **519,** 431–435 (2015).

222. Deegan, T. D., Baxter, J., Ortiz-Bazán, M. Á., Yeeles, J. T. P. & Labib, K. P. M. Pif1-Family Helicases Support Fork Convergence during DNA Replication Termination in Eukaryotes. *Mol. Cell* **74,** 231–244.e9 (2019).

223. Rossi, S. E., Ajazi, A., Carotenuto, W., Foiani, M. & Giannattasio, M. Rad53-Mediated Regulation of Rrm3 and Pif1 DNA Helicases Contributes to Prevention of Aberrant Fork Transitions under Replication Stress. *Cell Rep.* 80–92 (2015). doi:10.1016/j.celrep.2015.08.073

224. Pawłowska, E., Szczepanska, J. & Blasiak, J. DNA2-An Important Player in DNA Damage Response or Just Another DNA Maintenance Protein? *Int J Mol Sci* **18,** 1562 (2017).

225. Johansson, E., Garg, P. & Burgers, P. M. J. The Pol32 subunit of DNA polymerase delta contains separable domains for processive replication and proliferating cell nuclear antigen (PCNA) binding. **279,** 1907–1915 (2004).

226. Khakhar, R. R., Cobb, J. A., Bjergbaek, L., Hickson, I. D. & Gasser, S. M. RecQ helicases: multiple roles in genome maintenance. *Trends Cell Biol.* **13,** 493–501 (2003).

227. Glineburg, M. R., Johns, E. & Johnson, F. B. Deletion of ULS1 confers damage tolerance in sgs1 mutants through a Top3-dependent D-loop mediated fork restart pathway. *DNA Repair (Amst.)* **78,** 102–113 (2019).

228. Marrero, V. A. & Symington, L. S. Extensive DNA end processing by exo1 and sgs1 inhibits break-induced replication. *PLoS Genet.* **6,** e1001007 (2010).

229. Jain, S. *et al.* A recombination execution checkpoint regulates the choice of homologous recombination pathway during DNA double-strand break repair. *Genes Dev.* **23,** 291–303 (2009).

230. Brachmann, C. B. *et al.* Designer deletion strains derived from Saccharomyces cerevisiae S288C: a useful set of strains and plasmids for PCR-mediated gene disruption and other applications. *Yeast* **14,** 115–132 (1998).
231. Hong, Y. *et al.* LEM-3 is a midbody-tethered DNA nuclease that resolves chromatin bridges during late mitosis. *Nat. Commun.* **9,** 728 (2018).
232. Hong, Y. *et al.* The conserved LEM-3/Ankle1 nuclease is involved in the combinatorial regulation of meiotic recombination repair and chromosome segregation in Caenorhabditis elegans. *PLoS Genet.* **14,** e1007453 (2018).
233. Mendoza, M. *et al.* A mechanism for chromosome segregation sensing by the NoCut checkpoint. *Nat. Cell Biol.* **11,** 477–483 (2009).
234. Amaral, N. *et al.* The Aurora-B-dependent NoCut checkpoint prevents damage of anaphase bridges after DNA replication stress. *Nat. Cell Biol.* **18,** 516–526 (2016).
235. Tarnauskaitė, Ž. *et al.* Biallelic variants in DNA2 cause microcephalic primordial dwarfism. *Hum. Mutat.* **40,** 1063–1070 (2019).
236. Klingseisen, A. & Jackson, A. P. Mechanisms and pathways of growth failure in primordial dwarfism. *Genes Dev.* **25,** 2011–2024 (2011).
237. Macheret, M. & Halazonetis, T. D. DNA replication stress as a hallmark of cancer. *Annu. Rev. Pathol.* **10,** 425–448 (2015).
238. Liu, W. *et al.* A Selective Small Molecule DNA2 Inhibitor for Sensitization of Human Cancer Cells to Chemotherapy. *EBioMedicine.* **6,** 73–86 (2016).
239. Kumar, S. *et al.* Inhibition of DNA2 nuclease as a therapeutic strategy targeting replication stress in cancer cells. *Oncogenesis* **6,** e319 (2017).
240. Kachroo, A. H. *et al.* Evolution. Systematic humanization of yeast genes reveals conserved functions and genetic modularity. *Science* **348,** 921–925 (2015).